Investigation of the polymerisation and trimerisation of olefins catalysed by triazacyclohexane complexes of chromium

Smith, David Matthew

Award date:
2005

Awarding institution:
University of Bath

Investigation Of The Polymerisation And Trimerisation Of Olefins Catalysed By Triazacyclohexane Complexes Of Chromium

by

David Matthew Smith

A thesis submitted for the degree of Doctor of Philosophy

University of Bath

Chemistry Department

June 2005

COPYRIGHT

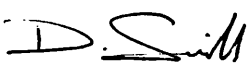

ProQuest LLC
789 East Eisenhower Parkway
P.O. Box 1346
Ann Arbor, MI 48106-1346

Declaration

The work described in this thesis was carried out at the University of Bath, Department of Chemistry, between September 2001 and May 2005. All the work is my own unless stated otherwise, and it has not been submitted previously for a degree at this or any other university.

Financial Support

The Engineering and Physical Science Research Council (EPSRC), BASF AG and Basell are gratefully acknowledged for providing funding for the work described herein.

Acknowledgements

During my four years at Bath I have had the pleasure of working alongside many wonderful people and made some great friends, and therefore if I miss anybody out who I owe a great deal of thanks then I apologise now and would just like to give my appreciation, Thanks!

First and foremost I would like to thank Dr. Randolf Köhn for allowing me to be a part of his group, and for being a very helpful and understanding supervisor. I also have to thank him for proof reading the many pages of drivel on the way to completing this thesis, and imparting me with some of his wisdom along the way. I would like to thank the Köhn group for being very friendly and a great bunch of people to work with. I thank Gabi for all her help with the X-ray crystallography and Pan, Ian, Freddy and Jeremy for all the great times in the lab. (Sorry Ian for not making the group meetings a little more exciting!)

For my time spent at BASF/Basell I would really like to thank Dr. Martina Egen for sorting out all my arrangements whilst I was there, showing me around Heidelburg, and providing an endless supply of ideas. Thanks also to Dr. Shahram Mihan for ideas for this project. I would like to thank all the members of the lab for making me feel welcome, Michael for all his help and advice, and a huge thank you to Jörg (the German king!) for being a great guide, translator, lab buddy, and an amazing friend. Thanks also have to go out to his family and Sara for their hospitality and friendship.

I must give a huge thanks to Dr. Andy Johnson for being an all round great guy, for giving me ideas, advice and a place to stay. (for a week or two!) I would like to thank Steve for putting up with hours of pointless conversations, lots of whining, but many happy times. Thanks to Cheryl for keeping my wardrobe well stocked from shopping, and thanks to Nichola for not letting me miss a film at the cinema. Thanks again to all the other students and lecturers in the chemistry department for making my time here very enjoyable. Thanks to the admin. and technical staff without whom this work would not be possible. Last but definitely not least a huge thanks to my mum, dad, Richard and Nicola for lots of love and support.

Abbreviations

acac	acetylacetonate
Ar	Aryl
Bu	n-Butyl
^{i}Bu	Iso-Butyl
^{t}Bu	Tertiary-Butyl
Bz	Benzyl
Cp	Cyclopentadienyl
Cp*	Pentamethyl cyclopentadienyl
Cy	Cyclohexyl
γ_I	Magnetogyric Ratio of nucleus I
d	Density
DCM	Dichloromethane
DMA	Dimethylaniline
DMAH	Dimethylanilinium
DMAB	Dimethylanilinium Tetrakispentafluorophenylborate
DMSO	Dimethyl Sulfoxide
Do	n-Dodecyl
en	Ethylenediamine
2-EH	2-Ethylhexanoate
Et	Ethyl
EtBu	2-Ethylbutyl
2-EtHex	2-Ethylhexyl
FBz	*para*-Fluorobenzyl
FPh	*para*-Fluorophenyl
g_e	Free-Spin Electron g Factor
η	Viscosity
HDPE	High Density Polyethylene
HOTf	Triflic Acid
k	Boltzmann Constant
L	Ligand
LDPE	Low Density Polyethylene

λ	Line Width
MAO	Methylaluminoxane
Me	Methyl
MW	Molecular Weight
μ_0	Permeability of Vacuum
μ_{eff}	Effective Magnetic Moment
n	Number of Unpaired Electrons (in connection with magnetic moments)
N_A	Avogadro Constant
OTf	Triflate
PE	Polyethylene
Ph	Phenyl
Pr	n-Propyl
^{i}Pr	Iso-Propyl
R	Alkyl Group
R_2	Transverse Relaxation Rate Constant
R_3TAC	1,3,5-Trialkyl-1,3,5-triazacyclohexane
R_3TACN	1,4,7-Trialkyl-1,4,7-triazacyclononane
S	Spin Quantum Number
Sen	Thiophene-2-methyl
T	Temperature
T_2	Transverse Relaxation Time
T_{dec}	Decomposition Temperature
TEA	Triethylaluminium
THF	Tetrahydrofuran
τ_c	Correlation Time
τ_M	Exchange Correlation Time
τ_r	Rotational Correlation Time
τ_s	Electronic Relaxation Correlation Time
V	Volume
X	Halide
χ	Magnetic Susceptibility

Numbering Of Compounds

1 1,3,5-tridodecyl-1,3,5-triazacyclohexane

2 1,3,5-tridodecyl-1,3,5-$d_6$triazacyclohexane

3 1,3,5-triallyl-1,3,5-triazacyclohexane

4 1,3,5-tri-(2-ethylbutyl)-1,3,5-triazacyclohexane

5 1,3,5-tri-(2-ethylhexyl)-1,3,5-triazacyclohexane

6 1,3,5-tri-para-fluorobenzyl-1,3,5-triazacyclohexane

7 1,3,5-(2-thiophenemethyl)-1,3,5-triazacyclohexane

8 1,3,5-(propyl-tri-ethoxysilane)-1,3,5-triazacyclohexane

9 1,3,5-Tris-(*o*-methoxyphenyl)-1,3,5-triazacyclohexane

10 N,N'-bis-(2-methoxy-phenyl)-methanediamine

11 1-(2-Ethylbutyl)-3,5-*p*-fluorophenyl-1,3,5-triazacyclohexane

12 1-(2-Ethylbutyl)-3,5-*p*-chlorophenyl-1,3,5-triazacyclohexane

13 1-(2-Ethylbutyl)-3,5-*p*-bromophenyl-1,3,5-triazacyclohexane

14 $(Allyl)_3TACCrCl_3$

15 $(2\text{-}PhEt)_3TACCrCl_3$

16 $(2\text{-}EtBu)_3TACCrCl_3$

17 $(2\text{-}EtHex)_3TACCrCl_3$

18 $[(EtO)_3SiPr]_3TACCrCl_3$

19 $Do_3TACCrCl_3$

20 $Do_3(d_6\text{-}TAC)CrCl_3$

21 $Do_2PhTACCrCl_3$

22 $Do_2[p\text{-}(F_3C)Ph]TACCrCl_3$

23 $(2\text{-}EtHex)_2(p\text{-}FPh)TACCrCl_3$

24 $(p\text{-}FPh)_2(2\text{-}EtBu)TACCrCl_3$

25 $Do_3TACCr(OTf)_3$

26 $(2\text{-}EtHex)_3TACCr(OTf)_3$

27 $(Do_3TAC)_2Cr(OTf)_3$

28 $PhNHMe_2B(C_6F_5)_4$

29 $PhNHEt_2B(C_6F_5)_4$

30 $n\text{-}Bu_4NB(C_6F_5)_4$

31 $(2\text{-}PhEt)_3TACCrCl_3DMAB$

32 $(2\text{-EtBu})_3TACCrCl_3DMAB$

33 $(2\text{-EtHex})_3TACCrCl_3DMAB$

34 $Do_3(d_6\text{-TAC})CrCl_3DMAB$

35 $(p\text{-FBz})_3TACCrCl_3DMAB$

36 $^tBu_3TACCrCl_3DMAB$

37 $Me_3TACCrCl_3DMAB$

38 $(2\text{-EtHex})_2(p\text{-FPh})TACCrCl_3DMAB$

39 $[Do_3TACCr^iBu_2][B(C_6F_5)_4]$

40 $[Do_3TACAl^iBu_2][B(C_6F_5)_4]$

41 $[(2\text{-EtBu})_3TACAl^iBu_2][B(C_6F_5)_4]$

42 $[(toluene)_2Cr][B(C_6F_5)_4]$

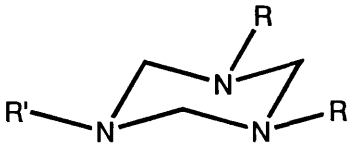

1 R' = R = Do

3 R' = R = Allyl

4 R' = R = 2-EtBu

5 R' = R = 2-EtHex

6 R' = R = *p*-FBz

7 R' = R = 2-thiophenemethyl

8 R' = R = propyl-tri-ethoxysilane

9 R' = R = *o*-methoxyphenyl

11 R' = 2-EtBu, R = *p*-FPh

12 R' = 2-EtBu, R = *p*-ClPh

13 R' = 2-EtBu, R = *p*-BrPh

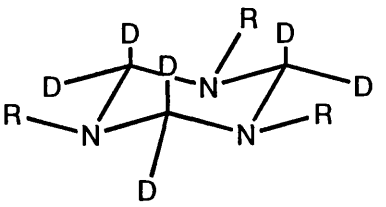

2 R = Do

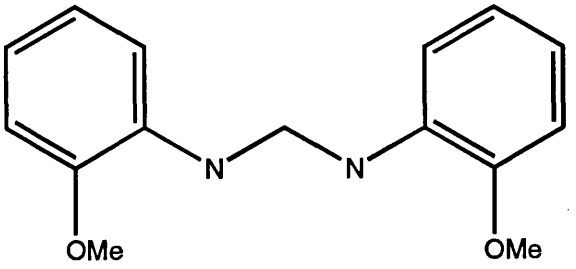

10

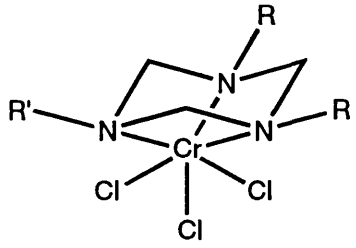

14 R' = R = Allyl

15 R' = R = 2-PhEt

16 R' = R = 2-EtBu

17 R' = R = 2-EtHex

18 R' = R = propyl-tri-ethoxysilane

19 R' = R = Do

21 R' = Ph, R = Do

22 R' = *p*-(F_3C)Ph, R = Do

23 R' = *p*-FPh, R = 2-EtHex

24 R' = 2-EtBu, R = *p*-FPh

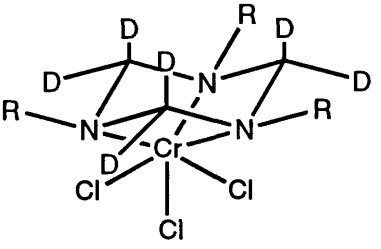

20 R = Do

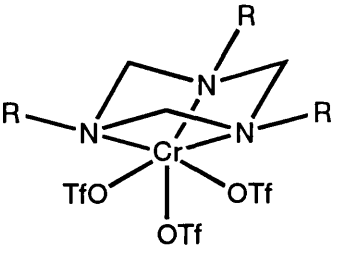

25 R = Do

26 R = 2-EtHex

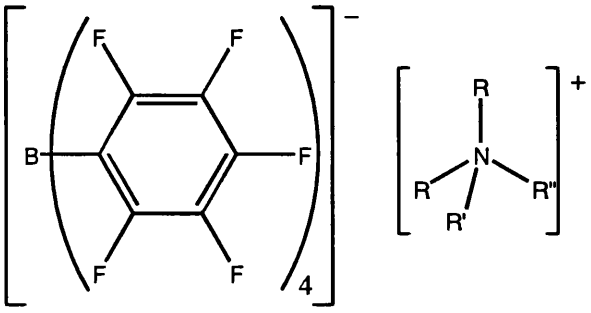

28 R = Me, R' = H, R'' = Ph

29 R = Et, R' = H, R'' = Ph

30 R = R' = R'' = *n*-Bu

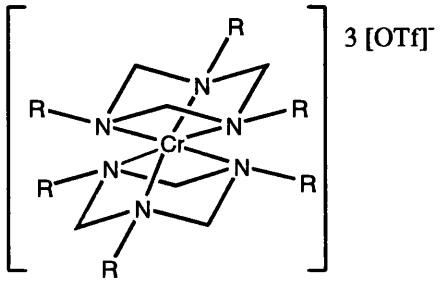

27

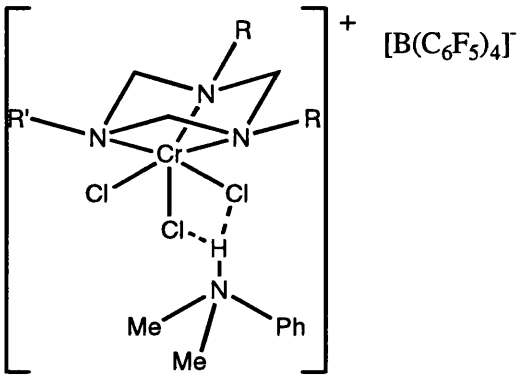

31 R = R' = 2-PhEt

32 R = R' = 2-EtBu

33 R = R' = 2-EtHex

35 R = R' = *p*-FBz

36 R = R' = ^{t}Bu

37 R = R' = Me

38 R = 2-EtHex, R = *p*-FPh

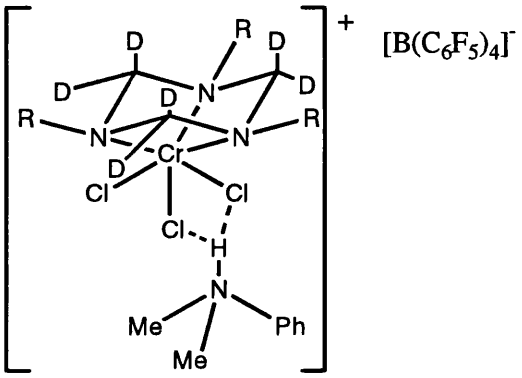

34 R = Do

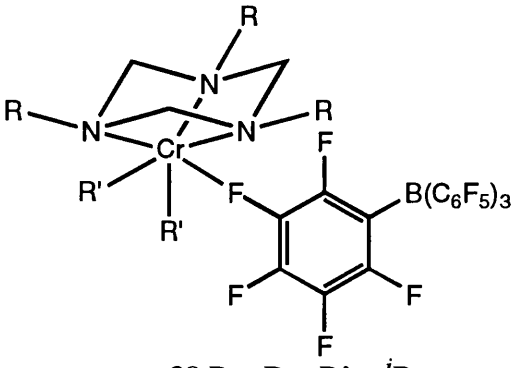

39 R = Do, R' = ^{i}Bu

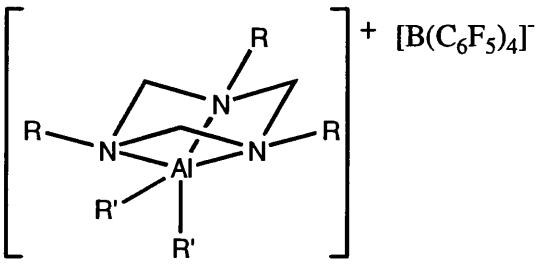

40 R = Do, R' = ^{i}Bu

41 R= 2-EtBu, R' = ^{i}Bu

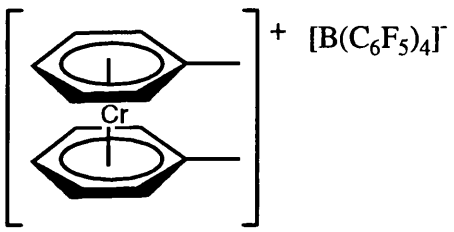

42

Abstract

This thesis describes an investigation into the activation, catalytic cycle and decomposition of 1,3,5-trialkyl-1,3,5-triazacyclohexane chromium complexes involved in the selective trimerisation of α-olefins. These studies include an in depth look into the mechanisms involved in each of these processes. Using these findings a development of the ligand system is illustrated to devise more highly active and long lived catalyst systems.

Chapter 1 highlights the industrial application of polymerisation and trimerisation along with the catalytic systems involved. Homogeneous model systems have been devised to aid in the understanding of these systems and hence, have led to the development of more highly active systems for the selective trimerisation of olefins. Attention is made to the difference in mechanism between the two processes and the problems associated with the study of paramagnetic Cr(III) complexes.

Chapter 2 describes the synthesis and structure of 1,3,5-trialkyl-1,3,5-triazacyclohexanes with comparisons made to substituted cyclohexanes and 1,3,5-triaryl-1,3,5-triazacyclohexanes.

Chapter 3 concentrates on the merits of 1,3,5-trialkyl-1,3,5-triazacyclohexanes as ligands with a variety of metals in a number of coordinating modes. The synthesis of 1,3,5-trialkyl-1,3,5-triazacyclohexane chromium complexes are described along with their solubility characteristics and ligand exchange reactions.

Chapter 4 focuses on the role of weakly coordinating anions in stabilisation and characterisation of active sites. The two step activation of the chromium complexes by firstly addition of the salt of the weakly coordinating anion followed by the trialkylaluminium activator is described. This process is probed by ^{1}H, ^{2}H and ^{19}F NMR spectroscopy alongside X-ray crystallography to identify key intermediates and comparison with MAO activation.

Chapter 5 describes the trimerisation activity of the chromium catalysts with a variety of activators and α-olefins. Decomposition products are identified from these reactions and lead to postulations on more active and long lived systems. Magnetic moment measurements lead to the most probable oxidation couple for this system.

Chapter 6 gives experimental details and characterisation data for chapters two to five.

Contents

1: Introduction

1.1: Olefin Polymerisation

Olefin polymerisation produces a wide range of exceptionally versatile polymers for a variety of industrial products. Polypropylene is produced in various forms whose properties depend largely on the polymer molecular weight and its stereochemistry. These in turn are largely determined by the particular catalyst system used for the polymerisation. Polyethylene is probably the polymer most often seen in daily life. Polyethylene is the most popular plastic in the world. This is the polymer that makes grocery bags, shampoo bottles, children's toys, and even bullet proof vests.

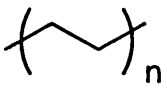

If the polymer produced is a straight chain this is known as high density polyethylene (HDPE). If the chain is highly branched, this is known as low density polyethylene (LDPE).

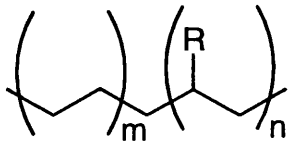

1.2: Phillips Catalyst

Polymers produced by homopolymerisation and/or copolymerisation of small olefins such as ethene and propene are amongst the most widely used plastics. In the last few years the worldwide consumption of polymers made from these small olefins has been over $40x10^6$ and $20x10^6$ tons per year, respectively.[1] In industry these materials are

products of metal-catalysed reactions conducted on an enormous scale. Two different types of catalyst are responsible for this production. One group consists of group 4 metals, such as Ti and Zr, and can be traced to the Nobel Prize winning discoveries of Ziegler and Natta, [2] *Scheme 1.*

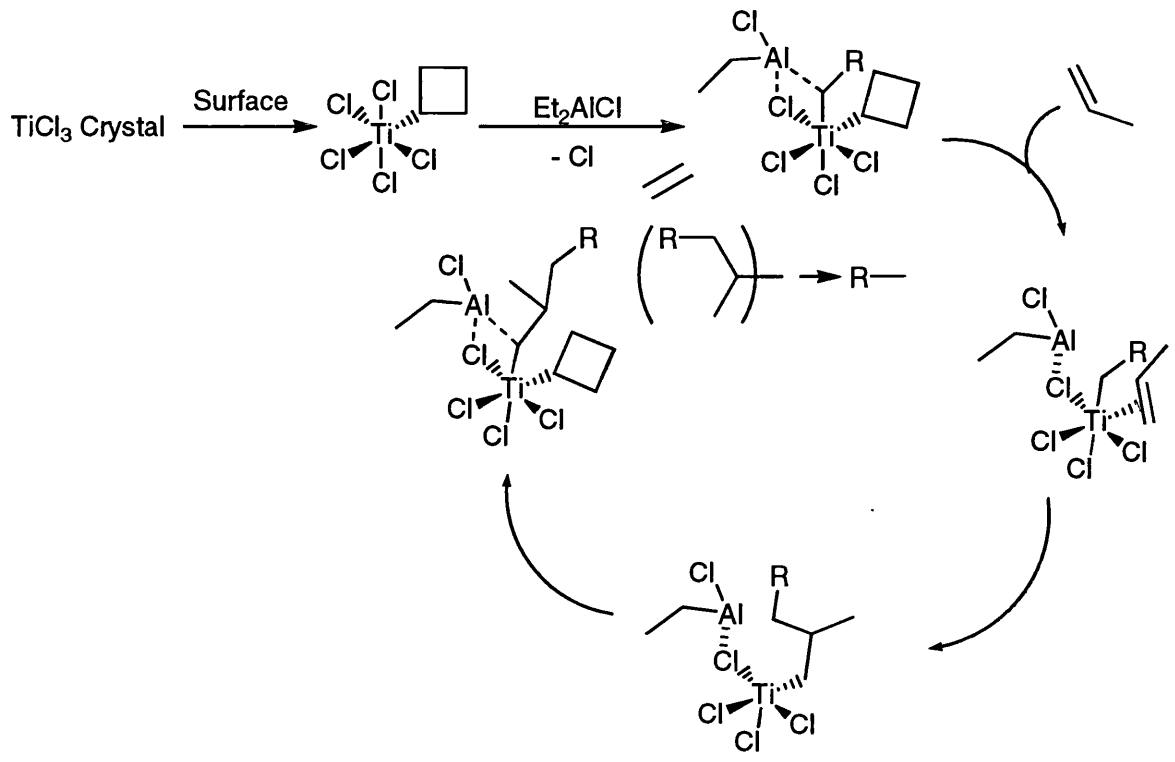

Scheme 1: Catalytic cycle for a titanium Ziegler – Natta olefin polymerisation

In recent times there has been much interest in this area due to developments in metallocene chemistry. This progress has brought about the creation of catalysts based on sophisticated organometallic molecules that give a greater control of polymer structure and properties, [3] *Scheme 2.*

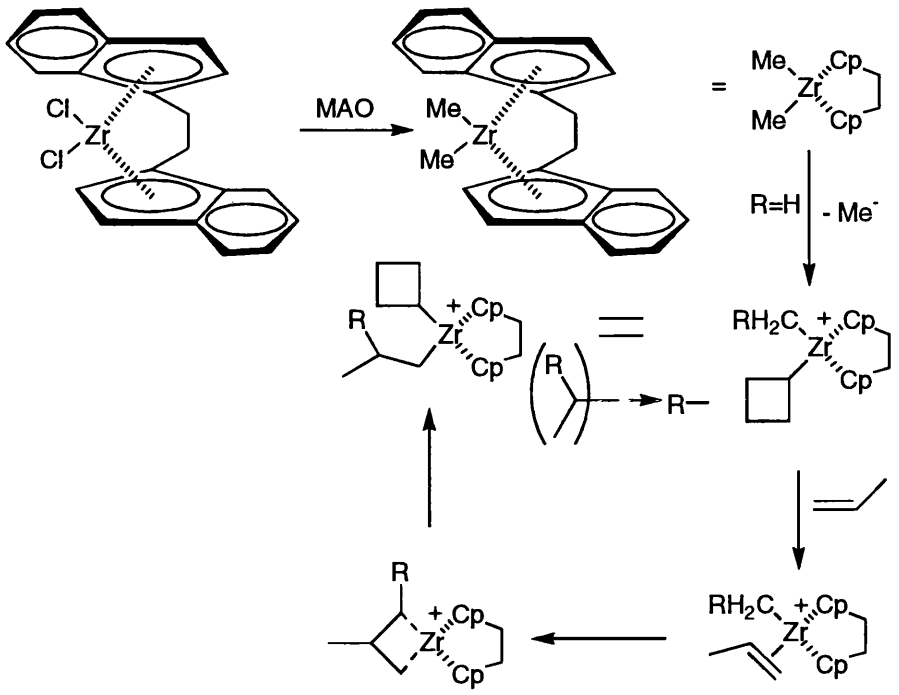

Scheme 2: Catalytic cycle for olefin polymerisation with a Zr metallocene system

The second type of catalyst was discovered independently by Hogan and Banks at Phillips Petroleum Co. in the early 1950s, [4] and still produces a large fraction of the world's HDPE. [5] This system has many unusual features compared to other transition metal catalysts. Firstly it is notable for not requiring any co catalyst. Most systems require either aluminium alkyls or methyl aluminoxane for activation. Despite much investigation little is known about the mechanism and active site of this system. This lack of information is due to the small number of homogeneous model systems for chromium based heterogeneous catalysts. In the last few years this has changed.

The Phillips Cr/silica polymerisation catalyst is prepared by impregnating an inorganic chromium compound, CrO_3 or various Cr(III) salts, onto a wide pore silica and then calcining in oxygen to activate the catalyst. [6] This leaves the chromium in the hexavalent state. *Figure 1*

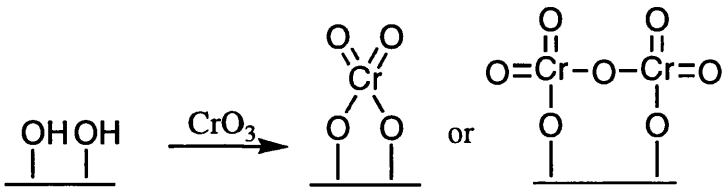

Figure 1: Preparation of the Phillips Cr/silica polymerisation catalyst

Upon contact with ethene, the metal is reduced; ultimately forming the catalytically active species. [7] However, the chemical structure, valence state, and mechanism of formation of the active site have been the subject of a longstanding controversy. *Figure 2* depicts some of the proposed structures.

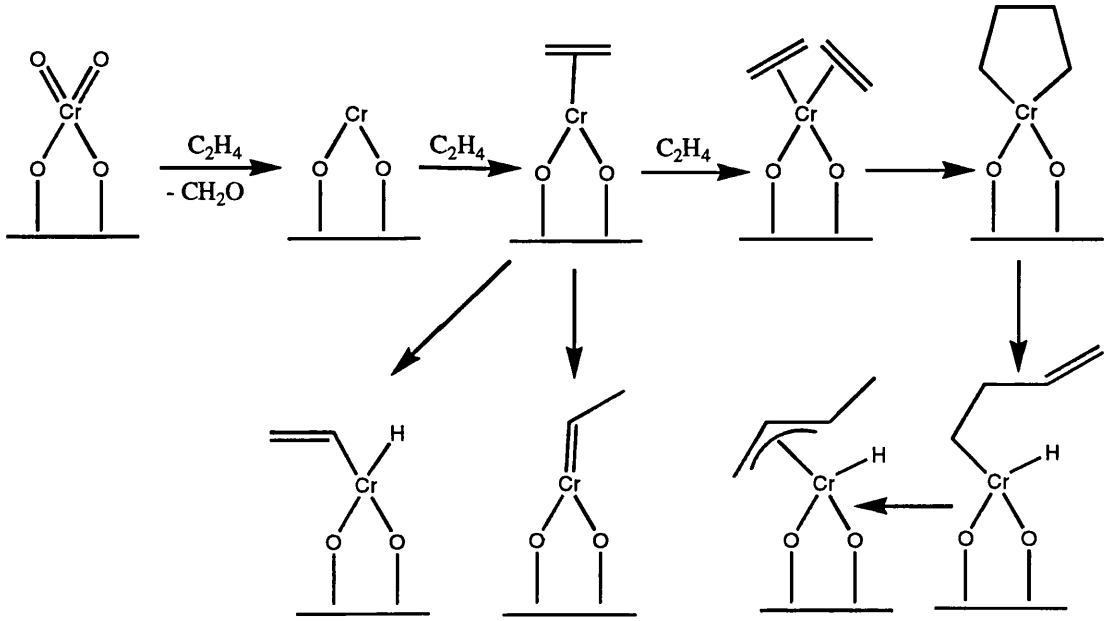

Figure 2: Proposed structures for the formation of the active site in the Phillips system

Activation can also be achieved with other reducing agents such as CO or aluminium alkyls. Contrary to most catalysts based on the hydride mechanism, the molecular weight of polymer is quite insensitive to hydrogen but can be regulated by the reaction pressure and temperature. End group analysis of the polymer shows not only the expected single methyl and vinyl end groups but also additional methyl groups, vinylidene and some internal olefin end groups. Such end groups have been seen for systems based on the hydride mechanism when additional isomerisation, mis-insertion

or chain-walking steps are involved. However, these groups are found in Phillips systems in consistently similar ratios.

When activated by aluminium alkyls the Phillips catalyst can also convert ethene to α-olefins that can be in-situ co-polymerised giving polymer with side chains. However, these oligomers do not follow the Flory-Schultz distribution typical for systems based on the hydride mechanism. There is a high selectivity for the trimer of ethene, 1-hexene, and subsequent co-polymers with butyl side chains.

1.3: Homogeneous Chromium Catalysts

As in the case of the Ziegler Natta system, homogeneous model systems of the Phillips catalyst were sought to try and gain a greater understanding of the mechanism and active species. The mimics prepared by Theopold et al., [8] were well characterised Cp* chromium alkyl complexes, $[Cp^*Cr(THF)_2Me]BPh_4$, that were able to polymerise ethylene, *Figure 3.* [9]

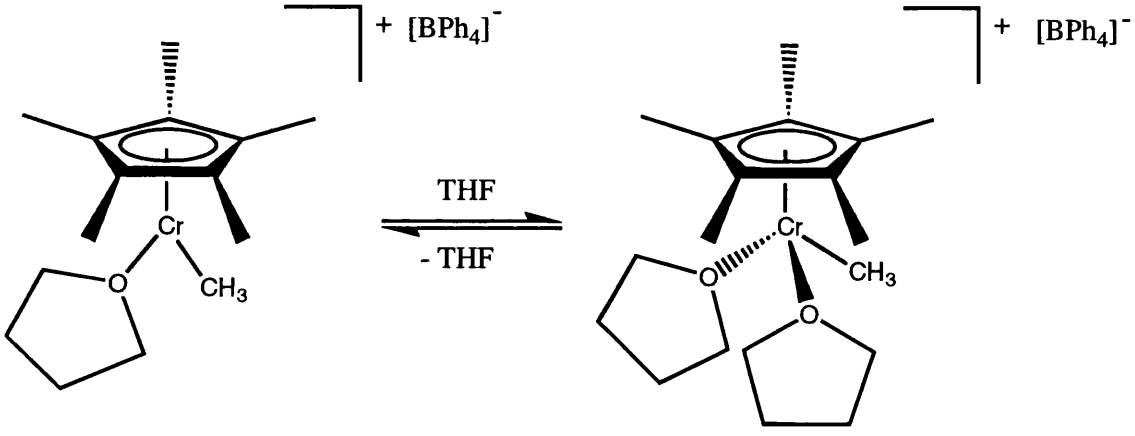

Figure 3: Labile THF in the $[Cp^*Cr(THF)_2Me]BPh_4$ system can provide free coordination sites

In solution this 15 electron complex exists in equilibrium with the co-ordinatively unsaturated mono THF complex, by dissociation of a THF ligand. The

Cp^*CrL_2X [10] complex is considered co-ordinatively saturated, despite being 3 electrons short of the 18 electron configuration, if the cyclopentadienyl ring acts as a tridentate chelating ligand. The Cp* would then occupy one trigonal face of an octahedron, with three other ligands filling the octahedral geometry of the Cr(III) ion. Attempts to polymerise propene with this complex were unsuccessful. However, with ethylene under typical conditions, 10mg of chromium complex dissolved in 50ml DCM produced 1-2g of polyethylene before activity ceased. The maximum activity measured was 1.1 turnover/sec a value within an order of magnitude of the quoted activity of commercial catalysts. The polymer produced was identified by IR spectroscopy as HDPE with melting points 135-140 °C. The molecular weights were relatively low, Mw: 22000-77000, with a narrow molecular weight distribution. The polymers were highly linear, showing no detectable branching.

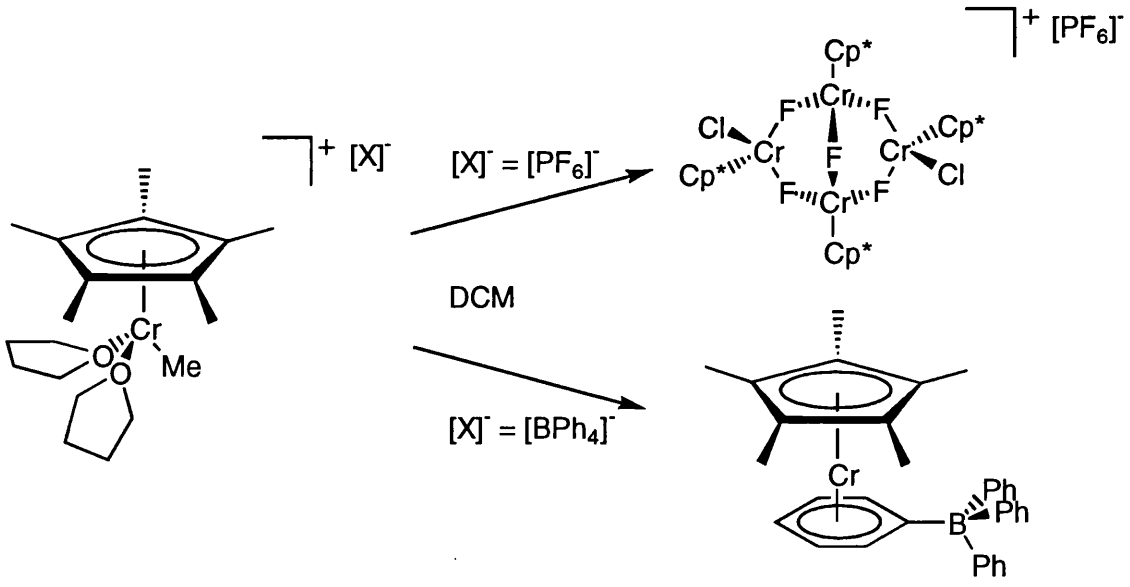

Figure 4: Decomposition of the $[Cp^*Cr(THF)_2Me]BPh_4$ system

This catalyst eventually became inactive and possible explanations of this were irreversible reactions of the highly electrophilic chromium cation with the solvent or its counterion. A few unusual chromium complexes resulting from the metal attacking anions have been isolated and characterised, *Figure 4.* [11]

A more active polymerisation catalyst was a neutral chromium complex $Cp^*Cr(CH_2SiMe_3)_2$, *Figure 5.* [12]

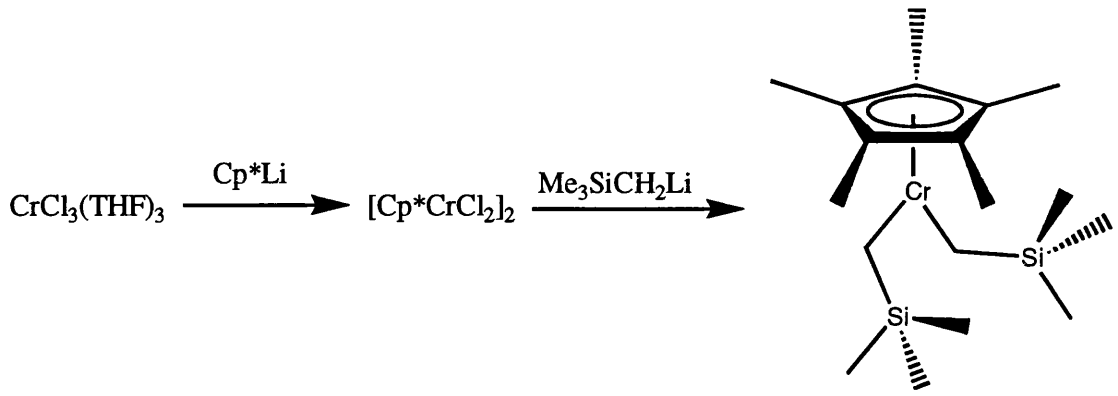

Figure 5: Formation of neutral complex $Cp^*Cr(CH_2SiMe_3)_2$

$Cp^*Cr(CH_2SiMe_3)_2$ is best described as a 13 electron complex. It is also a very good catalyst for the polymerisation of ethylene with activities as high as 5 Kg $molCr^{-1}h^{-1}$. Hydrocarbon solutions rapidly precipitated polyethylene at reaction temperatures 0 to – 42 °C, with the complex slowly decomposing at room temperature. The polymers formed were similar to those created by the previous system, Mw: 20000- 143000 and were also highly linear.

Unlike the Phillips catalyst these systems produce only linear polymer and show no reaction towards α-olefins, this is thought to be due to steric reasons. To try to account for this, complexes with extremely labile ligands were synthesised. The strongly binding THF ligands were replaced by dialkyl ethers to form $[Cp^*Cr(OEt_2)_2CH_2SiMe_3]BAr_4$, *Figure 6.* [13]

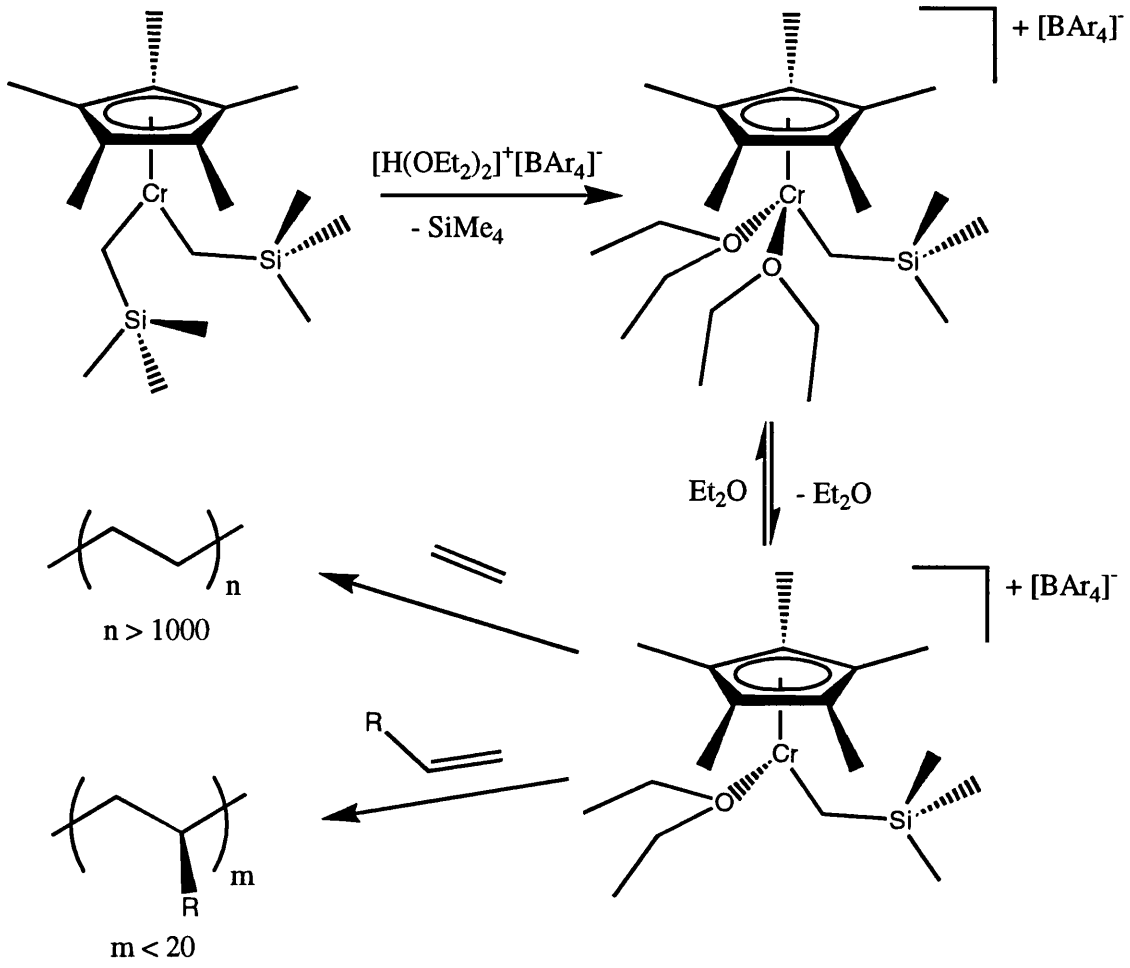

Figure 6: Formation and reactivity of the $[Cp^*Cr(OEt_2)_2CH_2SiMe_3]BAr_4$ system

This complex was a very reactive catalyst towards polymerisation of ethylene even below –104 °C, with activities up to 56 Kg $molCr^{-1}h^{-1}$. It was also capable of the oligomerisation of α-olefins. Copolymerisation of mixtures of ethylene and an α-olefin, yielded purely polyethylene without any indication of branching.

After these initial attempts Jolly reported that amino-substituted cyclopentadienyl chromium derivatives, in the presence of methylaluminoxane, MAO:Cr = 100:1, polymerise propene to atactic polypropylene, *Figure 7.* [14] It also has very high activity for the polymerisation of ethylene, with activities >6170 Kg $molCr^{-1}h^{-1}$. MAO is known to confer remarkable enhancements upon the catalytic activity of

group 4 metallocene catalysts, and so from the observation of the enhanced activity of this system over the non-activated Theopold systems, the same increased activity is seen in the case of chromium.

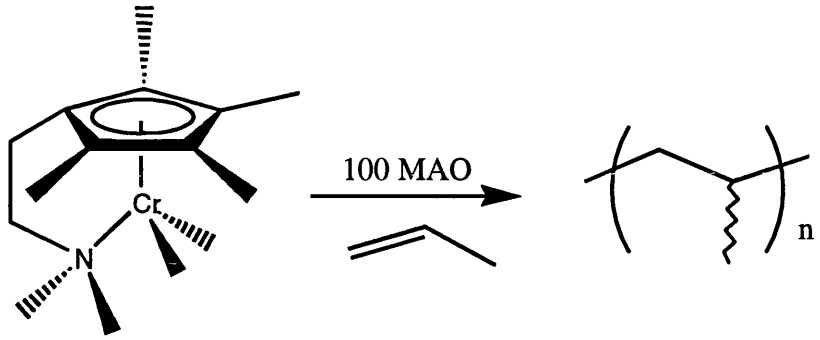

Figure 7: Propene polymerisation with the [(Cp*EtNMe$_2$)CrMe$_2$] system

Although these systems are highly active they have a tendency to decompose slowly after activation or are unstable at high temperatures during catalysis. Enders [15] adapted this system to include a more rigid structure for the nitrogen side arm, whilst maintaining the C_2 linker, by addition of quinolyl- and N,N-dimethylanilinyl-functionalities to the cyclopentadiene, *Figure 8*. With these rigid ligands intermolecular donor-metal interactions and formation of insoluble coordination polymers is impossible unlike with flexible spacer groups.

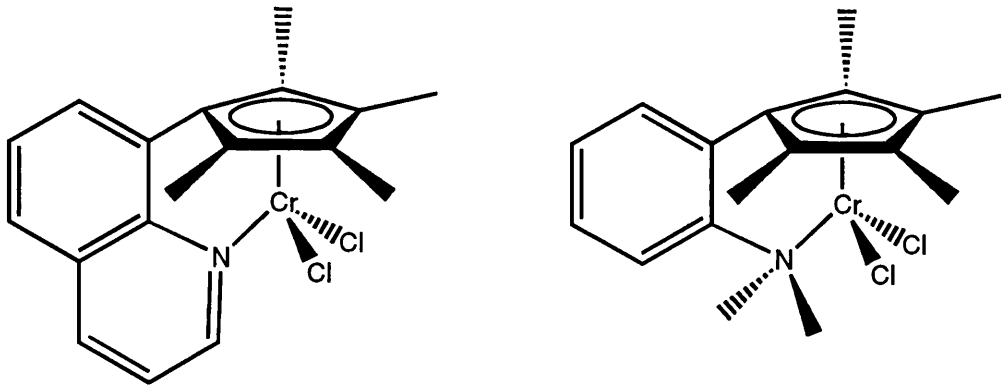

Figure 8: Chromium cyclopenadiene complexes with rigid nitrogen donor linkages

These complexes are more stable than the comparable complexes with flexible linkages with the complexes activated with MAO showing no detectable signs of decomposition after several weeks at room temperature. Ethylene polymerisation

activities for this type of complex are high, up to 3640 kg $mol^{-1}h^{-1}bar^{-1}$ at room temperature. Activities for propene polymerisation were dramatically reduced, up to 107 kg $mol^{-1}h^{-1}bar^{-1}$ at room temperature.

Other groups have also been trying to find potential well-defined catalyst for the polymerisation of ethylene, but concentrating on non-cyclopentadienyl chromium systems, where adjustment of steric and electronic properties will give them control over the molecular weight and microstructure of the resultant polymer. In 1994 Gibson reported an active homogeneous catalyst, [16] activity 65 Kg $molCr^{-1}h^{-1}$ for the polymerisation of ethylene, derived from bis(imido) chromium (VI) precursors, *Figure 9.*

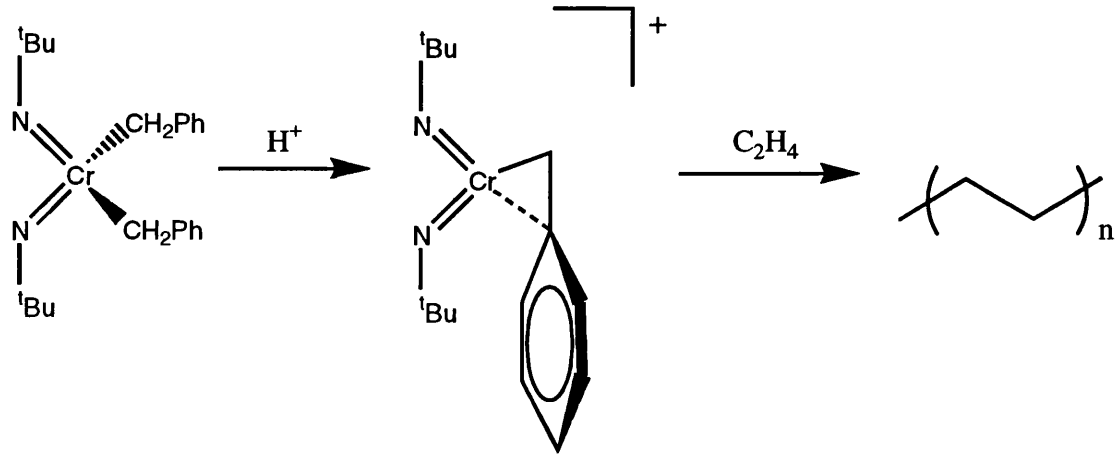

Figure 9: Activation of bis(imido)chromiumbis(benzyl) complex

While the active species in this system has not yet been fully characterised, this system resembles group IV metallocene chemistry much more than any known heterogeneous chromium catalyst.

In 1999 Gibson published new chromium catalysts based upon a bulky monoanionic N,O-chelating ligand derived from reduction of the corresponding Schiff-base precursor, *Figure 10.*[17]

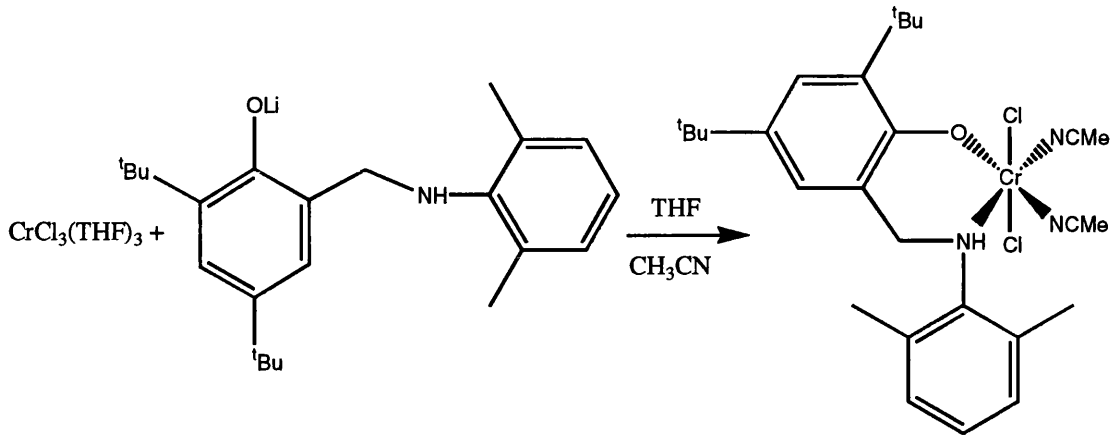

Figure 10: Formation of N,O-chelating Schiff-base Chromium complex

This chromium catalyst was found to be excellent for the polymerisation of ethylene in the presence of Et_2AlCl, with activities up to 130 Kg $molCr^{-1}h^{-1}$. In the presence of MAO as co-catalyst the activities were not as impressive.

1.4: Oligomerisation and Trimerisation Catalysts

In a patent to the Albemarle Corporation [18] Wu describes a selective ethylene oligomerisation in the presence of a chromium triazacyclononane catalyst system using aluminoxanes as activators. This process provided a Schultz-Flory distribution of α-olefins that is selectively enriched with 1-hexene, without the formation of excessive amounts of PE. In accordance with his reasoning the necessity of steric bulk for oligomerisation over polymerisation, he found that the complex with the absence of substituents on the nitrogens, gave a selectively polymerising system.

For the catalyst system [1,4,7-trimethyl-1,4,7-tri-azacyclononane]$CrCl_3$ / n-hexylaluminoxane 1 : 80 in toluene at 105 °C with an ethylene pressure of 29 bar the resulting products were 9.4% C_4, 39.9% C_6, 10% C_8, 8.5% C_{10}, 6.9% C_{12}, 6% C_{14}, 5% C_{16}, 4% C_{18} and 10.9% C_{20+} with an activity of around 12,309 g/g Cr per hour. Using the Schultz-Flory equation the expected amount of the C_6 fraction should be around 10%. This increased selectivity for this fraction along with the Schultz-Flory distribution of the other fractions suggests two competing pathways in action, both the linear chain growth mechanism well established for ethylene polymerisation and oligomerisation, and also the metallocycle mechanism the most accepted proposed mechanism for selective trimerisation. (See Chapter 5)

In 2000 Köhn reported that 1,3,5-triazacyclohexane chromium complexes were highly active ethylene polymerisation catalyst that resemble the Phillips catalyst in many properties and so may represent the first good homogeneous model system, *Figure 11.* [19] Activities for ethene polymerisation are up to 800 Kg $molCr^{-1}h^{-1}$ in the presence of MAO as co-catalyst. The system can also be activated by DMAB (dimethylanilinium tetrakis(pentafluorophenyl)borate) and $Al(^iBu)_3$, giving similar activities. (See Chapter 3) The molecular weights of the polymer are around Mw: 40000.

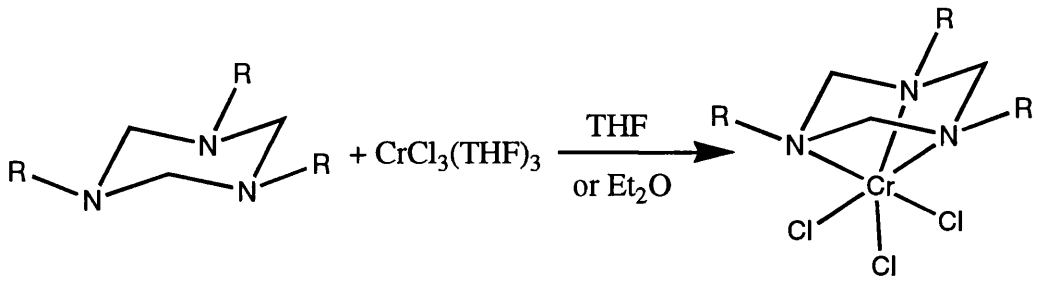

Figure 11: Formation of $R_3TACCrCl_3$ complexes

End group analysis of the polymer produced showed more methyl groups than expected and additional vinylidene and some internal olefin as well as the expected vinyl end groups. This distribution is very similar to that of the Phillips catalyst. As the molecular weights of the polymers differ the values for the end groups, in *Table 1*, are best compared relative to the total number of olefinic groups.

End Group	$H_2C=CHR$	$H_2C=CR_2$	RHC=CHR	Me
PE (Phillips)	84-92%	7-13%	1-4%	150-300%
PE (produced)	82%	12%	6%	240%
Decenes (Produced)	87%	8%	5%	200%

Table 1: End group analysis of polymer produced by $R_3TACCrCl_3$ catalysis

In addition, 1-hexene the trimer of ethylene, and some decenes as co-trimers of 1-hexene and ethene can be found in the solution. The butyl side chains are indicative of some 1-hexene built into the polymer. This shows that this system is also able to reproduce the selectivity for trimerisation. However due to the similarity of the end group distribution between the polymer and co-trimer suggests that the same mechanism is operating in both cases. The system can also be adjusted, via the alkyl arms of the triazacyclohexane, to form predominantly a trimerisation catalyst for both ethene and α- olefins, with up to 90% conversion.

Some possible reasons for this similarity to the Phillips catalyst and why this system is capable of adding α-olefin units are that the three hard nitrogen donor atoms facially co-ordinate chromium and may be a good model for the two or three oxygen atoms, in the hard ligand sphere of the silicate, believed to be bound in the

heterogeneous system. Without severe distortions during complexation of the triazacyclohexane the nitrogen lone pairs are orientated essentially parallel to each other and cannot overlap with the chromium orbitals as well as other amine ligands. Therefore this system is much more comparable to Cp ligands where the metal bonding p-orbitals are also parallel to each other. This can be seen in *Figure 12* with a comparison with the larger tiazacyclononane ligand, and the relevant cone angles. [20]

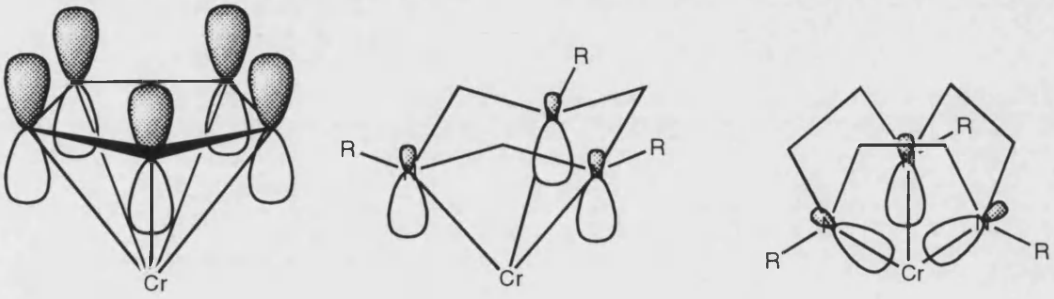

Cone Angle: 32° 36° 49°

Figure 12: Cone angles and directing of nitrogen lone pairs in Cp^*, R_3TAC and R_3TACN chromium complexes

However differences between Cp^* and R_3TAC complexes can be seen in UV/Vis spectroscopy. Complexes of both ligand systems show two absorptions that can be assigned to the d-d transitions $A_{2g} \rightarrow T_{2g}$ and $A_{2g} \rightarrow T_{1g}$. Average values for R_3TAC complexes being $10Dq(TAC) = 15822\ cm^{-1}$ $B'(TAC) = 670\ cm^{-1}$, and for Cp^* complexes $10Dq(Cp) = 15800\ cm^{-1}$ $B'(Cp) = 200\ cm^{-1}$. This shows that the ligand field splitting caused by Cp^* is similar to R_3TAC, but B' is much smaller showing a more covalently bound Cp^*.

The Tosoh Corporation found that tris(pyrazolyl)methane chromium complexes can be activated by MAO or trialkyl aluminiums to give active species for selective ethylene trimerisation. Four chromium trichloride complexes, tris(3,5-dimethyl-1-pyrazolyl)methane chromium trichloride, tris(3-phenyl-5-methyl-1-pyrazolyl)methane

chromium trichloride, tris(3-phenyl-1-pyrazolyl)methane chromium trichloride and tris(3-(4-tolyl)-1-pyrazolyl)methane chromium trichloride have been used to give selectivities up to 99.1% in 1-hexene, [21] *Figure 13.*

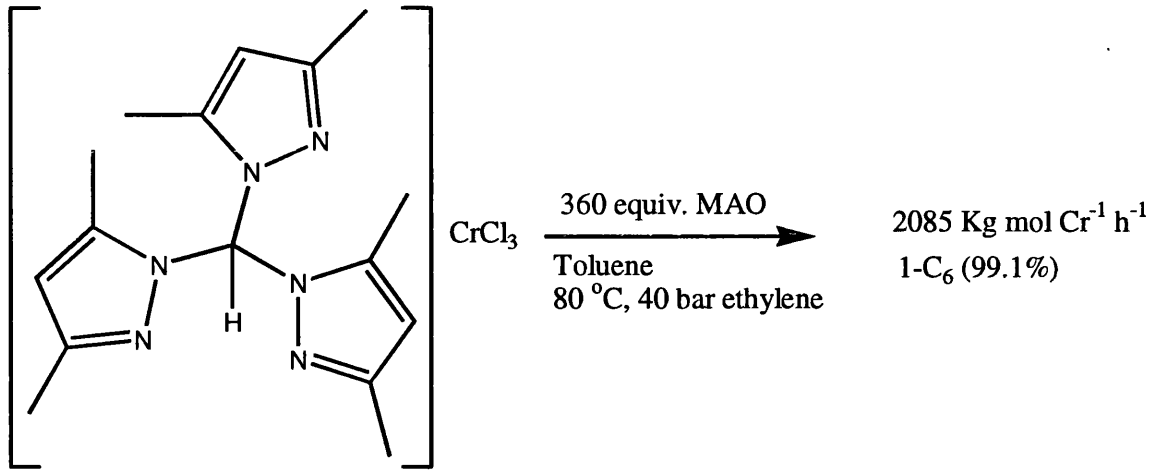

Figure 13: Activity of a tris(pyrazolyl)methane chromium complex in selective ethylene trimerisation

Diimine ligands have been used in transition metal catalysed polymerisations and have been extensively reviewed by Ittel. [22] Sumitomo Chemical Co. has patented the use of diimines of the form $R^1N=CR^2(CR^3R^4)_mCR^5=NR^6$ or $R^7R^8C=N(CR^9R^{10})_nN=CR^{11}R^{12}$ with Cr(III) 2-EH, and triethylaluminium (TEA) for the use of ethylene trimerisation. [23] A reaction comprising of Cr(III) 2-EH, glyoxalbis(1,1,3,3-tetramethylbutylimine) and TEA at molar ratios of 1:15:79, *Figure 14*, in heptane solution at 40 bar ethylene pressure and 120 °C afforded a reaction mixture of 12.2% C_4, 72.4% C_6 (80.5% 1-C_6, 58.3% 1-C_6 overall), 1.5% C_8, 9.4% C_{10} and 3% PE.

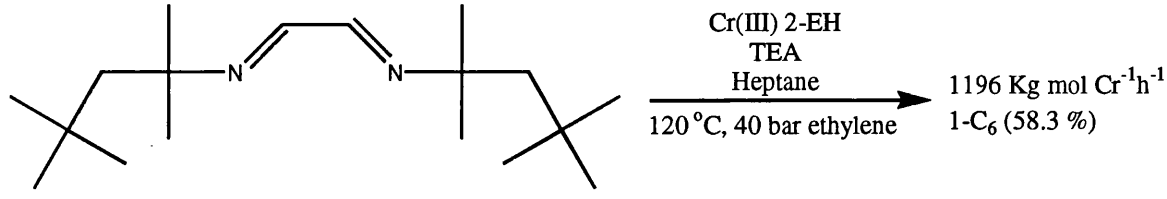

Figure 14: Activity of a diimine chromium complex in selective ethylene trimerisation

Although this system does show selectivity towards 1-hexene formation, the chain growth mechanism is once again competing, and leads to a distribution of products. Also the relatively low selectivity towards 1-hexene in the C_6 fraction causes problems in the industrial application of this system due to the difficulty in separating 1-hexene from the internal isomers.

Amoco Corporation [24] developed an ethylene trimerisation catalyst based on a tridentate phosphine ligand of the general formula $R_2P(CH_2)_mP(R')(CH_2)_nPR_2$ activated by an aluminoxane co-catalyst. Unlike the octahedral triazacyclohexane, triazacyclononane and tris(pyrazolyl)methane chromium complexes in which the named ligands are facially co-ordinating the PPP ligand occupies a meridional arrangement around the octahedral metal centre. The chromium complex of the unsymmetrical ligand, (2-dimethylphosphinoethyl)(3-dimethylphosphinopropyl) phenylphosphine in toluene activated by 214 molar equivalents of butylaluminoxane (BuAO) at 42 bar ethylene pressure and 80 °C afforded 1% C_4, 97.7% C_6 (98.8% 1-C_6, 96.5% 1-C_6 overall), 1% C_{10} and 0.3% PE, *Figure 15.*

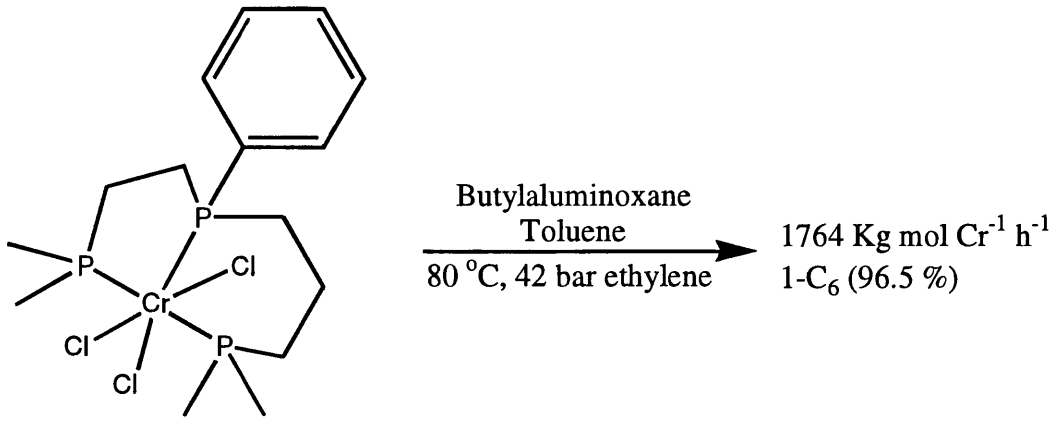

Figure 15: Activity of a PPP chromium complex in selective ethylene trimerisation

For this system it was found that symmetrical ligands gave active complexes with a much-shortened lifetime and catalysts were required to be preformed without a significant loss in activity and also a higher percentage of PE formation. In favour of this system was the exceptionally high selectivity for 1-hexene and low PE formation. This is compromised by the high cost of these PPP ligands that require a difficult synthetic route involving the use of radical chemistry.

Diphosphazane ligands $R_2PN(R)PR_2$ have previously been used with palladium to give active ethylene/CO co-polymerisation catalysts. [25] In conjuction with nickel they give complexes effective in ethylene polymerisation. [26] Wass published [27] an ethene trimerisation catalyst with a $Ar_2PN(Me)PAr_2$ chromium complex, where Ar is an *o*-methyoxy-substituted aryl group, *Figure 16*, and was patented by British Petroleum. [28] When activated by MAO this system is extremely active and selective towards 1-hexene formation.

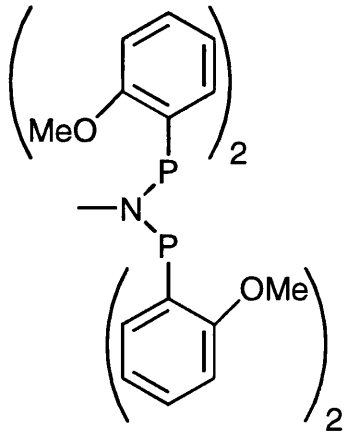

Figure 16: Structure of (2-methoxyphenyl)$_2$PN(Me)P(2-methoxyphenyl)$_2$

Over a one hour period at 80 °C and 20 bar ethylene pressure using 1.1125 mmol $CrCl_3THF_3$ and (2-methoxyphenyl)$_2$PN(Me)P(2-methoxyphenyl)$_2$ in 500ml toluene and activated by 300 equivalents MAO the catalyst produced 90% C_6 (99.9% 1-C_6, 89.9% 1-C_6 overall), 1.8% C_8 and 8.5% C_{10}. No PE was produced and the catalyst

activity was an unprecedented 53726 Kg mol Cr^{-1} h^{-1}. The main by products from this catalysis are decenes that form from the incorporation of one equivalent of 1-hexene cyclising with 2 equivalents of ethylene. This only occurs occasionally and trimerisation of exclusively α-olefins does not proceed. Catalysts with different ligand structure were studied, but for the cases in which there was no o-methoxy group, activities were extremely low. The authors postulated that the *o*-methoxy group is an important pendant donor that can co-ordinate to vacant sites during the catalytic cycle and unlike previously assumed were just a steric influence.

The *o*-ethoxy analogue was also tested and found to be inactive under the reaction conditions. The analogous complexes with carbon bridges between the two phosphorus atoms are also inactive under the same conditions indicating a requirement for the nitrogen bridge.

Sasol technology has recently patented [29] and published [30] a trimerisation catalyst based upon a bis-phosphinoamine ligand $R_2PCH_2CH_2NHCH_2CH_2PR_2$. As with the tridentate phosphine ligand these ligands opt for a meridional co-ordination to the chromium. Variation of the alkyl substituents on the phosphorus atoms was attempted to try and increase activity. Sterically demanding subtituents led to a decreased activity and increased PE production. Sterically undemanding groups led to an increased activity and better selectivity towards 1-hexene formation. Using [bis-(2-diethylphosphino-ethyl)amine]$CrCl_3$ activated by 850 equivalents of MAO at 100 °C and 40 bar ethylene pressure, afforded a reaction mixture containing 94% C6 (99.1% 1-C6, 93.2% 1-C6 overall) and 2.1% PE, *Figure 17.*

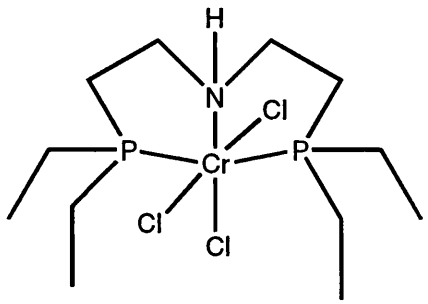

850 equiv. MAO
Toluene
100 °C, 40 bar ethylene

1945 Kg mol Cr^{-1} h^{-1}
1-C_6 (93.2)

Figure 17: Activity of a PNP chromium complex in selective ethylene trimerisation

Variations on this catalyst system can lead to 97% overall 1-hexene selectivity but at the cost of catalyst activity. Catalytic runs at 80 °C revealed that the system was more stable than at 100 °C, whereas extended run times revealed a dramatic deactivation over time.

More recently this system has been adapted for the role of ethylene tetramerisation [31] starting from the $[(R^2)_2P]_2NR^1$ motif a variety of alkyl and aryl substituents have been tested. Catalysts formed in-situ from the ligands $[Ph_2P]_2N^iPr$ and $[(p\text{-}MeOPh)_2P]_2N^iPr$ [32] gave the best results, *Figure 18.*

2 $[Ph_2P]_2N^iPr$ + $Cr(acac)_3$ — 300 MAO, Toluene, 45 °C, 45 bar ethylene pressure →
17% C_6, 70 % 1-C_6, (11.9% 1-C_6 overall)
68% C_8, 99% 1-C_8, (67.3% 1-C_8 overall)
7% C_{10}-C_{14}, 1% PE
14165 Kg mol Cr^{-1} h^{-1}

2 $[(p\text{-}MeOPh)_2P]_2N^iPr$ + $CrCl_3THF_3$ — 300 MAO, Toluene, 45 °C, 45 bar ethylene pressure →
24% C_6, 74 % 1-C_6, (17.8% 1-C_6 overall)
68% C_8, 99% 1-C_8, (67.3% 1-C_8 overall)
4% C_{10}-C_{14}, 3% PE
5860 Kg mol Cr^{-1} h^{-1}

Figure 18: Tetramerisation results with PNP chromium catalysts

Ethylene trimerisation has been proposed to follow the same metallacycle mechanism as trimerisation and hence, the fine-tuning of this system towards a greater selectivity in either trimer or tetramer. As the competing factors between the two processes are the coordination and insertion of the fourth equivalent of ethylene vs. the

β-hydride elimination from the metallacycloheptane addition of steric bulk to the phenyl substituents, especially close to the metal centre, favour trimerisation.

Following from the PNP ligands a natural progression was to exchange the phosphorus atoms for sulphur, as they are also soft donor atoms capable of facile association-dissociation equalibria. Initially substituents on sulphur were evaluated that had a low steric demand as these proved most effective for the PNP complexes. However, the solubility of the complexes became the most influential factor with the decyl substituted ligand giving a much more productive catalyst than the ethyl equivalent. An ethylene trimerisation reaction at 90 °C and 40 bar ethylene pressure using the [bis-(2-decylsulphanyl-ethyl)-amine]$CrCl_3$ complex activated by 280 equivalents of MAO afforded 98.4% C_6 (99.7% 1-C_6, 98.1% 1-C_6 overall), 0.16 % PE, [33] *Figure19.*

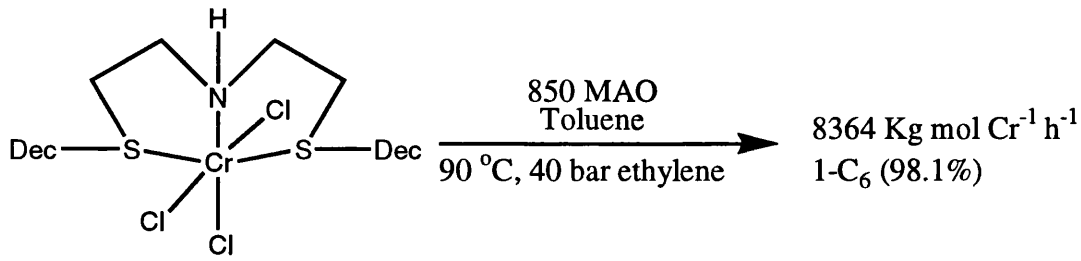

Figure 19: Activity of a SNS chromium complex in selective ethylene trimerisation

It was found that the complexes with a high solubility could be activated by much lower amounts of MAO (30-100 equivalents). Due to the high cost of MAO this proves to be a bonus for the cost efficiency.

1.5: Other Metal Trimerisation Catalysts

There has been a keen interest in trimerisation catalysts based on alternative transition metals, spearheaded by both UCC [34] and Phillips Petroleum, [35] to investigate the effect of new properties in the metal, a hopeful increase in performance and remove environmental concerns with chromium. UCC have tested salts of uranium, cerium, titanium, vanadium and zirconium with only uranium giving comparable yields of 1-hexene to chromium. [34] However there is no detailed experimental data on these results provided by UCC. Phillips Petroleum has published considerably more experimental details and has focused on zirconium, vanadium, titanium and nickel.

Phillips Petroleum [35] investigated a catalyst system comprising of $Zr(acac)_2$, pyrrole and TEA in molar ratios of 1:3:22 at 80 °C and 38 bar ethylene pressure. The reaction carried out in cyclohexane afforded 26.8% liquid products containing 26.9% C_6 (100% 1-C_6, 7.2% 1-C_6 overall) and 73.2% PE at a low activity of 2.7 Kg mol Zr^{-1} h^{-1}. With this being the most productive trimerisation result for zirconium based systems it is clear that they currently have low activity and selectivity towards 1-hexene formation. This catalyst system produces large quantities of PE that from a process point of view is problematic.

A very similar reaction was found to be the most productive in the case of vanadium, with reaction conditions comprising of $V(O)(acac)_2$, pyrrole and TEA in molar ratios 1:3:22 in cyclohexane at 80 °C and 38 bar ethylene pressure. This reaction afforded 56.8% liquid oligomers containing 63% C_6 (79.4% 1-C_6, 45% 1-C_6 overall)

and 43.2% PE with another low activity of 5.9 Kg mol V^{-1} h^{-1}. As with zirconium the activities and selectivities are low combined with the problematic PE production.

Enichem S.P.A. [36] has subsequently patented a vanadium trimerisation catalyst based on the motif $(arene)_2VX$, X = Cl, Br, I, $B(Ar)_4^-$, $AlCl_4^-$, carboxylates and sulphonates. It was demonstrated that this system could be initiated without the need of any co-catalyst. The best results were recorded with the system $V(Mesityl)_2$ and $Cp_2Fe(BPh_4)$ combined in a 1:1 molar ratio with the trimerisation carried out at room temperature and 7 bar ethylene pressure. This reaction afforded 99% 1-hexene at an activity of 30.3 Kg mol V^{-1} h^{-1}. This system shows a remarkable increase in selectivity over the Phillips Petroleum systems tested but is still lacking in the high activities of the chromium systems and those needed to be economically viable in industry.

The use of tantalum as a trimerisation catalyst resulted as the discovery of branches in the polymer formed from the polymerisation of ethylene with $TaCl_5$ activated by an alkylaluminium halide in chlorobenzene. [37] These branches were the result of a dual mechanism occurring with this catalyst system, the ethylene would be oligomerised combined with the co-polymerisation with the oligomers formed. Fine-tuning of this catalyst system with additives and ratios resulted in a greater selectivity towards 1-hexene formation. Best results were obtained with a combination of $TaCl_5$, a trialkylaluminim, and a tetraalkylammonium chloride in chlorobenzene producing 90% liquid product of which 75% was 1-C_6 (67.5% 1-C_6 overall). Following from this discovery Andes [38] found that using $TaCl_5$ with the methylating agent $Zn(CH_3)_2$ in a 1:1 molar ratio in chlorobenzene at 45 °C and 48 bar ethylene pressure gave an overall 1-C_6 selectivity of 96% with a catalyst activity of 38.7 Kg mol Ta^{-1} h^{-1}.

Phillips Petroleum [35] investigated a titanium system comprising $Ti(O)(acac)_2$, pyrrole and TEA at molar ratios of 1:3:22 at 80 °C and 38 bar ethylene pressure. The reaction afforded 71.2 % liquid oligomers of which 55% was C_6 (87.3% 1-C_6, 34.2% 1-C_6 overall) with a catalyst activity of 10.7 Kg mol Ti^{-1} h^{-1}. Titanium was first believed to be a contender as a highly selective ethylene trimerisation catalyst with the development of the Cp^*TiMe_3-$B(C_6F_5)_3$ system by Pellecchia. [39] This system devised for the production of LLDPE was found to produce only butyl branching in the polymer and 1-hexene was detected in high selectivity in the liquid fraction.

In 2001 Hessen [40] reported a titanium system that could be changed from an ethene polymerisation catalyst into an ethene trimerisation catalyst, *Figure 20.*

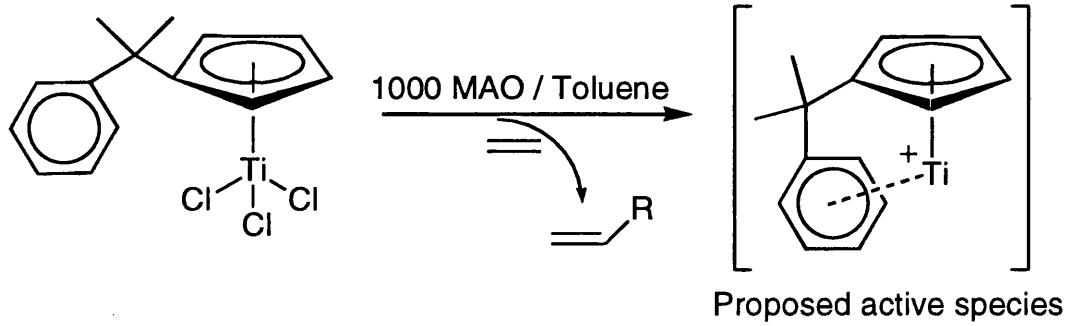

Figure 20: Activation of $[CpCMe_2Ph]TiCl_3$ system

From the observation that the toluene solvent stabilised the active Ti(II) trimerisation catalyst species for the Cp^*TiMe_3-$B(C_6F_5)_3$ system the Cp ligand was developed to include a pendent arene to mimic this solvent stabilisation role. As with the OMe group of the diphosphazane PNP chromium trichloride catalyst system, the phenyl group is thought to act as a labile donor to help stabilise active intermediates by binding in vacant co-ordination sites but always remain in close proximity when not involved in co-ordination. With this addition the activity towards ethene trimerisation

increased dramatically. In one catalytic example ethylene was trimerised using $[CpCMe_2Ph]TiCl_3$ and 1000 equivalents of MAO at 2 bar ethylene pressure and 30 °C, affording a reaction mixture containing 97.4% liquid oligomers comprising 87% C_6 (98% 1-C_6, 83% 1-C_6 overall), 1% 1-C_8, 11% C_{10} and 2.6% PE the catalyst activity was 1073 Kg mol Ti^{-1} h^{-1}. In the development of this system the effect of, the hemi-labile pendant group, aromatic vs. aliphatic solvents, various bridges between the Cp and arene ring, substituents on the arene ring and substituents on the Cp ring were all considered. Combination of all these factors produced the most competitive non-chromium ethylene trimerisation catalyst to date. Although this system is competitive in terms of activity and selectivity with the chromium competitors, one major disadvantage is the large excess of MAO required (1000 equivalents).

Although the majority of ethylene trimerisation catalysts are based upon early transition metal systems it is not inconceivable that late transition metals may form active catalysts. Phillips Petroleum [35] investigated the first of these systems combining $Ni(acac)_2$, pyrrole and TEA in molar ratios of 1:3:22 at 80 °C and 38 bar ethylene pressure to afford a reaction mixture containing 95.4 % liquid oligomers of which 69% was C_6 (65% 1-C_6, 62% 1-C_6 overall) with an activity of 19.0 Kg mol Ni^{-1} h^{-1}.

Mitsui Chemicals [41] have shown that the $NiBr_2(PhN{=}CHC_5H_4N)$ complex activated by 250 equivalents of MAO at 25 °C and 1 bar ethylene pressure affords a liquid product containing 60% trimer, 24% dimer and 16% tetramer with a catalyst activity of 611.6 Kg mol Ni^{-1} h^{-1}.

$(Ph_3P)_2NiBr_2$ has been activated by $MeAlCl_2$ [42] in a molar ratio of 1:300 to form a trimerisation catalyst. At 100 °C and 30 bar ethylene pressure this system afforded a reaction mixture containing 95% trimer at an activity of 6958 Kg mol Ni^{-1} h^{-1}. These trimers contained 47% 3-methyl-2-pentene, 21% 2-ethyl-1-butene and 25% 2-hexene, *Figure 21.*

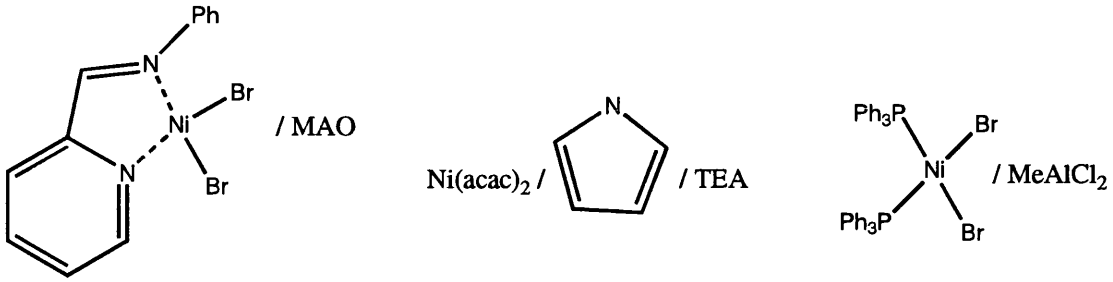

60% hexenes 62% 1-hexene 95% hexenes

Figure 21: Activity of $NiBr_2(PhN{=}CHC_5H_4N)$/MAO, $Ni(acac)_2$/pyrrole/TEA, $(Ph_3P)_2NiBr_2/MeAlCl_2$ sytems in trimerisation of ethylene

1.6: Trimerisation Mechanism

In 2000 Köhn [43] expanded upon a previously proposed mechanism, (See Chapter 5) by Briggs, [44] for the trimerisation of 1-hexene by triazacyclohexane chromium complexes activated by MAO, *Scheme 3.* This mechanism via metallacycles has also been supported by studies carried out by Jolly [14] in which a chromacyclopentane was isolated from a reaction of the appropriate dichloride with active magnesium in the presence of ethene. A chromacycloheptane derivative was also isolated from a reaction of the appropriate dichloride with 1,6-dichloromagnesiohexane. The metallacyclopentane derivative was more stable than the corresponding metallacycloheptane with decomposition temperatures of T_{dec} = 151 °C and 56 °C respectively. The chromacycloheptane decomposes to give 1-hexene, and protonolysis

of the product of the reaction of a chromacyclopentane derivative with ethene leads to the liberation of hexene and butane (1:3), *Figure 22*.

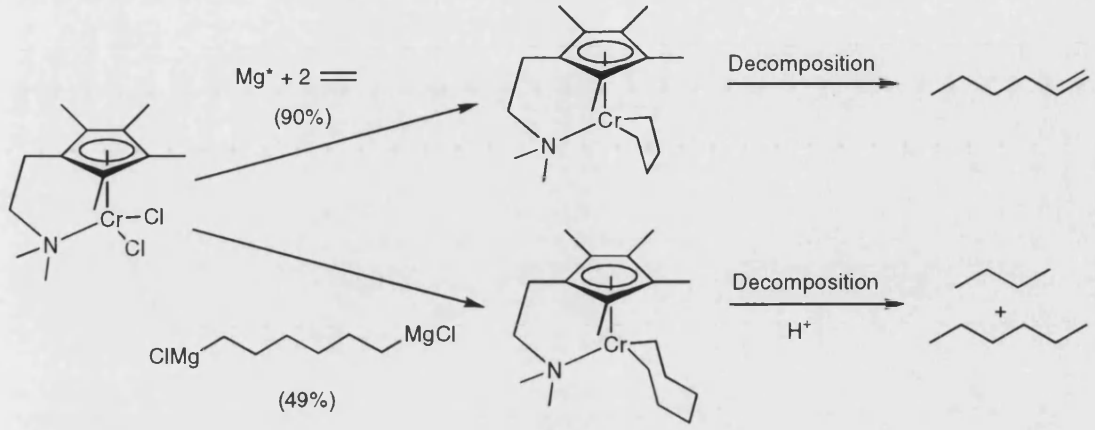

***Figure 22*:** Formation and reaction of chromium metallacyclopentane and metallacycloheptane complexes

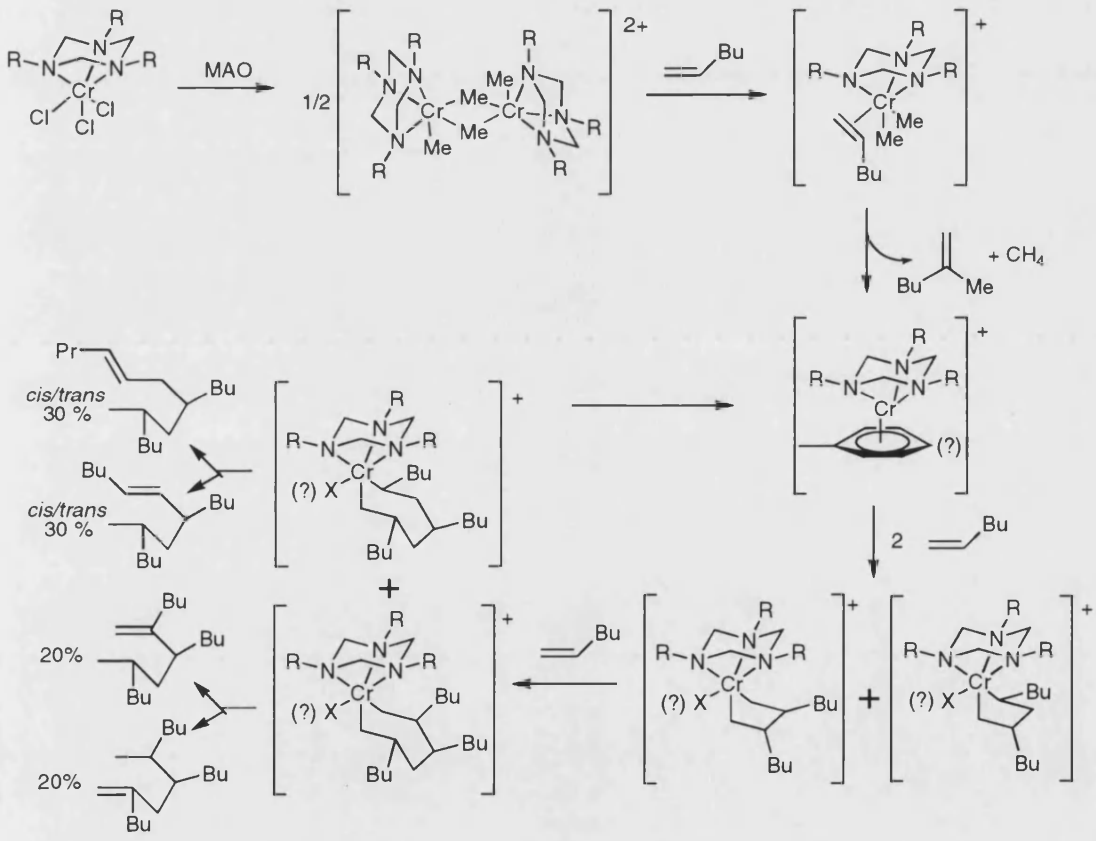

Scheme 3: Proposed mechanism for the MAO activated $R_3TACCrCl_3$ 1-hexene trimerisation

The mechanism consists of the initial chromium trichloride complex being alkylated by the MAO and a methyl/chloride anion is abstracted to give a cationic complex. After insertion of a first olefin, β-hydride transfer with reductive alkane and alkene elimination gives a Cr(I) complex and the formation of methane and 2-methyl-1-hexene. Oxidative addition of two olefins gives the metallacyclopentane steady-state complex. The rate determining insertion of a third olefin molecule into one of the Cr-C bonds of the complex gives a metallacycloheptane which is unstable towards β-hydride and reductive alkane elimination to the Cr(I) complex to start the cycle again.

1.7: Chromium

As mentioned earlier there have been limited studies on the Phillips catalyst type system compared to other transition metal polymerisation catalyst. One major factor in the lack of characterised intermediates for this system is the paramagnetism of chromium. Cr(III) has a d^3 electron configuration. In an octahedral arrangement the three electrons go into separate t_{2g} molecular orbitals, as this configuration is more favourable than pairing any of the electrons. With no electrons needing to be paired the spins of all three electrons align with each other, and hence results paramagnetism, *Figure 23.*

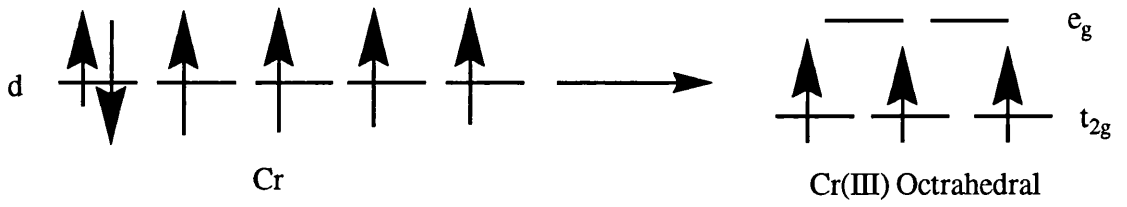

Figure 23: d electrons in chromium and octahedral Cr(III)

In an NMR experiment (See Chapter 3) these three unpaired electrons produce a paramagnetic shift. Unpaired electrons give rise to large dipolar magnetic fields, the gyromagnetic ratio of the electron is 660 times that of the proton, which can result in substantial nuclear shielding/deshielding.

Another feature of the NMR of paramagnetic compounds is a line broadening associated with the distance of the nucleus under study from the paramagnetic centre. The spin-lattice relaxation rate of a pair of interacting nuclei is proportional to r^{-6}.

$$R_2 = \frac{1}{T_2} = \frac{4}{3}\left(\frac{\mu_0}{4\pi}\right)^2 \frac{\gamma_I^2 g_e^2 \mu_B^2 S(S+1)}{r^6} \tau_c$$

Linewidths associated with relaxation are inversely proportional to the relaxation time.

$$1/\pi T_2 = \lambda$$

Therefore $\lambda \propto 1/r^6$

Factors affecting the amount of paramagnetic broadening are temperature, the viscosity of the solution and the size of the molecules.

$$\tau_c^{-1} = \tau_s^{-1} + \tau_r^{-1} + \tau_M^{-1} \qquad \tau_r = \frac{4\pi\eta a^3}{3kT} = \frac{\eta MW}{dN_A kT}$$

The correlation time τ_c is made up of the electronic relaxation correlation time τ_s, the rotational correlation time τ_r and the exchange correlation time τ_M. The rotational correlation time is Temperature T dependant, proportional to the viscosity η, and molecular weight MW.

Due to this relationship between the line broadening and the distance from the chromium centre, measurement of line width can provide valuable structural information of complexes in solution. This information in conjunction with X-ray

crystallographic data of the solid state are valuable tools to understanding intermediates and mechanism.

2: 1,3,5-trialkyl-1,3,5-triazacyclohexanes

2.1: Introduction

Wellington and Tollens, [45] and also Henry, [46] first studied the condensation reaction between formaldehyde and ammonia or primary amines in basic conditions. Their assignments of the products were alkylmethyleneimines ($RNCH_2$). Work by Brocher and Cambier [47] and also Duden and Scharff [48] provided a new interpretation on the products obtained a heterocyclic structure $(RNCH_2)_3$, *Figure 1.* The structure of these 1,3,5-trialkylhexahydro-sym-triazines or 1,3,5-trialkyl-1,3,5-triazacyclohexanes was demonstrated conclusively in a series of papers by Graymore. [49] In these papers Parachor determinations were calculated and show that the molecule has a cyclic structure with no significant equilibrium with its alkylmethyleneimine.

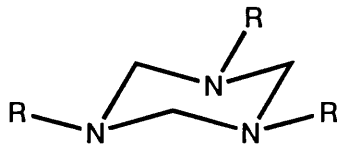

Figure 1: Structure of 1,3,5-trialkyl-1,3,5-triazacyclohexane

With a vast selection of primary amines commercially available or easily synthesised a large array of triazacyclohexanes is readily produced from a variety of procedures: -

1. Direct combination of primary amine and an aqueous solution of formaldehyde [49c]
2. Addition of aqueous formaldehyde to a primary amine in alcohol solution [50]
3. Addition of paraformaldehyde to a primary amine in aromatic solvent with [51] or without additional base [52]

The triazacyclohexanes are stable in basic or neutral conditions but on addition of acid they readily decompose. In acidic conditions the cyclic structure of the triazacyclohexane is in equilibrium with its alkylmethyleneimine that can react with water to give the corresponding primary amine and formaldehyde, [49b] *Scheme 1.*

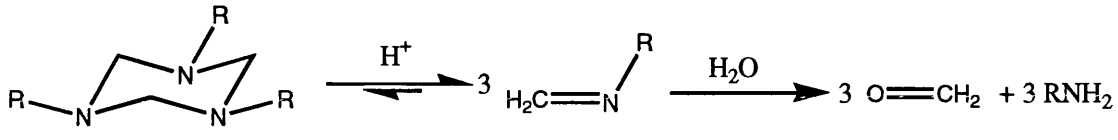

Scheme 1: Decomposition of R_3TAC in acidic conditions

With the addition of zinc to the acidic conditions, hydrogen is liberated, which can also react with the alkylmethyleneimine to produce an alkylmetylamine, [49c] *Scheme 2.*

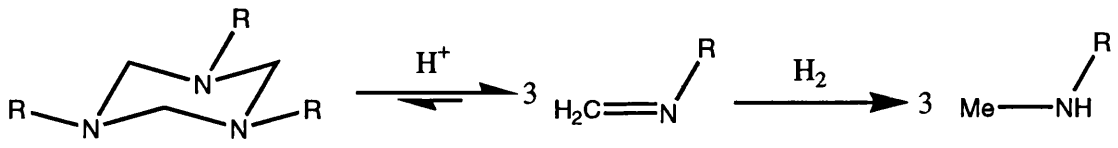

Scheme 2: Decomposition of R_3TAC in acidic conditions with the addition of zinc

Conformationally triazacyclohexanes could be thought of as being similar to cyclohexanes. Both can adopt boat, twist, and most common chair conformations, *Scheme 3.* In the case of cyclohexane the chair conformation is the most stable as it is free of angular and torsional strain. The chair is 5.5 kcal/mol more stable than the twist conformation [53] that in turn is 0.9 kcal/mol more stable than the boat. The boat conformation is also free of angular strain but has considerable torsional strain added to destabilised by van der Waals repulsions between the flagpole hydrogen atoms. The twist conformation has reduced torsional strain but in doing so acquires angular strain. Due to the destabilising forces in the boat and twist, chair conformations constitute over 99.9% of the mixture of isomers in cyclohexanes and also triazacyclohexanes. [54]

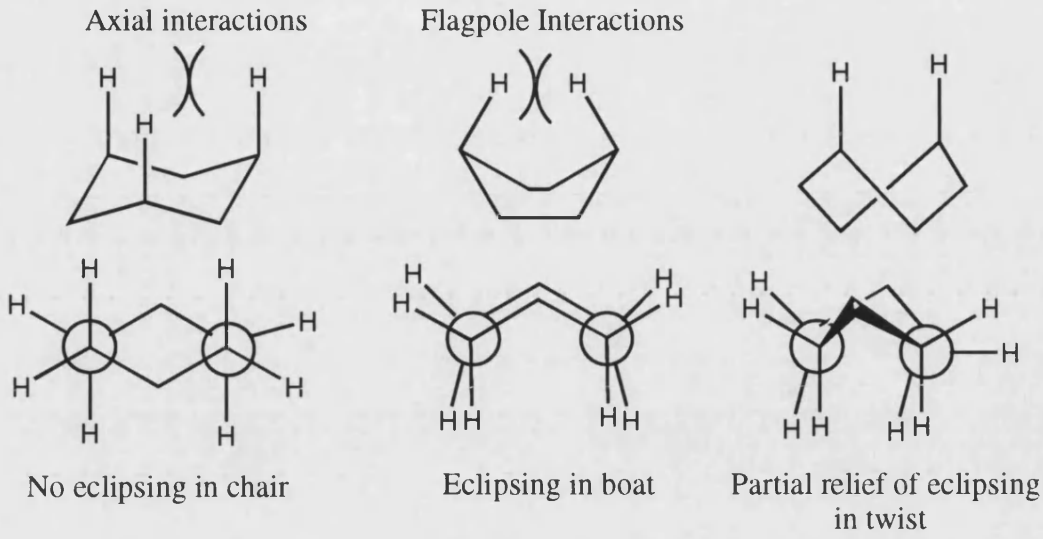

Scheme 3: Conformations of cyclohexanes

In a chair conformation the governing forces are the axial interactions, in the case of substituted cyclohexanes these will be substituent - substituent, substituent – proton, or proton - proton interactions. For triazacyclohexanes these interactions are now between lone pairs instead of protons *Scheme 4*. This change has a dramatic effect upon the preferences of preferred geometry between the cyclohexanes and triazacyclohexanes. [54]

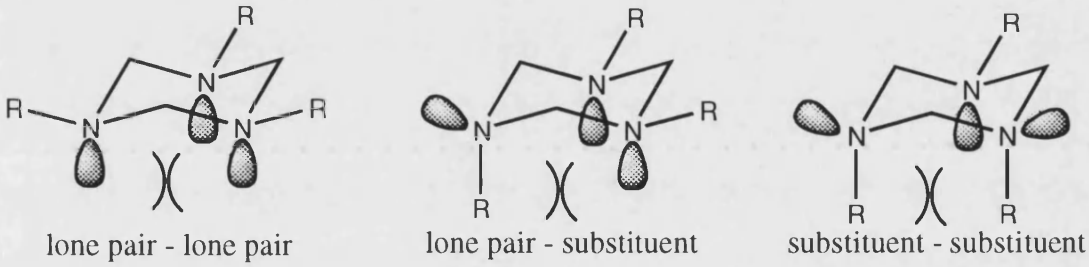

Scheme 4: Interactions between axial substituents and lone pairs in R_3TAC

Triazacyclohexanes and cyclohexanes can undergo ring inversions from one chair form to another, this process put groups that were in an equatorial position to being axial. The nitrogen atoms in triazacyclohexanes can also undergo nitrogen inversion; this process, that is much more readily occurring, has the effect of switching just one substituent from equatorial to axial or vice versa. These two conformational

changes mean that any cyclohexane or triazacyclohexane can be in equilibrium between different conformations with the balance being pushed in favour of its preferred geometry, *Scheme 5.*

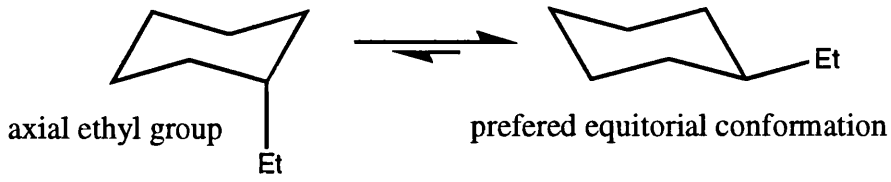

Scheme 5: Equilibrium between conformations of substituted cyclohexanes

With this in mind consider the two molecules methylcyclohexane and 1,3,5-trimethyl-1,3,5-triazacyclohexane. Both molecules would be expected to place the methyl groups in equatorial positions, as they are greater in size than either a proton or lone pair, and so reduce to axial interactions. This is in fact the outcome for methylcyclohexane with the axial methyl conformation being 1.7 kcal/mol higher in energy than the equatorial arrangement. [55]

Dipole moment studies on the triazacyclohexane system suggested equilibrium between a one axial methyl group and two axial methyl groups' conformations. [56] A ^{1}H dynamic NMR study on the same system showed an almost exclusive preference for the one axial methyl conformation. [57] This result was later supported by a ^{13}C dynamic NMR study that reported the same outcome. [58] It must be noted that these two studies were run at low observation frequencies with a low signal to noise ratio. This may mean that any signals due to minor conformations may not have been detected.

These results show that there are some surprising differences in preferred conformations between the two systems. These variances in conformation have been attributed to reduced steric repulsions between the axial methyl group and the axial

nitrogen lone pairs as opposed to lone pair – lone pair repulsions. [54] In addition there is a preferential orientation of bond dipoles, i.e., the anomeric effect. [59] In the one axial methyl group conformation the equatorial nitrogen lone pair is vicinal and anti to two electronegative nitrogen atoms. This orientation enhances n-σ* orbital overlap, postulated to be an important stabilisation associated with the anomeric effect. There would also be an increase in dipole – dipole interactions.

Systems in which there is an increase in the steric bulk of the substituents on the triazacyclohexane have also been studied. For 1,3,5-triethyl-,1,3,5-tri-isopropyl, and 1,3,5-tri-tertbutyl-1,3,5-triazacyclohexane the dipole moments measured all predict the one axial alkyl group conformation as being the most stable. [56] Early ^{13}C dynamic NMR spectra on the ethyl and isopropyl cases supported these findings. [58] A more recent study into the conformations of these three systems, and 1,3,5-trimethyl-1,3,5-triazacyclohexane, by ^{1}H and ^{13}C dynamic NMR, in different solvents, reveals some surprising results. [60] The ^{1}H NMR spectrum of 1,3,5-trimethyl-1,3,5-triazacyclohexane in dichlorodifluoromethane, (CF_2Cl_2) a solvent that does not hydrogen bond to nitrogen, shows a single resonance due to the methyl groups and a broadened singlet due to the methylene protons at 340 K. On cooling the methylene signal decoalesces due to slowing chair – chair interconversions. At 210 K these signals sharpen into an AX spectrum with a doublet representing the axial protons and a second doublet for the equatorial protons. At temperatures below 210 K there is a more complex decoalescence due to the slowing inversion of the nitrogen atoms. At 126 K the signals sharpen into a slow exchange spectrum with the methylene protons shown as an AX spectrum for two protons and a CM spectrum for the other four. The methyl groups show two singlet

resonances one for each axial and equatorial. The spectrum at 126 K shows only the three equivalent monoaxial conformations, [57] *Scheme 6.*

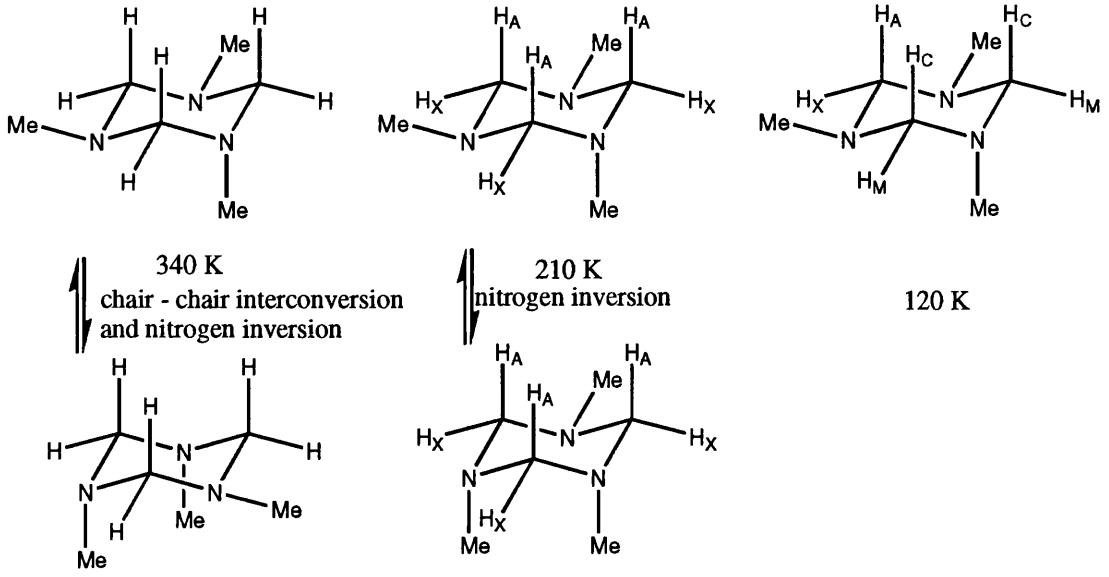

Scheme 6: Assignment of ring protons in Me_3TAC at changing temperature

The same type of decoalescence spectra are found, in solvents that do not hydrogen bond to nitrogen (CF_2Cl_2, CH_2=$CHCH_3$, CH_2=CHCl), for 1,3,5-triethyl-, 1,3,5-tri-isopropyl, and 1,3,5-tri-tertbutyl-1,3,5-triazacyclohexane. In comparison with alkyl cyclohexanes in which isopropylcyclohexane and tertbutylcyclohexane preferentially adopt the equatorial conformation by 2.2 kcal/mol and 4.9 kcal/mol respectively, it is surprising to find a preferred axial conformation.

The same dynamic NMR studies performed in dichlorofluoromethane, ($CHFCl_2$) a solvent that does hydrogen bond to nitrogen, [61] the 1,3,5-trimethyl-, 1,3,5-triethyl-, and 1,3,5-tri-isopropyl-1,3,5-triazacyclohexanes all show a strong preference, over 98 %, for the monoaxial conformation. However the 1,3,5-tri-tertbutyl-1,3,5-triazacyclohexane unanimously chose the triequatorial conformation. This is due to destabilisation in the monoaxial conformation by a sterically hindered axial *t*-butyl with the axial lone pairs, *Figure 2.*

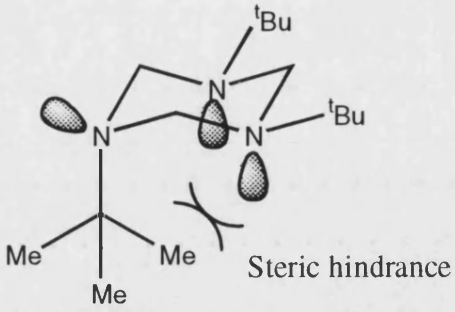

Figure 2: Steric hindrance in eea conformation of $^{t}Bu_3TAC$

Conformations of triazacyclohexanes have also been studied by x-ray crystallography. Three systems in which this method has been employed are the 1,3,5-tricyclohexyl-, [62] 1,3,5- tribenzyl-, [63] *Figure 3* and the 1,3,5-tri-*p*-tolylmethyl-1,3,5-triazacyclohexane. [64] The tricyclohexyl system resides in the mono axial conformation, which given the previous results would be the proposed structure, due to the close resemblance in structure to isopropyl substituents. However the same is not true for the tribenzyl and tri-*p*-tolylmethyl cases. The tri-*p*-tolylmethyl compound adopts a mono equatorial conformation in the solid state, as does the tribenzyl compound below *ca* 250 K. At higher temperatures, in the latter case, there is a disordered mixture between the mono axial and mono equatorial.

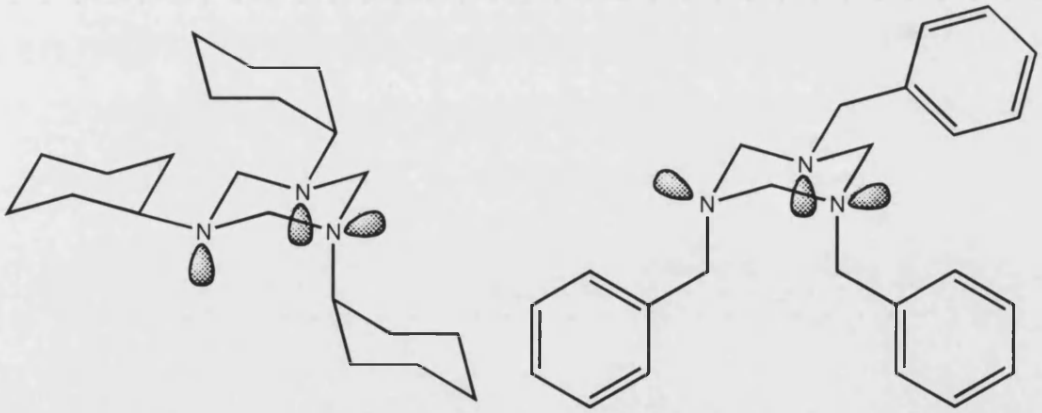

Figure 3: Preferred conformations of $(cyclohexyl)_3TAC$ and $(benzyl)_3TAC$

At temperatures above 250 K nitrogen inversion is occurring in the solid state and so more of the equatorial conformation is populated.

Another class of triazacyclohexanes whose conformations have been almost exclusively studied by x-ray crystallography are the 1,3,5-triaryl-1,3,5-triazacyclohexanes. These are prepared in the same manner but starting from aniline instead of the amine. This class of compounds have been known for some time and were first synthesised by Wellington and Tollens. [45] X-ray analysis of the unsubstituted triphenyl system shows a preference for the mono equatorial conformation. The phenyl rings are aligned perpendicular to the symmetry plane of the triazacyclohexane ring that maximises the overlap between the phenyl π-orbitals and the nitrogen lone pair, [65] *Figure 4.*

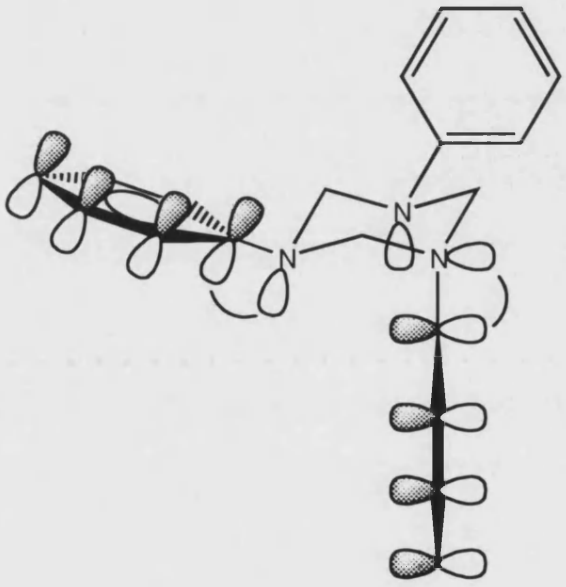

Figure 4: Overlap between phenyl substituents and nitrogen lone pairs

The down side to this preferred orientation of the phenyl rings is unfavourable steric repulsions between the *ortho-* hydrogens on the equatorial phenyl rings and the neighbouring methylene protons in the triazacyclohexane ring. In the case of cyclohexylbenzene it is this steric factor that makes the perpendicular phenyl orientation

3.9 kcal/mol higher in energy than the parallel phenyl. [66] There is also some steric hindrance due to the *ortho-* protons on the axial phenyl groups and axial lone pairs on the triazacyclohexane ring but these interactions are much less influential than those for the equatorial case.

These two factors can be seen more clearly with the conformational study of the *ortho-*, *meta-*, and *para*-fluorophenyl compounds [52] and the *ortho-* and *para*-chlorophenyl compounds. [67] 1,3,5-Tri-*para*-fluorophenyl-1,3,5-triazacyclohexane and its chloro counterpart preferentially adopt the mono equatorial conformation. The halophenyl group in the equatorial position lies perpendicular to the triazacyclohexane symmetry plane being 90 °. This orientation gives the maximum π-orbital and nitrogen lone pair overlap. The *meta*-fluorophenyl compound, which has slightly more steric bulk due to fluorine being larger than hydrogen, skews the phenyl ring by 54.1° to the symmetry plane. This orientation incorporates a significant degree of π-orbital and nitrogen lone pair overlap, whilst reducing steric interactions with methylene protons in the triazacyclohexane ring. The *ortho*-fluorophenyl compound, which has a larger steric bulk still, is orientated at 22.5 ° to the symmetry plane. To an even more exaggerated degree the *ortho*-chlorophenyl compound, which has the largest steric bulk of the five compounds, is orientated parallel or 0 ° to the symmetry plane and so has no π-orbital and nitrogen lone pair overlap.

A less pronounced effect is seen in the case of the axial phenyl groups with a change in orientation of 61-68 ° in the *para-* and *meta-* substituted phenyls to 44-46 ° in the *ortho*-halophenyls.

In all the triphenyl compounds the nitrogen atoms are distinctly pyramidal in character with the N – C(aryl) bonds of the fluorophenyl series inclined at 32.6 – 48.5 ° to the corresponding H_2C – N – CH_2 plane, *Figure 5*. In comparison to the out of plane angle in the tetrahedral arrangement of 54.7 ° the N – C(aryl) bonds are clearly fanned out from their positions in the ideal chair conformation to alleviate the repulsion between the axial aryl groups.

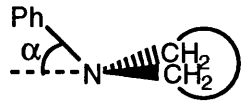

Figure 5: Angle between H_2C – N – CH_2 plane and phenyl substituent

Changing the halogen substituent for a methoxy group also reproduces the same results. [51] With the methoxy group in the *ortho-* position the aryl ring is much closer to the parallel orientation to the triazacyclohexane symmetry plane than the *para-* substituted with 32.8 – 40 ° and 62.4 – 63.6 ° respectively. The N – C(aryl) bonds are inclined at 30.8 – 44.9 ° to their respective H_2C – N – CH_2 planes.

2.2: Results and Discussion

2.2.1: Triazacyclohexanes

The condensation reaction between a primary amine and paraformaldehyde in a 1 : 1 ratio in toluene has been used to selectively produce a multitude of 1,3,5-trialkyl-1,3,5-triazacyclohexanes, [68] *Figure 6*. Among the possibilities are straight chained substituents, 1,3,5-tridodecyl-1,3,5-triazacyclohexane, **1** and 1,3,5-triallyl-1,3,5-triazacyclohexane, **3** branched substituents, 1,3,5-tri-(2-ethylbutyl)-1,3,5-triazacyclohexane, **4** and 1,3,5-tri-(2-ethylhexyl)-1,3,5-triazacyclohexane, **5** aromatic

substituents, 1,3,5-tri-*para*-fluorobenzyl-1,3,5-triazacyclohexane, **6** and 1,3,5-(2-thiophenemethyl)-1,3,5-triazacyclohexane, **7** and deuterated triazacyclohexanes 1,3,5-tridodecyl-1,3,5-$d_6$triazacyclohexane. **2**

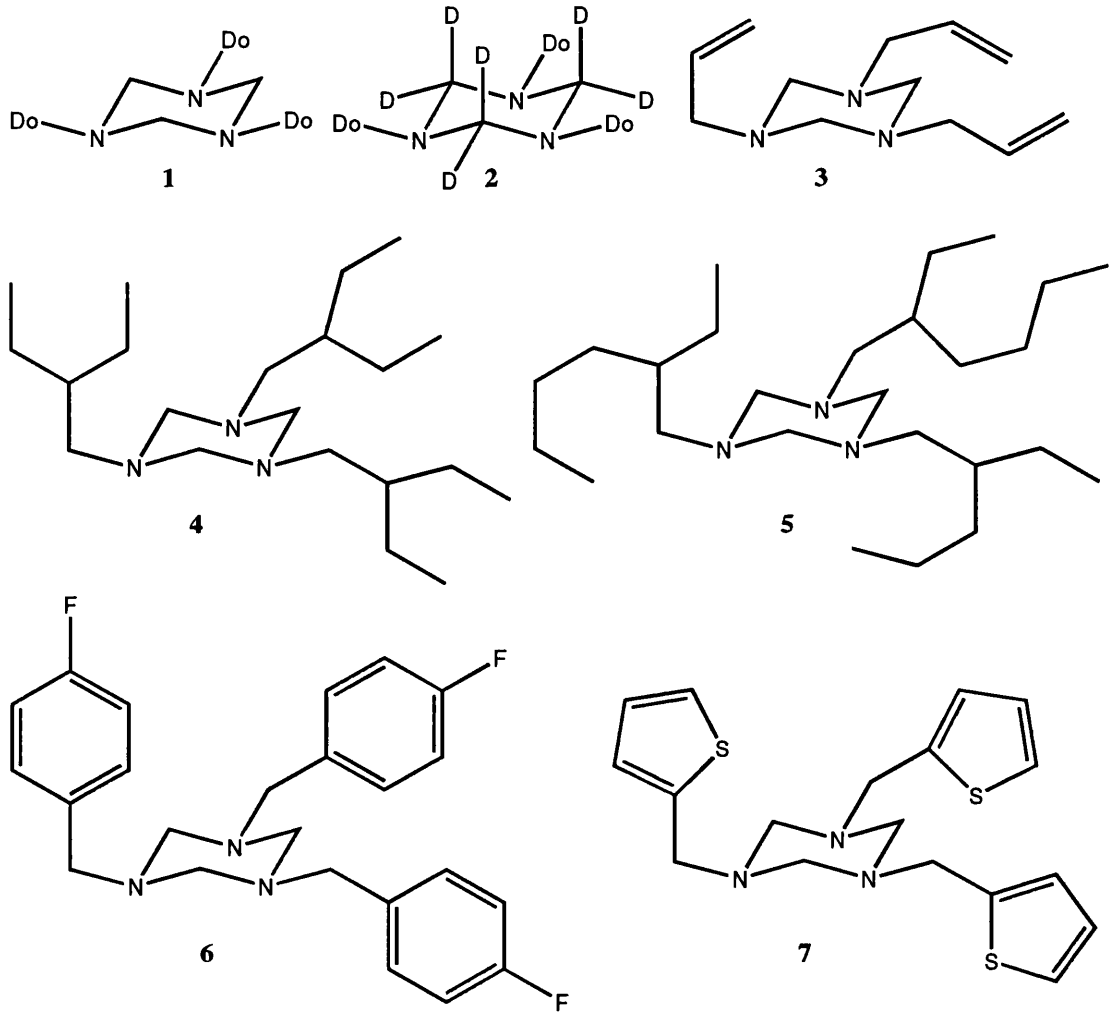

Figure 6: Synthesised 1,3,5-trialkyl-1,3,5-triazacyclohexanes

The ^{1}H NMR spectra of all these triazacyclohexane compounds show a characteristic broadened singlet at δ = 3.2 – 3.5 representative of the six methylene protons, except compound **2** which shows a similar peak in ^{2}H NMR due to the six methylene deuteriums. As the triazacyclohexane is undergoing chair – chair interconversions on the NMR time scale an average of the axial and equatorial environments is observed and so the signal appears slightly broadened. All other signals appear sharp and as expected.

The compound 1,3,5-(propyl-tri-ethoxysilane)-1,3,5-triazacyclohexane **8**, *Figure 7*, was synthesised in a similar fashion as the previous triazacyclohexane compounds except using the oxygen free equivalent of formaldehyde, N,N,N,N-tetramethylmetylenediamine, as to avoid water production and hence substitution of ethoxy for hydroxy groups on the silicon. This proceeds in toluene which after reaction is removed under reduced pressure along with the N,N-dimethylamine produced.

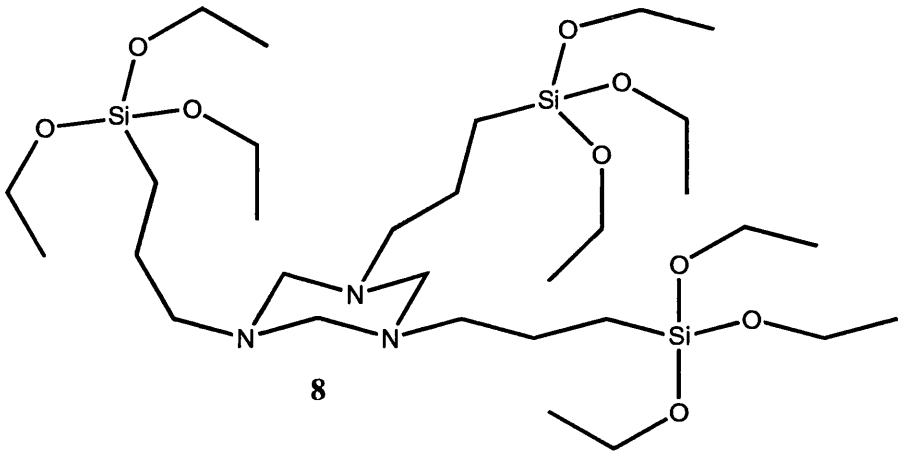

8

Figure 7: 1,3,5-(propyl-tri-ethoxysilane)-1,3,5-triazacyclohexane

1,3,5-Tris-(o-methoxyphenyl)-1,3,5-triazacyclohexane **9** has previously been synthesised [51] by the 1 : 1 reaction between 2-anisidine and paraformaldehyde in xylene solution containing sodium hydroxide. The 1 : 1 reaction performed in toluene solution with no additional base yielded N,N'-bis-(2-methoxy-phenyl)-methanediamine **10**, *Figure 8*, as the major product with no triazacyclohexane evident. The same compound **10** is the only product from the 2 : 1 reaction under the same conditions. On cooling a solution of compound **10** in petroleum ether at 4 °C overnight colourless crystals formed which were characterised by X-ray analysis.

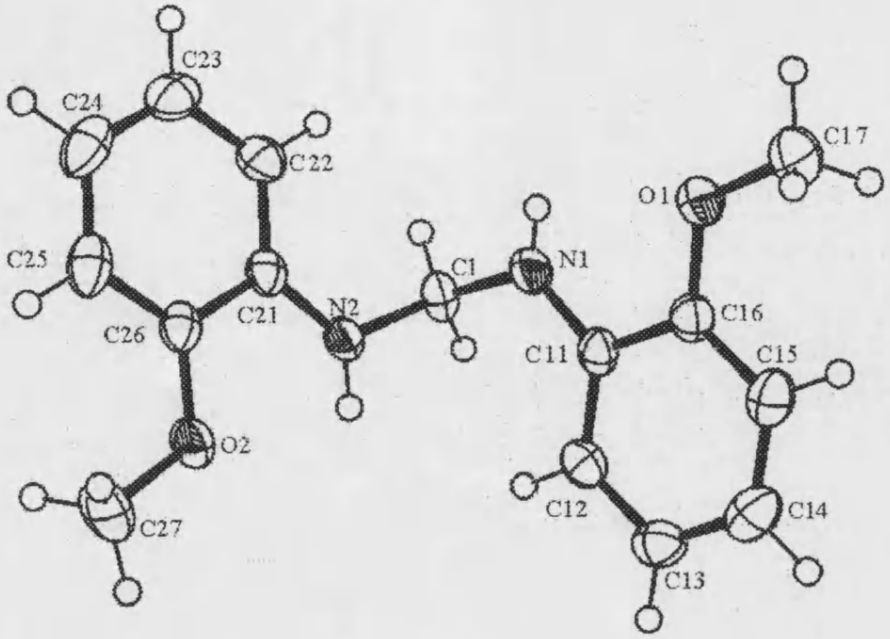

Figure 8: Compound **10** viewed down the C_2 axis

The N – CH_2 bond lengths are 1.4480 (16) and 1.4415 (17) Å similar to them seen in the triazacyclohexane 1.445 (2) – 1.481 (2) Å. However the N – C(aryl) bonds 1.3852 (19) and 1.3886 (18) Å are significantly shorter in **10** than the cyclic compound 1.422 (2) - 1.429 (2) Å, in addition the N – CH_2 – N angle 117.14 (11) ° in **10** is appreciably wider than the internal ring angles 112.3 – 113.5 °. These angles provide verification that compound **10** has less strain than the triazacyclohexane and bond lengths imply a reduction in steric hindrance of the aryl groups as they are able to adopt a position in which a stronger bond to the nitrogen is formed and no unfavourable interactions with methylene protons endured.

The reaction, in either toluene or ethanol solution, between 2-anisidine and n-dodecylamine in a 1 : 2 ratio with 2.5 equivalents of paraformaldehyde, *Scheme 7*, results in Do_3TAC and **10** as the only two products with no signs of a mixed triazacyclohexane.

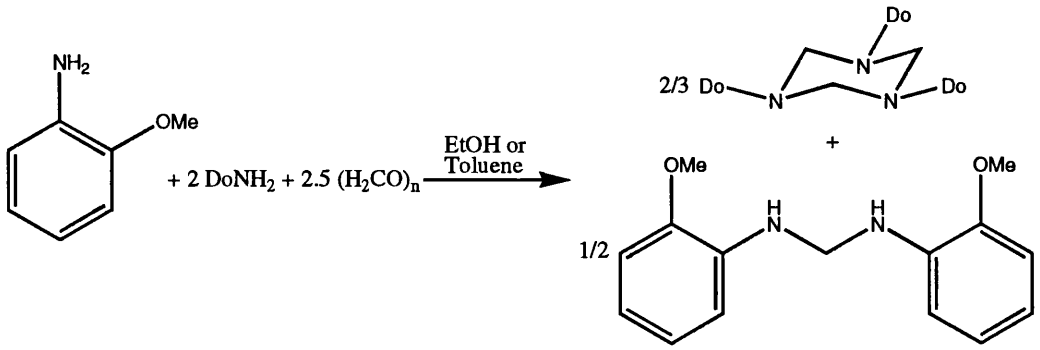

Scheme 7: Equation for the simultaneousformation of Do_3TAC and compound **10**

Due to the weaker nucleophilicity of 2-anisidine compared with n-dodecylamine the formation of Do_3TAC proceeds much quicker than reactions involving the anisidine. Once again the anisidine stops reacting after the formation of **10**. Hence, the need for the stronger base to promote the dehydration of the more sterically hindered anisidine to form the triazacyclohexane.

2.2.2 Mixed Triazacyclohexanes

The condensation reaction between two different primary amines or anilines and paraformaldehyde can be conducted in toluene solution stirring overnight followed by azeotropic distillation of the toluene with the water produced in the reaction. *Scheme 8*

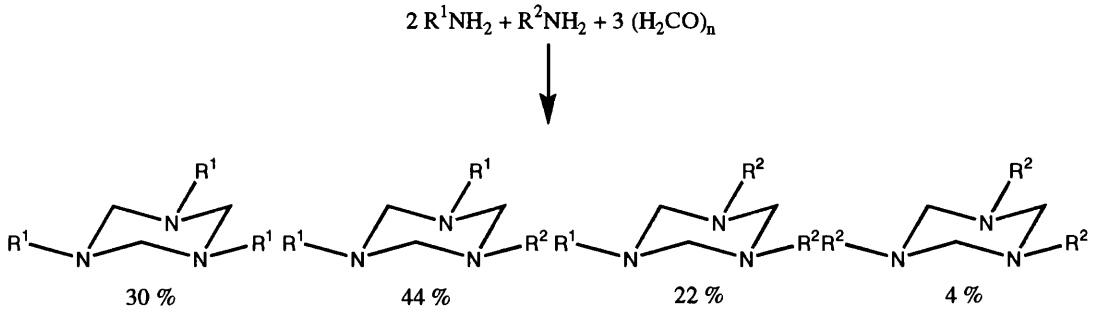

Scheme 8: Statistical mixture of triazacyclohexanes from the reaction of a 2:1 mixture of two amines with paraformaldehyde

When a ratio of 1 : 2 of the two primary amines is used a statistical mixture of four different products are expected, the symmetrical $R^1{}_3TAC$ 30 % and $R^2{}_3TAC$ 4 %, and the unsymmetrical $R^1{}_2R^2TAC$ 44 % and $R^1R^2{}_2TAC$ 22 %. The actual ratio is dependent upon the reactivity of the two amines. This reactivity includes both the donor strength of the nitrogen lone pair to an electrophile, such as formaldehyde, and any steric effects imparted by the size and shape of the alkyl group attached to that nitrogen. As stated earlier anilines react at a reduced rate compared with aliphatic amines and therefore in this mixed reaction, between an aniline and a primary amine, an unstatistical mixture of the four products is formed.

A number of reactions have been carried out with the following results. *Table 1* The chemical shifts from ^1H NMR are given for the methylene protons of the two unsymmetrical products, *Figure 9*, The symmetrical triaryl compound was not formed in any significant, i.e. not observable by ^1H NMR, amount in any of the reactions. For comparison the methylene protons for 1,3,5-tridodecyl-1,3,5-triazacyclohexane and 1,3,5-tri-2-ethylbutyl-1,3,5-triazacyclohexane appear as singlets at δ = 3.300 and 3.194 ppm.

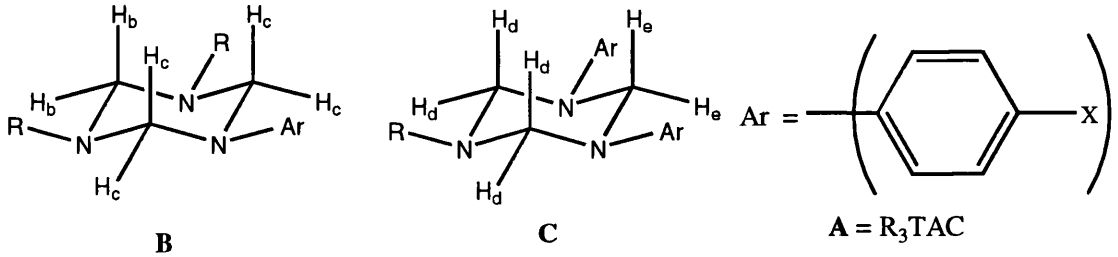

Figure 9: Assignment of ring protons in mixed triazacyclohexanes

	R_3TAC Ha	Hb Hc	Hd He	Ar_3TAC	A : B : C %
R = Do, X = H	3.48	3.64			14 : 60 : 26
		4.15	4.38		
			4.72	4.94 [68]	
R = Do, X = F	3.48	3.51			21 : 63 : 16
		4.04	4.20		
			4.67	4.76 [52]	
R = Do, X = Cl	3.48	3.52			28 : 64 : 8
		4.08	4.25		
			4.71	4.78 [67]	
R = Do, X = Br	3.48	3.52			21 : 63 : 16
		4.08	4.25		
			4.74		
R = Do, X = CF_3	3.48	3.56			6 : 84 : 10
		4.20	4.40		
			4.92		
R = Do, Ar = C_6F_5	3.48	3.62			8 : 79 : 13
		4.08	4.40		
			4.69		
R= EtBu, X = H	3.22	3.42			24 : 53 : 23
		4.03	4.22		
			4.70	4.94	
R= EtBu, X = F	3.22	3.51			25 : 50 : 25
		4.07	4.20		
			4.68	4.76	
R= EtBu, X = Cl	3.22	3.43			23 : 60 : 17
		4.02	4.16		
			4.65	4.78	
R= EtBu, X = Br	3.22	3.41			16 : 65 : 19
		4.01	4.15		
			4.64		
R= EtBu, X = CF_3	3.22	3.55			4 : 68 : 28
		4.21	4.39		
			4.93		
R= EtBu, Ar = C_6F_5	3.22	3.58			26 : 68 : 6
		4.07	4.32		
			4.68		

Table 1: Chemical shifts of ring protons and composition of reaction mixture on formation of mixed triazacyclohexanes

The ^1H NMR spectra, *Figure 10*, of each of the unsymmetrical triazacyclohexane compounds consist of two singlets in the ratio of 1 : 2, at 298 K, for

the methylene protons. There are two distinct methylene environments on an unsymmetical triazacyclohexane, one between two nitrogen atoms with the same substituants, and one between two differently substituted nitrogen atoms. The latter of these two cases occurs twice in the molecule; hence the signal due to these protons is twofold the size of the signal for the other methylene protons. At room temperature both nitrogen inversion and chair – chair interconversions occur rapidly, therefore on the NMR time scale methylene protons are interconverting between axial and equatorial positions and so are seen as an average of the two environments.

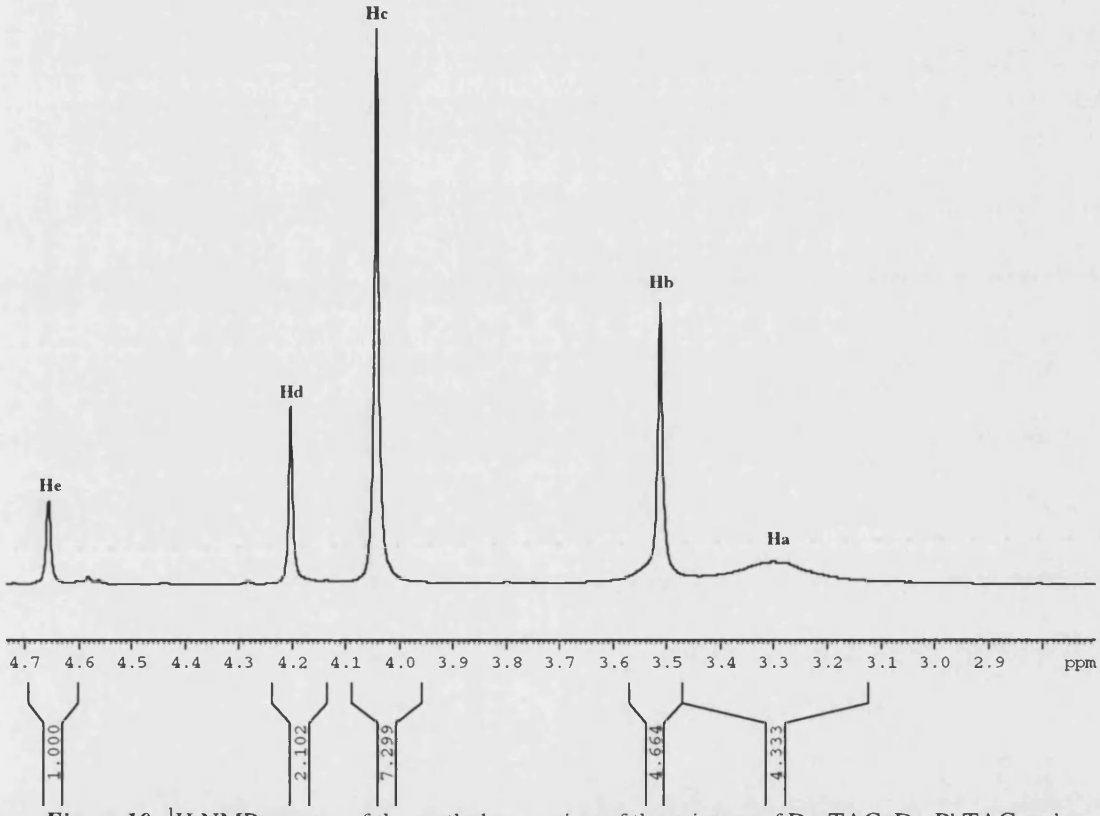

Figure 10: ^{1}H NMR spectra of the methylene region of the mixture of Do_3TAC, Do_2PhTAC and Ph_2DoTAC

The chemical shift of the methylene protons is dictated by the substituents on the nitrogen atoms adjacent to it in the triazacyclohexane ring. A methylene group between two N(aryl) groups gives a proton chemical shift higher than that seen for methylene protons between a N(aryl) and a N(alkyl), in turn these are higher than between two

N(alkyl) groups. This ordering of chemical shifts can be more refined by including the electronegativity of the substituent on the aryl groups. As the aryl groups have the effect of drawing the electron density away from the nitrogen nucleus, and hence reducing the shielding created by that atom on the metylene protons, which is increased by additional electron withdrawing groups in the *para-* position. This deshielding effect increases in the order F > Cl > Br > H.

1-(2-Ethylbutyl)-3,5-bis-*p*-fluorophenyl-1,3,5-triazacyclohexane **11** was studied by x-ray crystal analysis, *Figure 11*, and was found to adopt a mono equatorial conformation with the two fluorophenyl substituents in axial positions and the 2-ethylbutyl group occupying an equatorial arrangement. This orientation is comparable to the tri-*p*-fluorophenyl compound with one of the aryl groups replaced by a 2-ethylbutyl group.

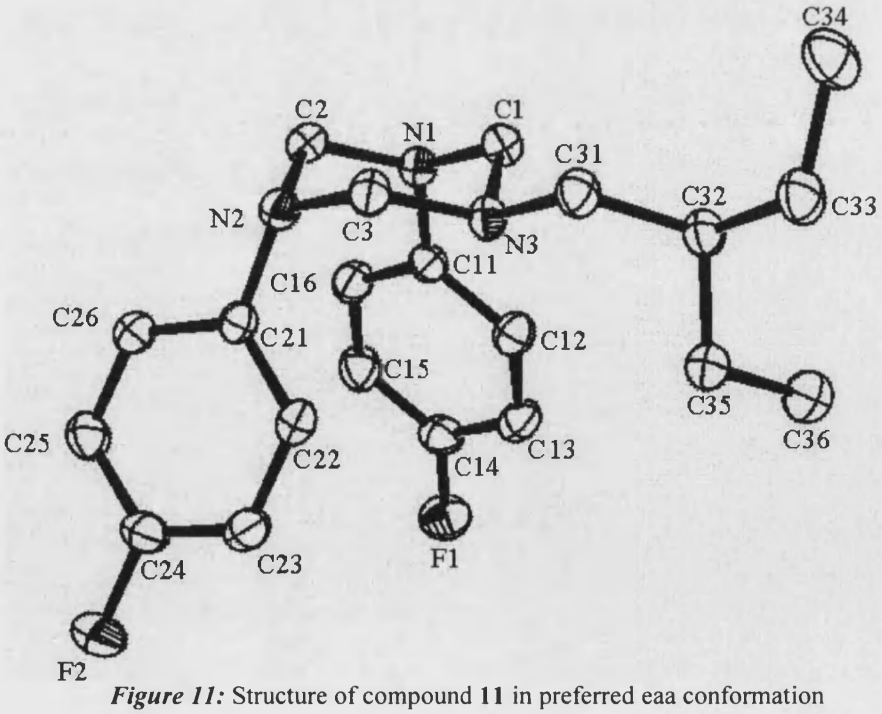

Figure 11: Structure of compound **11** in preferred eaa conformation

In the triazacyclohexane ring the H_2C – N bond lengths are 1.4525 (19) – 1.4731 (18), mean 1.463 Å similar to those in the tri-*p*-fluorophenyl compound which are 1.443 – 1.479, mean 1.460 Å. The H_2C – N – CH_2 angles are 107.92 (12) – 110.19 (12); mean 108.9 ° and the N –CH_2 – N angles are 111.91 (12) – 113.27 (12), mean 112.59 °. The C(aryl) – N bond lengths are 1.4249 (19) and 1.4259 (19) Å and the C(aliphatic) – N bond length is 1.4746 (19) Å. The shorter bond lengths for the C(aryl) – N bonds are consistent with a nitrogen bonding to an sp^2 hybridised carbon as opposed to an sp^3 carbon atom in the C(aliphatic) – N bond. A bond to an sp^2 carbon atom will have more s character than to an sp^3 hybridised carbon atom. The electrons are therefore held closer to the nucleus and so forms stronger and shorter bonds.

1-(2-Ethylbutyl)-3,5-bis-*p*-chlorophenyl-1,3,5-triazacyclohexane **12** was studied by x-ray crystal analysis, *Figure 12*.

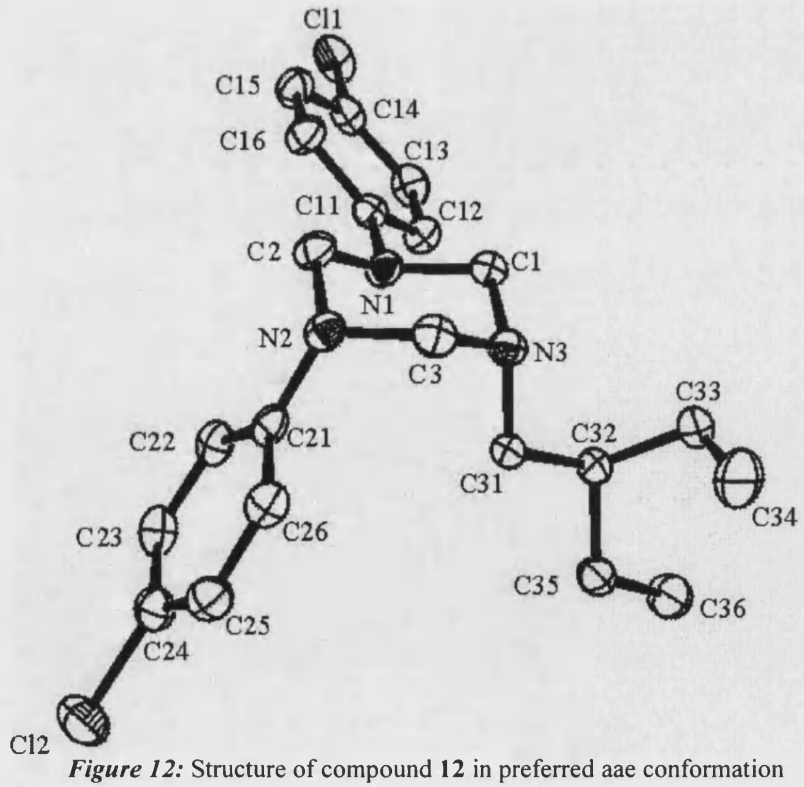

Figure 12: Structure of compound **12** in preferred aae conformation

Triazacyclohexane **12** was found to adopt a mono axial conformation with one of the chlorophenyl substituents being axial, the other one and the 2-ethylbutyl group preferring an axial arrangement. This orientation is comparable to the tricyclohexyl compound or most other trialiphatic triazacyclohexanes.

In the triazacyclohexane ring the H_2C – N bond lengths are 1.444 (2) – 1.488 (2), mean 1.462 Å similar to those in the tri-*p*-chlorophenyl compound which are 1.440 (6) – 1.478 (7), mean 1.457 Å. The H_2C – N – CH_2 angles are 108.29 (13) – 109.86 (13); mean 109.15 ° and the N –CH_2 – N angles are 110.25 (13) – 114.02 (14), mean 112.18 °. The C(aryl) – N bond lengths are 1.416 (2) and 1.412 (2) Å and the C(aliphatic) – N bond length is 1.471 (2) Å.

1-(2-Ethylbutyl)-3,5-*bis*-*p*-bromophenyl-1,3,5-triazacyclohexane **13** was studied by x-ray crystal analysis, *Figure 13*, and was also found to adopt a mono axial conformation, analogous to the 1-(2-Ethylbutyl)-3,5-*bis*-*p*-chlorophenyl compound, with one of the bromophenyl substituents being axial and the other one in an equatorial position with the 2-ethylbutyl group occupying an axial arrangement.

In the triazacyclohexane ring the H_2C – N bond lengths are 1.446 (4) – 1.491 (4), mean 1.464 Å similar to those in the tri-*p*-chlorophenyl compound which are 1.440 (6) – 1.478 (7), mean 1.457 Å. The H_2C – N – CH_2 angles are 108.3 (2) – 109.7 (2); mean 108.9 ° and the N –CH_2 – N angles are 110.0 (2) – 114.2 (2), mean 112.1 °. The C(aryl) – N bond lengths are 1.411 (4) and 1.420 (4) Å and the C(aliphatic) – N bond length is 1.462 (4) Å.

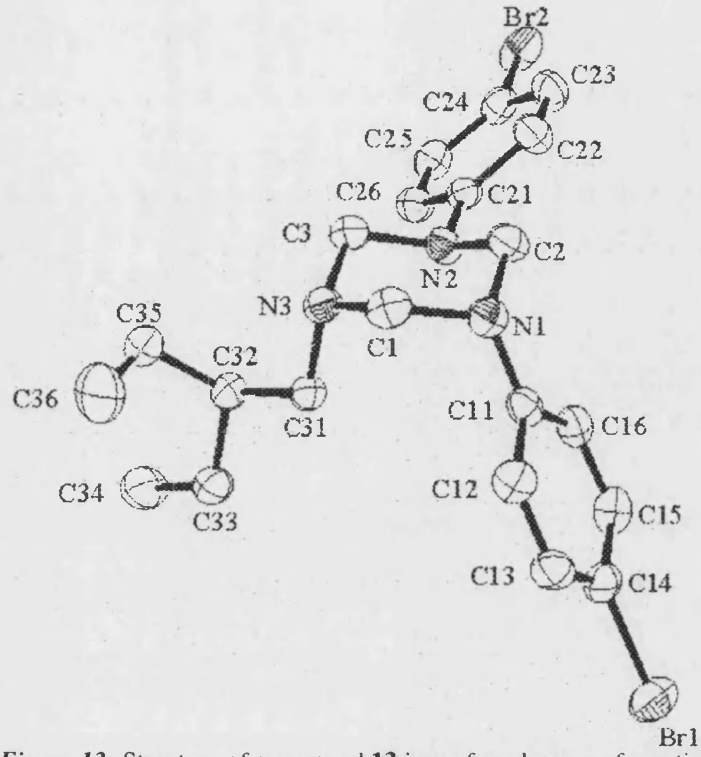

Figure 13: Structure of compound **13** in preferred aae conformation

As previously mentioned for 1,3,5-triphenyl-1,3,5-triazacyclohexane the phenyl rings are aligned perpendicular to the symmetry plane of the triazacyclohexane ring. A comparison of this angle σ between these two planes *Figure 14* shows that these unsymmetrical triazacyclohexanes do not follow in the same vein and adopt a slightly skewed orientation in which some π-orbital – nitrogen lone pair overlap is sacrificed for less steric hindrance between *o*-arylhydrogens and methylene protons on the triazacyclohexane. This skewed orientation was observed with the axial aryl groups in the fluorophenyltriazacyclohexane compounds, *Table 2*.

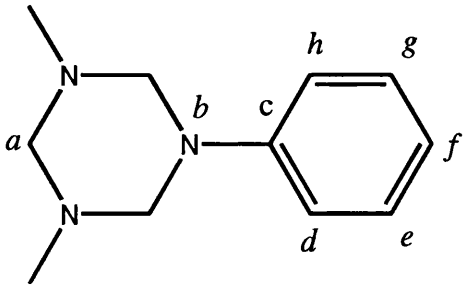

σ is angle between bent planes *abcf* and *cdefgh*

Figure 14: Definition of phenyl plane and plane perpendicular to the triazacyclohexane

	σ (°) equatorial aryl	σ (°) axial aryl
Ph_3TAC [68]	90.0	90.0
(*p*-FPh)$_3$TAC [52]	90.0	61.3
2-EtBu(*p*-FPh)$_2$TAC **11**	-	68.8 and 75.6
2-EtBu(*p*-ClPh)$_2$TAC **12**	61.2	64.3
2-EtBu(*p*-BrPh)$_2$TAC **13**	69.8	66.0

Table 2: Angle between plane of phenyl substituent and perpendicular plane of triazacyclohexane

2.3 Summary

Reported herein is the synthesis of a diverse range of 1,3,5-trialkyl-1,3,5-triazacyclohexanes. From the simple condensation reaction between a primary amine and paraformaldehyde in a 1:1 molar ratio the majority of primary amines will selectively cyclise to give the triazacyclohexane product. Primary amines that are much weaker nucleophiles and are also sterically cumbersome are shown to be much less readily reactive and reside at an intermediate compound $RNHCH_2NHR$ that consists of

two amine units bridged by a methylene moiety. Primary amines of this type can be driven through to the triazacyclohexane by the addition of sodium hydroxide.

The condensation reaction between two primary amines, in a 1:2 molar ratio, with paraformaldehyde forms a mixture of triazacyclohexanes with a greater than statistical selectivity for the mixed triazacyclohexane $R_2R'TAC$ that includes the two amine moieties in the same ratio as the initial primary amines. A number of such compounds have been synthesised with the amine in lowest quantity being a substituted aniline derivative.

In solution both symmetrical and mixed triazacyclohexanes undergo conformation changes rapidly, on the NMR time scale, either by ring flipping or nitrogen inversion. Hence, ^1H NMR spectra at 298 K show a single broad peak for all six methylene protons in symmetrical triazacyclohexanes and two singlets of intensity 2:1 for the two different environments of methylene protons in the mixed triazacyclohexanes.

Selective crystalisation of the bis-aryl mixed triazacyclohexane product from the reaction mixtures has been achieved in most cases. Analysis by X-ray diffraction gives evidence for these systems to prefer the aae conformation in the solid state. This observation has been previously observed for symmetrical triazacyclohexanes with substituted aryl substituents.

3: 1,3,5-Trialkyl-1,3,5-triazacyclohexane Complexes

3.1: Introduction

Organometallic complexes play a vital role in homogeneous catalysis. These complexes are of such importance due to their vast versatility and their ability to be fine-tuned to any given reaction and as a source of activated catalysts. A general form for organometallic complexes could be written as L_mMX_n, and comprises of a metal centre (M), a ligand set (L), and a number of labile groups (X). The active site of an organometallic complex is the metal centre that can be any metal from an alkali metal to a *p*-block element. After selecting a metal there is usually a choice of oxidation states that can dramatically change the hard- or softness of that metal and hence it's affinity for different substrates. This variable oxidation state is prominent in transition metal complexes, with the addition of *d*-orbitals which are ideally suited to overlap with π-orbitals of unsaturated organic molecules, these compounds are the most widely used in catalysis. These choices also dictate the nature of binding of various ligands to the metal centre from covalent to ionic or somewhere in between. The ligands are the essence, which make the catalyst selective for a specific reaction. The ligands dictate the electronic properties of the metal centre, apply steric hindrance to control the size and shape of the active site, and also provide any chirality governing the orientation of molecules at the active site. There are endless possibilities for the ligands, with a different type and number of donor atoms, various binding modes, a range of backbone frameworks, and a choice of charges. There is also a wide range of labile groups that vary in their binding ability to different metals and therefore can be tuned to help

stabilise intermediates and precatalyst or to not interfere with the active site during catalysis.

1,3,5-Trialkyl-1,3,5-triazacyclohexanes have three nitrogen atoms that have the possibility of donating one, two, or three lone pairs of electrons to form bonds with metal species. To date only two of these coordination modes have been structurally characterised by X-ray crystallographic methods, but a κ^3 binding mode in a couple of copper complexes have been found to have only two strong bonds to the triazacyclohexane and so is considered as a κ^2 binding mode, despite this binding mode being less common it can not be rejected as an important binding mode during catalysis.

The κ^1 binding mode, in which only one of the three nitrogen atoms is bound to one metal centre, has been observed with dimethylzinc, dimethylcadmium, [69] and trimethylaminoaluminiumhydride. [70] Reaction of either dimethylzinc or dimethylcadmium with a greater than 1:2 ratio of metalalkyl to triazacyclohexane results in the formation of the bis adduct, *Figure 1.*

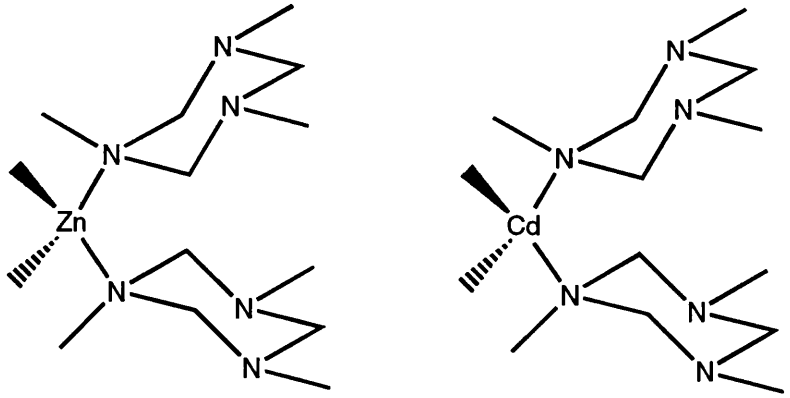

Figure 1: $Zn(Me)_2(\kappa^1\text{-}Me_3TAC)_2$ and $Cd(Me)_2(\kappa^1\text{-}Me_3TAC)_2$ complexes with triazacyclohexane involved in κ^1 coordination

In both the zinc and cadmium cases two triazacylohexanes are bound to the metal centre, each by only one metal – nitrogen bond, in which the lone pair has been

donated from the nitrogen to form the bond. For all the triazacyclohexane ligands the metal has been bound into an equatorial position in relation to the ring, this is a consequence of reducing the 1,3,5-axial interactions, by placing a relatively smaller methyl group into the axial position instead. The nitrogen – metal bond lengths 2.41 Å, in the zinc complex, are relatively long compared with another like donor zinc compound $Zn((CH_2)_3N(CH_3)_2)_2$ with a Zn – N bond length of 2.32 Å.

Reaction of trimethylaminoaluminiumhydride with 1,3,5-trimethyl-1,3,5-triazacyclohexane in a 1:1 ratio results in a polymeric species $[H_3Al(Me_3TAC)]_\infty$, whereas in a 1:2 ratio in favour of the triazacyclohexane, a bis complex is produced, *Figure 2.*

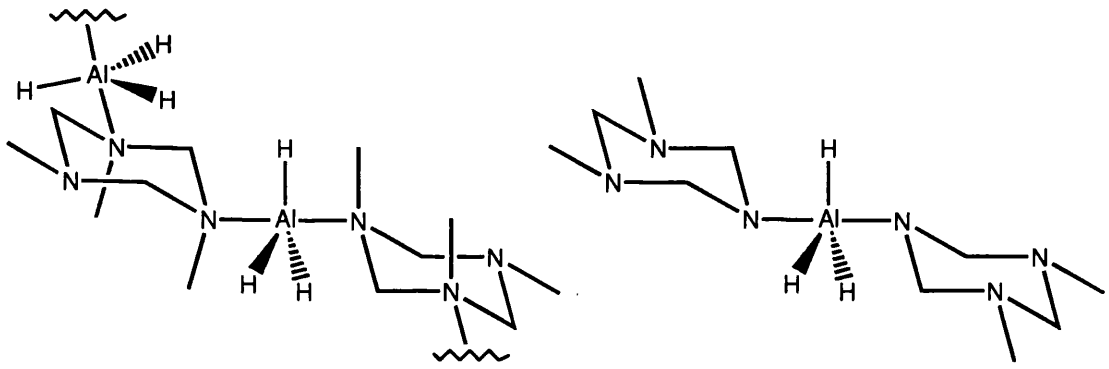

Figure 2: $[H_3Al(Me_3TAC)]_\infty$ polymer and $H_3Al(Me_3TAC)_2$ complex with triazacyclohexane involved in κ^1 coordination

In both the polymeric and the monomeric forms the triazacyclohexanes bind to any given metal centre in a κ^1 fashion with the metal fragment in an equatorial orientation, as with the zinc and cadmium complexes, to reduce the amount of steric interactions. The mean nitrogen – aluminium bond lengths in the monomeric form 2.19 Å, and the polymeric form 2.22 Å are much longer than for the weakly associated $[(H_3Al(BzNMe_2))_2]$ complex with a mean Al – N bond length of 2.09 Å, and slightly

longer than in $H_3Al(NMe_3)_2$ with an average Al – N bond length of 2.18 Å. These weaker bonds between Al – N(TAC) and also Zn – N(TAC) as compared with the corresponding M – N(none heterocyclic) bonds show that in the κ^1 binding mode triazacyclohexane nitrogen binding is slightly weaker than other amine donor ligands.

This κ^1 type of binding has been observed for a triazacyclohexane to more than one metal centre, in an axial position, in some copper cluster compounds, [71] *Figure 3.*

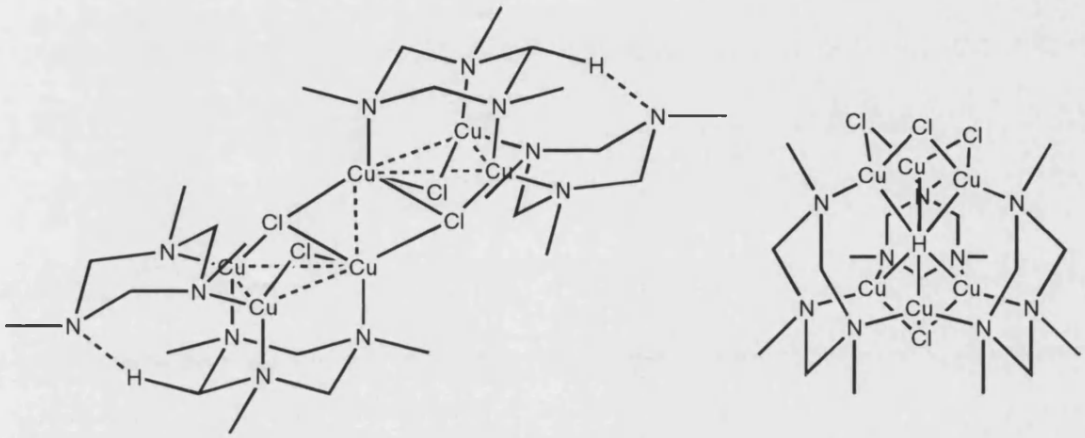

Figure 3: Copper clusters involving triazacyclohexanes in κ^1 coordination bridging metal centres

Both cluster compounds show a triazacyclohexane binding to three different Cu(I) metal centres that show metal – metal bonds in a triangular arrangement. All the copper atoms are bound in the axial position placing them all on the same face of the triazacyclohexane. In the first example there are also two triazacyclohexanes binding only two copper metal centres, that are also bound in axial orientations, but show no significant change in bond length to the previously described triazacyclohexane - copper bonds.

In contrast complexes of copper bound to triazacyclohexane in a κ^3 fashion, but have a significant degree of κ^2 character, have been reported, [72] *Figure 4.*

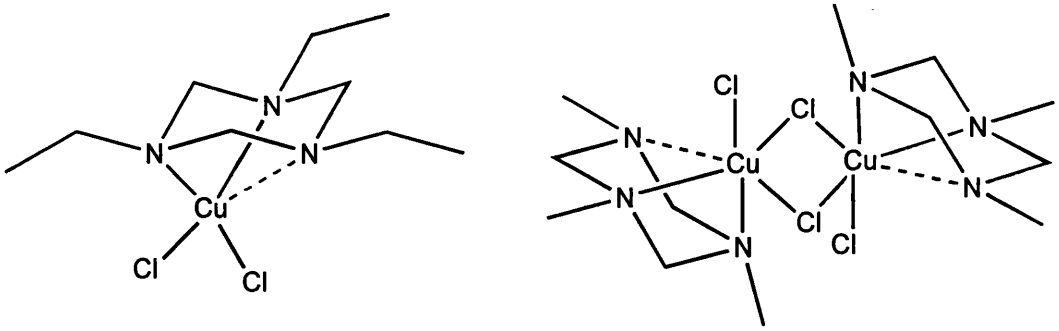

Figure 4: $Et_3TACCuCl_2$ and $[Me_3TACCu(\mu_2\text{-}Cl)Cl]_2$ complexes involving triazacyclohexanes in κ^2 coordination

In these Cu(II) complexes the bonding atoms attempt to arrange in octahedral geometry, but due to the Jahn-Teller effect arising from the unequal occupation of the e_g pair of orbitals when a d^9 ion is subjected to an octahedral crystal field, there is an elongation of the octahedron. As the coordination number of these copper complexes is 5 there are four short bonds in an almost square plane and one long bond at approximately 90° to this plane forming a square pyramidal structure. For the first complex the Cu – N bonds part of the square plane are 2.0706 (12) and 2.0952 (13) Å whereas the third Cu – N bond is 2.5218 (13) Å showing this to be a much weaker interaction.

The most common binding mode of triazacyclohexanes to a Lewis acidic metal centre is by κ^3 coordination by which all three nitrogen lone pairs donate to the same metal. The first metal alkyl group found to form an adduct with a triazacyclohexane was $Et_3TACInMe_3$ [73] but as this complex was a liquid at room temperature nothing could be interpreted about the nature of bonding. However since this first discovery the methyl-, *iso*-propyl-, and *tert*-butyl- triazacyclohexane trimethyl indium adducts have been prepared. [74,75] From this group of compounds the iso-propyl- complex, *Figure 5*, was

studied by X-ray crystallography to reveal the familiar piano stool structure of a *fac*-octahedral geometry of a six coordinate indium metal centre.

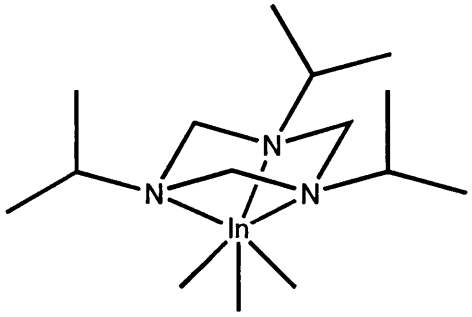

Figure 5: $^{i}Pr_3TACInMe_3$ involving triazacyclohexane in κ^3 coordination

All three alkyl substituents on the triazacyclohexane ring must adopt equatorial positions as to allow the nitrogen lone pairs to point in the same direction, towards the indium *p*-orbitals, and hence bind to the metal centre. Although there are three nitrogen atoms bound to the indium the strength of the coordination between the triazacyclohexane and the metal is not in the vicinity of the sum of three monodentate amine ligands, in fact it is much lower.

A variable temperature study on this class of indium complexes [74] reveals that ring inversion of the ligand also occurs in these compounds, as was seen in the free triazacyclohexanes, but during the process must remain associated with the metal by one In – N bond. In comparison of this process with that of the free triazacyclohexane it is found that the increase in strength given to the adduct by the two extra In – N bonds amounts to about 4.5 kJ / mol. In context this means that the triazacyclohexane is bound to indium by 85 – 90 kJ / mol compared with one NMe_3 group binding to indium with 83 kJ / mol.

This lower than expected binding energy between the three equivalent nitrogen atoms and the indium metal centre are the cause of long In – N bonds observed for these complexes and in the case of $^{i}Pr_3TACInMe_3$ the longest In – N bond to date 2.78 Å.

Dynamic ^{1}H NMR spectra on a class of titanium triazacyclohexane complexes, *Figure 6*, [76] confirms the view that 1,3,5-trimethyl-1,3,5-triazacyclohexane is not as strongly binding as would be expected. However larger alkyl- substituted triazacyclohexanes show a larger affinity for coordination to the titanium metal centre.

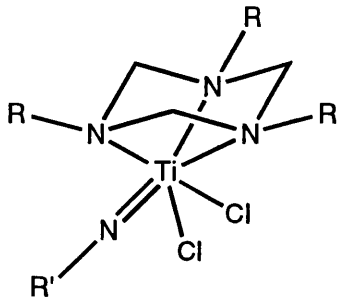

R = Me or ^{t}Bu
R' = ^{t}Bu or 2,6-$C_6H_3{}^{i}Pr_2$

Figure 6: Structure of $R_3TACTi(Cl)_2$=NR' complexes

The room temperature ^{1}H NMR spectra of the *tert*-butyl compounds and the low temperature (slow exchange) spectra of the methyl complexes show resonances consistent with a *tert*-butyl or 2,6-$C_6H_3{}^{i}Pr$ group and a coordinated triazacyclohexane. The signals due to the triazacyclohexane reveal two environments of substituents on the nitrogen atoms, methyl or *tert*-butyl, being in either *cis*- or *trans*- positions to the Ti=N-R', and two pairs of inequivalent methylene linkages. At room temperature the Me_3TAC complexes do not retain these same spectra, the *tert*-butyl or 2,6-$C_6H_3{}^{i}Pr$ signals remain sharp and are temperature independent but the resonances due to the Me_3TAC are broad. The dynamic NMR spectra of these compounds were assigned to an in-place trigonal twist of the triazacyclohexane ligand. Variable temperature NMR spectroscopic experiments including spin saturation transfer [77] were used to identify site exchange of the methyl groups with respect to Ti=N-R, and also between the two sets of

axial metylene protons, and equatorial protons. There was however no exchange between axial and equatorial methylene protons with each other, indicating that the process occurring does not proceed via complete dissociation of the triazacyclohexane, as was observed in the indium complexes.

1,4,7-trialkyl-1,4,7-triazacyclononanes (R_3TACN) are a slightly larger counterpart to the triazacyclohexane, due to the larger ring size the nitrogen atoms have much more flexibility. This reduced torsional strain allows for a greater directing ability of the lone pairs for a more preferential overlap with metal *d*-orbitals than in a triazacyclohexane complex. It has therefore been proposed that triazacyclononanes form more stable complexes than triazacyclohexanes. [78] Ligand substitution reactions performed on the titanium triazacyclohexane complexes support the weaker binding of the Me_3TAC ligand. Addition of Me_3TACN to the methyltriazacyclohexane titanium complex resulted in 50 % ligand substitution at room temperature after seven days; heating at 75 °C for a further 24 hours pushed the reaction to completion. The same procedure on the *tert*-butyltriazacyclohexane titanium complex resulted in only minor traces of the Me_3TACN complex. As there is no reaction between the Me_3TACN titanium complex and free triazacyclohexane under the same temperature conditions Me_3TACN complexes are more stable than the corresponding triazacyclohexane compounds with Me_3TAC forming less stable complexes than $^tBu_3TAC$. However triazacyclohexane exchange reactions are slow and a significant activation energy barrier must be overcome.

In comparison of triazacyclonanes and triazacyclohexanes as ligands for metal complexes the compounds of both tin and germanium with each ligand, *Figure 7*, have been studied by x-ray crystallography. [79]

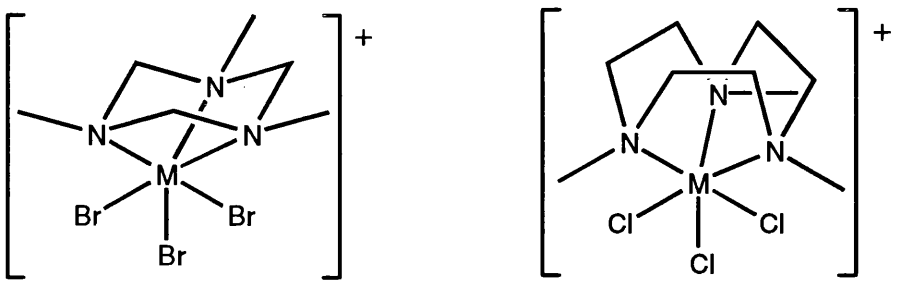

M = Sn or Ge

Figure 7: Structures of tin and germanium [$Me_3TACMBr_3$] and [$Me_3TACNMCl_3$] cations

1,3,5-trimethyl-1,3,5-triazacyclohexane and 1,4,7-trimethyl-1,4,7-triazacyclononane react with MBr_4 and MCl_4 (M = Sn or Ge) respectively in a 1 : 1 ratio to give complexes in which the specified ligand binds in a κ^3 fashion to both tin and germanium. The heterocyclic-metal fragments are all cationic species with various anions from simple halide ions in salt formation for the germanium complexes to the hexahalogenostannate anion $[SnX_6]^{2-}$ in the tin complexes. In all the complexes the tin and germanium are six coordinate in a skewed octahedral geometry. The chelating triazacyclononane has a mean N – Sn – N bond angle of 79.1 ° and a mean N – Ge –N bond of 82.9 ° the corresponding angles for the triazacyclohexane complexes are 59.7 ° and 64.3 °coordinating in a *fac-* orientation but with smaller acute N – M –N angles than optimal octahedral geometry of 90 °. The much larger and more optimal geometries of the triazacyclononane complexes emphasises the larger ring size, with reduced ring strain, and so greater aptitude for lone pair directing, *Figure 8*.

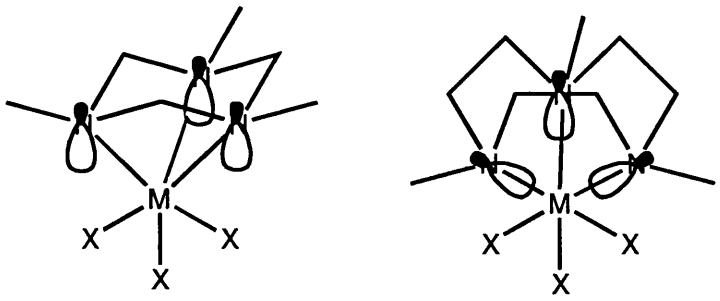

Figure 8: Direction of nitrogen lone pairs in R_3TAC and R_3TACN complexes

The mean metal – nitrogen bond length in the triazacyclononane complexes are Sn – N 2.244 Å and Ge – N 2.113 Å whereas the corresponding bond lengths for the triazacyclohexane compounds are 2.311 Å and 2.142 Å respectively. The longer metal – nitrogen bond lengths in the triazacyclohexane complexes is another sign of the weaker bonding and hence the misdirected donating lone pairs.

Many group 6 triazacyclohexane complexes have been synthesised [80-83] the first group of which we will look at are the tricarbonyl compounds, *Figure 9.*

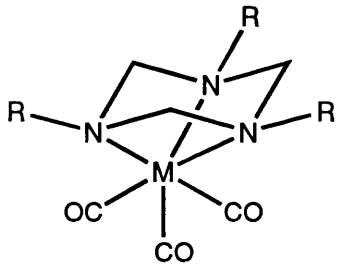

M = Cr, Mo, W
R = Me, ^{t}Bu, $PhCH_2$

Figure 9: Structure of chromium, molybdenum and tungsten triazacyclohexane tricarbonyl complexes

All these triazacyclohexane complexes form the familiar piano stool conformation in which the heterocycle is bound in a κ^3 *fac-* coordination. Once again the lack of stability given to the complexes by the Me_3TAC ligand is evident as all it's associated complexes are air sensitive whereas all the complexes with $^tBu_3TAC$ are stable in air indefinitely. This lack in coordination strength of the Me_3TAC ligand has been exploited in the preparation of a number of molybdenum and tungsten products *fac*-$[M(CO)_3(CH_3CN)_3]$ (M = Mo, W), $[W(CO)_3(alkyne)_3]$, $[W(CO)_3(PR_3)_3]$ and

$[W(CO)_3(\eta^6\text{-arene})]$. [84] The Me_3TAC ligand can be easily displaced by acetonitrile, PPh_3, P^iPr_3, and DMSO at room temperature and at reflux for two hours with diphenylacetylene, benzene, and toluene.

As nitrogen atoms are particularly hard donors they should bind most strongly with harder metal acceptors, this is the case with these group 6 metal carbonyls. Taking the $^tBu_3TAC$ complexes as examples the chromium is the hardest of the three metals with molybdenum and tungsten quite similar in size, hence the mean metal – nitrogen bond lengths are Cr – N 2.210 Å, Mo – N 2.347 Å, and W – N 2.332 Å and the respective N – M – N bond angles are 63.2 °, 59.5 °, and 59.8 °. From these values it can be seen that chromium gets closer to the triazacyclohexane ring and binds more strongly, than the other two metals, and is the reason why the Me_3TAC ligand displacements are much more demanding for the chromium complexes. The same trend is observed for the corresponding metal amine complexes with average bond lengths of 2.15, 2.26 and 2.26 Å for chromium, [85] molybdenum, [86] and tungsten [87] respectively.

Trans to the triazacyclohexane the three carbonyl groups have close to optimal octahedral geometry 90 °. The mean C – M – C bond angles for the $^tBu_3TAC$ metal carbonyl complexes are C – Cr – C 85.6 °, C – Mo – C 85.0 °, and C-W – C 86.1° showing that the triazacyclohexane is imparting very little, if any, steric hinderance on these groups. The carbonyl region of the infrared spectrum of these compounds show two bands centred at 1900 (A_1 mode) and 1760 cm^{-1} (E mode) as expected for facial tricarbonyl complexes of C_{3v} symmetry with the lower band broadened or split due to lower site symmetry in the crystal. For the $^tBu_3TAC$ chromium tricarbonyl complex the stretching frequencies for the carbonyl groups are 1901, 1771, and 1756 cm^{-1} these are

higher than the corresponding values for the $^{i}Pr_3TACN$ chromium compound 1886, 1750, and 1720 cm^{-1}. The triazacyclononane is a stronger σ-donor in these complexes, due to the more directing nature of the nitrogen lone pairs; this therefore increases the electron density at the metal centre. Through increased metal to CO back bonding the carbonyl bond will be weaker and so lower stretching frequencies in these complexes than the triazacyclohexane compounds.

Another class of chromium triazacyclohexane complexes have been reported, [88, 19, 20] *Figure 10*, these are the trichloride compounds that adopt the same configuration as the carbonyl complexes. Unlike the carbonyl compounds that involve zero valent chromium, these complexes have a chromium centre in a +3 oxidation state. As these complexes are six coordinate and are in octahedral geometry the chromium is paramagnetic. These trichloride complexes are purple solids that are inert to air and moisture.

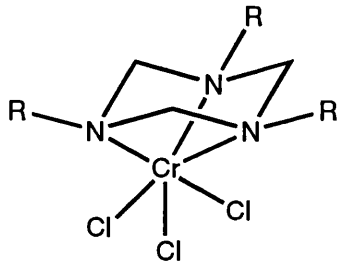

R = Me, n-Pentyl, n-Octyl, n-Dodecyl
^{i}Pr, Cy, Bz

Figure 10: Structure of $R_3TACCrCl_3$ complexes

The choice of alkyl substituent on the triazacyclohexane ring is of vital importance in terms of solubility of these complexes as short chain alkyl substituents lead to insoluble compounds in most common solvents and are only slightly soluble in polar solvents such as DMSO. The cyclohexyl- and benzyl- substituents form complexes that show solubility in chlorinated solvents (up to 6 g l^{-1}) whereas long chain

alkyl substituents produce compounds soluble in most common solvents and even to some degree in warm hexane.

The UV-Vis spectra of Bz_3TAC and Cy_3TAC chromium trichloride complexes in DCM show the first two absorptions due to the octahedral Cr(III) d – d transitions $A_{2g} \rightarrow T_{2g}$ and $A_{2g} \rightarrow T_{1g}(F)$. The average ligand field parameters were derived as Δ_o = 13989 cm^{-1}, 13651 cm^{-1}, and B' = 570 cm^{-1}, 550 cm^{-1} respectively. A third transition $A_{2g} \rightarrow T_{1g}(P)$ was seen as a shoulder at 29917 and 27400 cm^{-1} respectively. With the ligand field parameters for $[CrCl_6]^{3-}$ and $[Cr(en)_3]^{3+}$, an average Δ = 17500 cm^{-1} and B' = 600 cm^{-1} can be expected for $(amine)_3CrCl_3$. These values show that triazacyclohexanes cause a much weaker ligand field splitting and a smaller Racah parameter B' than normal amine ligands. These two complexes have been modified into trialkyl complexes, *Scheme 1*.

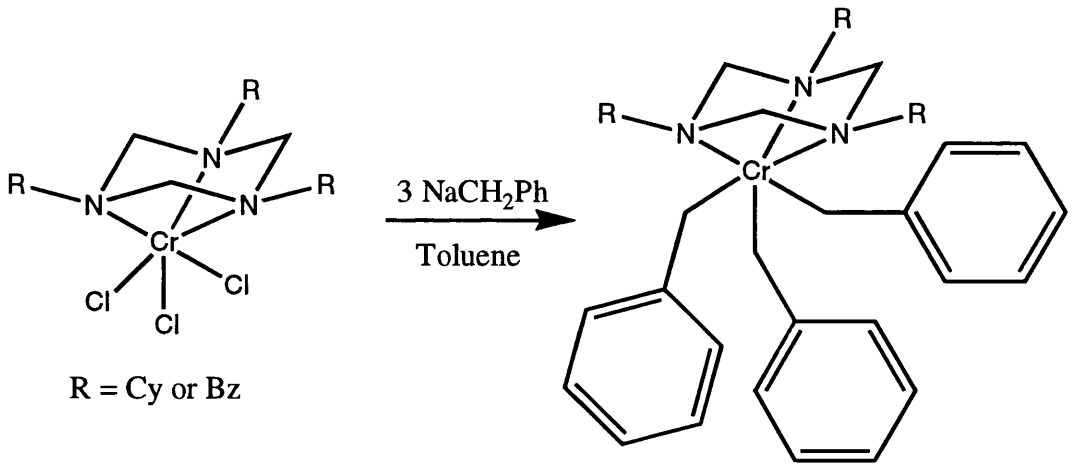

Scheme 1: Formation of $R_3TACCr(Bz)_3$ complexes

The UV-Vis spectra of these two alkylated complexes show two absorptions due to d –d transitions as with the trichloride compounds giving ligand field parameters Δ = 15822 cm^{-1} and B' = 670 cm^{-1} for the Bz_3TAC complex and Δ = 15820 cm^{-1} and B' = 470 cm^{-1} for the Cy_3TAC compound. As would be expected the ligand field splitting is increased on alkylation. On comparison of these spectra with those of $[Cp^*Cr(CH_2Ph)_3]^-$

and $[Cp^*Cr(CH_2Ph)_3]Li$ [20] Δ = 15800, 16600 cm^{-1} and B' = 200, 180 cm^{-1} respectively, it can be seen that the ligand field splitting caused by Cp* is similar to that of triazacyclohexane, but B' is much smaller due to the more covalently bound Cp^*.

3.2: Results and Discussion

3.2.1: Triazacyclohexane Chromium Complexes

1,3,5-trialkyl-1-3-5-Triazacyclohexane chromiumtrichloride complexes can be easily prepared from a couple of different methods, *Scheme 2*.

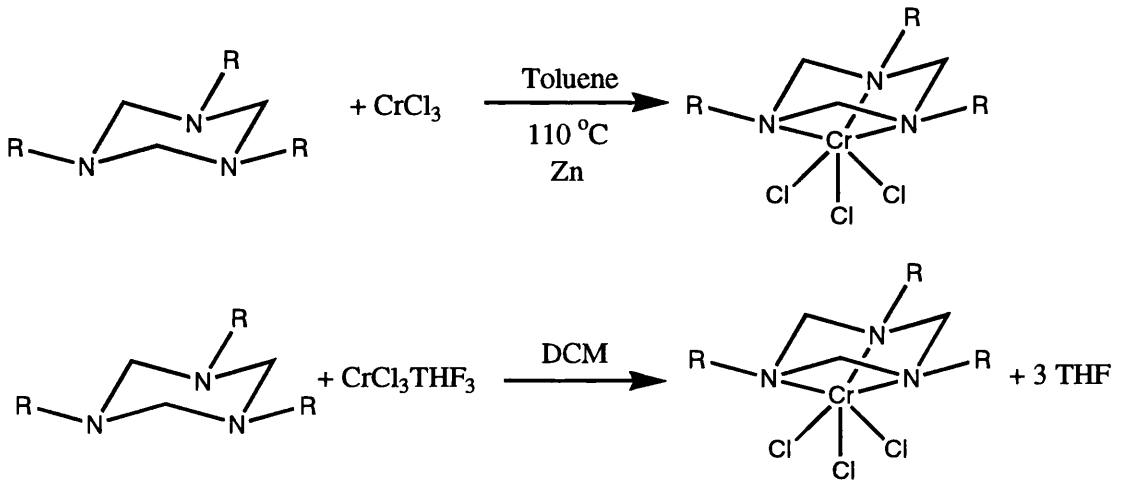

Scheme 2: Preparation of $R_3TACCrCl_3$ complexes

Each of these methods has their own advantages and limitations. A slight excess of trialkyltriazacyclohexanes can be reacted in toluene solution with chromium trichloride, a metallic purple solid insoluble in most solvents, in the presence of a small amount of zinc powder. The mixture is heated to reflux until a purple solution is formed and no more unreacted chromium trichloride is observed. The solution is then filtered to remove the zinc powder and after removal of solvent under reduced pressure a crude purple solid complex is formed. Various complexes of this type are cleaned in different ways depending upon solubility and reactivity. Readily soluble complexes in DCM can

be separated from any impurities by column chromatography through silica gel. Collection of the purple fraction followed by removal of solvent at reduced pressure and thrice washing with hexane yields a clean purple powder of the desired triazacyclohexane chromiumtrichloride complex. Less soluble complexes can usually be cleaned by washing the crude product with diethyl ether that removes most impurities, followed by the thrice washing with hexane to yield the required product.

The small amount of zinc in this reaction is to promote a redox process in the chromium. The chromium trichloride initially is unreactive toward triazacyclohexane but can be reduced by the zinc powder to Cr(II) that will readily react to form the complex. On formation the chromium will then undergo oxidation back to Cr(III) with the self-perpetuating motion of reducing more of the chromium trichloride, or with the zinc ion produced in the initial reduction.

This method for producing this type of chromium complex is very valuable in the production of fairly large quantities as all the starting reagents are cheap. The reagents, and in most cases the products, are not air or moisture sensitive and so the presence of an inert atmosphere may be employed but is not essential during reaction. This lack of sensitivity leads to much more simple set up and manipulations of the reagents and reaction mixture.

The second preparative method involves the moisture sensitive purple chromiumtrichloride tristetrahydrofuran complex [$CrCl_3(THF)_3$] that on contact with water becomes a green aqua complex and is inactive towards triazacyclohexane. This form of chromiumtrichloride, as can be seen from the reaction with water, is much more

reactive than $CrCl_3$. The tetrahydrofuran groups are labile in solution and so vacate coordination sites that are readily filled by a lone pair on a triazacyclohexane molecule. The manipulation of this compound and the following reaction must be performed under inert atmosphere. This reaction proceeds for different triazacyclohexanes in a variety of solvents but in the majority of cases proceeds in DCM. After addition of $[CrCl_3(THF)_3]$ to a solution of triazacyclohexane in DCM the mixture is stirred until a purple solution of the desired complex is formed, that usually requires less than 24 hours at room temperature. Once the reaction has gone to completion the product can be worked up in the same ways as previously described for the other method. This method is much more active than with $CrCl_3$ and so can be used for much less donating triazacyclohexanes. The conditions required for reaction are less harsh as no heating is required and the yields tend to be higher. However due to the expense of the $[CrCl_3(THF)_3]$ starting material and the inert conditions this reaction is not as economical for larger quantities of complex.

All the complexes formed by either of these two methods are Cr(III) complexes bound to a single triazacyclohexane in a κ^3 fashion. This general structure can be observed in the single crystal x-ray analysis of the 1,3,5-triallyl-1,3,5-triazacyclohexane chromium trichloride complex. **14**, *Figure 11*, This complex was prepared using the $[CrCl_3(THF)_3]$ method in THF and single crystals were grown from the mother liquor when left to stand at room temperature.

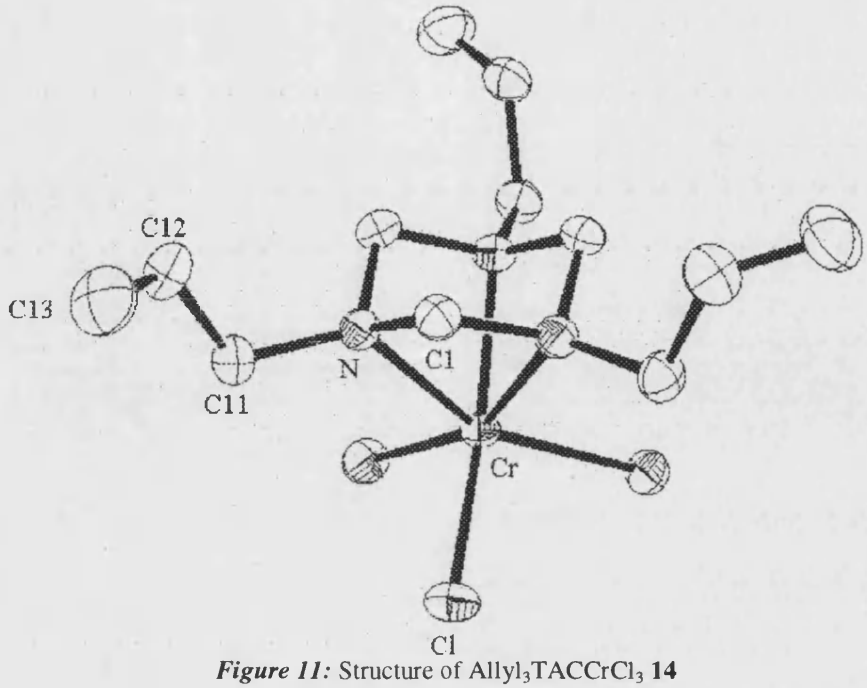

Figure 11: Structure of $Allyl_3TACCrCl_3$ **14**

As is common with a number of complexes of this type this compound has a C_3 symmetry that indicates a symmetrical molecule about a 120 ° rotation about an axis going through the centre point of the triazacyclohexane and the chromium atom. This symmetry element indicates that the corresponding bond lengths and angles in each of the (allyl)$N(CH_2)CrCl$ fragments are the same, *Table 1.*

Cr – N	2.099 (2)	N – Cr – N (1)	66.12 (10)
Cr – Cl	2.283 (7)	N – Cr – Cl	95.71 (6)
C (1) – N	1.483 (3)	N – Cr – Cl (2)	157.35 (7)
N – C (11)	1.480 (3)	Cl – Cr – Cl (1)	99.34 (3)
C (11) – C (12)	1.491 (4)	C (11) – N – Cr	127.47 (17)
C (12) – C (13)	1.309 (5)	C (1) – N – C (2)	109.6 (2)

Table 1: Selected bond lengths and angles for complex **14**

The Cr – N bond lengths are at the lower limit of the range observed in other Cr(III) – triazacyclohexane complexes (2.10 – 2.30 Å) [20,88,89] and is similar to the Cr –

N bond length seen in the (n-Octyl)$_3$TACCrCl$_3$ complex 2.095 (7). [43] This bond is even shorter than that in the analogous tri-n-butyl- substituted 1,4,7-triazacyclononane chromiumtrichloride complex (2.15 Å). [90] This comparison shows that that the lower steric demand of the triazacyclohexane can overcome the weakening of the bond caused by the miss-directed lone pairs. As seen with other triazacyclohexane complexes bound in the κ^3 fashion the N – Cr – N angles are much smaller than the ideal octahedral angle of 90 ° and therefore allow the chloride substituents to be a bit more relieved from this angle.

The crystal packing, *Figure 12*, shows a continuation of the C_3 symmetry. The allyl substituents have been removed for clarity but are not involved in the hydrogen bonding network or significant interaction with neighbouring molecules. The triazacyclohexane chromium complexes are staked in columns with the three chlorides of one molecule sitting over the axial methylene proton of the triazayclohexane of the complex below. These Cl···H hydrogen bonds (2.729 Å) are the strongest in this structure. The other hydrogen bonds, in this stucture, that connect the columns together are between the chloride substituents of one complex molecule with the equatorial methylene protons on a neighbouring columns molecule (2.733 Å). The complexes are all orientated the same way with the hydrogen bonds to the equatorial methylene protons being to the molecule above that in which the corresponding chloride is bound, this gives a skewed pattern to adjoining columns.

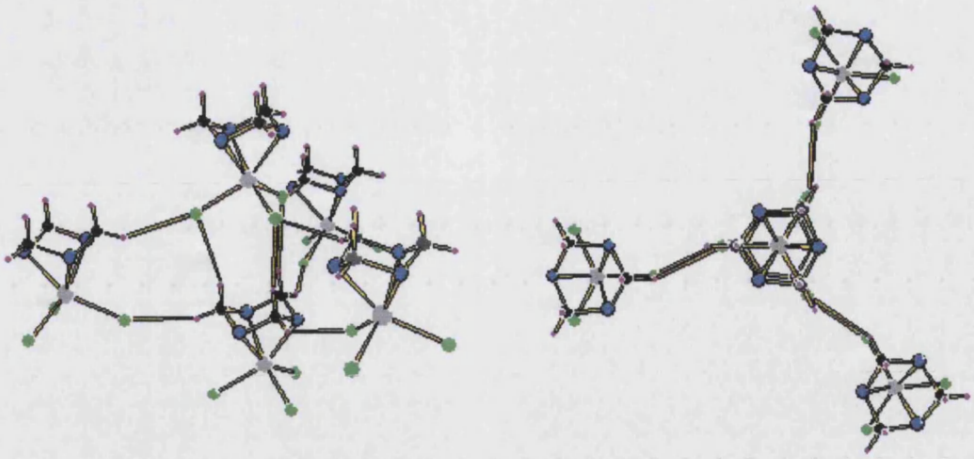

Figure 12: Intramolecular Cl ··· H hydrogen bonding within **14** (allyl groups removed for clarity)

The 1,3,5-tri(2-phenylethyl)-1,3,5-triazacyclohexane chromium trichloride complex **15** has been synthesised by the $CrCl_3THF_3$ method and single crystals, that have been studied by x-ray crystallography, *Figure 13*, were grown from a saturated solution of DCM left to stand at 4 °C.

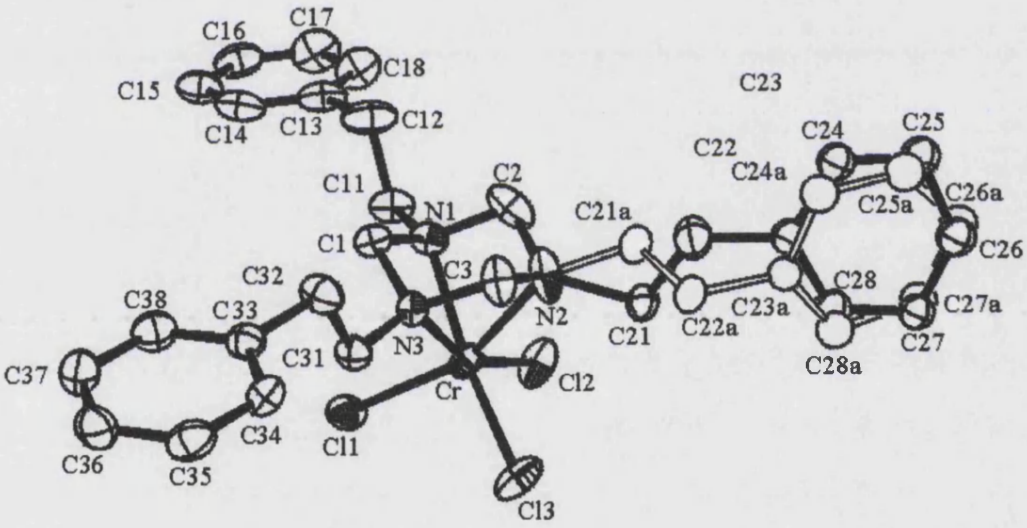

Figure 13: Structure of $(PhEt)_3TACCrCl_3$ **15**

Unlike the previous compound this complex does not have the same C_3 symmetry due to disorder in the crystal of one of the phenylethyl group substituents on the triazacyclohexane. However this disorder does not affect the similarity in bond lengths and angles, *Table 2*, significantly more the majority of the molecule but some

changes are noted around the disordered substituent. The triazacyclohexane still binds in a κ^3 fashion with all its substituents in equatorial positions and forming a complex in a distinctive piano stool arrangement.

Cr – N (1)	2.097 (18)	N (1) – Cr – N (2)	66.03 (8)
Cr – Cl (1)	2.285 (6)	N (1) – Cr – Cl (1)	94.28 (5)
C (1) – N (1)	1.481 (3)	N (1) – Cr – Cl (3)	157.87 (5)
N (1) – C (11)	1.476 (3)	Cl (1) – Cr – Cl (2)	97.84 (3)
N (2) – C (21)	1.583 (5)	Cr – N (1) – C (11)	125.23 (13)
N (2) – C (21a)	1.491 (5)	C (1) – N (1) – C (2)	109.10 (17)

Table 2: Selected bond lengths and angles for **15**

The Cr – N bond lengths are similar to that noted for the triallyltriazacyclohexane complex showing no distinctive differences between the steric and electronic properties of the ligands towards the chromium metal centre. The N – Cr – N angles are also very similar, but with slightly larger N – Cr – Cl bond angles the three chloride substituents are pushed fractionally closer together. This is probably due to the phenylethyl substituents being to some extent more bulky, and the Cr – N – C (11) angles being smaller suggesting the substituents are not quite as far spread than in the allyl case.

Although there are no significant changes in the bond lengths and angles in the $TACCrCl_3$ section of this complex, compared with the same vital unit in the crystal structure of **14**, there are many differences to be noted in the packing of the this structure, *Figure 14*. These discrepancies are due to the phenyl ethyl groups, although not aligned dissimilarly to the allyl substituents, are larger and create more steric bulk.

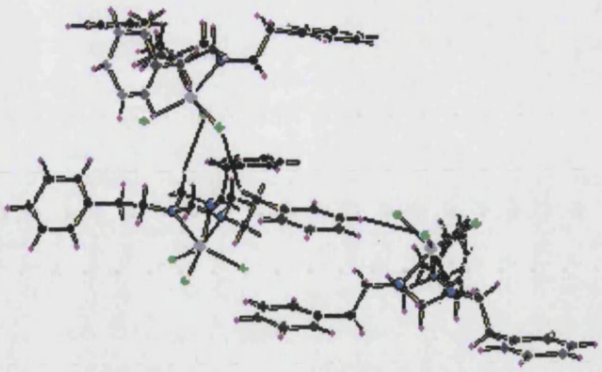

Figure 14: Intramolecular Cl ··· H hydrogen bonding in **15**

Unlike complex **14** the molecules in this structure are not aligned with consecutive $TACCrCl_3$ units eclipsing each other in the column. Instead the molecules in a column are skewed with only one chloride substituent from a given molecule hydrogen bonded to an axial proton on the triazacyclohexane of the complex below (2.842 Å). This is still the strongest hydrogen bond found in this structure but is not as strong as those seen in the allyl complex. One of the other chloride substituents finds a proton on the β-carbon of a phenylethyl subsituent in which to hydrogen bond with (2.880 Å). The third chloride substituent is involved in hydrogen bonding between the columns and interacts with a *meta-* proton of a phenyl group (2.870 Å). Along with this hydrogen bonding between columns there is π-stacking between phenyl rings that are orientated parallel to each other. The orientation of the molecules in a column is anti to that of the following column.

3.2.2: Paramagnetic NMR

NMR studies on these type of compounds is not as informative as of many other complexes due to the highly paramagnetic nature of Cr(III) in an octahedral field with a d^3 configuration, hence three unpaired electrons all aligned in the same direction. The

effects of this paramagnetism are a line broadening of the signals and a shift in parts per million (ppm).

In a typical inversion recovery NMR experiment the magnetization in the z plane M_z is initially inverted by applying a 180 ° pulse. It's recovery along the z axis is given by $M_z(t) = M_z(\infty) - 2M_z(\infty)\exp(-R_1 t)$ where $M_z(\infty)$ is the equilibrium value of M_z. $M_z(t)$ at various times t is sampled by applying a 90 ° pulse and measuring the intensity of the detected signal. R_1 is then extracted from a fitting of the data to an exponential recovery. If the rate of reaching equilibrium is measured orthogonally to the magnetic field, by sampling the projection of the magnetization in the xy plane, a different rate constant is obtained R_2. R_1 and R_2 are known as the longitudinal and transverse relaxation rates respectively and correspond to the relaxation times T_1^{-1} and T_2^{-1}. The longitudinal process only involves energy exchanging with the lattice, or environment, through switches of energy levels. Hence the longitudinal relaxation time is also called the spin lattice relaxation time. These processes also contribute to the transverse relaxation including spin-spin flip-flop transitions, for this reason R_2 is also known as spin-spin relaxation. Due to the extra contributions to R_2 the relation $R_2 \geq R_1$ always holds.

In a pulsed experiment the rate of reaching equilibrium is equal to the rate of disappearance of magnetization in the xy plane. This process is exponential with time constant T_2. The cosine Fourier transform of this exponential decay is:

$$\int_0^{\infty} \exp(-t/T_2)\cos(\omega t)\, dt = \frac{T_2}{1+\omega^2 T_2^2}$$

The frequency function is a Lorentzian with line width at half height of $\lambda_{1/2} = R_2/\pi$. Due to this relation between relaxation and the line width the faster the relaxation of any given nuclei the more broad that signal will appear. Nuclear relaxation can be prompted by three different mechanisms, electron relaxation, rotation of the molecular frame, and chemical exchange. For paramagnetic Cr(III) complexes the most prominent of these is the electron relaxation. In paramagnetic molecules, the magnetic nucleus does not see an unpaired electron as localised, but as spin density distributed throughout space, with an integrated intensity equal to that of a single electron. As a result, in every unit volume, the spin density corresponds to just a small fraction of an electron. Such a fraction will spend some time in the low Zeeman energy levels (negative M_s) and a slightly reduced time in the higher energy levels (positive M_s). Changes in the M_s value involve adjustments in the orientation of the electron magnetic moment. The time-sharing of the levels occurs through electron relaxation. Electron relaxation thus provides fluctuating magnetic fields and cause nuclear relaxation. For the chromium complexes the nuclear relaxation is metal centred with the unpaired electrons providing the fluctuating electron dipolar field, *Figure 15*.

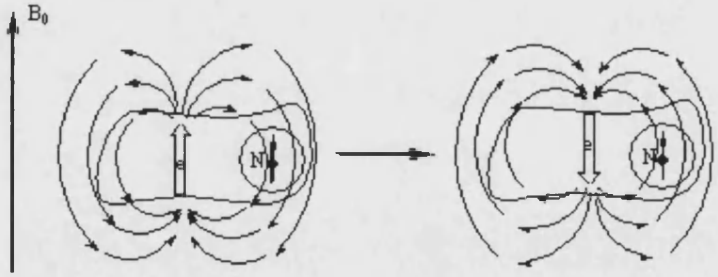

Figure 15: Electron relaxation causing fluctuating magnetic fields

Due to this type of relaxation, line widths at 500 MHz of a proton at 5 Å distance from a Cr(III) centre are reported as 3000 – 25 000 Hz.[91,92,93]

Unpaired electrons have a preference to align with an external magnetic field in the absence of any restrictions. Therefore, their magnetic moment will add to that of the external field and hence increase the effective magnetic field felt by a nucleus. This interaction between unpaired electrons and nuclei is known as hyperfine coupling.

Due to a combination of these two factors some interesting results can be interpreted and to a small degree characterisation of compounds can be conducted. The most commonly preferred nucleus in NMR experiments is ^{1}H in which compounds can quite often be characterised by its spectra alone. However, for these Cr(III) complexes the ^{1}H NMR spectra are dominated by couple of broad signals that swamp the spectra covering many of the other signals resulting in futile integration and somewhat meaningless chemical shift values.

^{13}C NMR can be used to a much greater effect. With a much larger window for the signals and with larger differences in ppm between signals, means that resonances tend to overlap less often, leading to a greater ability to interpretation. Although the study of the carbon nucleus seems more promising the line broadening still causes problems with nuclei close to the paramagnetic centre. For a dipolar coupling between an electron and a nucleus, the effect of which on the relaxation rates is found to be inversely proportional to the distance between the two bodies to the sixth power.[94a] Hence the closer the nucleus under observation is to the paramagnetic chromium centre

$$R_2 = \frac{4}{3}\left(\frac{\mu_0}{4\pi}\right)^2 \frac{\gamma_I^2 g_e^2 \mu_B^2 S(S+1)}{r^6} \tau_c$$

the larger the line width will be. In practical terms carbon atoms that are within three

bonds from the chromium will be too broad to be recognised in the NMR spectra, *Figure 16.*

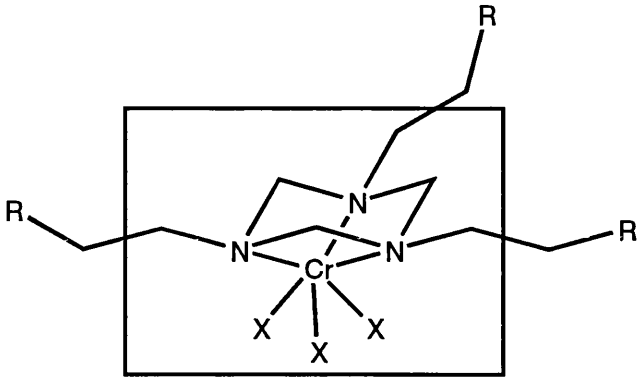

Figure 16: Unobservable carbon environments by ^{13}C NMR inside the box

Other nuclei, such as ^{2}H and ^{19}F prove to be easiest to be observed as only selected positions are doped with these nuclei there is no over saturation of resonances at any given frequency and so each signal is clearly seen. This technique is especially useful for observing events taking place close to the active metal centre. Unlike in the proton and carbon spectra, where only the periphery of the triazacyclohexane substituents that play no part in catalysis are seen, deuterium and fluorine signals can be observed within the three bond length limit.

For well-resolved NMR spectra, especially ^{13}C that only has a natural abundance of 1%, dissolving a significant amount of the complex 50 mg is essential. Complexes **14** and **15** are not very soluble, even in the more polar solvents, and so compounds that have larger substituents on the triazacyclohexane were synthesised, *Figure 17.*

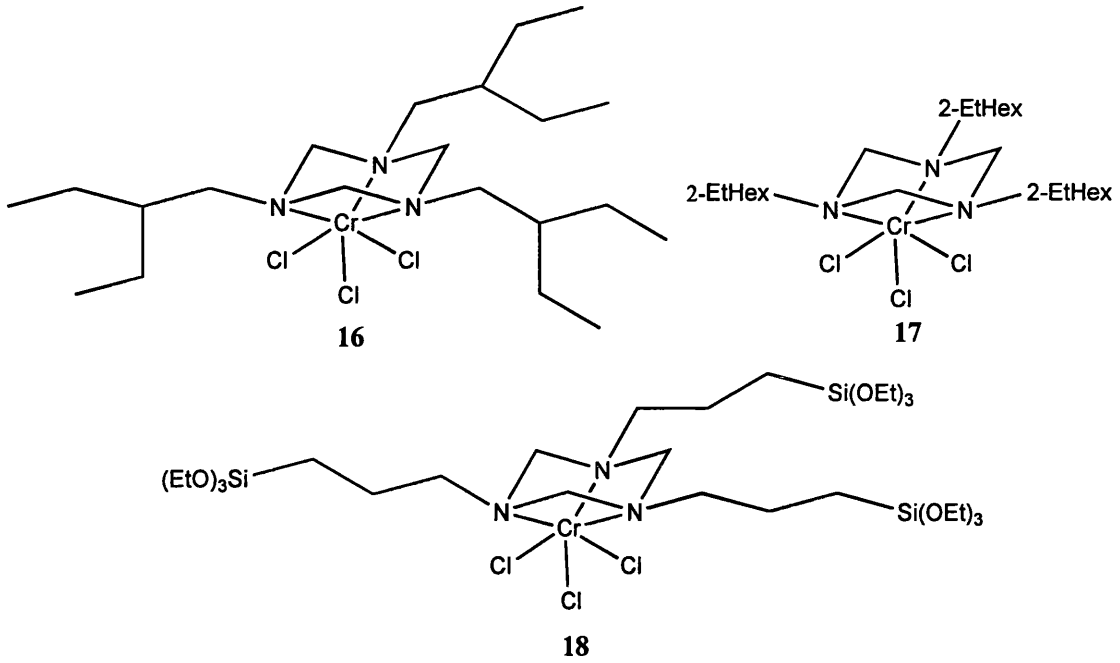

Figure 17: $R_3TACCrCl_3$ complexes with large alkyl substituents

The $(2\text{-EtBu})_3TACCrCl_3$ **16** and $[(EtO)_3SiPr]_3TACCrCl_3$ **18** complexes were both synthesised from the corresponding triazacyclohexane and $CrCl_3THF_3$ in DCM, whereas the $(2\text{-EtHex})_3TACCrCl_3$ **17** and the previously reported $Do_3TACCrCl_3$ complexes were both prepared from the corresponding triazacyclohexane and $CrCl_3$ in toluene. All of these complexes are soluble in DCM with the later two complexes being the most soluble compounds of this type showing some solubility in warm hexane.

The ^{13}C NMR spectral data of these compounds can be compared with that of the corresponding triazacyclohexane data, *Table 3*, along with the spectrum for **17**, *Figure 18*. Assignment of the ^{13}C signals was predominantly due to the relation between line width and distance from the paramagnetic centre, but also with comparison to similar complexes previously studied by ^{13}C isotope labelling studies. [94b]

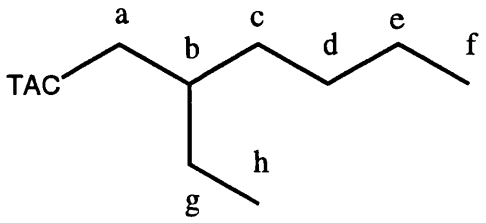

	a	b	c	d	e	f	g	h
^{13}C CrTAC	-	-49.56	42.14	29.39	21.86	12.02	46.15	14.45
^{13}C TAC	57.15	37.71	31.84	25.01	23.58	11.20	29.38	14.54

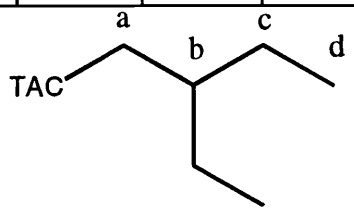

	a	b	c	d
^{13}C CrTAC	-	-	39.22	12.98
^{13}C TAC	56.74	39.17	24.45	11.25

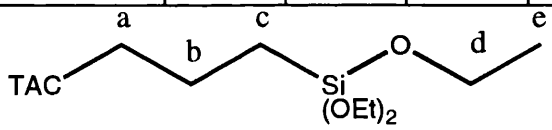

	a	b	c	d	e
^{13}C CrTAC	-	-	41.82	62.18	21.60
^{13}C TAC	56.30	18.77	8.47	58.64	21.88

Table 3: Comparative ^{13}C {^{1}H}NMR data for free ligand and chromium trichloride complex of (2-EtHex)$_3$TAC, (2-EtBu)$_3$TAC and [(EtO)$_3$SiPr]$_3$TAC

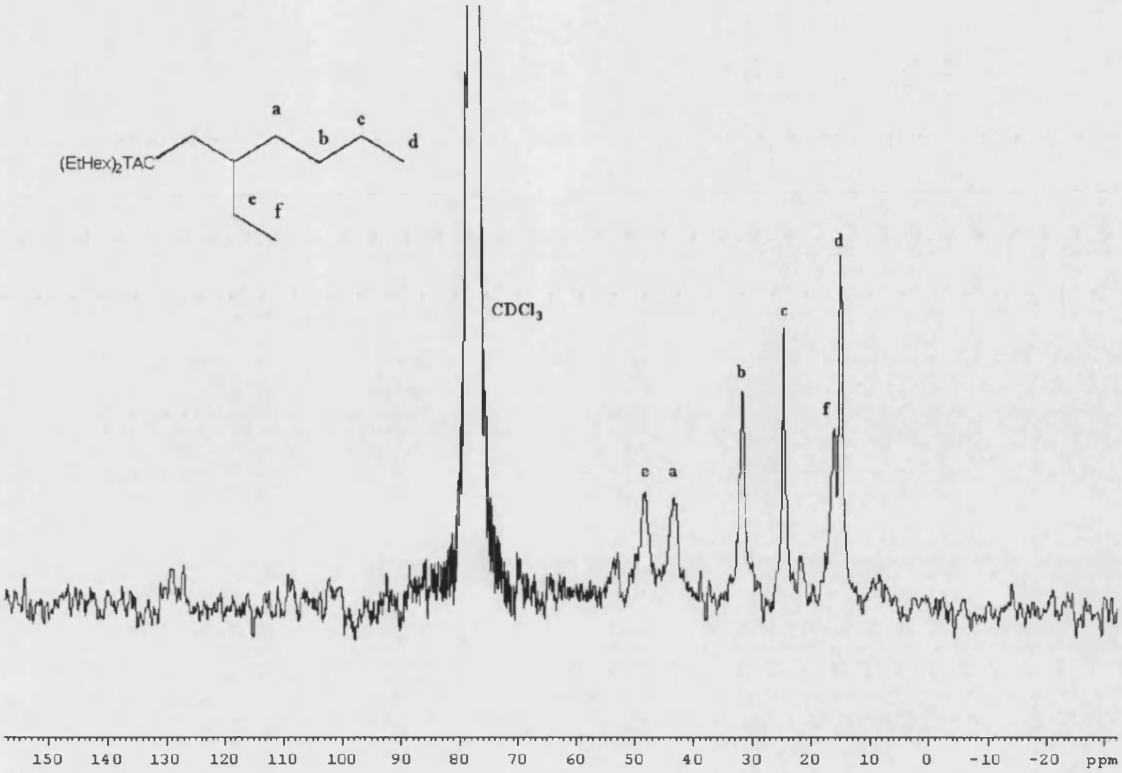

Figure 18: $^{13}C\{^{1}H\}$NMR 100 MHz, 298 K spectrum of **17** in $CDCl_3$

As can be seen from the data the hyperfine shifts increase with the reduced distance between the nucleus under observation and the chromium centre. This is emphasised by the 87 ppm shift of the β-carbon resonance in **17**. This signal is usually not observable but as this is the most soluble compound of its type a concentrated enough sample was prepared to be able to amplify the very broad resonance. The shift of this signal is negative due to another mechanism in operation involving spin polarisation. The spin polarisation yields alternate positive and negative unpaired spin density along the ligand backbone.

Not only does the paramagnetism of the chromium cause a shift on the nuclei of the complex involved, but also on the diamagnetic solvent. By measuring the shift between the paramagnetic and the diamagnetic environment, measured simultaneously, a determination of the magnetic susceptibility of the solute dependent upon the

concentration can be found. This experimental procedure is known as Evans method, [95] and constitutes one of the best ways of measuring magnetic susceptibilities in solution around room temperature.

For these measurements a capillary of the diamagnetic solvent is placed into the NMR tube along with a solution of known concentration of the paramagnetic solution. The ^1H NMR spectrum is run and a chemical shift difference is found between the solvent in the paramagnetic solution and the diamagnetic solvent. This shift can then be related to the susceptibilities of the components in the mixture.

$$\frac{3\delta[ppm]}{4\pi} = \frac{m_x}{V}\chi_x^{para} + \frac{m_x}{V}\chi_x^{dia} + \frac{m_y}{V}\chi_y^{dia} + \left(\frac{m_L}{V} - d_L\right)\chi_L \qquad \chi^{dia}[10^{-6}\,cgs] = \frac{\chi_M^{dia}}{M_W}$$

For the diamagnetic susceptibilities of each component in the system values can be calculated from Pascals constants. Therefore using these equations a value for the paramagnetic susceptibility can be calculated. From this value an effective magnetic moment is evaluated and hence the number of unpaired electrons (n).

$$\chi_x^{para}[10^{-6}\,cgs] = 10^6 \frac{(\mu_{eff}/\mu_B)^2}{8.066 \cdot T \cdot M_W} \qquad \mu_{eff}/\mu_B = [n\,(n+2)]^{1/2}$$

	$\mu_{eff}/\mu_B \pm 0.05$	n
$(2\text{-EtHex})_3TACCrCl_3$ in DCM	3.97	3
$(2\text{-EtHex})_3TACCrCl_3$ in benzene	3.69	3
$(2\text{-EtHex})_3TACCrCl_3$ in toluene	3.75	3
$Do_3TACCrCl_3$ in toluene	3.77	3

Table 4: Effective magnetic moments for the $(2\text{-EtHex})_3TACCrCl_3$ **17** and $Do_3TACCrCl_3$ **19**

Using this method effective magnetic moments have been calculated for the complexes **17** and $Do_3TACCrCl_3$ **19** in DCM, benzene, and toluene, *Table 4*. The effective magnetic moment associated with three unpaired electrons is $\mu_{eff} = 3.87\ \mu_B$. The values for both these complexes are found to be close to the expected value and so seem to be a classical mononuclear complex, as those seen by x-ray crystallographic analysis, in solution. The more viscous solutions, benzene and toluene, appear to give slightly lower effective magnetic moments than those observed in DCM.

The $Do_3(d_6\text{-}TAC)CrCl_3$ complex **20** has been prepared from the corresponding ring deuterated triazacyclohexane and $CrCl_3THF_3$ in DCM. Unlike complex **19** the triazacyclohexane ring deuteriums are observable in the ^2H NMR spectrum in DCM. The broad singlet observed in the ^2H NMR spectrum of the methylene deuteriums in the $Do_3(d_6\text{-}TAC)$ compound at $\delta = 3.37$ with a line width of 14.4 Hz becomes split into two broad signals of axial and equatorial environments in the $Do_3TACCrCl_3$ complex. These two signals are far shifted from that of the triazacyclohexane, the axial deuterium atoms produce a signal at $\delta = 41.80$ with a linewidth of 384 Hz, whilst the equatorial deuterium atoms resonate at $\delta = -5.73$ with a line width of 612 Hz. These large linewidths along with the hyperfine coupling causing a shift as large as 38 ppm show a close relation between the triazacyclohexane and the chromium centre. No additional signals are observed in the ^2H NMR spectrum relating to none coordinated triazacyclohexane. Hence the triazacyclohexane ligand does not appear to be labile in solution or binding in a κ^1 fashion in which case both axial and equatorial deuterium atoms would appear equivalent.

The ^{2}H NMR spectrum of this compound have also been studied in acetone, toluene, and a range of mixtures of the two named solvents at constant concentration.

Table 5

Toluene : Acetone	Axial δ	Axial λ / Hz	Equa. δ	Equa. λ / Hz
0 : 1	41.2	175.6	-6.2	265.9
0.15 : 1	40.3	197.3	-5.1	272.1
1 : 1	39.5	345.5	-4.7	470.3
12 : 1	~47	~1400	-	-
1 : 0	~52	~3500	-	-

Table 5: ^{2}H NMR data for **20** in toluene/acetone solutions

As the concentration of toluene increases the deuterium signals become more broadened, up until the point at which the signals are no longer distinguishable from the baseline and so no values can be reported. This broadening of the linewidth occurs in the less polar solvents in which the solutions are much more viscous. Hence it is proposed that the molecules tend to bunch up into pairs or higher numbered clusters, possibly interacting via the hydrogen bonds between chloride substituents and triazacyclohexane methylene groups, *Figure 19.*

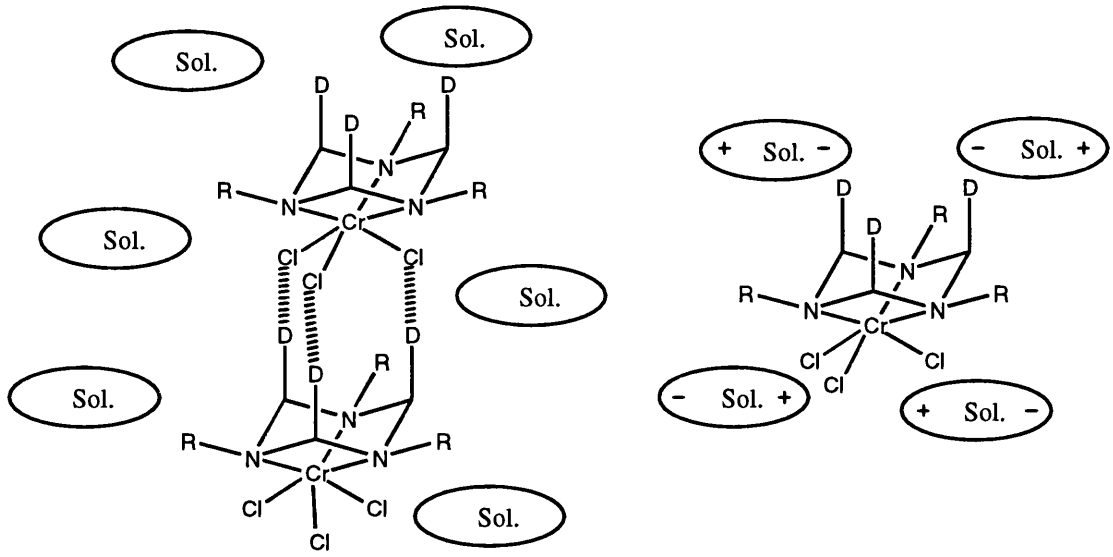

Figure 19: Effect of polarity of solvent upon grouping of chromium complexes in solution

This observation has been reinforced by preliminary molecular weight, by freezing point calculations by Köhn. [96] In these calculations solutions of **17** in benzene were measured. For concentrations of 12, 5 and 1 mM values of MW were calculated as 2500, 2200 and 600 respectively. (MW of **17** = 582) These results suggest that above very low concentrations the $R_3TACCrCl_3$ complexes aggregate into clusters of approximately 4 units. This clustering coincides with an increase in viscosity η = 0.67, 0.90, and 3.75 kg $m^{-1}s^{-1}$ for concentrations of 0.28, 1.4, and 6.9 mM respectively. At the low concentration 0.28 mM the viscosity is close to that of the C_6H_6 solvent η = 0.67 kg $m^{-1}s^{-1}$.

In polar solvents the dipoles in the complex molecules can interact with solvent molecules and therefore do not have the attraction towards other complexes. This keeps the individual complex molecules apart and so a less viscous solution is formed. The concurrent line broadening with the formation of the pairs is due to two neighbouring paramagnetic centres to the deuterium nucleus under investigation.

3.2.3: Mixed Triazacyclohexane Chromium Complexes

Chromium trichloride complexes of mixed triazacyclohexanes have been synthesised, *Figure 20.*

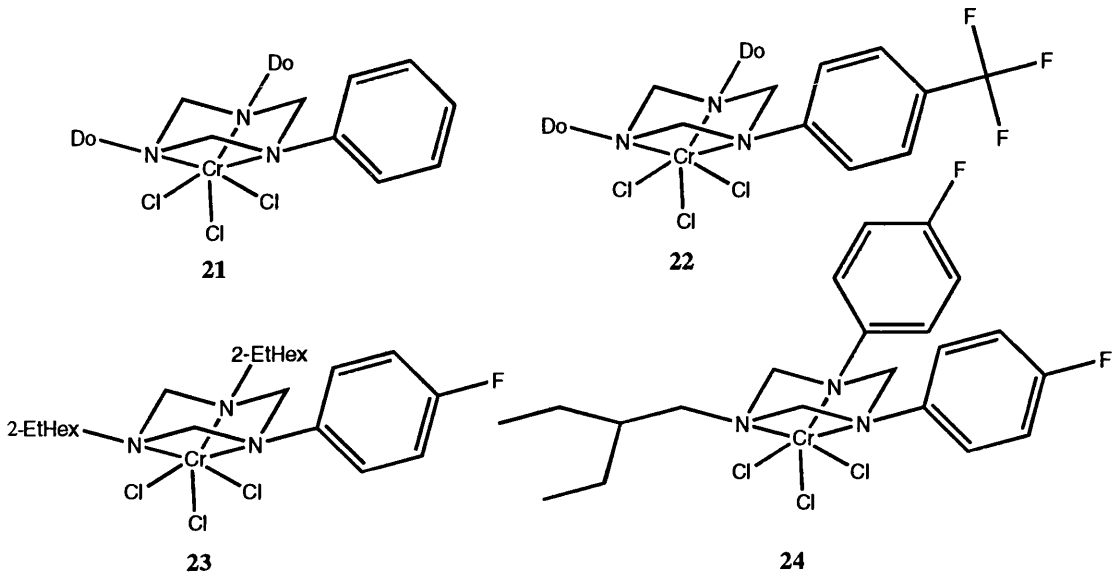

Figure 20: Mixed triazacyclohexane chromium complexes

The 1,3-di-dodecyl-5,-phenyl-1,3,5-triazacyclohexane chromium trichloride, **21** 1,3-di-dodecyl-5,-(*para*-trifluoromethyl)phenyl-1,3,5-triazacyclohexane chromium trichloride, **22** and 1,3-di-(2-ethylhexyl)-5,-*para*-fluorophenyl-1,3,5-triazacyclohexane chromium trichloride **23** were all synthesised from the corresponding mixtures of triazacyclohexanes, discussed in chapter 2, with $CrCl_3THF_3$ in DCM. The resulting mixture of complexes was separated using column chromatography through silica gel. The only two products recovered from each of these reactions were the symmetrical $(alkyl)_3TACCrCl_3$, and $(alkyl)_2PhTACCrCl_3$. The symmetrical $Ph_3TACCrCl_3$ complex was never recovered as in some cases the corresponding ligand did not form in the preceding reaction, or the complex did not form due to the poor donor strength of the triazacyclohexane nitrogen lone pairs. The $Ph_2(alkyl)TACCrCl_3$ complex, although is thought to have formed, decomposes before leaving the column. This lack of stability is

also due to the lack in donor strength of two of the three nitrogen lone pairs. The ligand will have a predominantly κ^1 binding mode and in this state will be quite labile. Once in solution the ligand will be lost from the chromium during the chromatography.

Crystals were grown of 1-(2-ethylbutyl)-3,5-*para*-fluorophenyl-1,3,5-triazacyclohexane from a mixture of triazacyclohexanes. (see chapter 2) This compound was reacted with $CrCl_3THF_3$ in DCM. The complex **24** precipitated out of the solution, showing very little solubility in DCM.

3.2.4: Chromium Triflate Complexes

Triazacyclohexane chromium trichloride complexes can be converted into the corresponding tritriflate complex by the simple reaction with triflic acid, *Figure 21*.

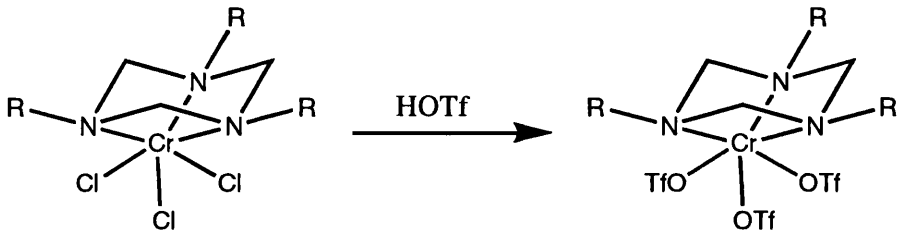

Figure 21: Preparation of $R_3TACCr(OTf)_3$ complexes

An excess of triflic acid is condensed onto the chromium trichloride complex, reaction with the purple solid is almost instantaneous at room temperature to yield a blue / green mixture. After condensing the unreacted triflic acid along with the HCl produced away, and washing thrice with diethyl ether a blue / green solid of the corresponding triazacyclohexane chromium tritriflate is produced. The complexes $Do_3TACCr(OTf)_3$ **25** and $(2\text{-EtHex})_3TACCr(OTf)_3$ **26** have both been synthesised by this method. These compounds are moisture sensitive, with the solid decomposing into

a brown oil within one week exposure to the air, and a solution decomposing within two days. With more labile triflate ligands these complexes were synthesised to be able to under go activation with $ZnEt_2$, to remove the need for aluminium that has found to be harmful to the lifetime of the catalyst (See chapter 5). Due to the hydroscopic nature of these complexes and the difficulties in purifying these samples (See elemental analysis results chapter 6) no trimerisation activity was found for these complexes.

The NMR spectra of the triflate complexes are very similar to those observed for the trichloride compounds. With the chromium also in the +3 oxidation state with a d^3 electronic configuration the molecules are paramagnetic. In comparison is the data from the ^{13}C NMR spectra of **17** and **26**, *Table 6.*

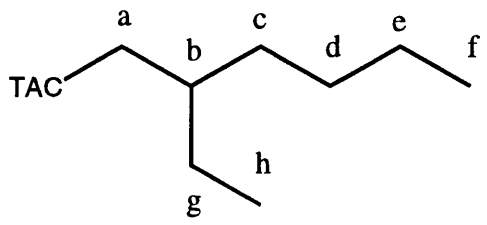

	a	b	c	d	e	f	g	h
^{13}C $TACCrCl_3$	-	-49.56	42.14	29.39	21.86	12.02	46.15	14.45
^{13}C $TACCr(OTf)_3$	-	-	-	28.09	22.40	14.45	-	10.03

Table 6: ^{13}C $\{^1H\}$NMR data of the $(2\text{-EtHex})_3TACCr(OTf)_3$ complex

Due to the reduced solubility of the tritriflate complexes compared with the trichlorides the signals due to carbons a, b, c, and g were not observable. A similar picture is observed with complex **25** as when compared to the corresponding trichloride compound **19**. The ^{19}F NMR spectra of these compounds show only one broad signal

due to the nine equivalent fluorine nuclei δ = -77.55, λ = 123.5 Hz for the **26** and δ = -77.74, λ = 515.1 Hz for the **25**.

In an NMR tube reaction, *Figure 22*, to a solution of **25** in toluene was added one equivalent of Do_3TAC.

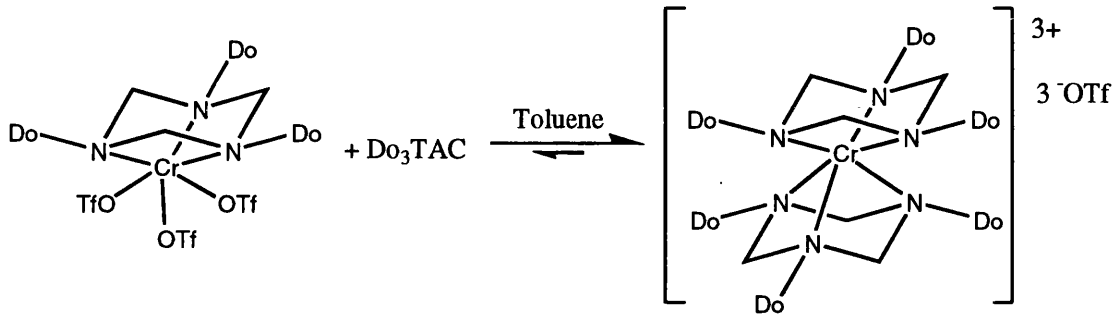

Figure 22: Formation of $(Do_3TAC)_2Cr(OTf)_3$ complex **27**

Upon addition of the triazacyclohexane a colour change from the deep blue / green solution to a pale blue solution, a greater colour change than just dilution alone, was observed. The ^{13}C NMR spectrum consisted mainly of relatively sharp signals due to uncoordinated triazacyclohexane. However the ^{19}F NMR revealed a dramatic sharpening of the signal at δ = -77.74 from λ = 515.1 Hz to 113.5 Hz with very little change in the chemical shift δ = -78.33. This suggests that the average fluorine nuclei are situated further from the chromium than in the tritriflate complex alone but are still in a state of equilibrium with the parent complex as the average signal is still the only observable signal in the spectrum.

3.3: Summary

This chapter reports the synthesis of a number of diverse 1,3,5-trialkyl-1,3,5-triazacyclohexane chromium complexes. Many previously reported complexes of this type and also the initial complexes synthesised herein show only very limited solubility with most common solvents and hence the potential as α-olefin trimerisation catalysts are seriously diminished. Lengthening as well as incorporation of branching of the alkyl substituents on the triazacyclohexane leads to a much greater solubility in the corresponding chromium complex. These Cr(III) complexes are highly paramagnetic that has a significant effect upon the NMR spectra of these compounds. Line broadening has an inverse relation with the distance between the chromium and nucleus under investigation. This property has been utilised in the determination of aggregation of the chromium complexes in non-polar solvents. The second effect of paramagnatism upon NMR spectra is a chemical shift, this has also been exploited in determination of effective magnetic of the complexes by the Evans method.

Mixed triazacyclohexane chromium complexes can be prepared from mixtures of ligands with different alkyl substituents. Column chromatography can be used to separate the mixture of complexes formed. They can also be synthesised in the same manner as the symmetrical triazacyclohexane complexes but from the isolated mixed ligand $R_2R'TAC$.

$R_3TACCrCl_3$ complexes can under go ligand exchange with triflic acid to give the corresponding $R_3TACCr(OTf)_3$ complex with a dramatic colour change from purple to green/blue. The triflate ligands are much more labile than chloride substituents and

hence this complex can react with free ligand, unlike the trichloride complex, to give a $(R_3TAC)_2Cr(OTf)_3$ complex, *Scheme 3*.

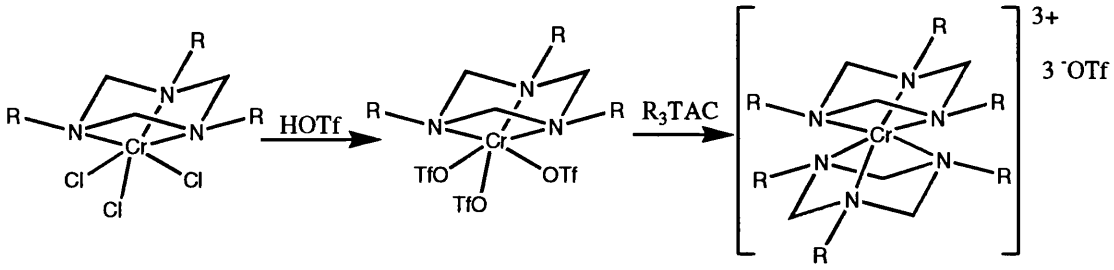

Scheme 3: Transformation of $R_3TACCrCl_3$ complex to $(R_3TAC)_2Cr(OTf)_3$

4: Cationic Complexes With Weakly Coordinating Anions

4.1: Introduction

The 'weakly coordinating anion' has become an area of great interest in both academia and industry over the couple of decades. This is due to their potential in many homogeneous catalytic systems including the catalytic synthesis of organic molecules and especially olefin polymerisation. The primary role of the weakly coordinating anion is to replace a coordinating anion such as a halide and hence create a more reactive metal species but still offer stabilisation. The initial weakly coordinating anions devised we originally dubbed 'noncoordinating anions' these included $[CF_3SO_3]^-$, $[BF_4]^-$, $[ClO_4]^-$, $[AlX_4]^-$, and $[MF_6]^-$ (X = Cl, Br, I; M = P, As, Sb). [97] However, with the rise of X-ray crystallographic methods all these anions were found in some cases to coordinate, *Figure 1*, and so the term weakly coordinating anion was born. [98-102]

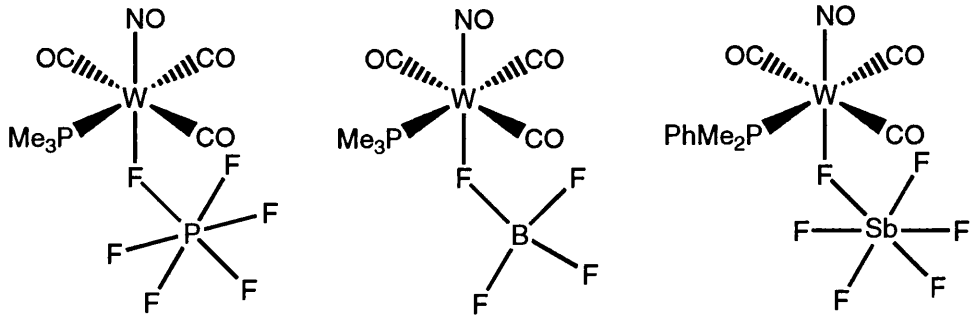

Figure 1: $[PF_6]^-$, $[BF_4]^-$ and $[SbF_6]^-$ coordinating in tungsten complexes

Since these findings many more anions have been devised to achieve the title of 'noncoordinating anion'. To achieve this the anion should not have any lone pairs, nucleophilic, or basic sites. It should also not contain any double bonds or easily polarisable single bonds that may lead to smaller more coordinating fragments. It should be kinetically and thermally stable with a large degree of charge delocalisation over a large structure, so that no one atom bears a high concentration of charge, this structure

also minimises electrostatic attractions. In addition it requires a good solubility in most common solvents. To achieve most of these features a number of much less coordinating anions have been found and are classed as 'super weak anions'. The first set of this new class of anion is the borate-based anion.

Starting with the $[BF_4]^-$ motif the fluoride substituents were replaced by phenyl groups to give $[BPh_4]^-$. This anion found extensive use as a phase-transfer catalyst and as the counter ion in Ziegler-Natta olefin polymerisation with the cationic group 4 metallocene complex $[(Cp)_2ZrR]^+$. [103] But this anion is also known to coordinate to metal ions through π-interactions of one of the phenyl rings. [104, 105] In only one example does this anion coordinate in any other fashion. That is in $Cu(BPh_4)(CO)(en)$ in which the anion binds in a η^2 fashion, [106] *Figure 2.*

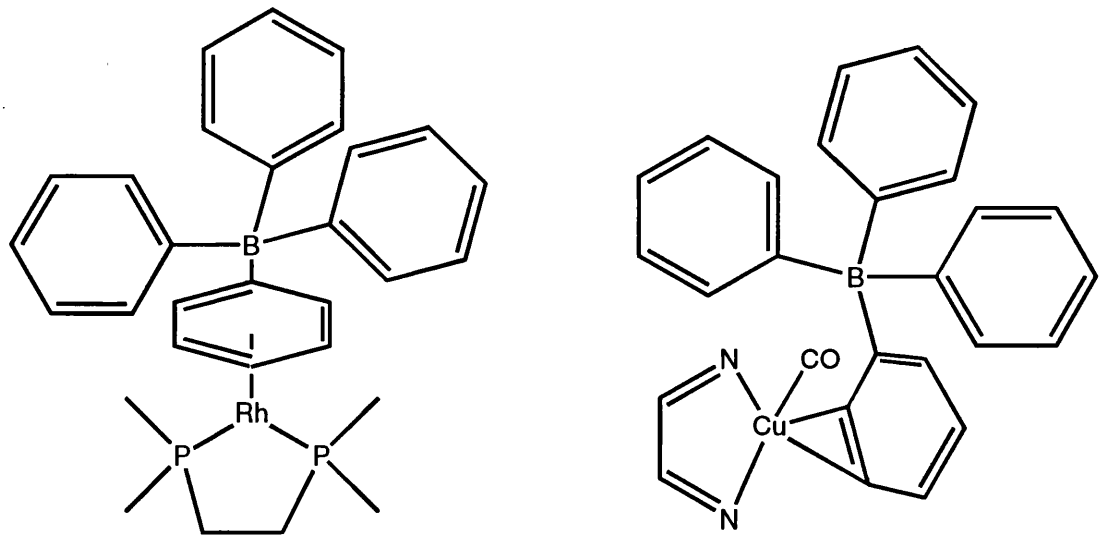

Figure 2: Examples of η^6 and η^2 coordination of the $[BPh_4]^-$ anion

$[BPh_4]^-$ is involved in many reactions that make this anion unsuitable for a number of applications. These reactions include metalation, [107] phenyl group transfer, [108] and electron transfer. [109] In addition it is also susceptible to photochemical decomposition.

To try and overcome the coordinating and reactivity problems with $[BPh_4]^-$ the phenyl groups were fluorinated to give $[B(C_6F_5)_4]^-$ [110] and trifluoromethylated to give $[B\text{-}(3,5\text{-}C_6H_3(CF_3)_2)_4]^-$, [111] *Figure 3.*

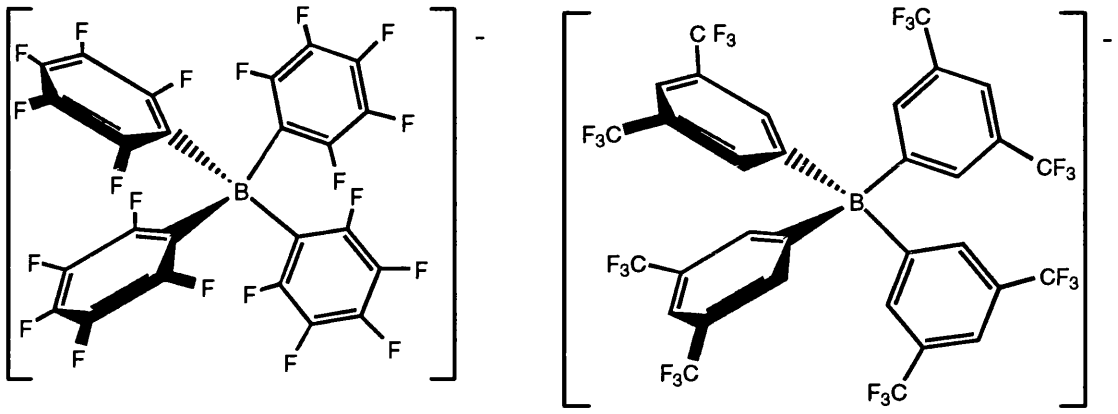

Figure 3: Stucture of the $[B(C_6F_5)_4]^-$ and $[B\text{-}(3,5\text{-}C_6H_3(CF_3)_2)_4]^-$ anions

By placing electron withdrawing groups, fluoride and trifluoromethyl, onto the aromatic rings the π-coordination is suppressed and the reduction potential is raised. In fact there are no examples of either of these two anions coordinating to a metal centre via π-interactions. The electron withdrawing substituents also reduce the tendancy for B – Ar cleavage by decreasing the amount of negative charge in the ipso carbon atoms.

Although these anions are much more stable than $[BPh_4]^-$ and are weaker coordinating anions they are still not the 'noncoordinating anion'. $[B(C_6F_5)_4]^-$ can coordinate to metal ions through lone pairs on fluorine. The X-ray crystal structure of $Th(Cp^*)_2(Me)(B(C_6F_5)_4)$ shows that there are two Th – F –C bridges, involving an *ortho, meta* pair of fluorine atoms, [112] *Figure 4.* The Th – F(*ortho*) and Th – F(*meta*) bond lengths are 2.757(4) and 2.675(5) Å respectively and are longer than the sum of the Th^{4+} and F^- ionic radii (~2.3 Å) [113] and shorter than the sum of the Van der Waals radii(~3.26). [114]

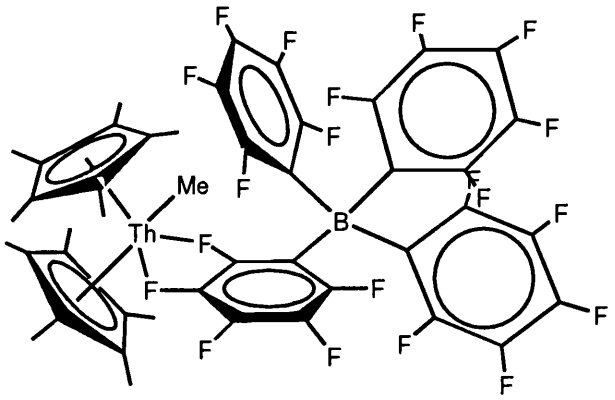

Figure 4: Coordination of $[B(C_6F_5)_4]^-$ anion to a Th metal centre

This compound is more than three orders of magnitude more reactive for olefin polymerisation than $Th(Cp^*)_2(Me)(BPh_4)$ for which the anion is found by ^1H NMR to be bound by π-coordination. [115]

Another related weakly coordinating anion is formed when $B(C_6F_5)_3$ is added to complexes such as $[M(Cp^*)_2R_2]$, $[M(Cp^*)R_3]$, and MR_4 (M = Ti, Zr R = alkyl). [116] In one case with the $Zr(1,2\text{-}C_6H_3Me_2)(Me)_2$ complex the resulting anion is $[(Me)B(C_6F_5)_3]^-$, this system has been structurally characterised and found to have the anion linked to the metal centre via Zr – H_3CB interactions, [117] *Figure 5.*

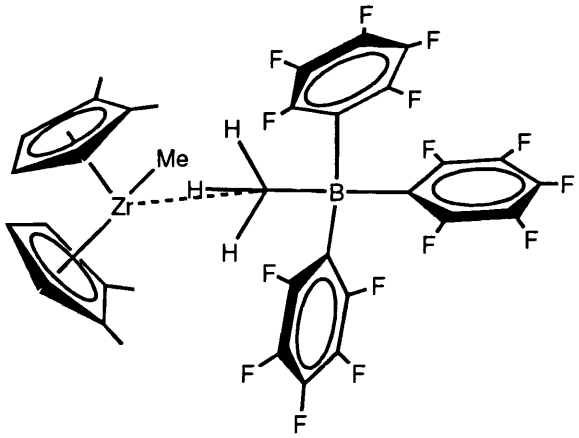

Figure 5: Coordination of the $[(Me)B(C_6F_5)_3]^-$ anion through a Zr – Me interaction

The methyl group with a formal δ^- charge migrates onto the Lewis acidic boron atom, the Zr – C (bridging) bond length is 2.549 (3) Å compared with the shorter Zr – C (methyl) bond length 2.252 (4) Å. The shortest Zr – H (bridging) length is 2.25 (3) Å

greater than typical terminal and bridging Zr – H bond distances 1.78 (2), 1.94 (2), and 2.05 (3) Å. [118] This anion has also been found to involve the assistant coordination of one *ortho-* fluorine atom in the complex $[(Cp^*SiMe_3)_2Y(Me)(MeB(C_6F_5)_3]$, [119] *Figure 6.*

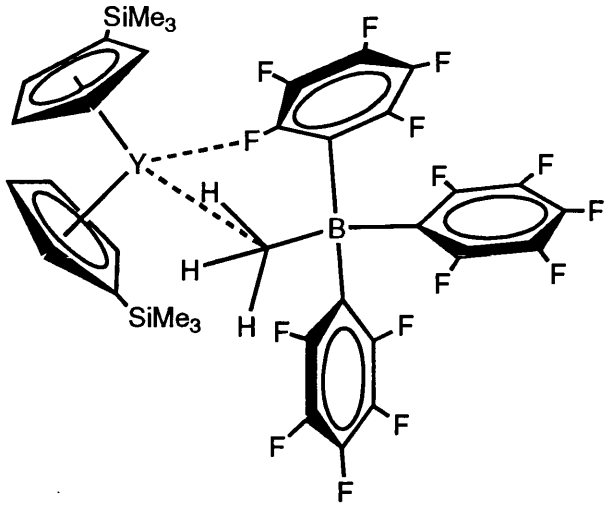

Figure 6: Coordination of $[(Me)B(C_6F_5)_3]^-$ anion through Y – Me and Y – F interactions

In this complex the agostic interactions of two of the three hydrogen atoms of the boron – methyl group, have Y – H contacts of 2.18 (5) and 2.43 (4) Å. These Y – H interactions are similar in length to those observed for the previous Zirconium complex, with yttrium and zirconium having nearly identical covalent radii, but the Y – C distance (bridging) of 2.853 (7) Å is much longer and cannot be considered as a bonding interaction as in the zirconium case. The Y – F bond length is 2.366 (3) Å a relatively strong interaction as compared with another weakly fluorine coordinating anion complex $(Cp^*)_2Zr(H)HB(C_6F_5)_3$ with Zr – F bond lengths 2.416 (3) and 2.534 (3) Å. [120]

Variations on these fluorinated anions have recently been synthesised tris(2,2',2''-perfluorobiphenyl)borane, [121] bis(pentafluorophenyl)(2-perfluorobiphenyl) borane, tris(β-perfluoronaphthyl)borane, [122] and octafluoro-9,10-bis(pentafluorophenyl)-9,10-diboraanthracene [123] being just a select few, *Figure 7.*

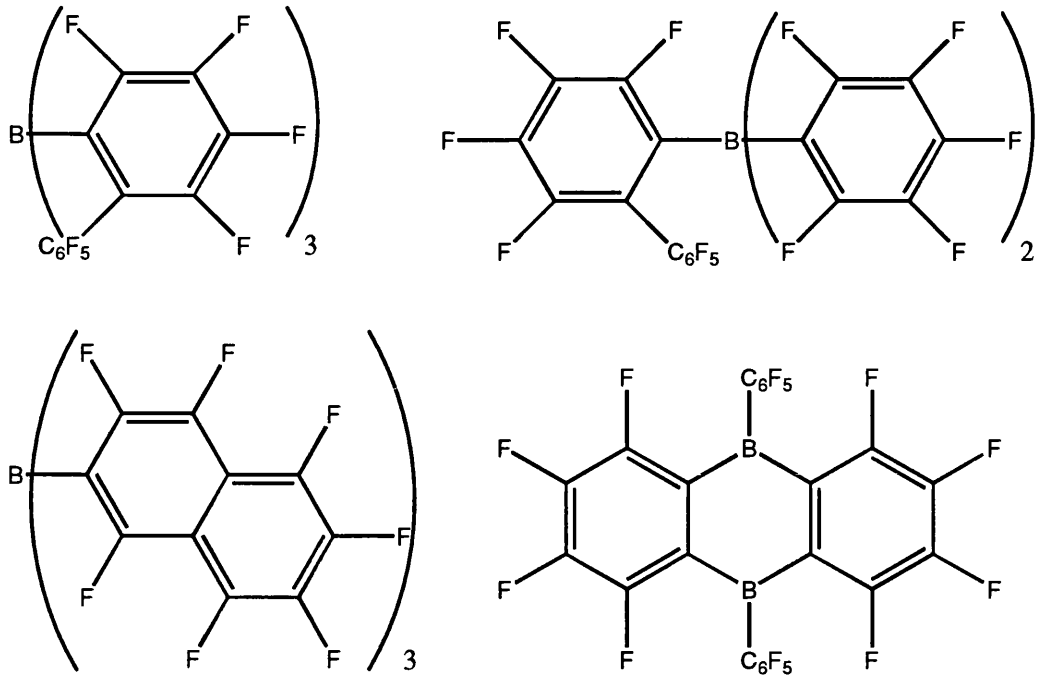

Figure 7: Selection of fluorinated borate anions

These anions all add different qualities to the reactive system, reducing decomposition rates, enhancing solubility, or elevating reaction efficiency.

Aluminium containing anions, of similar form to the borate anions, have also been synthesised and found also to be weakly coordinating. A couple of examples are $[Al(F)(C_{12}F_9)_3]^-$, [124] and $[Al(OC_6F_5)_4]^-$, [125] *Figure 8.*

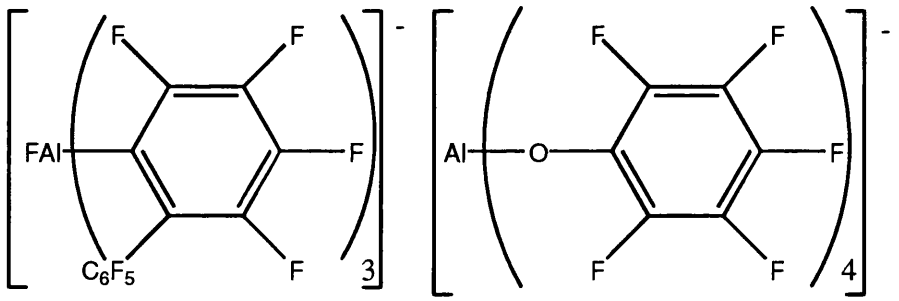

Figure 8: Selection of fluorinated aluminium anions

Ethylene polymerisation activities achieved by in-situ activation of $(Cp^*)_2ZrMe_2$ are comparable to those seen with the borate anions. The $[Al(F)(C_{12}F_9)_3]^-$ anion is the stronger coordinating anion of the two forming an almost linear Zr – F – Al bridge in

the structure rac-$Me_2Si(Ind)_2Zr(CH_3)$ $Al(F)(C_{12}F_9)_3$ [126] with a Zr – F bond length of 2.123 (6) Å.

Another class of weakly coordinating anions are the carborane anions, instead of being based upon a Lewis acidic central atom strongly bound to ligands that are weakly coordinating, these anions involve the use of a stable univalent polyhedral moiety. The *closo*- carbaboranate ions $[CB_{11}H_{12}]^-$ and $[CB_9H_{10}]^-$ are classic examples with all the B – H bonds being very stable and only weakly coordinating, however both these ions are prone to oxidation. It was found that halogenation of these parent anions resulted in much more robust systems, one of the most stable weakly coordinating anions to date, and so anions of the form $[CB_{11}H_6X_6]^-$ (X = Cl, Br), *Figure 9*, were developed. [127, 128]

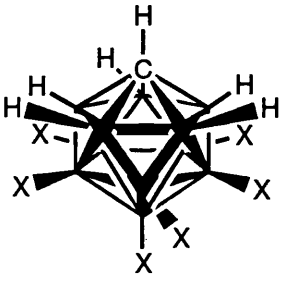

Figure 9: Structure of *closo*-carbaboranate anions

These anions can be almost completely halogenated to give ions of the type $[HCB_{11}X_5Y_6]^-$ (X, Y = Cl, Br, I) [129] and exclusively methylated $[CB_{11}Me_{12}]^-$. [130] Of all the carborane anions the most weakly coordinating is $[1\text{-}R\text{-}CB_{11}F_{11}]^-$ (R = Me, Et). [131] But despite carboranes proven ability as weakly coordinating anions as well as their stability, the halogenated ions are not widely used due to the expensive and time consuming multistep procedure of their preparation.

For a metal catalysed olefin polymerisation or oligomerisation using any given metal (M) usually starts with a precatalyst of the form L_nMX_m that is relatively stable, but in its present state is unreactive towards olefins. To transform this precatalyst into an active species a co-catalyst(s) is required. The preferred geometry of this active catalyst $[L_nMR_{(m-1)}]^+$ (R = H, alkyl) involves a metal with a vacant coordination site that is able to bind a molecule of olefin and an alkyl group, or hydride, into which the olefin will be able to insert. (Further mechanistic details will be discussed in chapter 5)

To produce these active species it was found that aluminium alkyls and alkylaluminium chlorides were very useful activators in classical heterogeneous Ziegler – Natta catalysis. [132, 133] As an example, Vanadium catalysts activated by aluminium alkyls were found to promote the syndiospecific polymerisation of propylene at temperatures below –60 °C. [134] Cp_2TiCl_2 in the presence of diethylaluminium chloride was found to promote the homogeneous polymerisation of ethylene under mild conditions. [135] Subsequent studies and detailed spectroscopic, kinetic and isotope-labelling studies have contributed significantly to the understanding of olefin polymerisation using homogeneous Ziegler – Natta systems in terms of cocatalyst function. [136, 137, 138] These studies demonstrated that ligand exchange between Cp_2TiCl_2 and the R_2AlCl cocatalyst forms the alkyl titanocene complex $Cp_2Ti(R)Cl$ which on adduct formation polarises the Ti – Cl bond $Cp_2Ti^{\delta+}(R)\text{-}Cl\cdots Al^{\delta-}R_2Cl$. This species can then undergo insertion of a molecule of olefin into the Ti – R bond. A suggestion was put forth on the possible participation of the cationic species $[Cp_2TiMe]^+$ in the polymerisation process [139] based upon electrochemical results. This species could be generated by the abstraction of Cl^-, by an aluminium species, and ethylene insertion could take place at a true cationic centre, [140] *Figure 10.*

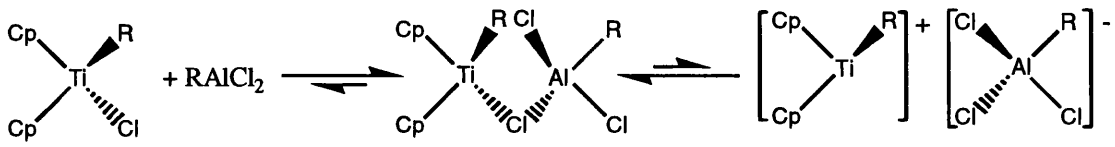

Figure 10: Generation of a cationic Ti centre from the Cp_2TiCl_2 system

Capture of the complex after first insertion of a silylacetylene molecule revealed a structure, *Figure 11*, that argued strongly in favour of the cationic species $[Cp_2TiR]^+$ ion paired with $AlCl_4^-$. [141]

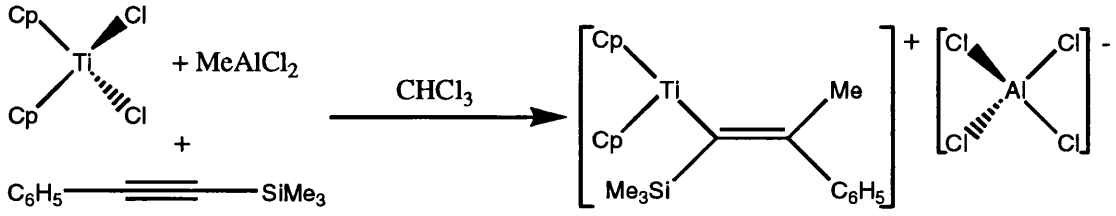

Figure 11: Mimic structure of the first insertion of olefin into Ti – Me bond

Extensive kinetic and reactivity studies as well as multinuclear NMR investigations have demonstrated that dynamic equilibria exist between the contact ion pairs $Cp_2Ti(R)\cdots Cl\cdots AlCl_3$ and the solvent separated ion pairs $[Cp_2TiR]^+[AlCl_4]^-$ which are the most catalytically active sites. [142, 143] The contact ion pairs that are the dominant species in solution are relatively unreactive sites. In polar solvents and at higher dilution the equilibrium is pushed in favour of the solvent separated ion pairs and therefore enhances catalytic activity. However these systems activated by alkylaluminium chlorides only exhibit polymerisation activities for ethylene and no α-olefins. This inability to polymerise larger olefins limited the use of this activator.

The tandem activation by trialkyl aluminium and an ion pair with a weakly coordinating anion has been used to great effect to generate the active catalytic species

for polymerisations. The chemistry of trialkyl aluminium is predominantly due to its high Lewis acidity. As the aluminium is short of a full shell of electrons it desires an extra lone pair of electrons to be donated to it, and therefore has a large affinity towards elements such as oxygen and halogens that are able to fulfil this need. Trialkyl aluminium is therefore attracted towards chloride ligands and on formation of a relatively strong Cl – Al bond will undergo ligand substitution and replace the chloride with an alkyl group thus breaking a relatively weak Al – C bond. Via this process a metal chloride precatalyst can be alkylated and then can proceed to an active catalytic species by interacting with a precursor weakly coordinating anion. There are a number of ways of introducing the weakly coordinating anion to promote the formation of the active cationic metal species, *Scheme 1*.

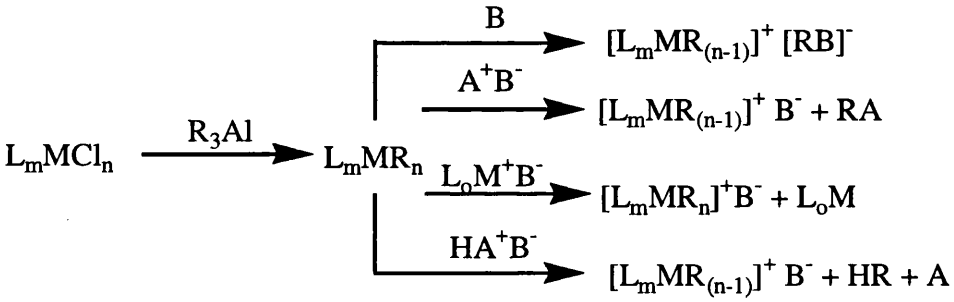

Scheme 1: Methods for introducing borate anions

Reaction of a borane (B), or with a coordinatively unsaturated Lewis acid such as surface sites on dehydroxylated alumina, [144] with the alkylated complex gives the desired cationic metal species with a borate anion which has abstracted an alkyl group from the metal. Reaction of a trityl (Ph_3C^+) salt of a weakly coordinating anion (A^+B^-) with the alkylated complex gives the metal cation – weakly coordinating anion pair and a non-coordinating organic compound Ph_3CR. The Lewis acidic trityl cation is able to abstract an alkyl group from the metal centre thus cleaving the M – C bond and forming an inert species in further reaction. A one electron redox reaction can take place between the metal complex and a silver salt, [145] or ferrocenium salt [122] of the borate.

One other method is via protonolysis of the M – C bond by reacting the alkylated complex with a trialkylammonium ($[HNR_3]^+$) or protonated diethyl ether ($[H(OEt_2)_2]^+$) salt of the weakly coordinating anion. This method also produces the metal – weakly coordinating ion pair but with an equivalent of alkane and either a tertiary amine or diethyl ether. On successful activation the tertiary amine or the diethyl ether is sometimes found to be the most Lewis basic component in the reaction mixture and so has been found to coordinate to the metal centre, in what would be the vacant coordination site, *Figure 12*. [146, 147, 148] Dimethylaniline (DMA) is less basic than trialkylamines due to resonance stabilisation of the nitrogen lone pair into the phenyl ring therefore, is more weakly coordinating and the preferred amine on introduction of the borate anion.

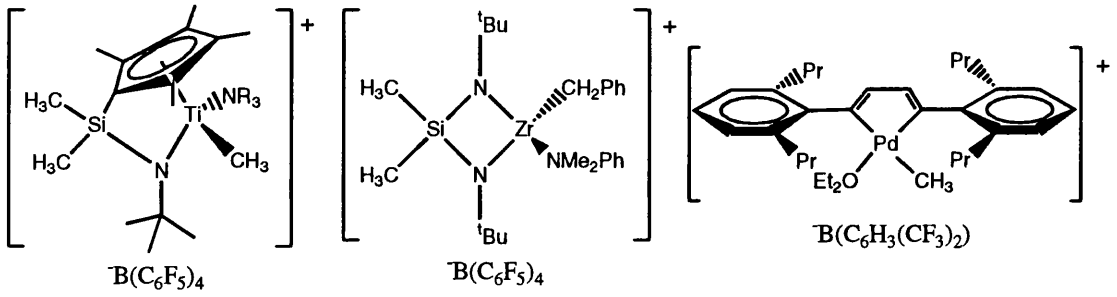

Figure 12: Coordination of amine after activation

In contrast there are also cases where the amine or diethyl ether are found to play no role in coordinating to the electrophilic metal centre. In two zirconium complexes incorporating 8-quinolinato ligands with similar steric environments, it is shown that increased electrophilicity of the metal induced by the electron withdrawing ligand governs the strength of amine coordination. [149] The effect of the coordination of amine during polymerisation is contested. A study on the Cp^*TiMe_3 / Al^iBu_3 / $[ammonium]^+[B(C_6F_5)_4]^-$ system shows a sharp increase in activity with decreasing pK_a of the ammonium salt. [150] However, other reports [151, 152] suggest that the presence of

amine have no detectable effect upon the polymerisation activity. This is thought to be due to the catalyst being dissociated from the amine at dilute concentrations, and that amine coordination is not a limiting factor in the ethylene polymerisation by the $(C_5H_4SiMe_3)_2ZrMe_2$ / $PhNHEt_2^+B(C_6F_5)_4^-$ system. [148]

What is now the most common form of activation for metal catalysed polymerisations was discovered by the addition of water to the halogen free polymerisation inactive Cp_2ZrMe_2 / $AlMe_3$ system. On this addition a surprisingly high activity was found for the polymerisation of ethylene. [153] This discovery brought about the highly efficient methyl aluminoxane (MAO) activator. [154] MAO is prepared by the controlled hydrolysis of $AlMe_3$ and typically having 5 – 20 [-Al(Me)-O-] units in the polymeric structure, but its exact structure is still unclear. [155, 156] Proposed structures include one dimensional linear polymers, or cyclic rings, which contain three coordinate aluminium centres, two-dimensional structures and three-dimensional clusters with four coordinate aluminium, *Figure 13.*

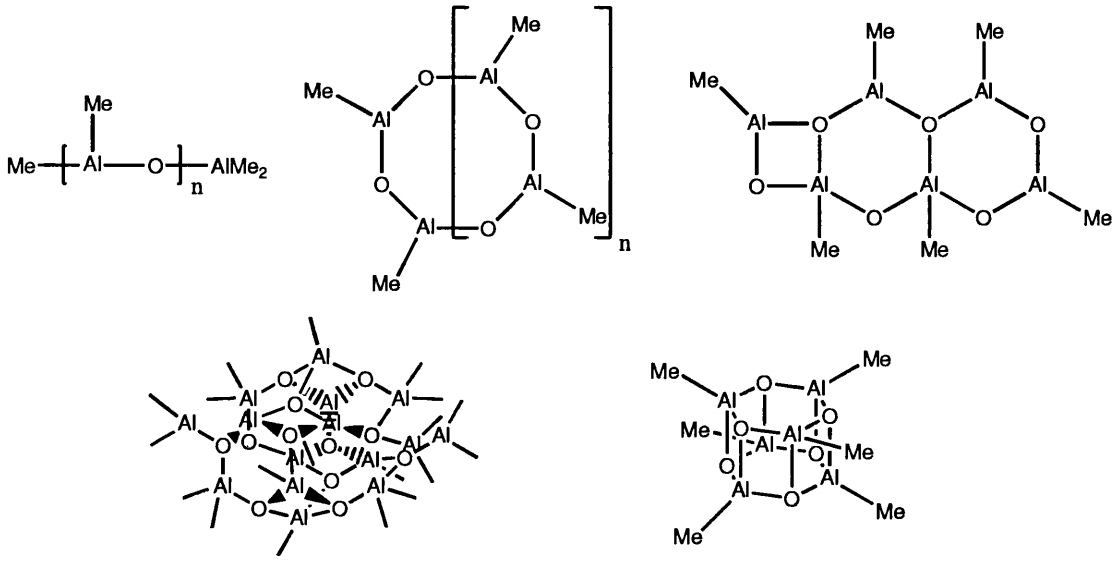

Figure 13: Proposed structures of MAO

The most recently proposed of these structures is the three-dimensional cage structure [157] with the basic formula $[Al_4O_3(CH_3)_6]_4$ with a CH_3 : Al ratio of ~1.5 which is in agreement with the general formula $[AlO_{0.8\text{-}0.75}(CH_3)_{1.4\text{-}1.3}]_n$ reported from ^1H NMR studies. [158] This structure contains four coordinate aluminium in the main body of the cluster with three coordinate aluminium on the periphery. From the ^{27}Al NMR spectroscopy of MAO it is found that the majority of the aluminium environments are four coordinate but there are some three coordinate aluminium species in the structure. [159]

Toluene solutions of MAO can be used to activate such complexes as Cp_2ZrCl_2 upon which there is a rapid ligand exchange generating predominantly the mono-methyl complex $Cp_2Zr(Me)Cl$. [160] Under the usual conditions when using MAO, at least a two hundred fold excess of the MAO to catalyst, the reaction can be pushed through to the dimethyl complex Cp_2ZrMe_2. After initial ligand exchange it is generally assumed that some of the aluminium centres have an affinity towards chloride abstraction from $Cp_2Zr(Me)Cl$ or $^-CH_3$ abstraction from Cp_2ZrMe_2. From ^{13}C and ^{91}Zr NMR spectra Cp_2ZrCl_2 / MAO solutions it was found that ion pairs such as $Cp_2ZrMe^+Cl[\text{-}Al(Me)O\text{-}]_n^-$ or $Cp_2ZrMe^+Me[\text{-}Al(Me)O\text{-}]_n^-$ are formed. [161]

On activation with MAO it is now generally accepted that Cp_2ZrCl_2 is only mono alkylated, by the MAO directly or by residual $AlMe_3$ in the MAO, followed by abstraction of the second chloride substituent to form the catalytically active species, *Scheme 2.*

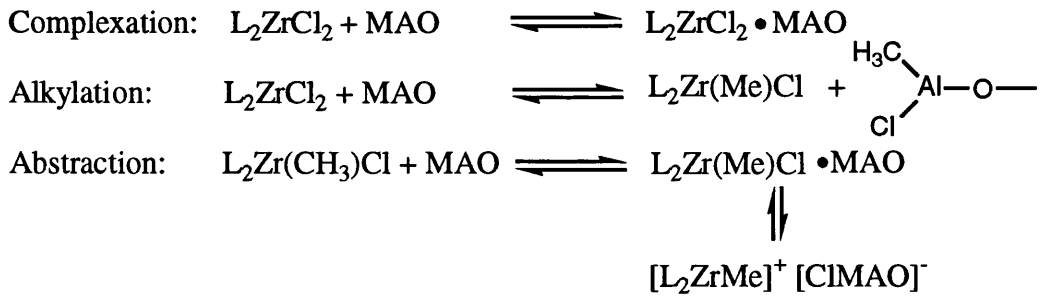

Scheme 2: Activation of Cp_2ZrCl_2 with MAO

Comparative NMR studies between the two systems $Cp_2Ti(CH_3)Cl + AlMe_3$ and $Cp_2Ti(CH_3)Cl$ + MAO reveal that MAO is the superior alkylating agent, the stronger Lewis acid, and so the greater ability to undergo the abstraction process, and also forms a less coordinating anion compared with $AlMe_3$. [162] In fact the equilibrium for the abstraction process involving $AlMe_3$, *Scheme 3,* is way over to the left, the opposite of which is seen in the case of MAO.

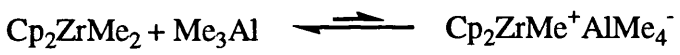

Scheme 3: Equilibrium for methyl extraction with $AlMe_3$

From this information it is evident that the free trimethyl aluminium is not the active cocatalyst. ^{13}C NMR studies have been conducted upon a ^{13}C enriched $Cp_2Zr(^{13}CH_3)_2$ complex and MAO during ethylene polymerisation. The results of which provide evidence for the formation of monomeric $Cp_2ZrMe^+MeMAO^-$, dinuclear $(Cp_2ZrMe)_2(\mu\text{-}Me)^+MeMAO^-$, as well as the heteronuclear $Cp_2Zr(\mu\text{-}Me)_2AlMe_2^+MeMAO^-$ species. [163] The two dinuclear complexes are possible dormant states for the active sites in olefin polymerisation.

4.2: Results and Discussion

4.2.1: Borates

The $[B(C_6F_5)_4]^-$ anion has been synthesised with a variety of different cations by modified methods of published procedures, [164,165] *Scheme 4*. Starting from the lithium salt of the anion the dimethylanilinium ($PhMe_2NH^+$) salt, diethylanilinium ($PhEt_2NH^+$) salt, and tetrabutylammonium (*n*-Bu_4N) salt have been made. Synthesis can also be performed going through the very useful $B(C_6F_5)_3$ borane using Grignard reagents [166] that are cheaper than alkyl lithium reagents and can also be handled, in larger quantities more safely. By passing the borane can also lead to the $BrMg^+B(C_6F_5)_4^-$ ion pair that has also been converted into the dimethylanilinium borate salt.

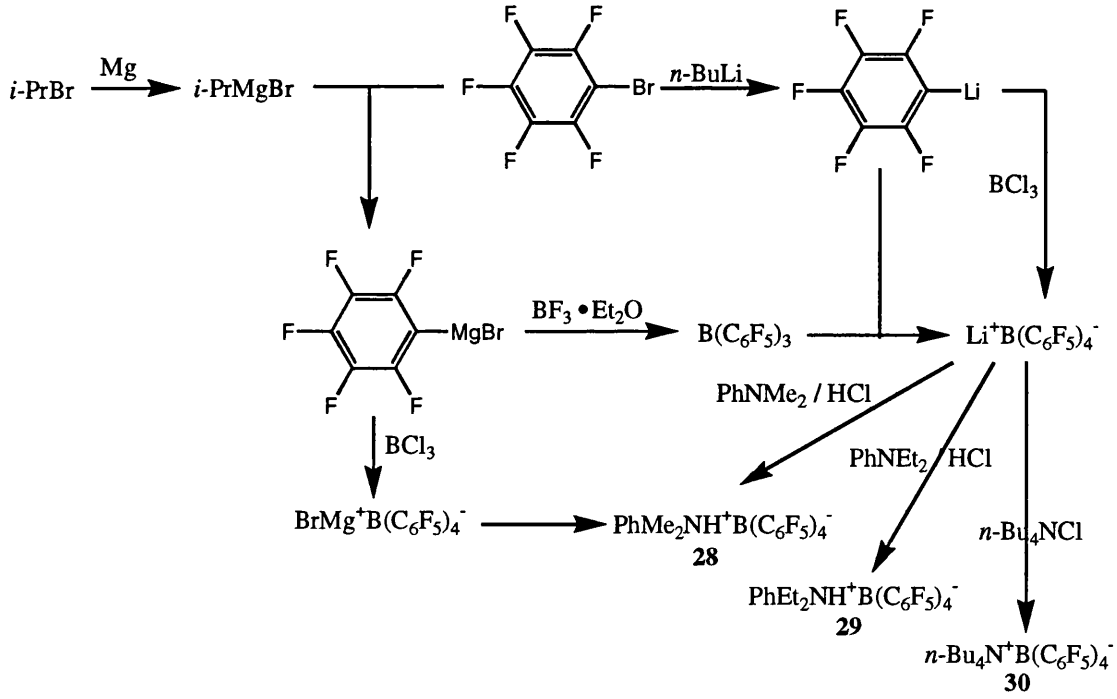

Scheme 4: Reaction scheme of the formation of borate salts

The ^{19}F NMR spectra of the three ammonium borate salts are very similar to each other and in comparison with the spectra of the trityl salt [167] of the same borate

apart from a slight upfield shift due to the effect of a different solvent but the shift difference between the peaks remains almost constant, *Table 1*.

	o-F / ppm	*m*-F / ppm	*p*-F / ppm
$PhNHMe_2B(C_6F_5)_4$	-133.2 (bs)	-167.5 (dd, J 15.7 Hz)	-163. 5 (t, J 20.5 Hz)
$PhNHEt_2B(C_6F_5)_4$	-133.3 (bs)	-167.4 (dd, J 16.0 Hz)	-163.4 (t, J 21.0 Hz)
$Bu_4NB(C_6F_5)_4$	-132.4 (bs)	-166.2 (bm)	-162.3 (t, J 19.6 Hz)
$Ph_3CB(C_6F_5)_4$ [168]	-125.7 (bs)	-160.0 (dd, J ca. 18 Hz)	-156.1 (t, J 20.6 Hz)

Table 1: ^{19}F NMR data for **28, 29, 30** and the trityl salt of the same borate anion

Other than the chemical shifts the spectra have the same form in all of the compounds. The *ortho*-fluorine signal portrayed as a broad singlet λ = 58 Hz in both cases showing no distinctive coupling pattern. The *meta*-fluorine signal is a doublet of doublets with both F – F couplings of equal strength with the neighbouring substituents and hence takes the appearance of a triplet pattern. The *para*-fluorine signal has the distinctive triplet pattern due to F – F coupling to two neighbouring fluorine substituents in identical environments.

4.2.2: DMAB Chromium Complexes

$R_3TACCrCl_3$ complexes have been activated in a two stage process first the addition of the weakly coordinating anion with anilinium counter ion followed by trialkyl aluminium. Following this procedure a single site catalyst with a well-defined anion is produced. The corresponding activation with MAO, with an indefinite structure and active site, causes greater problems in the interpretation of the catalytic cycle.

Treatment of one equivalent of the dimethylanilinium borate (DMAB) **28** to a $R_3TACCrCl_3$ complex in benzene, toluene, or DCM solution at room temperature yields an adduct by which dimethylanilinium (DMAH) is associated with the chloride substituents of the chromium complex via hydrogen bonds, [169] *Scheme 5.*

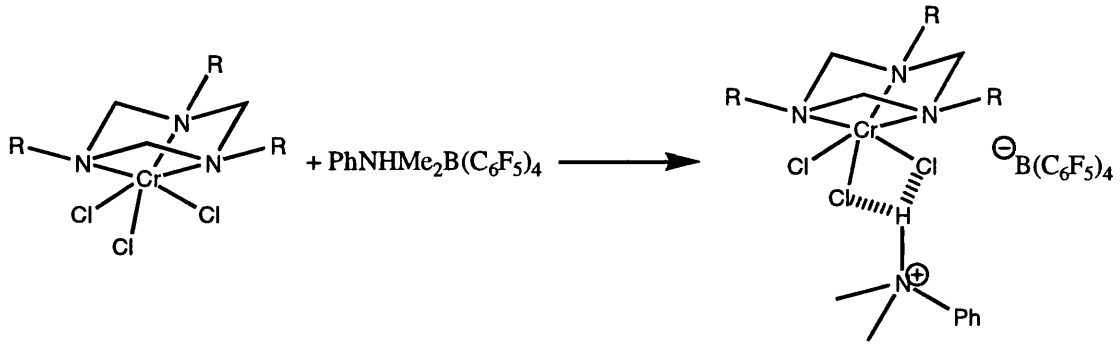

Scheme 5: Formation of $R_3TACCrCl_3$DMAB complexes

Formation of the DMAH adduct dramatically enhances the solubility of the parent $R_3TACCrCl_3$ complex, to the extent that previously insoluble complexes, i.e $Me_3TACCrCl_3$ in DCM, is soluble as the anilinium adduct.

Reaction of the $(2\text{-}PhEt)_3TACCrCl_3$ complex with **28** in toluene solution yields $(2\text{-}PhEt)_3TACCrCl_3(PhNHMe_2)[B(C_6F_5)_4]$. **31** After partial removal of solvent to give a saturated solution and layering with hexane purple crystals of the named product were formed after 4 days. These crystals were analysed by X-ray crystallography, *Figure 14.*

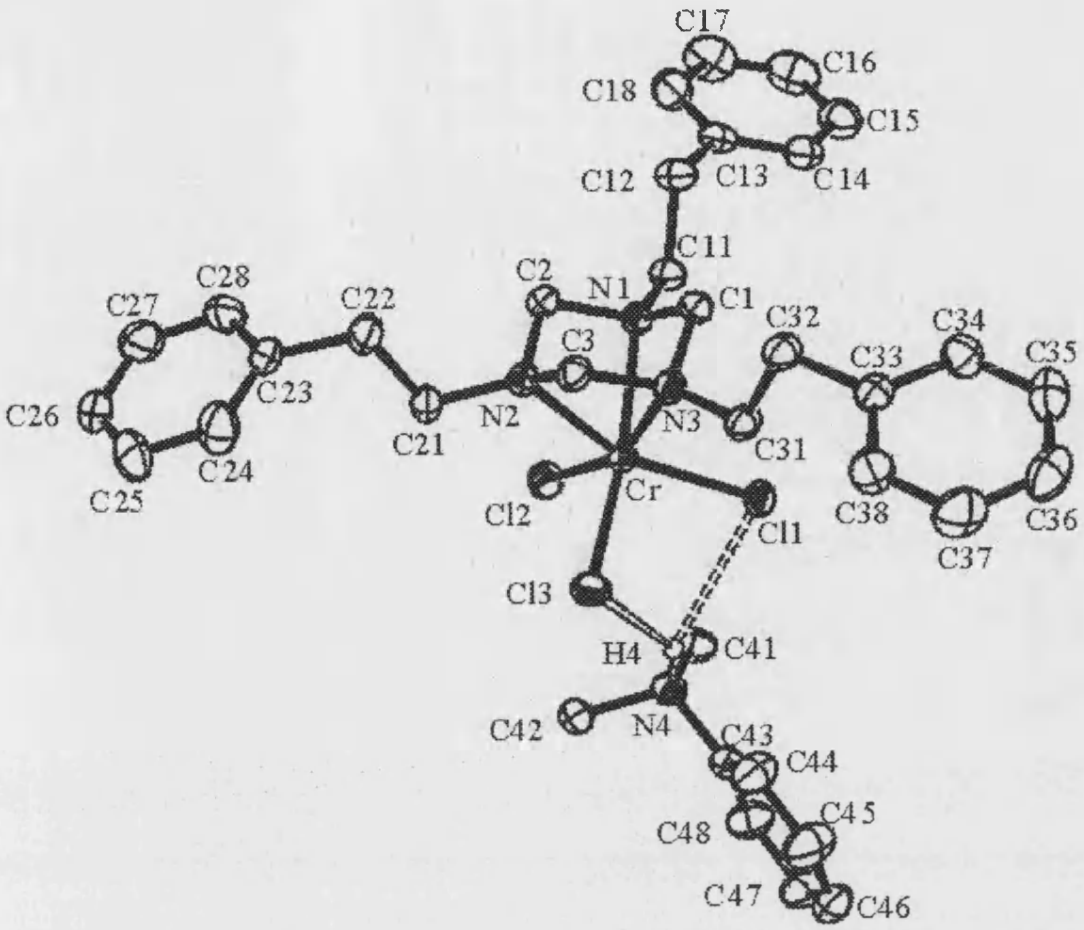

Figure 14: Structure of the cation in the $(2\text{-PhEt})_3TACCrCl_3DMAB$ complex

The dimethyl anilinium ion does not sit central to the three chloride substituents as this would involve the positively charged moiety at a relatively close distance to the electropositive chromium centre. Instead a bifurcated H bridge is formed between two of the chlorides with H – Cl crystallographic distances of 2.65 and 2.60 Å. This strong hydrogen bonding has a slight weakening effect upon two of the Cr – Cl bonds, hence a lengthening of theses bonds with respect to the third Cr – Cl bond whose bond length is slightly shorter than those seen in the $(2\text{-PhEt})_3TACCrCl_3$ complex, *Table 2*.

	Cl – Cr / Å	Cr – N / Å	Cl – Cr –Cl / °	N – Cr – N / °
(2-PhEt)$_3$TACCrCl$_3$ [PhNHMe$_2$]B(C$_6$F$_5$)$_4$	2.296 (5) 2.270 (5) 2.292 (5)	2.116 (14) 2.083 (14) 2.098 (14)	99.9 (19) 95.9 (18) 99.7 (19)	66.03 (8) 65.77 (7) 65.73 (7)
(2-PhEt)$_3$TACCrCl$_3$	2.277 (6)	2.103 (17)	99.0 (3)	66.2 (5)

Table 2: Selected bond lengths and angles of **31**

The attraction of the anilinium proton towards the two chloride substituents pulls them closer together and hence decreases the Cl – Cr – Cl bond angle by 3 ° with respect to the parent chromium complex. The greatest influence of the interaction between the chromium complex and the anilinium is to disrupt the hydrogen bonding network between chloride substituents and triazacyclohexanes of neighbouring molecules. (See chapter 3) For this complex there is no extensive hydrogen bonding throughout the structure, but just between two molecules to form an isolated di-nuclear structure, *Figure 15*.

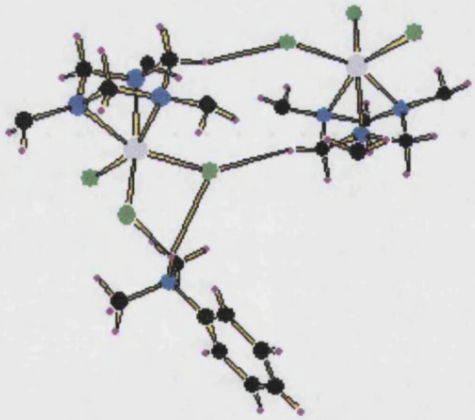

Figure 15: Intermolecular Cl···H hydrogen bonding within **31** (CH_2Ph groups removed for clarity)

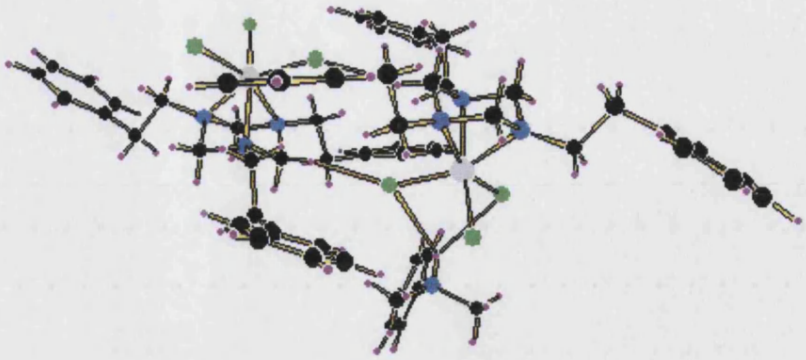

Figure 15 cont.: Intermolecular Cl ··· H hydrogen bonging within **31**

The first diagram with ($PhCH_2$) moieties removed from the triazacyclohexane arms, gives a clear image of the two relatively strong Cl – H hydrogen bonds (2.52 Å) are formed between a chloride substituent on one molecule with an equatorial methylene proton on the other molecule and vice versa. The chloride responsible for this interaction is also involved in hydrogen bonding to the anilinium and not the third chloride substituent that does not contribute to intra-molecular interactions. There are no more additional H ··· Cl contacts in the crystal structure with a shorter length than 3 Å. This disruption of the extensive hydrogen bonding network in the parent complex is a major contributing factor to the increased solubility, on addition of the borate salt, as interactions with solvent molecules will become more prolific. The second diagram gives a more complete picture of all interactions between the pair of molecules that includes π stacking between phenyl rings on neighbouring molecules.

Formation of this anilinium adduct does not lead to any significant change in the structure of the triazacyclohexane ligand or its bonding to the chromium with all bond lengths and angles being comparable to that seen in the $(2\text{-}PhEt)_3TACCrCl_3$ complex.

The same procedure for the preparation of the previous anilinium adduct was followed starting from the $(2\text{-EtBu})_3TACCrCl_3$ complex. Purple crystals of $(2\text{-EtBu})_3TACCrCl_3(PhNHMe_2)[B(C_6F_5)_4]$ **32** were formed, *Figure 16*.

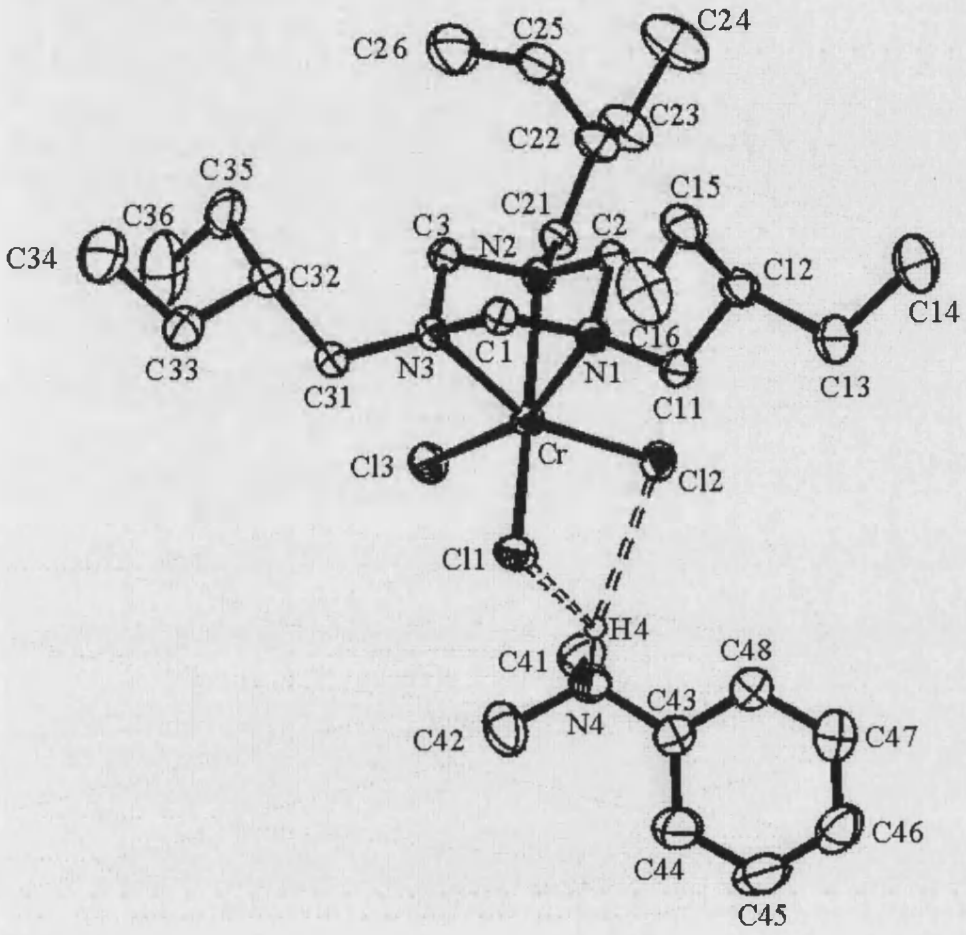

Figure 16: Structure of the cation in the $(2\text{-EtBu})_3TACCrCl_3DMAB$ complex

Once again the bifurcated hydrogen bonds to two of the three chloride substituents are formed. (2.74 and 2.59 Å) As before there is an extension of the Cr – Cl bonds of the respective chlorine substituents, *Table 3*.

	Cl – Cr / Å	Cr – N / Å	Cl – Cr –Cl / °	N – Cr – N / °
$(2\text{-EtBu})_3TACCrCl_3$	2.293 (7) $_a$	2.103 (18)	97.4 (3)	66.0 (7)
$[PhNHMe_2]B(C_6F_5)_4$	2.283 (7) $_b$	2.115 (19)	98.4 (2)	66.3 (7)
	2.282 (6) $_c$	2.095 (19)	98.0 (3)	66.4 (7)

$_a$ Cr – Cl(1), $_b$ Cr – Cl(2), $_c$ Cr – Cl(3)

Table 3: Selected bond lengths and angles for **32**

The attraction of the anilinium to the two chloride substituents making the Cl – Cr – Cl bond angle smaller also occurs in this complex but is much less pronounced with a difference of only 1 ° compared with the other two bond angles. Once again the extensive hydrogen bonding network of the parent complexes is disrupted, but unlike with the previous anilinium adduct the relatively strong hydrogen bonds to form the dinuclear structure are also not formed due to the larger steric bulk of the nitrogen substituents, close to the triazacyclohexane, preventing the close interaction. Instead much weaker hydrogen bonds (2.91 Å) are formed to give a zig-zag chain of molecules, *Figure 17*. The structure is shown with (Et_2CH) groups removed from the arms of the triazacyclohexanes for clarity, but must be noted do not participate in intra-molecular interactions.

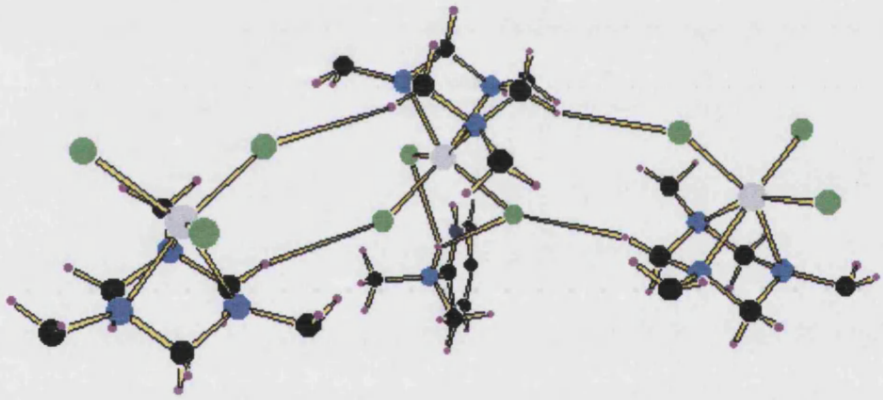

Figure 17: Intermolecular Cl···H hydrogen bonds within **32** ($CHEt_2$ groups removed for clarity)

NMR experiments on these anilinium adduct complexes have the same problems as with the precursors, (See chapter 3) hence the ^{1}H and ^{13}C spectra are very similar, *Table 4*. The nuclei close to the chromium, that may show differences compared with the parent molecules, give signals that are too broad to be analysed.

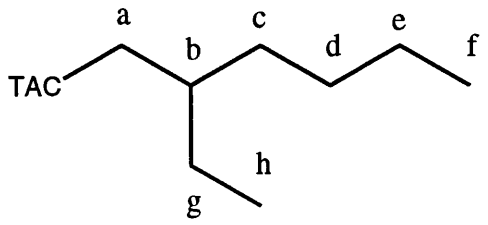

λ / Hz	a	b	c	d	e	f	g	h
$R_3TACCrCl_3$ DMAB	-	-	37.89	29.86	24.03	14.68	44.54	12.49
$R_3TACCrCl_3$	-	-49.56	42.14	29.39	21.86	12.02	46.15	14.45

Table 4: Comparative ^{13}C {^1H}NMR data for $(2\text{-EtHex})_3TACCrCl_3DMAB$ **33** and **17**

Deuterium nuclei closer to the chromium centre can be analysed by ^2H NMR in the $Do_3(d_6\text{-TAC})CrCl_3DMAB$ complex, **34** that was prepared in toluene solution in an NMR tube, the two methylene signals can be compared in **20**, *Table 5*.

	20 / DCM		**20** / Toluene		**34** / DCM		**34** / Toluene	
	Ax.	Equ.	Ax.	Equ.	Ax.	Equ.	Ax.	Equ.
δ / ppm	41.8	-5.7	~52	-	59.3	-5.6	58.3	-5.9
λ / Hz	384	612	~3500	-	443	656	703	1152

Table 5: Comparative ^2H NMR data of **20** and **34**

There is a significant downfield shift of the axial methylene deuterium signals on formation. These axial deuterium atoms are much more variable in these triazacyclohexane complexes as the C – D bond is trans- to the N – Cr bond and thus trans to Cr-Cl···DMA, hence any variation in the strength of the latter has an effect upon the former, and changes the environment of the deuterium nucleus respectively. In contrast with complex **20**, in which only the axial signal can be identified due to

association in solution, the signals for both the methylene deuterium signals can be observed for **34** in toluene. The toluene solution of **34** is still much more viscous than in DCM due to ion pairing and forming quadrupoles that would tend to be more sparse in polar solvent with a high dielectric constant which leads to more electrostatic interactions with the complex ions.

The behaviour of the anion can be monitored via ^{19}F NMR spectroscopy, in studying them in solution more information can be discovered about the metal species from the anion – cation interactions. On addition of the anilinium salt to the chromium pre-catalyst, analysis by ^{19}F NMR reveals the same pattern of three signals for the *ortho-*, *meta-*, and *para-* fluorine substituents. An average of all the fluorine environments in these designated positions are amalgamated to give the signals observed. These signals are broadened, compared with the spectra of a DMAB solution, due to paramagnetism of the solution generated by the chromium centres. Comparison of the three individual line widths can be made to give a guide on the average distance to a chromium centre for fluorine substituents in a given position in relation to the fluorine atoms in another position.

There are a number of variables that can affect these line widths and so comparison of line widths between spectra from different samples is speculative and should only be used as a rough guide. The line widths are dependent largely upon the viscosity of the solution, which means that they are concentration, temperature, and solvent dependent. They are also indirectly influenced by the size and shape of any ligands present on the metal centre as they determine the closest approach of the anion to the metal. These factors can be seen in the equation for the relaxation rate constant R

that is proportional to the line width, and the equation for the rotational correlation time τ_r which can be a significant factor in the value of the correlation time τ_c.

$$R_2 = \frac{4}{3}\left(\frac{\mu_0}{4\pi}\right)^2 \frac{\gamma_I^2 g_e^2 \mu_B^2 S(S+1)}{r^6}\tau_c \qquad \tau_r = \frac{4\pi\eta a^3}{3kT} = \frac{\eta MW}{dN_A kT}$$

τ_r is found to be dependent upon temperature T, proportional to both the viscosity η and molecular weight of the substrate MW.

NMR tube reactions of a variety of $R_3TACCrCl_3$ complexes with DMAB have been studied by ^{19}F NMR spectroscopy, *Table 6.*

$R_3TACCrCl_3$ DMAB (Solvent)	o- λ / Hz (δ / ppm)	m- λ / Hz (δ / ppm)	p- λ / Hz (δ / ppm)	Other F λ / Hz (δ / ppm)
R = Do **34** (Benzene)	220 (-131.07)	205 (-164.90)	146 (-161.74)	
Do (DCM)	44 (-132.86)	52 (-166.92)	44 (-162.98)	
2-EtHex **33** (Benzene)	233 (-131.65)	255 (-164.83)	186 (-161.60)	
FBz **35** (Chloroform)	49 (-130.14)	56 (-163.76)	49 (-160.01)	50 (-107.70)
2-EtBu **32** (Benzene)	218.4 (-132.91)	229 (-165.93)	174 (-162.47)	
^{t}Bu **36** (Benzene)	86 (-132.08)	74 (-165.86)	48 (-162.47)	
Me **37** (Toluene)	74 (-131.83)	67 (-168.60)	49 (-164.68)	
PhEt **31** (Chloroform)	149 (-130.48)	150 (-163.29)	111 (-159.95)	
2-$EtHex_2$FPh **38** (Benzene)	229 (-131.37)	255 (-164.28)	175 (-161.03)	343 (-114.34)

Table 6: ^{19}F NMR data for $R_3TACCrCl_3$DMAB complexes

As the peaks observed for the fluorine signals should be Lorentzian in shape: the line width λ of the peak can be measured by line fitting in the NMR computer software or by measuring at half peak height. As the peaks obtained are not all ideal Lorentz curves values measured at 1/5 height and 1/10 height give values of 2λ and 3λ

respectively. Averaging of all these three values are the line widths given in Table 6. For all solutions the concentration is approximately 0.026 mol/l except for $Me_3TACCrCl_3DMAB$, **37** that was not soluble enough at this concentration, and so a less concentrated saturated solution was used in this case.

For a freely rotating anion in which all the fluorine atoms occupy all positions at a fixed distance r from the boron atom then the average value for $<R^{-3}>^2$ (R is the distance F···Cr) can be calculated to $1/[D^2(D^2-r^2)^2]$ (with D the distance Cr...B). This average assumes that internal motions within the anion and cation are faster than the molecular tumbling of the ion pair. Cases in which the molecular tumbling is known to be faster an average of $<R^{-6}>$ is used. [170] Using the distances r (F...B) obtained from the crystal structures, that should be similar in solution, *ortho* 299 pm, *meta* 505 pm, *para* 584 pm. This means that *para* should be broader than *meta* and than *ortho*, and the difference in line width depends on D. For a value of D=10Å the ratio of line widths would be 1:1.5:1.9 for o,m,p. From the data the general trend for these anilinium adduct complexes is for a slightly less broadened *para* signal compared with similar *ortho* and *meta* signals. In solution the anion is not freely rotating but approaching the cation predominantly with a pair of *ortho* and *para* fluorine atoms. Solvent dependence is clearly evident from the two spectra of **34** in which the solvent system is changed from benzene to DCM. Addition of the more polar solvent produces a much less viscous solution the line widths observed in this case, and also **35** in chloroform, are reminiscent of those observed for the much less soluble complexes in less polar solvents i.e. **36** and **37**. This similarity in line widths is due to separation into freely moving cations and anions in these different solutions whereas in the more viscous solutions dipoles and possibly quadrupoles of ions are formed. (Discussed later in this chapter)

Inclusion of fluorine substituents onto the triazacyclohexane of the chromium complexes adds an internal reference by which the anion can be compared. Although the line width correlates to a distance between two nuclei that are not covalently bound it is attempted in this case as a rough guide with this in mind. To estimate whether this will be a significant factor the chemical shift of the fluorine under study can be compared with that of a similar fluorine atom in a diamagnetic complex. The fluorine signal of **35** is shifted by 6 ppm from that of a reported zinc complex $(FBz_3TAC)_2Zn^{2+}$ [171] with a shift of –113.5 ppm. This is not a large paramagnetic shift but still may distort the result. Assuming that the FBz groups adopt their most commonly observed orientations syn and anti, *Figure 18*, distances between metal and fluorine can be assumed to be similar to those in a previously published copper complex $(FBz_3TAC)_2Cu^{2+}$ [172] with a Cu-N bond length of 2.10 Å similar to chromium. In this complex Cu···F(syn) is 7.05 and Cu···F(anti) is 8.44 Å. The syn:anti ratio in this and other similar complexes is on average 1:1.

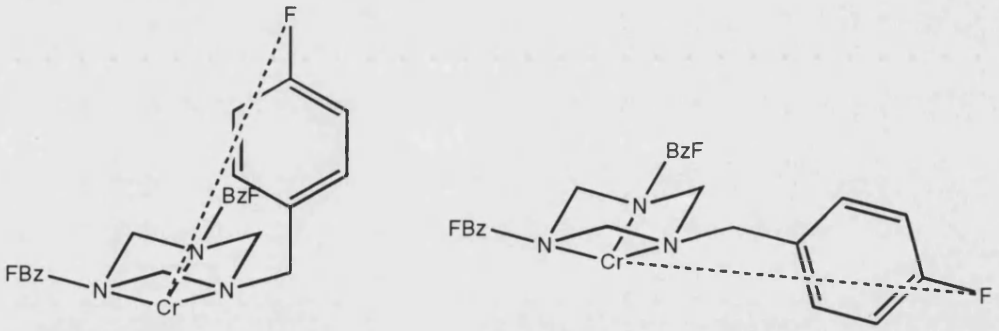

Figure 18: Cr···F Distances in syn and anti configurations of **35**

Taking this ratio and these bond lengths along with the line widths observed for **35** would give Cr···F values of 5.0, 4.9 and 6.4 ± 0.2 Å for *ortho*, *meta* and *para* fluorine atoms respectively considering that one set of *o,m,p* fluorine atoms dominate the R^{-3} sum. These values are in reasonable agreement with the solid state structure with the

closest Cr···F in the crystal structures of **31** and **32** of 5.5 Å. This value may be a bit longer due to the presence of many anions around a cation in the solid.

The $(2\text{-EtHex})_2(FPh)TACCrCl_3DMAB$ **38** complex provides a more reliable solution to this problem. The phenyl substituent on a triazacyclohexane only has a rotational motion around the N – C bond, *Figure 19*. The fluorine substituent on the phenyl group lies on this axis of rotation; hence there is no variation in distance between fluorine and chromium caused by this motion.

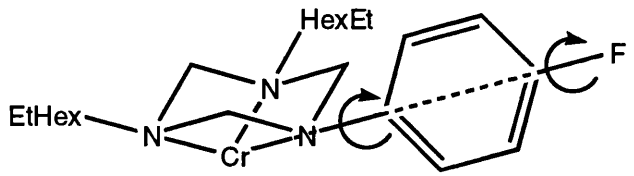

Figure 19: Cr...F Distance in **38**

As the Cr – F distance is fixed, 7.4 Å from average bond lengths and angles, comparison can be made with the anion fluorines. For relaxation due to dipolar coupling the line width is proportional to $1/r^6$. Using this relation averaging over all equivalent fluorine atoms in the anion, one set of *o,m,p* fluorine atoms are usually closest to Cr and dominate the sum of $\langle R^{-3} \rangle^2$, would lead to $R_{closest}$ of 5.0, 4.9 and 6.6 ± 0.2 Å for ortho, meta and para respectively. These values are in good agreement with those for the FBz calculation.

As mentioned earlier the line broadening caused by the chromium centres has concentration dependence. This property has been studied on complex **33** in toluene solution, *Figure 20.*

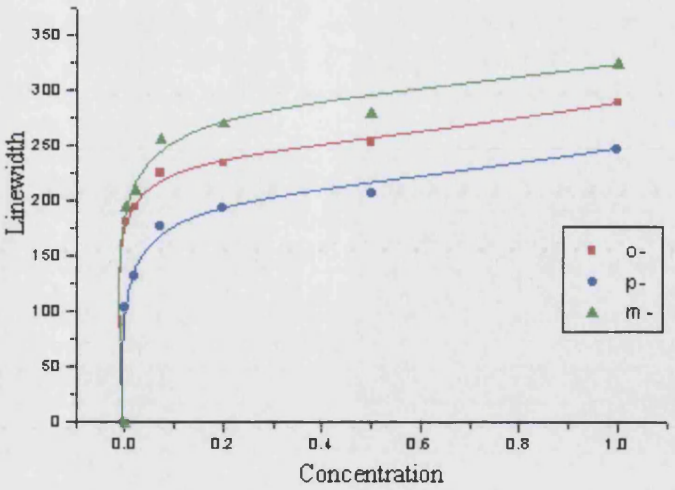

Figure 20: Dilution effect upon a toluene solution of **33**

All three fluorine positions follow the same trend on dilution of the solution, showing that the effect upon the anion is a general outcome and not a change in local orientation effecting the three fluorine positions differently. Starting from the most concentrated solution studied 0.138 M the line widths follow a steady linear decrease upon dilution. This constant change in line width is consistent with a reduction in viscosity of the solution. Extrapolation of the linear region to conc.=0 should give the line width at pure solvent viscosity if this is the only reason for the concentration dependence. This leads to an estimate for the mol volume of the dipolar complex. As the solution is diluted below a 0.01 M solution there is a dramatic increase in the rate of change of line width. This change is attributed to dissociation from dipoles in solution to separated ions as at extremely low concentration the distance between anion and cation will be great causing no paramagnetic line broadening, *Figure 21*.

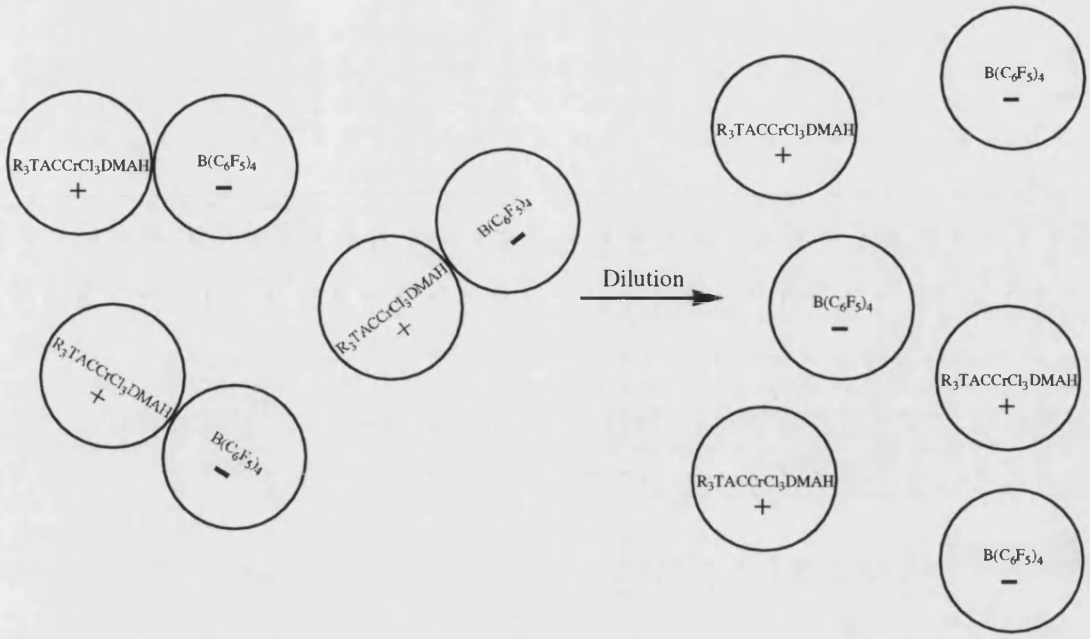

Figure 21: Dissociation of dipoles into separate ions upon dilution

For a dipolar solution the line widths of the fluorine signals will be larger than a corresponding separated ions solution as the anion is in close proximity to the paramagnetic centre of the cation. For solutions below 0.01 M once separated ions are the only species in solution there is another linear decrease in line width once again corresponding to a decrease in viscosity.

For more polar solvents this separated ions state is present at much higher concentrations, as solvation of the ions occurs, hence there is a reduced interaction between anion and cation.

4.2.3: Activation of Triazacyclohexane Chromium complexes

Addition of an excess of trialkyl aluminium solution to a purple solution of the anilinium adduct complex, under inert atmosphere, results in the formation of a green solution of alkylated chromium complex within seconds on stirring, *Scheme 6.*

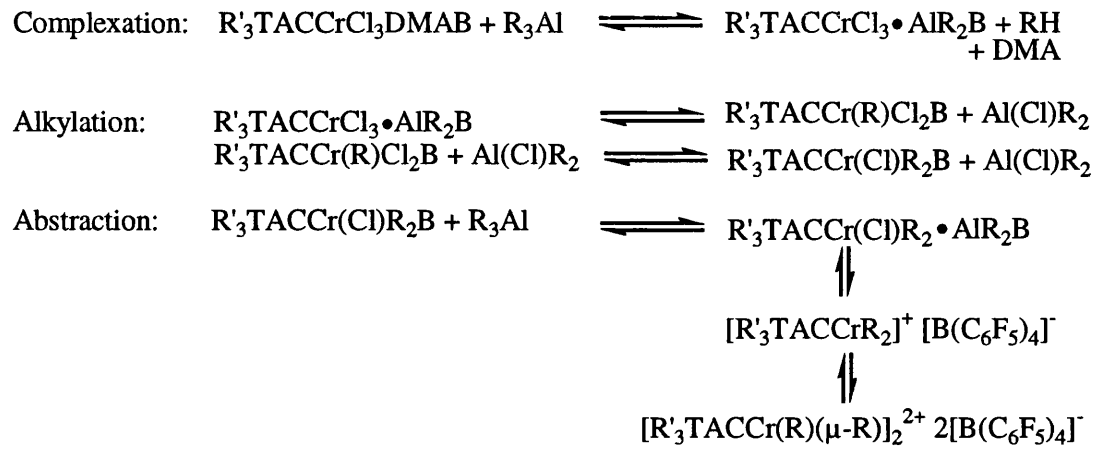

Scheme 6: Activation of $R_3TACCrCl_3DMAB$ with AlR_3

These alkylation reactions using various alkylaluminium compounds have mainly been carried out in NMR tubes and hence been studied by ^1H, ^2D, ^{13}C and ^{19}F NMR spectroscopy. As with the chromium trichloride precursor complexes these alkylated chromium compounds are also highly paramagnetic and therefore the signals in ^1H NMR of these complexes are measured with short acquisition times are very broad and show no distinctive difference than prior to alkylation. ^1H NMR spectra of these solutions run at standard parameters reveals no signals due to chromium complexes, due to fast relaxation, but a notable observation is the presence of sharp signals due to dimethylaniline. This observation can be seen in all cases and shows that the dimethylanilinium salt is no longer the counter ion of the borate anion and also that

the dimethylaniline is not involved in coordination with a chromium centre due to the sharp nature of the signals it produces.

^{13}C NMR spectra prove to be similar, as the ^{1}H NMR spectra the broad signals due to the alkylated complex show no distinctive differences to those previously observed for the corresponding chloride compound. As with the ^{1}H NMR spectra signals corresponding to the alkyl substituents (R = Me, Et, ^{i}Bu) on the chromium centre are not observable as the chain length is not sufficiently long enough to be at a distance at which the paramagnetic effect is not sufficiently strong to cause a line broadening too large to be observable. As with the ^{1}H NMR spectra the sharp dimethylaniline signals can be seen in the ^{13}C NMR spectrum.

^{19}F NMR spectra show quite distinct changes to those seen for the anilinium adduct complexes, *Table 7*, all the signals are significantly more broadened showing that on average the anion is closer to the chromium centre.

	o- λ / Hz (δ / ppm)	m- λ / Hz (δ / ppm)	p- λ / Hz (δ / ppm)
$Do_3TACCrCl_3DMAB$	317.4 (-131.37)	337.1 (-164.65)	237.9 (-161.77)
$Do_3TACCrCl_3DMAB$ / $Al^{i}Bu_3$	534.7 (-129.68)	-	913.0 (-158.14)
1 Day	278.6 (-130.98)	-	558.8 (-159.96)
2 Days	201.8 (-131.29)	(~-148)	407.6 (-160.64)
7 Days	78.4 (-132.05)	1594.0 (-163)	100.0 (-162.00)
17 Days	64.2 (-132.11)	923.3 (-164.49)	97.9 (-162.37)

Table 7: ^{19}F NMR data of **34** before and after activation with $Al^{i}Bu_3$

In the majority of cases the *meta-* signal shows the greatest effect and is quite often unobservable in the spectrum due to the extreme line broadening from the large paramagnetic effect over the short Cr – F distance. Hence, this would suggest a *m*-F – Cr close contact interaction. An estimated value for the line broadening of this signal can be extrapolated from the line widths of the **34** / Al^tBu_3 system during decomposition, *Figure 22*. Along with the line broadening there is a dramatic paramagnetic shift of the *meta-* fluorine signal. In the first spectrum where the broad peak is observable but still not measurable to a good degree of certainty it is found at δ ~ -148 ppm, hence, downfield of the *para-* fluorine signal. On decomposition the signal moves upfield until ending at a similar chemical shift to the *m*-F signal in **34**, a shift of approximately 17 ppm. The *ortho-* and *para-* fluorine signals show a much smaller paramagnetic shift of 2.5 and 4 ppm respectively.

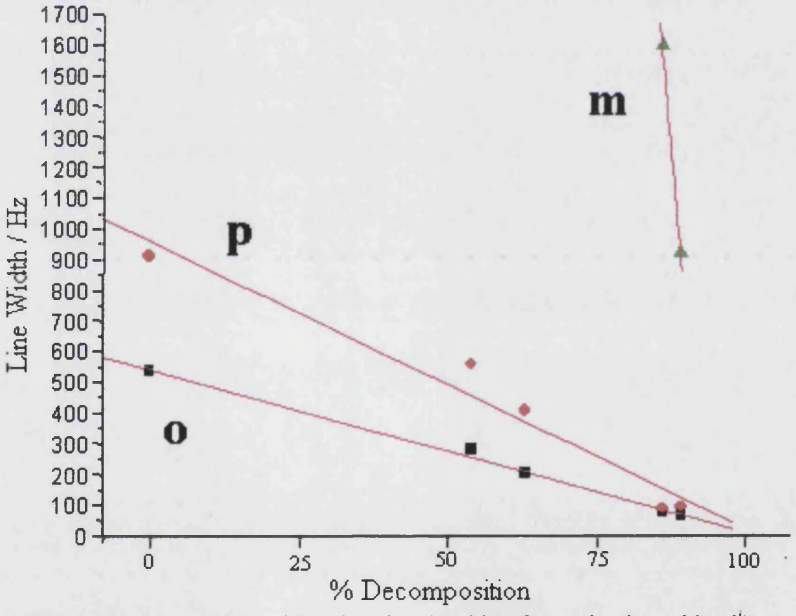

Figure 22: Line widths of fluorine signals of **34** after activation with Al^tBu_3

From an extension of the graph, (for more detail see chapter 5) the *meta-* fluorine has a line width of ~9000 Hz before decomposition. This value is a ten-fold

excess over either of the *ortho-* or *para-* signals and hence a *meta-* fluorine is the most strongly interacting part of the anion with the metal centre, *Figure 23.*

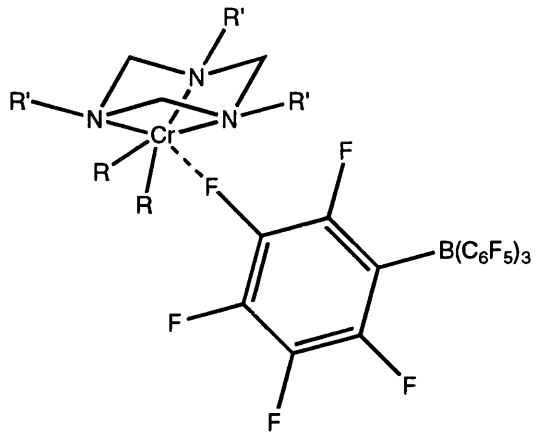

Figure 23: Proposed $R'_3TACCrR_2B(C_6F_5)_4$ activated complex

This proposed structure has a close interaction between the $[B(C_6F_5)_4]^-$ anion and the metal centre as seen previously in the $Th(Cp^*)_2(Me)(B(C_6F_5)_4)$ complex (mentioned earlier this chapter) with the *m*-F – M interaction being the strongest, but in this case a reduced contribution from the *ortho-* fluorine.

DFT calculations have been made by Molnar [173] on the $Me_3TACCr(\eta^1,\eta^1\text{-}CH_2(CH_2)_2CH_2)B(C_6F_5)_4$ system. Calculations were made on three structures with either *ortho*, *meta* or *para* fluorine forming the close contact. Only considering this interaction between anion and cation the relative energies of the structures were 0, +9, +3 kJ/mol respectively. This would suggest an *o*-F···Cr interaction would be favoured. However, a more realistic situation would be to involve F···H interactions as well. In this new model it was found that the relative energies of the three structures are +8, -10, +5 kJ/mol for o,m,p respectively. This model suggests that the structure with the *m*-F···Cr (2.16 Å) interaction and a hydrogen bond between a fluorine atom on the anion and an axial proton on the triazacyclohexane ring (H···F 2.42 Å) would be the most stable. Using the distances for the closest *o,m,p* fluorines ratios of $\langle R^{-3}\rangle^2$ can be calculated at 1.3 : 10 : 1

these are in close agreement with the observed values for $Do_3TACCr^iBu_2B(C_6F_5)_4$ with 1 : 10 : 2. The same generic ^{19}F NMR spectrum is seen for a range of $R'_3TACCrCl_3DMAB$ complexes activated by solutions of AlR_3 (R = Me, Et, ^{i}Bu), *Table 7.*

R'	R	Solvent	o- λ / Hz (δ / ppm)	m- λ / Hz (δ / ppm)	p- λ / Hz (δ / ppm)
^{i}Bu	^{i}Bu	Benzene	131 (-131.71)	251 (-163.88)	126 (-161.52)
2-EtHex	Me	Toluene	217 (-131.71)	244 (-165.27)	140 (-162.09)
2-EtHex	Et	Toluene	153 (-133.72)	~1000 (-163)	162 (-163.69)
2-EtHex	^{i}Bu	Toluene	192 (-131.58)	-	272 (-160.06)
2-EtHex	^{i}Bu	Benzene	289 (-131.76)	-	759 (-158.95)
2-HexOct	^{i}Bu	Benzene	318 (-131.78)	-	606 (-159.84)
Do	^{i}Bu	Toluene	600 (-126.81)	-	594 (-156.89)
Do	^{i}Bu	Benzene	535 (-129.69)	-	913 (-158.14)
Do	^{i}Bu	DCM	80 (-132. 32)	111 (-166.4)	48 (-162.88)

Table 7: ^{19}F NMR data for a series of $R_3TACCrCl_3DMAB$ complexes activated with AlR_3

The cases that do not show a disappearance of the *meta-* fluorine signal involve alternative factors at work. In polar solvents such as DCM, that has previously been shown to cause sharper signals for the $R_3TACCrCl_3DMAB$ complexes, the solvent molecules can solvate the metal cation, and borate anion fragments separately. Being charged species they have a large affinity for polar molecules and therefore receive more stabilisation from the solvent and less between anion – cation interaction causing a greater distance between the chromium metal centre and the fluorine substituents of the anion, *Figure 24.*

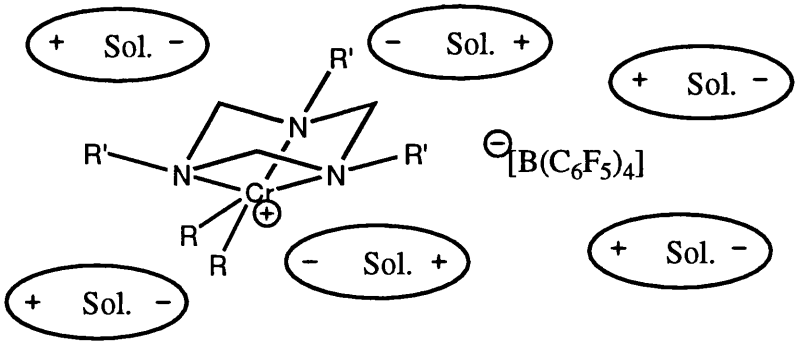

Figure 24: Reduced anion-cation interaction by solvation in polar solvents

For activation using different alkyl aluminium species (AlR_3 R = Me, Et, ^{i}Bu) essentially the same mono-nuclear complex is formed. However, all three alkyl aluminium species donate relatively small alkyl groups with low steric restraints and so are able to form three centre two electron bonds i.e. form bridged species. These chromium-bridged complexes are in equilibrium with the initially formed complex, *Figure 25.*

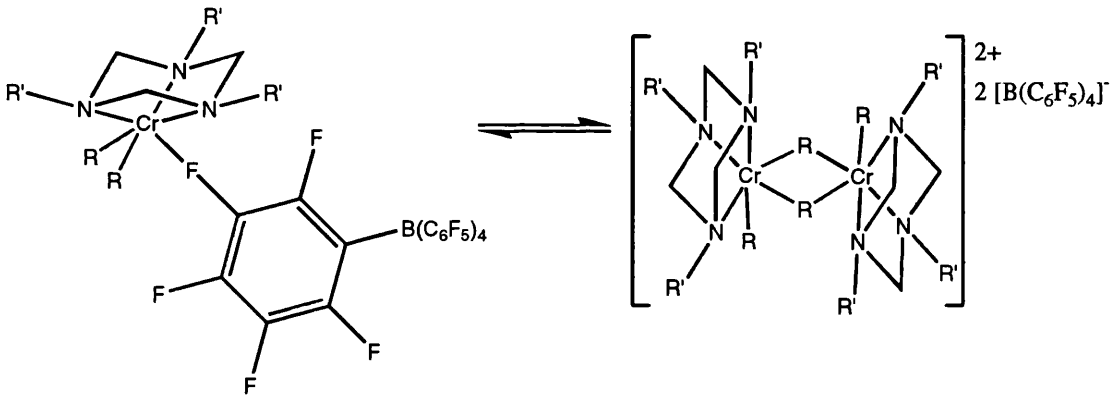

Figure 25: Equilibrium between active monomer and bridged alkyl complex

These two forms have different ^{19}F NMR spectra due to the borate anion either being involved in a close contact with the metal fragment or just associated with the chromium complex in solution, but in equilibrium an average signal for all the borate anions is seen. For activation with the $Al^{i}Bu_3$ the equilibrium will lie mainly to the left, as the ^{i}Bu groups have the largest steric bulk of the three alkyl substituents, and so will

prefer the mono-nuclear complex with less crowding, hence a ^{19}F NMR spectrum with unobservable *m*-F signal. On the other hand the much smaller methyl substituents present from the activation with $AlMe_3$ have a much stronger preference for the bridged structure with no Cr – F close contact and hence relatively sharp *m*-F signal. This preference for methyl bridging has been observed in a number of similar Cr(III) complexes. [174] In between the two extremes is the activation with $AlEt_3$ that has a much greater mix of the two possible states and hence an averaged ^{19}F NMR spectrum incorporating a visible yet very broad *m*-F signal, *Figure 26.*

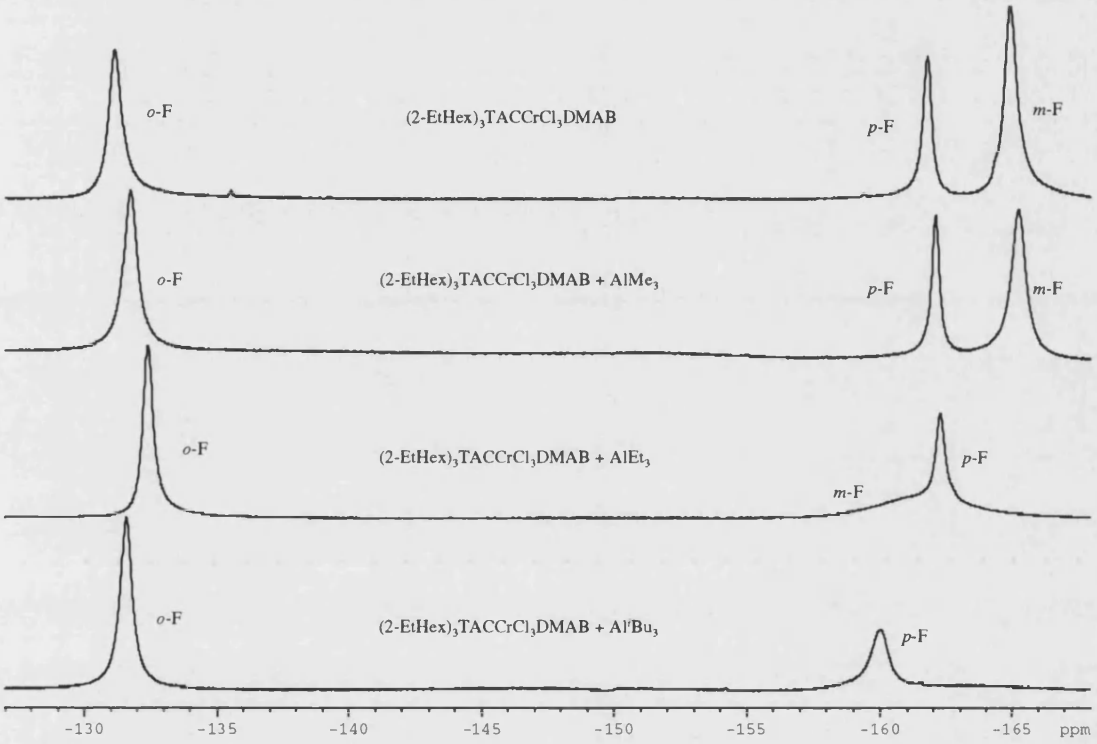

Figure 26: ^{19}F NMR 376 MHz, 298 K spectra of **33** in toluene activated by a series of AlR_3 activators

Although there is a close interaction between the anion and the metal fragment in the dialkyl mono-nuclear complex the borate anion is found not to be static in solution. Addition of $NBu_4B(C_6F_5)_4$, an excess of the borate anion with an inert counter ion, to a solution of $Do_3TACCr^iBu_2[B(C_6F_5)_4]$ **39** in toluene was studied by ^{19}F NMR spectroscopy, *Table 8.*

Equiv. $NBu_4B(C_6F_5)_4$	*o*- λ / Hz (δ / ppm)	*m*- λ / Hz (δ / ppm)	*p*- λ / Hz (δ / ppm)
0	521 (-128.45)	-	900 (-157.15)
0.5	515 (-128.25)	-	859 (-156.54)
1	447 (-128.63)	-	794 (-157.21)

Table 8: ^{19}F NMR data on addition of an excess of borate anions to **39**

The additional borate anion is found to mix with the original anions in solution and therefore average signals for the three fluorine positions are observed for all anions. There are no additional peaks in the spectrum suggesting that there are no anions in a fixed environment and not interchanging with the other anions. On addition of the excess of borate anions the line width of the *ortho*- and *para*- signals is reduced due to a larger proportion of the signal coming from fluorine substituents on anions that are not in close contact with a metal centre. Focusing upon the system in which there is a ratio of 1:1 of **39** and $NBu_4B(C_6F_5)_4$ one would expect that the line width would be roughly halved due to half the borate anions are in a paramagnetic environment and the rest in a pseudo diamagnetic environment. In reality this is found not to be the case, although there is a decrease in the line width, there is an increase in the viscosity of the solution that counteracts this effect thus causing a lower than expected change in line broadening.

As with the anilinium adduct complex an attempt at calculating the distance of the *m*-F of the borate anion from the chromium of the activated metal complex, by using the relation between the line broadening in ^{19}F NMR spectroscopy and the distance between the paramagnetic centre and nucleus under study, can be undertaken. A toluene

solution of (2-EtHex)$_2$(*p*-FPh)TACCrCl$_3$DMAB **38** activated with Al^{i}Bu$_3$ studied by ^{19}F NMR spectroscopy gives a spectrum with three signals one for the FPh group and one for each for the *ortho-* and *para-* substituents on the anion with chemical shifts / ppm and (line widths / Hz) of –97.58 (605), -131.75 (295), and –158.32 (850) respectively. The paramagnetic shift for FPh is larger than in the pre-activated complex probably due to the tighter binding by a cationic chromium. This will cause an increased contact contribution to the line width. As previously calculated the distance between the fluorine on the phenyl arm of the triazacyclohexane from the chromium is 6.77 Å (calculated from bond lengths and angles of similar structures). Using this value along with the three line width values for the average distances between *o*-F – Cr and *p*-F – Cr of 7.63 and 6.40 Å are calculated. Averaging over all fluorine atoms in the borane and considering that one half of one phenyl group is much closer to Cr than the other F atoms. Estimation of the closest contacts would lead to Cr···F(o) 3.8 and Cr···F(p) 4.0 Å, i.e. nearly equal at 3.9 Å. Using this value as the estimated distances of the closest *ortho-* and *para-* fluorine substituents to the chromium a distance of 3.1 Å can be calculated for the *m*-C – Cr distance, *Figure 27.*

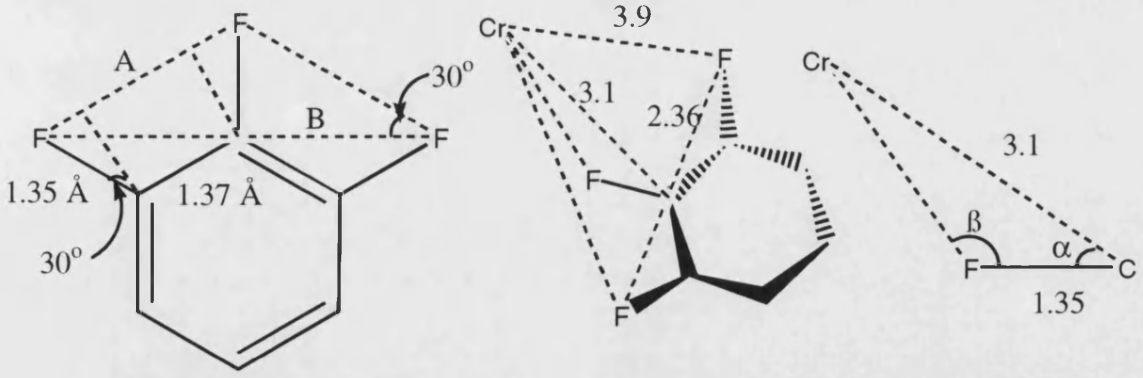

A = 1.37 + 2(1.37 Sin 30)
= 2.72 Å
B = 2.72 Cos 30
= 2.36 Å

Figure 27: Diagrams of the geometry of borate anion in relation to chromium

As the *m*-fluorine will bind to the chromium through one of its lone pairs an angle for β can be estimated at 109 °. This leaves the F_{meta}...Cr distance dependent on the angle α. At an angle of α=45° gives Cr···F of 2.35 Å and β=111° with the set of closest fluorine atoms of 3.8, 2.35 and 4.0 ± 0.2 Å for o,m,p respectively. These values are in excellent agreement with DFT calculations by Molnar [173] on the $Me_3TACCrR_2B(C_6F_5)_4$ system that gave 4.3, 2.2 and 3.9 Å for o,m,p respectively and Cr···F-C of 141 °. These results strongly suggest a close contact *m*-F···Cr interaction being within the range 2.5 – 3 Å. This value for the *m*-F – Cr distance converts back to a line width of 5500 Hz that fits with the data, as a signal that is significantly broad as not to be distinguished from the baseline. The calculated values are significantly shorter than the Cr – F distances seen for the **38**, showing that the anion is much closer to the chromium centre than before activation.

To try to understand more about the active metal centre after the activation a few techniques can be employed. One of these is an indirect method, the ^2H NMR sprectrum of **34** activated with Al^iBu_3. In toluene solution as with complex **20** (see chapter 3) the deuterium signals are not visible due to the high viscosity of the solution and aggregation into dipoles. The same is noticed in the activation of **20** with MAO in toluene solution. This activation also forms a green solution of the same type of methyl bridged chromium dimer, as with the activation with DMAB and $AlMe_3$, but in this case with an anion of MAO. However in DCM, where the solution is much less viscous, signals for both axial methylene deuterium atoms δ = 35.5 ppm and equatorial deuterium atoms δ = 3.8 ppm can be identified with line widths of 315 and 590 Hz respectively. Line widths are similar to those seen for both the trichloride complex and the anilinium adduct but there is a shift up field of the axial deuterium atoms. The

change from electron withdrawing chloride substituents to electron donating alkyl groups causes a change in the electrostatics of the chromium metal centre that is trans to the axial deuterium atoms.

4.2.4: Effective Magnetic Moments

Another method for of probing the metal centre is by magnetic moment measurements (See Evan's method in chapter 3) that give information about the spin state of chromium, *Table 9*.

	$\mu_{eff} / \mu_B \pm 0.05$	n
$Do_3TACCrCl_3DMAB$ Benzene	3.73	3
$Do_3TACCrCl_3DMAB / Al^iBu_3$ Benzene	3.99	3
$Do_3TACCrCl_3DMAB / Al^iBu_3$ Toluene	3.71	3
$Do_3TACCrCl_3$ / MAO Toluene	3.17	2 or 3
$(2\text{-EtHex})_3TACCrCl_3DMAB$ Benzene	3.74	3
$(2\text{-EtHex})_3TACCrCl_3DMAB$ Toluene	3.69	3
$(2\text{-EtHex})_3TACCrCl_3$ / MAO Toluene	2.95	2 or 3
$(2\text{-EtHex})_3TACCrCl_3DMAB / AlMe_3$ Toluene	3.62	3
$(2\text{-EtHex})_3TACCrCl_3DMAB / AlEt_3$ Toluene	3.81	3
$(2\text{-EtHex})_3TACCrCl_3DMAB / Al^iBu_3$ Toluene	3.89	3

Table 9: Effective magnetic moment measurements for a series of activated $R_3TACCrCl_3$ complexes

On formation of the anilinium adduct complex there is no significant change in the effective magnetic moment from that of the corresponding precursor parent complex with μ_{eff} values just below that of the ideal value for 3 unpaired electrons of 3.87 μ_B.

On activation of these compounds with a trialkyl aluminium source, to give alkyl chromium complexes, the effective magnetic moments remain around the values for 3 unpaired electrons giving evidence for chromium remaining in a 3+ oxidation state. Activation with $AlMe_3$ results in the lowest value of these activations and could be due to antiferromagnetic coupling in the methyl bridged dimer [174] species that cannot exist in the mono-nuclear complex, the predominant species in Al^iBu_3 activation. Activation of the parent trichloride complex with MAO reveals significantly lower effective magnetic moments. Although these values are closer to an effective magnetic moment value of 2.828 μ_B expected for 2 unpaired electrons, they are on the high side and are still thought to belong to chromium in a 3+ oxidation state. This activation is thought to also form a methyl bridged dimer structure that can incorporate some metal – metal bonding along with antiferromagnetic coupling, reducing the apparent number of unpaired electrons. This lowered effective magnetic moment due to metal – metal bonding in a chromium methyl bridged dimer complex has been observed previously by Theopold [175] in the $[Cp^*(CH_3)Cr(\mu\text{-}CH_3)]_2$ system with a $\mu_{eff} = 2.1\ \mu_B$, *Figure 28.*

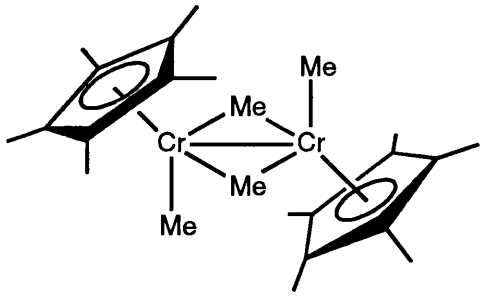

Figure 28: Methyl bridged dimer complex with a lower then expected effecive magnetic moment

This postulation has further justification on the addition of olefin when the dimer would be broken, in which the effective magnetic moment value increases to a value more respective of 3 unpaired electrons. (See chapter 5)

4.3: Summary

In this chapter is reported the synthesis of anilinium adduct complexes of the general formula $R_3TACCrCl_3DMAB$ from the corresponding chromium trichloride complex and DMAB. These complexes involve a cation, consisting of DMAH in a bifurcated hydrogen bond to two chloride substituents, and a weakly coordinating borate anion. The aggregation of this ion pair is both solvent and concentration dependent. In non-polar solvents at concentrations above 0.1 M the ions pair and so dipoles are the dominant species in solution. For less concentrated solutions the ions dissociate resulting in separate ions as the prevailing species. Polar solvents have the same effect as reduced concentration in that separate ions dominate the solution but in this case solvation of the ions is the cause.

Paramagnetic broadening of signals in ^{19}F NMR spectroscopy has been utilised in the estimation of anion-cation interaction in solution. By using the $1/r^6$ dependence on the line broadening, r being the distance between paramagnetic centre and nucleus under investigation, the closest fluorine atoms on the anion are found to be 4.5 Å from the chromium. This value in the solid state is slightly longer than the value calculated in solution due to more restrictions imparted by the close packed cations in the solid state.

Activation of the $R_3TACCrCl_3DMAB$ complexes with AlR_3 results in the extreme line broadening of the *meta* fluorine signal in the ^{19}F NMR spectrum. This result led to the postulated active complex $R_3TACCrR_2B(C_6F_5)_4$. Calculations involving the line broadening of the fluorine signals in comparison with a fluorine internal

standard on the coordinated triazacyclohexane concluded in a close contact m-F – Cr of 2.35 Å. This result has also been reinforced by DFT calculations by Molnar. [173]

Activation of $R'_3TACCrCl_3DMAB$ complexes with a selection of AlR_3 compounds, studied by ^{19}F NMR and effective magnetic moments by Evans method, led to the formation of mono-nuclear and an alkyl bridged dimer structures. These two structures are in equilibrium with the dominant species being dictated by the alkyl substituent R. Activation with $AlMe_3$ leads primarily to the dimer, $AlEt_3$ leads to a mixture, where as Al^iBu_3 forms dominantly the mono-nuclear complex.

5: Olefin Trimerisation

5.1: Introduction

Ethylene oligomerisation to form longer chained α-olefins is a well-understood process that produces a distribution of products varying in chain length of a statistical distribution known as a Schulz-Flory [176] or Poisson distribution. The generally accepted mechanism for this process, first proposed by Cossee and Arlman, [177] involves a chain growth by firstly coordination of ethylene followed by insertion into a transition metal alkyl bond. This chain growth results in a termination step via a β-hydrogen transfer to the metal to form a metal hydride species and releasing a molecule of a linear α-olefin, *Scheme 1.*

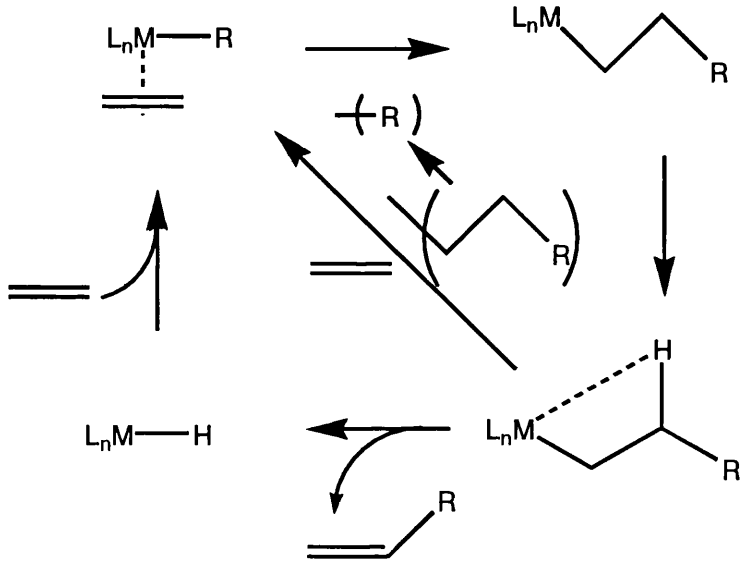

Scheme 1: Chain growth mechanism for polymerisation

Due to the undetermined number of insertion steps the distribution of products are formed from this type of mechanism. However, more recent discoveries have found a new set of catalysts which do not display this typical spread of products, instead these catalysts show a remarkable selectivity for the trimerisation product 1-hexene and recently even tetramerisation to 1-octene. This selectivity is not possible from the chain

growth mechanism and so a scheme involving metallacycle intermediates was adopted. McDermott had previously demonstrated metallacycles in the early 1970s at a Pt (II) centre [178] and thereby showed the possible existence of this type of intermediate. Manyik proposed the first metallacycle mechanism for the selective trimerisation of ethylene to 1-hexene in 1977, [179] *Scheme 2*.

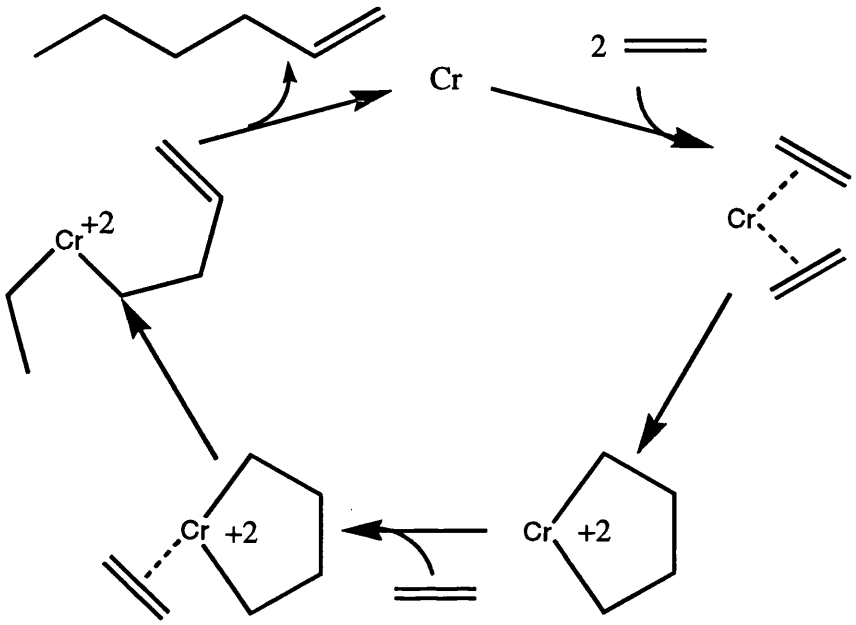

Scheme 2: Proposed metallacycle mechanism for ethylene trimerisaston

This mechanism started with the addition of two equivalents of ethylene to an unspecified chromium source followed by a ring closing process to the formation of a metallacyclopentane. After the coordination of the third equivalent of ethylene a β-hydrogen transfer occurs from the metallacyclopentane to the coordinated ethylene to form a chromium butenyl ethyl intermediate. Reductive elimination from this di-alkyl intermediate liberates 1-hexene and reproduces the initial chromium species. Kinetic studies were undertaken on this system and found a second order dependence with respect to ethylene and so formation of the metallacyclopentane was proposed as the rate-determining step.

Following this publication Briggs proposed an alteration to the step leading to the liberation of 1-hexene, [44] instead of the β-hydrogen transfer to ethylene, a fast insertion of the coordinated ethylene into the metallacyclopentane species occurs to form a metallacycloheptane. At this stage ring opening occurs with the formation of a chromium hexenyl hydride species that can undergo reductive elimination to liberate 1-hexene and return the original chromium species, *Scheme 3.*

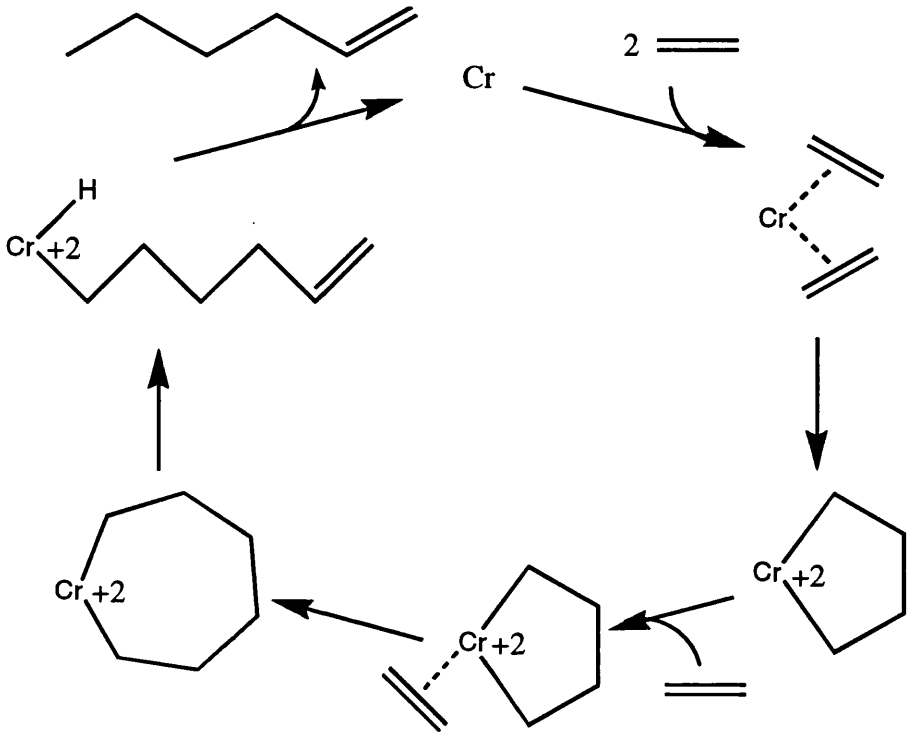

Scheme 3: Proposed trimerisatin mechanism with metallacycle growth

This postulation was based upon the thermal decomposition of platinacycles, reported by McDermott, [180] for the selective liberation of 1-hexene the insertion step must be faster than the decomposition of the metallacyclopentane to 1-butene. Following from this the liberation of 1-hexene must be a faster process than the insertion of another equivalent of ethylene into the metallacycloheptane to form a larger ring.

Greater support for this altered mechanism came in the form of two chromium metallacycles synthesised by Jolly, [14] *Figure 1.*

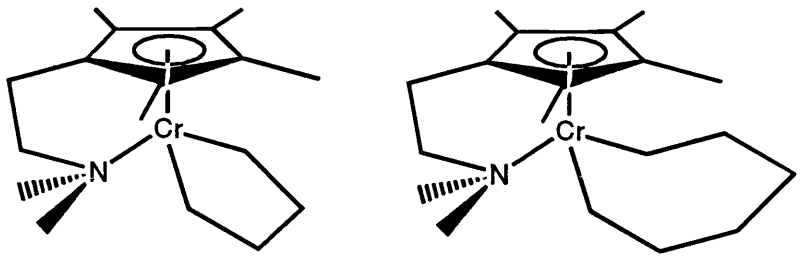

Figure 1: Chromium metallacycle complexes

The metallacyclopentane complex is found to be more stable than the metallocycloheptane analogue with T_{dec} = 151 °C and 56 °C respectively. The metallacycloheptane complex decomposes with the liberation on 1-hexene and the protonolysis of the product of the reaction of the metallacyclopentane complex with ethylene (0.1 bar, room temperature) leads to the liberation of hexane and butane 1 : 3. X-ray crystal structures of chromium alkyl hydride complexes have also been reported, by Theopold, [181] showing the possibility of the intermediate after β-hydrogen transfer. However, both the Jolly metallacycle complexes and the Theopold alkyl hydride complexes are unable to catalyse the selective trimerisation of ethylene. Using the Cp type ligands requires a labile pendant group for selective trimerisation as observed in the $[CpCMe_2Ph]TiCl_3$ / MAO system. [81]

A study by Bercaw et al. [182] using an equimolar mixture of C_2H_4 / C_2D_4 for trimerisation with the system $[((o\text{-}MeO\text{-}Phenyl)_2P)_2NCH_3]CrPh_3$ / $H(Et_2O)B(C_6H_3(CF_3)_2)_4$ revealed that there was no scrambling of the deuterium isotopes. For a classical Cossee-type mechanism it is expected that there will be some H / D scrambling as the metal hydride into which the first equivalent of ethylene inserts

/ D scrambling as the metal hydride into which the first equivalent of ethylene inserts comes from the last olefin to be produced. As either a proton or deuterium is donated from the previous olefin, and either a proton or deuterium is lost on liberation of the produced olefin, the products formed by this type of mechanism range from C_6D_{12} to C_6H_{12} with all the permutations of hydrogen and deuterium $C_6H_xD_{(12-x)}$, *Scheme 4*.

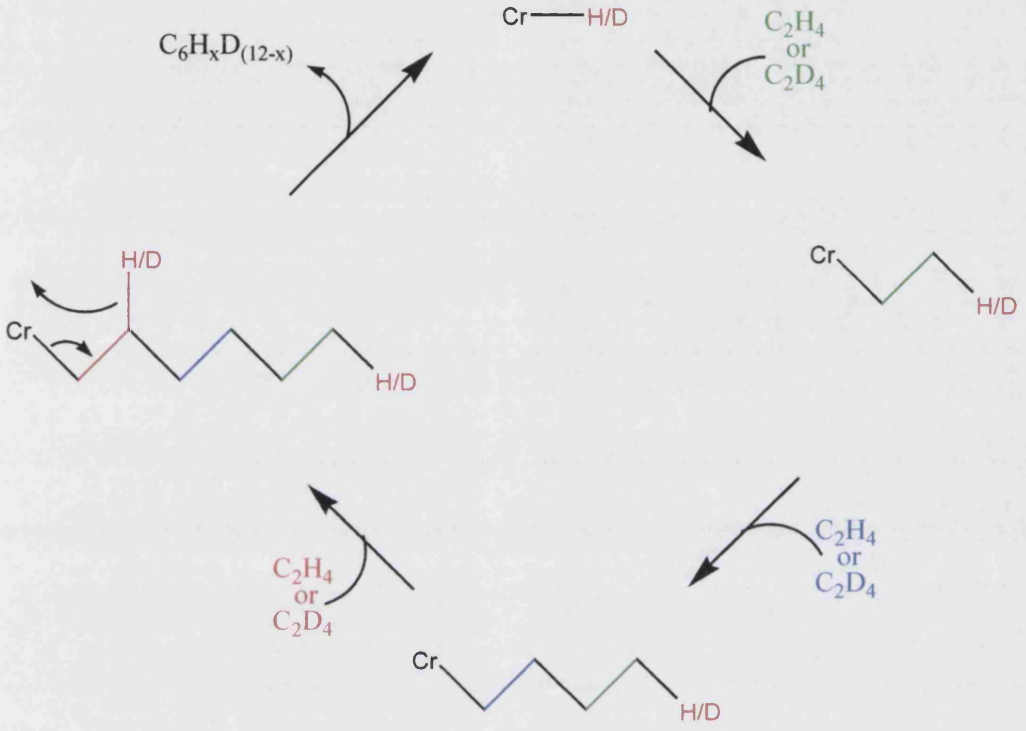

Scheme 4: Isotope experiment showing scrambling of hydrogen or deuterium from previous 1-hexene formed

For a metallacycle mechanism there are no hydrogen or deuterium atoms passed on from previously liberated olefin and hence all protons and deuterium atoms from the three equivalents of ethylene are contained within the one molecule of 1-hexene. Therefore, there is no H / D scrambling and only products with even numbers of hydrogen and deuterium are obtained (C_6H_{12}, $C_6H_8D_4$, $C_6H_4D_8$ and C_6D_{12}) in a ratio of 1 : 3 : 3 : 1.

One aspect of the mechanism that is still in contention is the oxidation state of the chromium during the catalytic cycle. Oxidative addition of two equivalents of ethylene to form a metallacyclopentane dictates that there is change in oxidation state of M^n to M^{n+2}. In this process the metal centre acts as both a Lewis acid and a Lewis base reacting with a molecule AB, in this case two molecules of ethylene, forming two new M – A and M – B bonds. This increases the coordination number of the metal centre by two and as A and B are considered to be more electronegative than M the formal oxidation state of M increases by two, *Scheme 5.*

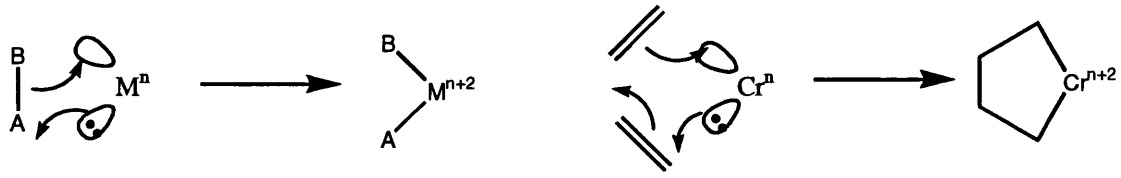

Scheme 5: Oxidative addition of ethylene to form metallacyclopentane

At the end of the catalytic cycle there is a decrease in the oxidation state from M^{n+2} to M^n via reductive elimination liberating 1-hexene. This process is the reverse of the oxidative addition with the formation of an H – C bond and the breaking of 2 Cr – C bonds whilst reducing the formal oxidation state of chromium by two, *Scheme 6.*

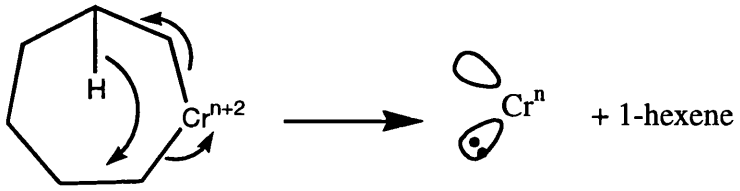

Scheme 6: Reductive elimination to liberate 1-hexene

Various pairs of oxidation couples have been proposed Cr(III) /Cr(V), [183] Cr(I) / Cr(III), [179] and Cr(II) / Cr(IV) [184] though none have been proven conclusively. Cr(III) complexes are typically the most stable, while Cr(II) and Cr(IV) complexes are less stable. Cr(V) and Cr(I) complexes are quite rare and unstable. Therefore in terms of stability a Cr(II) / Cr(IV) couple would be the most likely. Known Cr(V) complexes

typically only have oxygen or halide ligands, whereas organometallic Cr(I) complexes are possible with donor ligands such as aryl isocyanides and bipyridine. [185] Therefore the Cr(I) / Cr(III) couple seems more likely than the Cr(III) / Cr(V) couple. Also experimental evidence using X-ray photoelectron spectroscopy of the Phillips catalyst seems to indicate a Cr(I) / Cr(III) couple for this system [186] but still some Cr(II) and Cr(IV) sites are also detected so this couple can not be ruled out.

Although the metallacycle mechanism has been established over the last thirty years the first molecular modelling studies related to this mechanism were only published in 2003. The overriding factor for this slow arrival of computational support is due to the almost selective nature of this reaction to chromium catalyst. Modelling these systems would involve notoriously difficult open shell calculations in particular including spin state changes and there is also little fundamental experimental data on both the exact active chromium species and its electronic structure. However, van Rensburg [187] recently published a theoretical study assuming a Cr(II) / Cr(IV) couple for the Phillips (Cr-pyrrolyl) trimerisation catalyst system. A detailed analysis was conducted to determine the preferred spin ground state for the active Cr(II) and Cr(IV) species in the mechanism. It was determined that the triplet spin states for both the oxidation states are predicted to be the lowest in energy and hence, that there is no spin state crossing during the proposed mechanism, *Scheme 7.*

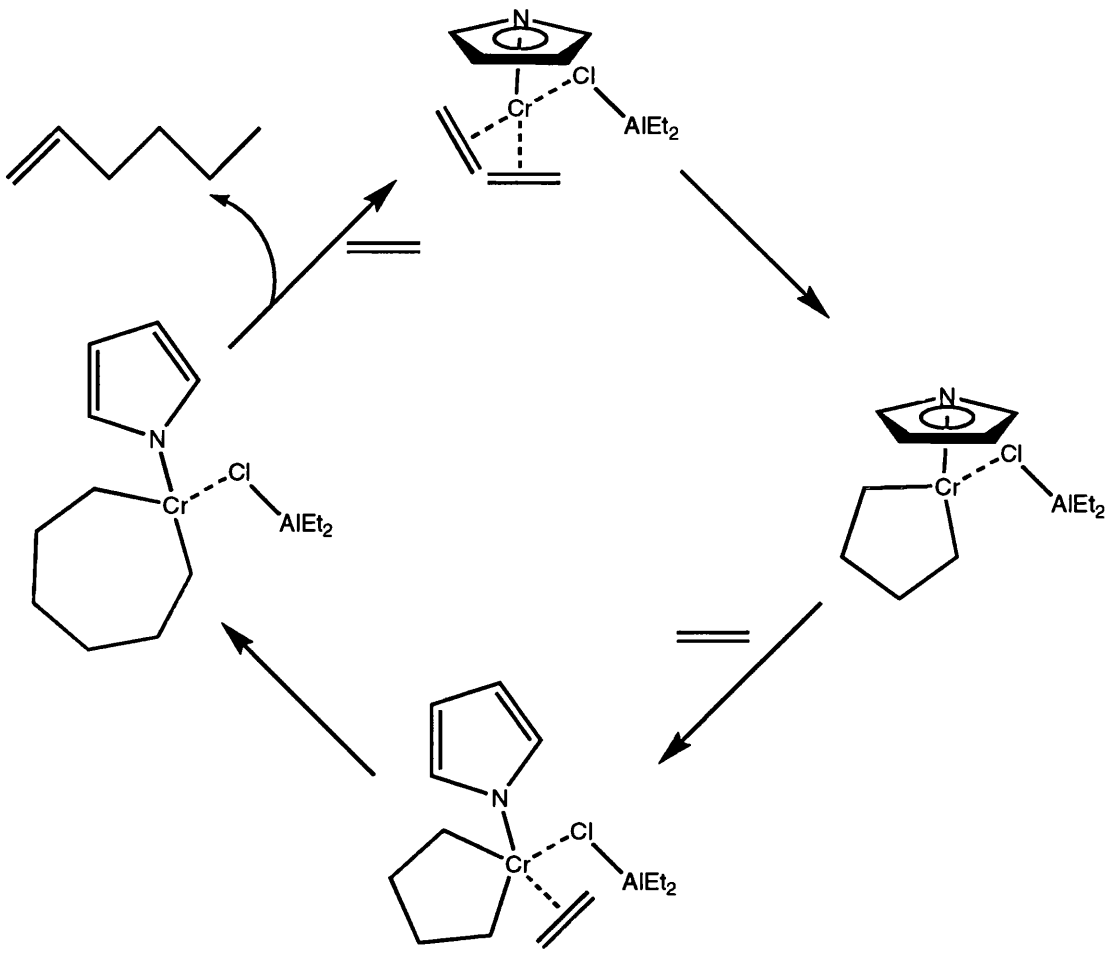

Scheme 7: Proposed metallacycle mechanism with no hydride species

Calculations of the Gibbs free energy profiles for the full potential energy surfaces of the η^5- and σ- coordinated binding modes of the pyrrole ligand found both pathways feasible. In both cases the rate determining step for this system was found to be the metallacycle growth from the corresponding metallacyclopentane to the metallacycloheptane complex but involves a lower energy in the σ-coordinated complex. Whereas metallacycle formation is favoured by η^5-coordination showing that a change in the pyrrole-binding mode is an important concept in this mechanism. Calculations on the counter ion during the catalytic cycle reveal that there is a significant reduction in the activation energy of the rate-determining step when a structure incorporating the whole $[ClAlMe_3]^-$ anion instead of the much simplified Cl^-

ion. Therefore suggesting that the full aluminate anion may have an important role in controlling the reactivity of the Cr-pyrrolyl catalyst system.

After the recently published discoveries of tantalum [188] and titanium [189] based trimerisation catalyst systems there was an increased interest in the understanding of this highly selective reaction. Yu and Houk [190] published a detailed study on the $TaCl_3$ catalysed trimerisation. The proposed mechanism for the reaction with the tantalum catalyst is a very similar metallacycle process as used to describe the trimerisation with chromium, *Scheme 8.*

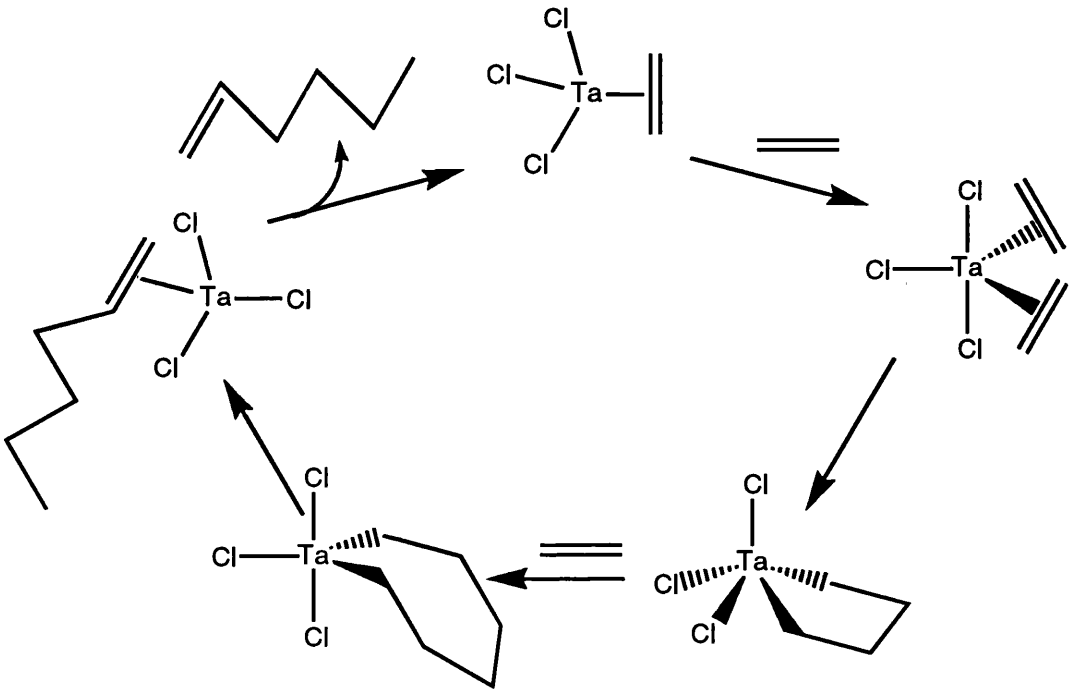

Scheme 8: Trimerisation mechanism used for the calculations of the $TaCl_3$ system

Starting from a tetrahedral ethylene coordinated tantalum complex a second equivalent of ethylene binds to form a trigonal bipyramidal complex. The two bound olefins form a metallacyclopentane complex that is found to be more stable as a square based pyramid complex. Insertion of a third equivalent of ethylene into the metallacycle forms a metallacycloheptane complex, more favourable back in a trigonal bipyramid

arrangement. β-hydrogen and reductive alkane elimination result in the formation of a 1-hexene bound complex that readily liberates the olefin and binds another equivalent of ethylene to continue the cycle.

From the calculations it is found that the energy barrier for ethylene addition to the metallacyclopentane is lower than for the reductive elimination process to liberate 1-butene. This energy barrier is also lower than the corresponding energy barriers to addition of ethylene to the mono-ethylene coordinated complex and the metallacycloheptane intermediate. Due to the ring strain in the metallacyclopentane, with a C – Ta – C angle much smaller than the ideal 120 °, there is less steric hindrance to the addition of another ethylene molecule. The relatively high energy barrier for the addition of ethylene to the metallacycloheptane complex, along with the somewhat easier reductive elimination step from this larger ring size, are the reasons for the termination of ring growth beyond a metallacycloheptane and the selectivity for 1-hexane production. The β-hydrogen elimination of the metallacycloheptane to form the 1-hexene coordinated complex occurs as a concerted process passing through a transition state with an agostic metal – hydrogen interaction, *Figure 2*.

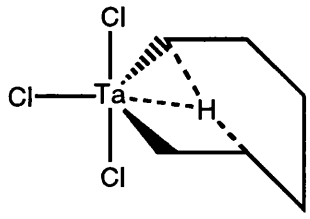

Figure 2: Agostic hydrogen intermediate during β-hydrogen elimination

The alternative two step process involving β-H abstraction and reductive elimination, which has been proposed for the chromium system, requires a higher activation energy barrier to form the metastable tantalum hydride intermediate and a very unfavourable second reductive elimination step.

Blok, [191] de Bruin, [192] as well as Tobisch and Ziegler [193] independently performed calculations on the half metallocene titanium catalyst system, *Figure 3.*

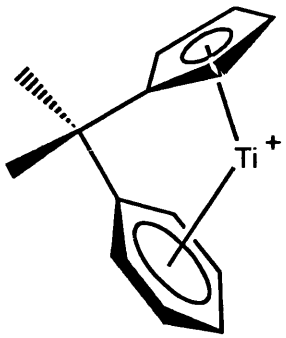

Figure 3: [$CpCMe_2Ph$]$TiCl_3$ / MAO system

Collectively their findings are very similar to those results found in the tantalum system. The poor selectivity for the dimerisation to form 1-butene is governed by the high-energy barriers of a two step β-H abstraction and reductive elimination, or conformationaly impossible concerted agostic β-H transfer, compared with the low energy addition and insertion of another equivalent of ethylene. The selectivity for 1-hexene production is credited to the low energy barrier for an agostic β-H transfer from the metallacycloheptane compared with the energy required for addition of another ethylene molecule. In this system the larger energy barrier for addition of this third ethylene molecule is due to steric constraints of the pendent arene ring. Calculations on the system with no labile arene moiety reveal a vastly reduced 1-hexene selectivity with a greater degree of oligomerisation and polymerisation. These calculations are supported by the practical observations seen by this catalyst under standard trimerisation conditions. [39]

As mentioned earlier both Manyik and Yang reported a second order dependence on ethylene for two different chromium catalyst systems. These

observations imply the rate determining step to be the formation of the metallacyclopentane. Studies by Köhn on the triazacyclohexane chromium system established a first order dependence of α-olefin in the trimerisation of the more bulky 1-hexene. Similarly Deckers reported a first order dependence with respect to ethylene with the $[C_5H_4C(CH_3)_2C_6H_5]TiCl_3$ system. This would imply that the rate determining step would be the insertion of the third equivalent of ethylene into the metallacyclopentane. Blok, as well as Tobisch and Ziegler who found that this insertion step is rate determining for the same system have endorsed this result in the molecular modelling results. Contrary to these findings de Bruin postulated that the liberation of 1-hexene from the titanacycloheptane ring and not metallacycle growth is rate limiting, although this would mean a zero order dependence with respect to ethylene, experimentally this was not observed. Molecular modelling calculations on the Phillips catalyst system, by van Rensburg, determined that insertion of ethylene is the rate determining step in that case.

5.2: Results and Discussion

5.2.1: Trimerisation

$R_3TACCrCl_3$ complexes activated by the co-catalyst MAO or by pre-formation of the DMAB adduct followed by activation with AlR_3 can perform selective trimerisation reactions of α-olefins. In accordance with the metallacycle mechanism a Schultz-Flory distribution of α-olefins is not produced. For ethylene trimerisation the major product is 1-hexene, *Scheme 3*, other minor products consist of decenes and higher oligomers resulting from co-trimerisation between ethylene and the 1-hexene

produced. For α-olefin trimerisation a number of isomers are produced based upon the same hexene backbone, *Scheme 9.*

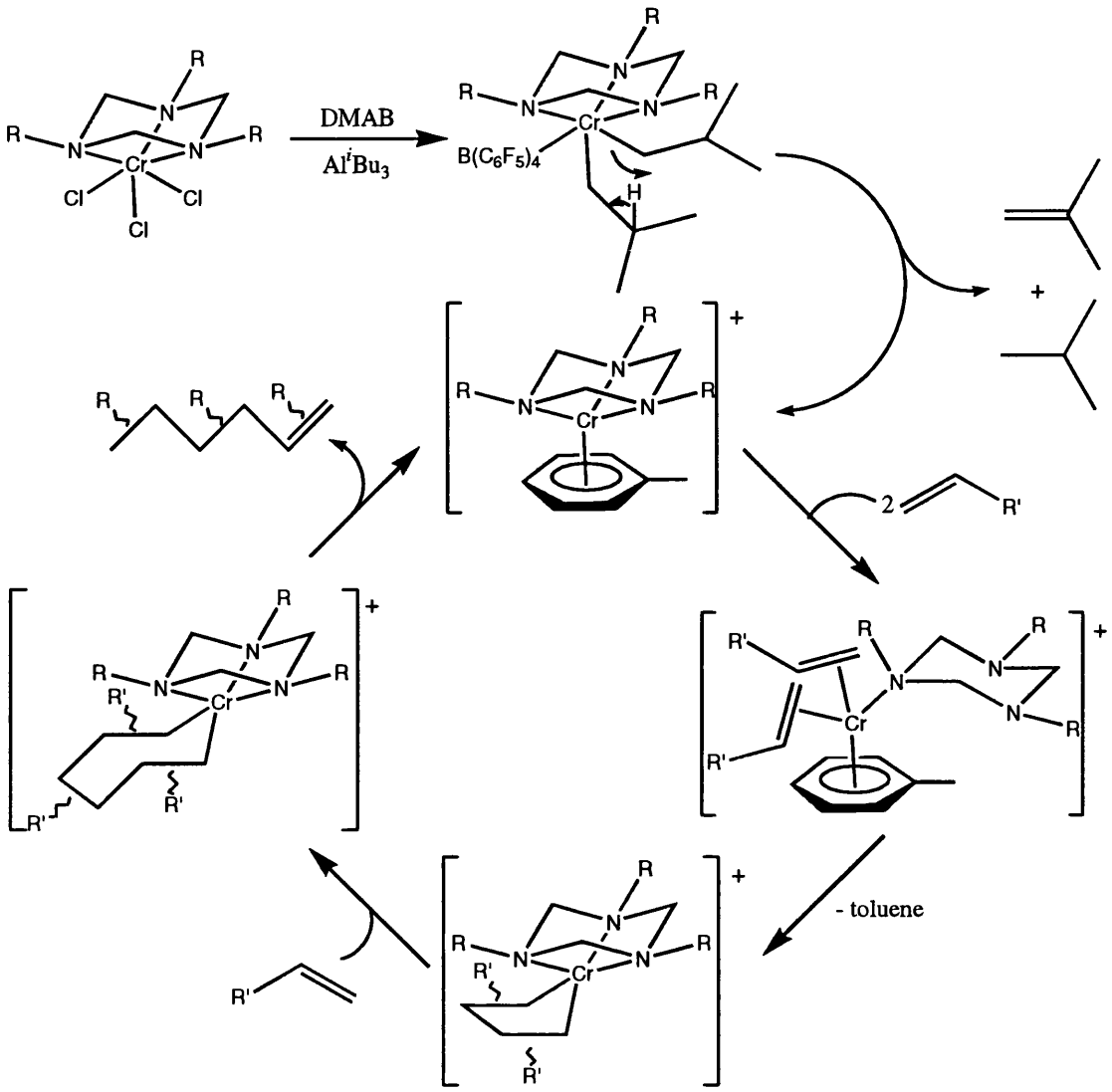

Scheme 9: Proposed trimerisation mechanism for the $R_3TACCrCl_3$ system

The following proposed mechanism is consistent with our observations: β-H transfer and reductive elimination of *iso*-butane and *iso*-butene from the activated di-alkyl complex results in the formation of a Cr(I) complex with an equivalent of the toluene solvent filling the vacant coordination sites. Addition of two equivalents of α-olefin to the chromium centre form a metallacyclopentane complex with the two branches of the α-olefins in a distribution of the four possible positions. Coordination and insertion of the third equivalent of α-olefin, orientated either way round, creates a

metallacycloheptane complex. After β-H transfer and reductive elimination the initial chromium-arene complex is formed with the liberation of the trimer product. The nature of the α-olefins produced varies between vinylidene and internal olefins, *Scheme 10.*

Scheme 10: A selection of olefin trimers formed from the metallacycle mechanism

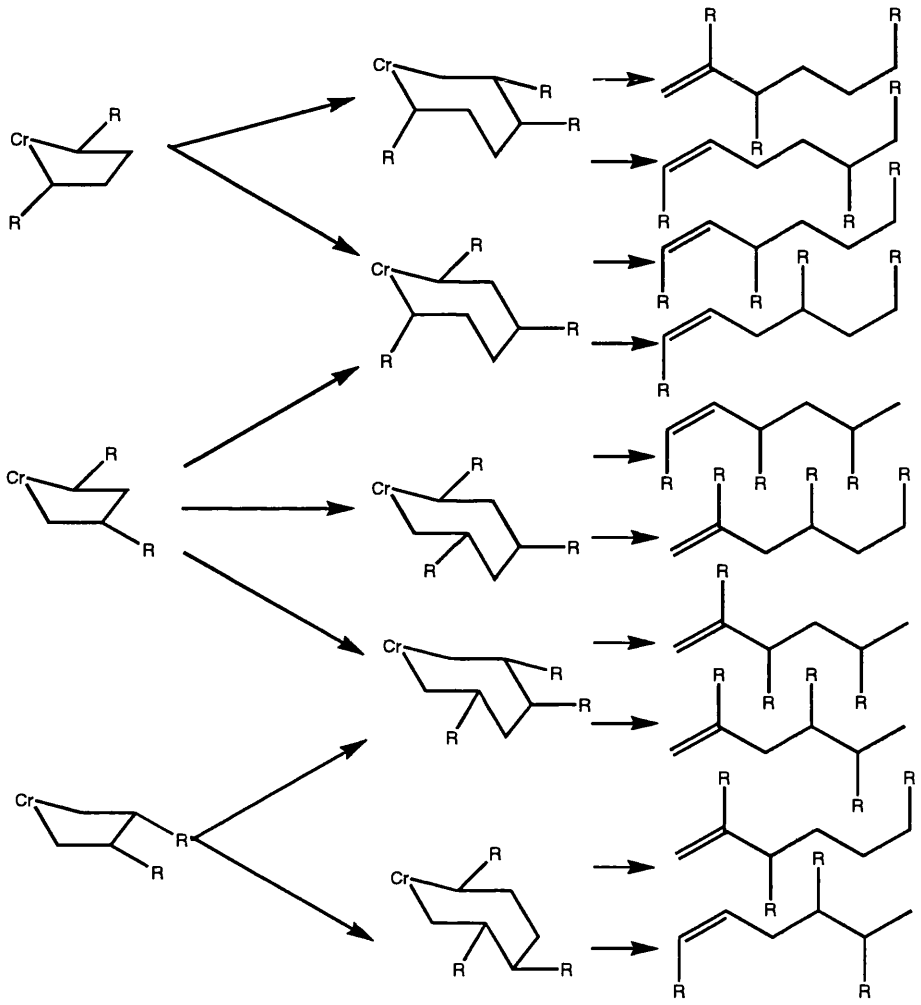

As well as the trimers shown above elimination can also occur onto an R group on the α-carbon of the metallacycle. In the case of propene trimerisation this can lead to vinyl end groups. Separation of these products can be achieved by GC but to be able to recover the separated fractions would be an extremely difficult process and so has not been attempted. However, confirmation of trimerisation can also be found from comparison of the integrals of the olefinic region with the aliphatic region of the ^{1}H NMR spectrum. As trimerisation occurs the difference in integral intensities increases

quite significantly in favour of the aliphatic region due to the number of C = C bonds being broken to form more C – C bonds. Decomposition of the catalyst during trimerisation or impurities in the solvent lead to complexes that are inactive for trimerisation but are still (slowly) active for olefin isomerisation, i.e from 1-hexene to 2-hexene. Both the trimerisation reaction and isomerisation show a loss of one of the vinyl signals of 1-hexene in the ^{1}H NMR spectrum but the ratio between olefinic and aliphatic integrals is much different in each case. For isomerisation the ratio would tend to 1 : 5 with 2 olefinic, and 10 aliphatic protons in the 2-hexene molecule. For trimerisation this ratio tends to 1 : 17 with the consumption of 1-hexene.

The trimerisation reactions carried out were all in NMR tubes with the products only identified by ^{1}H and ^{13}C NMR spectroscopy with no isolated yields. These reactions were primarily to identify active catalytic systems and only give a rough guide to the rate of reaction as the trimers were isolated and fully characterised before. [194] NMR tube trimerisation reactions have been performed using a number of different $R_3TACCrCl_3$ complexes with a variety of activators and olefins, *Table 1*. All reactions were carried out at room temperature with no stirring. For the ethylene trimerisations an ethylene pressure of 1 bar was used and hence reaction times in these cases include the diffusion time of the gas into the solution.

$R_3TACCrCl_3$	Activator	Solvent	Olefin	Time	Product /Purity
2-EtHex	DMAB / $AlMe_3$	Toluene	Ethylene	40 min	-
2-EtHex	DMAB / $AlEt_3$	Toluene	Ethylene	13 min	1-Hexene /80%
2-EtHex	DMAB / Al^iBu_3	Toluene	Ethylene	13 min	1-Hexene />99%
2-EtHex	MAO	Toluene	Ethylene	10 min	1-Hexene / 100%
2-EtHex	DMAB / $ZnEt_2$	Toluene	Ethylene	1 day	-
2-EtHex	DMAB / Al^iBu_3	Toluene	1-Hexene	1 day	2-Hexene / 100%
$PrSi(OEt)_3$	DMAB / Al^iBu_3	Toluene	1-Hexene	1 day	Trimer, 2-Hexene
$Do_2(Ph)TAC$	DMAB / Al^iBu_3	Toluene	1-Hexene	1 day	Trimer / 10%, 2-Hexene 90%
Sen	DMAB / Al^iBu_3	Toluene	1-Hexene	2 day	-
Do	DMAB / Al^iBu_3	Toluene	1-Hexene	3 days	Trimer / 77%
Do	DMAB / Al^iBu_3	Toluene	Allylbenzene	5 days	Isomerisation / 5%
Do	DMAB / Al^iBu_3	DCM	1-Hexene	7 days	2-Hexene / 2%
Do	MAO	Toluene	1-Hexene	5 days	Trimer / 69%
Do	MAO	Toluene	Allylbenzene	5 days	Isomerisation / 5%

Table 1: α-olefin trimerisations with activated $R_3TACCrCl_3$ complexes

The choice of activator can have a significant effect upon the formation of an active catalytic system. With the standard polymerisation activator MAO in a 100 fold excess the $(2\text{-EtHex})_3TACCrCl_3$ complex can be activated to give a very efficient ethylene trimerisation catalyst, with consumption of the monomer within 10 minutes to give selectively 1-hexene with no visible signs of side products in ^1H NMR. This reactivity and selectivity can be mirrored by addition of DMAB to the same chromium complex followed by activation with 3 equivalents of Al^iBu_3, *Figure 4.*

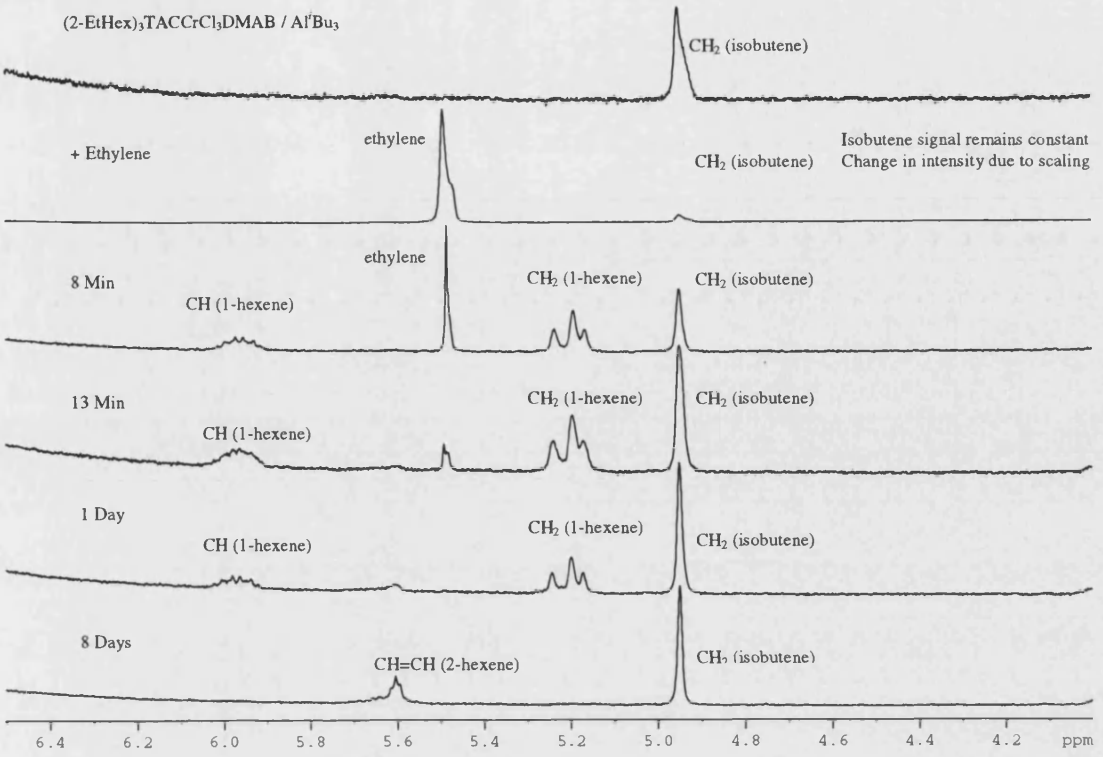

Figure 4: Consecutive ^{1}H NMR 400 MHz, 298 K spectra for the trimerisation of ethylene with the **33** / $Al^{i}Bu_3$ system in toluene

Activation of **33** with $Al^{i}Bu_3$ results in the formation of an alkyl chromium complex that is prone to β-hydrogen elimination to form the active trimerisation catalyst and isobutene. The static integrals for the isobutene, in comparison with the solvent peak, show that this olefin does not participate in any further reaction showing that olefins with vinylidene termini cannot form metallacycles in this system. Upon addition of ethylene to the activated complex there is rapid formation of 1-hexene with almost complete consumption of ethylene within 13 minutes. Decomposition of the active complex, within 1 day, results in a species that is slowly active for the isomerisation of 1-hexene into 2-hexene. This process consumes all the produced 1-hexene within 8 days.

A similar, but slightly slower, reactivity was observed on switching to $AlEt_3$ and may be due to the distribution of the activated complex between a mono-nuclear species and the alkyl bridged dimer complex. (See chapter 4) If the active species for the trimerisation can only be formed from β-H transfer and reductive elimination from the mono-nuclear species then a longer activation time would be expected as the rate of interconversion of the two equilibrium species is included, *Scheme 11*.

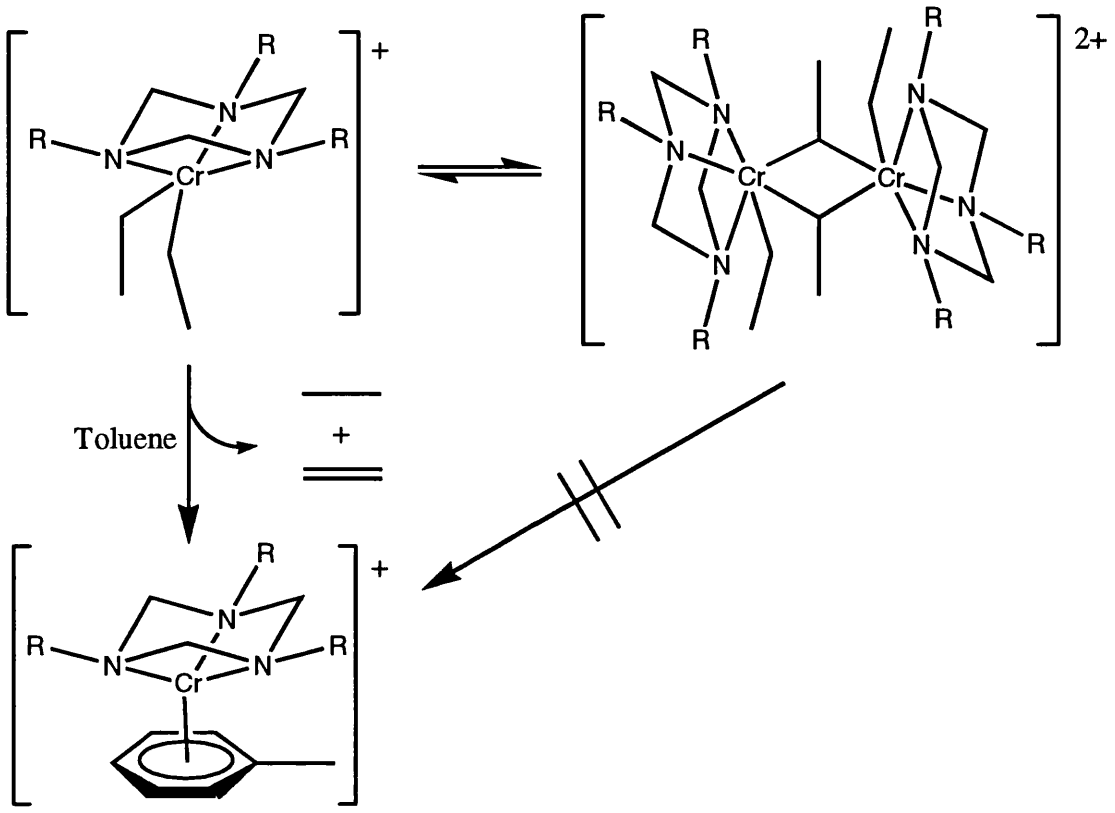

Scheme 11: Reactivity of mono-nuclear and alkyl bridged dimer complexes

Activation with $AlMe_3$ gives a trimerisation inactive solution, as the dimer complex is predominant in solution. There are no β-hydrogen atoms on either of the alkyl groups and therefore cannot undergo β-H transfer and reductive elimination from any monomer species formed. Instead activation would require the addition of an olefin

followed by insertion into a Cr – Me bond to give the required β-hydrogen. However, this process is slower than reformation of the dimer species.

Attempted activation of the $(2\text{-EtHex})_3TACCrCl_3$ / DMAB system with $ZnEt_2$, a substitute for aluminium that promotes decomposition, gives a green solution in appearance very similar to AlR_3 activation. However, this activated complex does not show any activity towards ethylene, either polymerisation or trimerisation.

Variation in the arms of the triazacyclohexane ligand also has a dramatic effect upon the reactivity of the trimerisation. This steric factor also dictates the selectivity of each triazacyclohexane chromium complex with different α-olefins. As the alkyl substituents of the triazacyclohexane are initially directed away from the metal centre the bulk of straight chained alkyl substituents apply a minimal amount of steric hindrance upon the active site of the chromium, as is observed for **19** that can be activated to give an active 1-hexene trimerisation catalyst. In comparison complex **17**, that incorporates an ethyl group branching in the β-position, is an excellent ethylene trimerisation catalyst. But due to a larger steric hindrance of the active site is found to lose all trimerisation activity with the larger 1-hexene olefin. When activated **18** incorporates branching of the arms further from the triazacyclohexane ring maintains some 1-hexene trimerisation ability, whereas the activated $(Sen)_3TACCrCl_3$ (Sen = 2-thiophenemethyl) complex with a short arm joining the sulphur containing heterocycle to the triazacyclohexane shows no reactivity towards 1-hexene. Changing one of the dodecyl substituents of **19** with a phenyl ring, to give the $Do_2(Ph)TACCrCl_3$ complex, seems to give a dramatic decrease in activity. However, in this case there is no significant increased steric factor to blame, but the phenyl ring does have a detrimental

effect. There is an electron withdrawing effect upon the nitrogen lone pair by the phenyl ring causing the N – Cr bond to be significantly weaker than the other two N – Cr bonds. This reduced ligand – metal interaction causes this activated complex to decompose much more readily than activated **19**. The more sterically bulky olefin, allyl benzene, has only been found to undergo isomerisation with any of the activated $R_3TACCrCl_3$ complexes.

Effective magnetic moment measurements have been calculated on a variety of activated $R_3TACCrCl_3$ systems during catalysis, *Table 2*.

	$\mu_{eff} / \mu_B \pm 0.05$	n
34 / Al^iBu_3 Toluene	3.78	3
34 / Al^iBu_3 / Hexene 30 min Toluene	3.77	3
17 / MAO Toluene	2.95	2 or 3
17 / MAO / Ethylene 3 min Toluene	2.89	2 or 3
17 / MAO / Ethylene 8 min Toluene	2.87	2 or 3
33 / $AlEt_3$ Toluene	3.81	3
33 / $AlEt_3$ / Ethylene 8 min Toluene	3.66	3
33 / Al^iBu_3 Toluene	3.99	3
33 / Al^iBu_3 / Ethylene 3 min Toluene	3.98	3
33 / Al^iBu_3 / Ethylene 11 min Toluene	3.97	3

Table 2: Effective magnetic moments of activated $R_3TACCrCl_3$ complexes during catalysis

On addition of α-olefin to the solution of activated $R_3TACCrCl_3$ complexes the effective magnetic moment drops slightly in all cases. In all but the MAO activation the effective magnetic moments during catalysis are still within experimental errors of the

values for three unpaired electrons and so the dominant complex in solution is Cr(III). The reduction in magnetic moment after activation is due to decomposition of the active complex and precipitation of a Cr(I) species. On activation with MAO the chromium complex formed is a methyl bridged dimer with a lower than expected magnetic moment, (see chapter 4) the same species must be a resting state for the active catalyst whilst not involved in the catalytic cycle.

5.2.2: Decomposition

All of the active activated $R_3TACCrCl_3$ complexes have a relatively short lifetime, showing significant decomposition within 1 hour. The same decomposition is observed from the activated $R_3TACCrCl_3$ complexes without addition of olefin, but in this case the process is much slower with complete decomposition occurring within 1 week.

The ^{19}F NMR data from the decomposition of **39** was compiled in a graph (See Chapter 4) of line width, of the fluorine signals, against the amount of decomposition. A more informative label for this latter axis, and the physical measurable quantity is the formation of one of the decomposition products $[Do_3TACAl^iBu_2][B(C_6F_5)_4]$, **40** *Figure 5.*

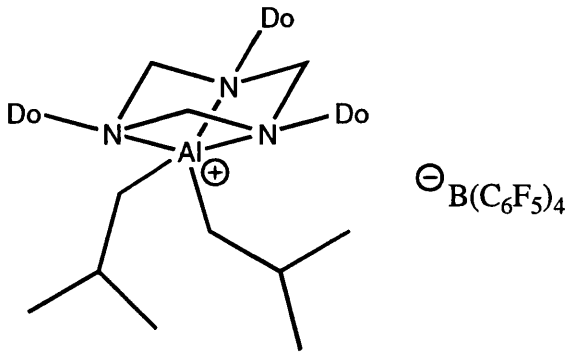

Figure 5: Complex **40** decomposition product

In parallel with the ^{19}F NMR spectra obtained for this period of decomposition ^{1}H NMR spectra were also obtained, *Figure 6.* These spectra were recorded using parameters convenient for identifying nuclei of diamagnetic compounds, i.e. relatively long acquisition times and delays, hence no chromium species were observed during the decomposition. Emerging from these spectra as the decomposition proceeded were a pair of doublets at δ = 3.48 and 2.88 with $J_{Ha,Hb}$ = 8.9 Hz corresponding to a triazacyclohexane ring with inequivalent axial and equatorial methylene protons, hence, a metal complex with coordinated triazacyclohexane. As the signals are sharp the protons belong to a diamagnetic species. Additional signals due to *iso*-butyl groups were found in the aliphatic region. Integration of these peaks in comparison with those of the triazacyclohexane revealed two *iso*-butyl groups per complex, hence, the structure given above.

An NMR tube reaction of Do_3TAC with $Al^{i}Bu_3$ in deuterated benzene solution did not result in any reaction and both ^{1}H and ^{13}C NMR spectra confirmed the existence of both starting reagents with no additional species in solution. Addition of one equivalent of DMAB to the solution resulted in the formation of the aluminium triazacyclohexane complex at room temperature, *Scheme 12.*

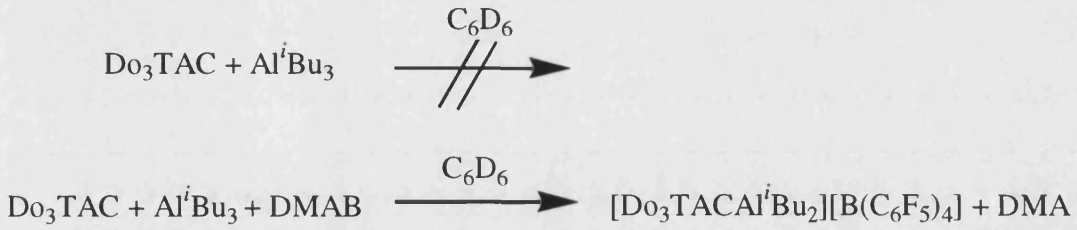

Scheme 12: Alternate formation of aluminium decomposition product

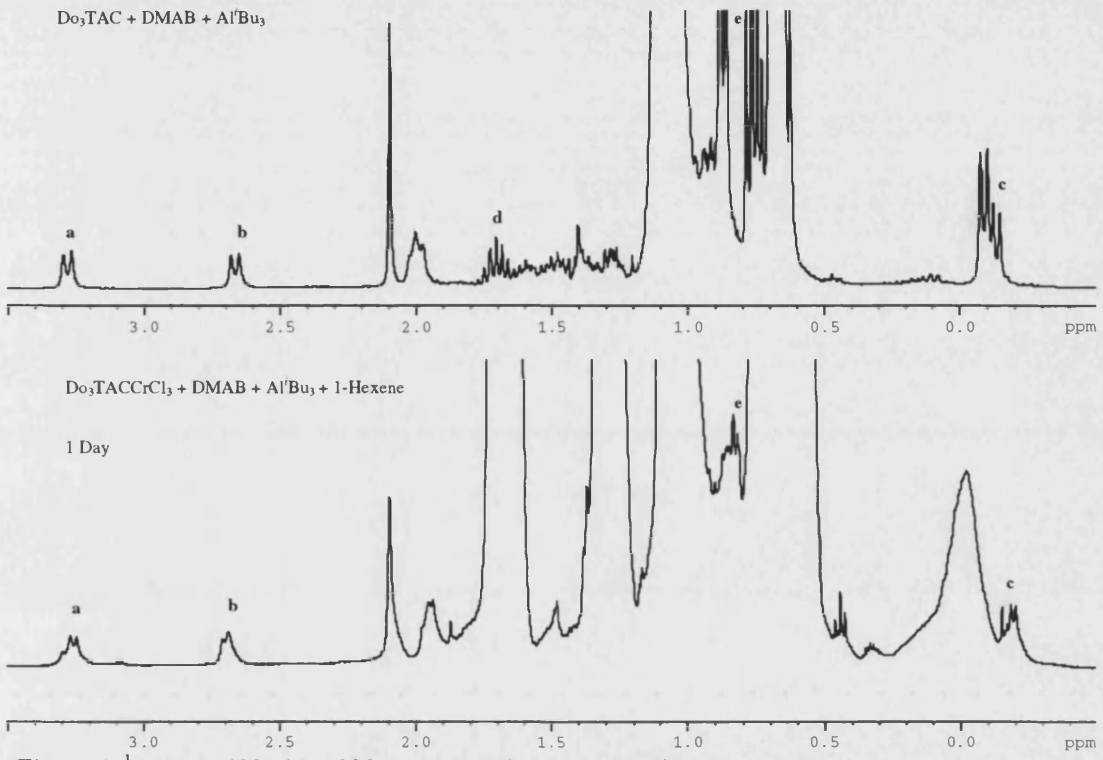

Figure 6: ^{1}H NMR 400 MHz, 298 K spectra of formation of **40** independently and as a decomposition product in benzene

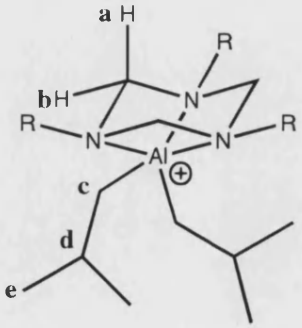

The same reaction was performed using the 2-EtBu$_3$TAC ligand and the corresponding aluminium complex [(2-EtBu)$_3$TACAl^{i}Bu$_2$][B(C$_6$F$_5$)$_4$] **41** was formed, *Table 3.*

	a	b	c	d	e
R = Do	3.48, 3H, d	2.88, 3H, d	0.07, 4H, d	1.76, 2H, m	0.95, 12H, d
R = 2-EtBu	3.73, 3H, d	3.08, 3H, d	0.24, 4H, d	1.70, 2H, m	0.92, 12H, d

Table 3: ^{1}H NMR data for complexes **40** and **41**

Upon addition of 1-hexene to the solution of **41** there is no change to the signals for the complex in the ^{1}H NMR spectra. After 1 day the doublet at 0.07 ppm had become a triplet and small quantities of isobutylene and 2-hexene were present. These observations are consistent with alkyl substitution on the aluminium of the isobutyl groups for 1-hexene. Very slowly these groups can be substituted with the liberation of 1-hexene or 2-hexene. In this way this decomposition product may be responsible for the isomerisation observed during the chromium catalysed trimerisations.

Using the relative process of the formation of this aluminium complex during the decomposition as the x-axis a new plot against line broadening of the fluorine anion signals can be drawn, *Figure 7.*

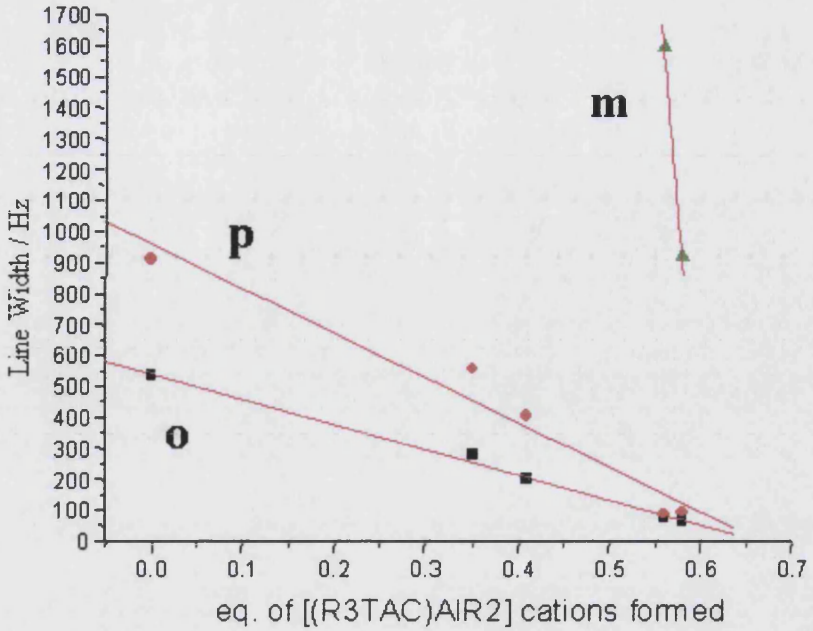

Figure 7: Graph of line widths of fluorine signals against the amount of decomposition product formed

Extrapolation of the lines for the *ortho-*, *meta-*, and *para-* fluorine signals to the convergence point at which the line broadening of all three signals are equal to each other, and to that of a diamagnetic solution of the same anion, is the point at which there is complete decomposition. At this point the aluminium complex that has been formed is present in about 2/3 of an equivalent with respect to the starting chromium complex. This value is determined by the integration of the triazacyclohexane methylene proton signals compared with the integration of the signals of a known quantity of the toluene solvent.

In conjunction with the formation of this aluminium complex is the crystallisation of yellow crystals of $[(toluene)_2Cr][B(C_6F_5)_4]$, **42** *Figure 8*.

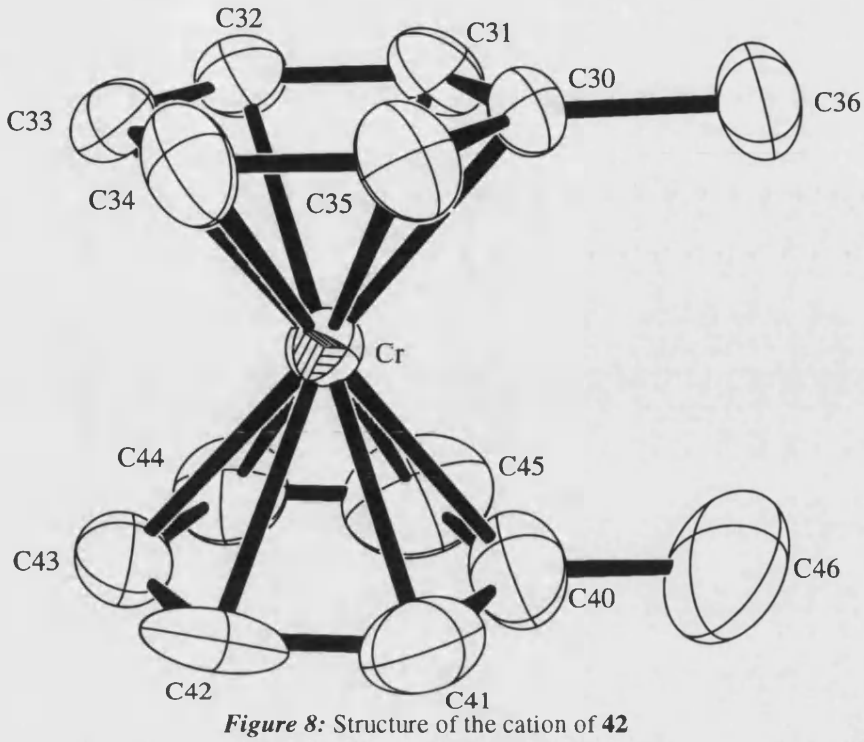

Figure 8: Structure of the cation of **42**

This Cr(I) sandwich compound has two toluene solvent molecules bound each in a η^6 fashion and parallel to each other. In the crystal structure is a significant degree of disorder, there are two sets of toluene rings with two chromium positions. The first structure has the methyl groups of ring 1 (C30-C35) and ring 2 (C40-C45) almost eclipsing, the second structure has ring 1A (C30A-C35A) skewed by about 60 ° from ring 2A (C40A-C45A). In each of the two structures the corresponding Cr(1) and Cr(1A) sit almost in line with the centroid of the ring, *Table 4*.

	Cr – Tol(centroid) / Å	Ring Slippage / Å
Cr(1) / Ring (1)	1.6208 (18)	0.049
Cr(1) / Ring (2)	1.655 (2)	0.032
Cr(1A) / Ring (1A)	1.621 (5)	0.074
Cr(1A) / Ring (2A)	1.541 (5)	0.185

Table 4: Orientation of coordinated toluene in **42**

The crystals are air and moisture sensitive decomposing in air within a few minutes. The crystals of this sandwich complex obtained from the decomposition account for about 1/3 of the total amount of chromium added to the system but clearly demonstrates that the reduction of the starting Cr(III) complex to give Cr(I) species is accessible in this system. Hence, the proposed Cr(III) / Cr(I) couple is a strong candidate for the trimerisation using the $R_3TACCrCl_3DMAB$ / AlR_3 catalyst system.

The triazacyclohexane ligand does not bind significantly stronger in the κ^3 bonding mode than in κ^1 fashion. (See Chapter 3) The ligand has a tendency to slip in solution to give a monodentate triazacyclohexane chromium intermediate that has the ability to bind electron donor molecules. (i.e. olefins) This slipping of the triazacyclohexane to vacate empty chromium d orbitals may be a key feature to the success of this type of complex as α-olefin trimerisation catalyst. However, during this process a pathway for decomposition is unveiled, *Scheme 13.*

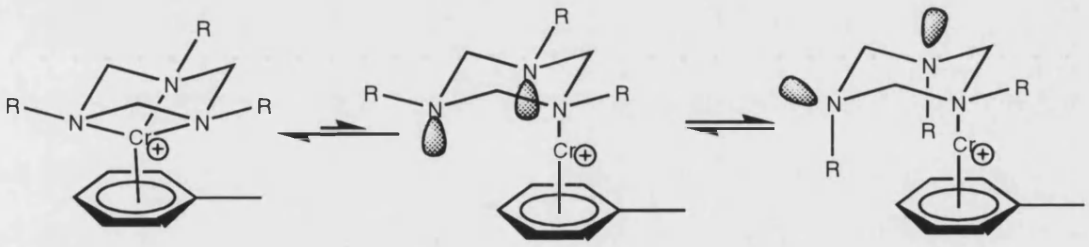

Scheme 13: Proposed decomposition pathway

After slipping of the triazacyclohexane the nitrogen lone pairs are in an axial orientation and are hindered towards donation to any species other than the d orbitals of the parent chromium centre. However nitrogen inversion may occur placing the nitrogen lone pairs in equatorial positions and hence exposing them to Lewis acids such as AlR_3. Once aluminium is coordinated all three nitrogen lone pairs may be donated and leave a

coordinatively unsaturated chromium species that rapidly finds a solvent molecule to fill the vacant sites. In this way both of the two identified decomposition species can be formed.

From a known quantity of pre catalyst and activators a proposed stoichiometry for the decomposition can be devised, *Scheme 14.*

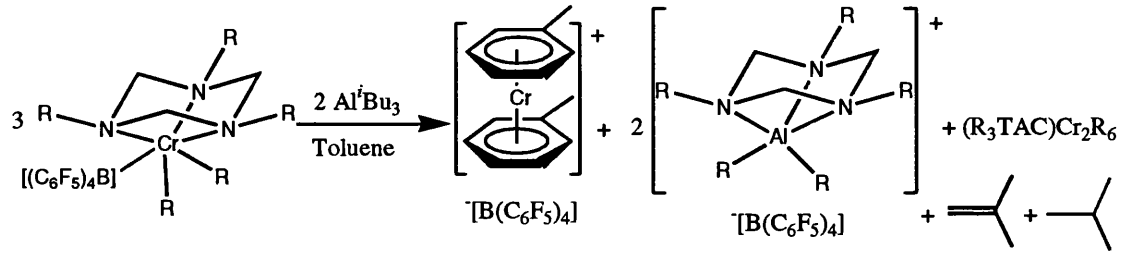

Scheme 14: Stoichiometry of decomposition

Accounting for the two known decomposition products the remaining stoichiometry gives a third neutral complex of formula "$(R_3TAC)Cr_2R_6$". As mentioned previously for copper complexes (See Chapter 3) the triazacyclohexane ligand can act as either a κ^1 or κ^2 ligand to more than one metal centre simultaneously. In this way the third decomposition product may take the form of a cluster compound with multiple metal centres linked via bridging triazacyclohexane ligands.

5.3: Summary

Reported herein is a number of $R_3TACCrCl_3$ complexes that can be activated by MAO or a combination of DMAB followed by AlR_3 to give active trimerisation catalysts for ethylene and 1-hexene. At room temperature and at 1 bar ethylene pressure both activation methods lead to active systems of comparable activity. It is found that activation with $AlMe_3$ leads to a complex that is inactive towards α-olefins. Upon

activation with AlR_3 the $R_3TACCrCl_3DMAB$ complexes form a pair of complexes that are in equilibrium one being a mono-nuclear species the other a dimer. The dimer is inactive towards olefins without firstly converting into the mono-nuclear complex. As the dimer species is the more stable on $AlMe_3$ activation the equilibrium of this system is found to be predominantly in favour of this complex and hence is an inactive catalyst.

Selectivity in the $R_3TACCrCl_3$ system towards different α-olefins can be achieved with variation of the alkyl substituent R. Branching of this subtituent especially in the β-position of the alkyl chain tends to lead to excellent selective ethylene trimerisation catalyst whilst their steric bulk tends to hinder the formation of metallacycles with larger α-olefins. Straight chained alkyl substituents are found to make catalysts with a good activity towards the larger α-olefins. Proposed in the catalytic cycle is the possible slipping of the triazacyclohexane ligand during the addition of the two equivalents of α-olefin. To try to enhance this feature mixed triazacyclohexane complexes, with either one or two weaker donor nitrogen atoms, were tested. However, these complexes had a dramatically shortened lifetime and so did not show the same activities as previously observed.

Effective magnetic moment measurements, by the Evans method, on these systems during catalysis reveals the principal complexes in solution are Cr(III). Upon decomposition of the active chromium complex, **42** crystallises out of the solution and is proof that Cr(I) is accessible in this system and that the most likely oxidation couple for this system is Cr(III) / Cr(I).

The other decomposition product found in this system was identified by signals in the ^1H NMR spectra that show the formation of a $R'_3TACAlR_2B(C_6F_5)_4$ complex. Confirmation of this complex came in the separate formation of this compound from the corresponding R'_3TAC with DMAB and an excess of AlR_3. Formation of this complex as a part of decomposition is also thought to be a product of the ring slipping process of the triazacyclohexane. This decomposition product may also be the source of isomerisation during catalysis.

6: Experimental

6.1: Materials, Techniques and Instrumentation

Solvents were freshly distilled from the appropriate drying agents. Any reactions involving air-sensitive species were carried out under a dry nitrogen atmosphere, using standard vacuum line techniques or under an argon atmosphere in a Saffron glove box. Where necessary, solvents were degassed by repeated and alternately exposing to vacuum and nitrogen. Transfers of air-sensitive materials were performed either *via* syringe, in a Saffron glove box, or using standard Schlenk techniques. Column chromatography was performed on Merck silica gel 60H, 230-300 mesh, and using standard chromatographic methods.

Reagents were purchased from Fisher, Aldrich, Avocado, or Lancaster. ^{1}H NMR spectra were recorded on a Bruker Avance 300 (300MHz), or a Bruker Avance 400 (400 MHz) spectrometer. $^{13}C\{^{1}H\}$ NMR spectra were recorded on a Bruker Avance 300 (75.5 MHz), or a Bruker Avance 400 (100.5 MHz) spectrometer. ^{19}F NMR spectra were recorded on a Bruker Avance 400 (376.2 MHz). COSY and DEPT experiments were used in cases where assignment of signals was unclear. ^{1}H NMR shifts are reported in ppm relative to $CDCl_3$ (δ7.27) or C_6D_6 (δ7.15), ^{13}C chemical shifts are reported relative to the central peak of $CDCl_3$ (δ77.0), or C_6D_6 (δ128.0). Abbreviations used in the description of spectra are s = singlet, d = doublet, t = triplet, q = quartet, quin = quintet, dd = doublet of doublets, m = multiplet, bs = broad singlet, bm = broad multiplet. Effective magnetic moments were measured by Evans method. Magnetic susceptibilities for diamagnetic components are: DMAB χ^{dia} = -0.506, MAO χ^{dia} = -0.558, $AlMe_3$ χ^{dia} = -0.796, $AlEt_3$ χ^{dia} = -0.807, $Al^{i}Bu_3$ χ^{dia} = -0.887.

6.2: Triazacyclohexanes

Synthesis Of (2-EtBu)$_3$TAC 4

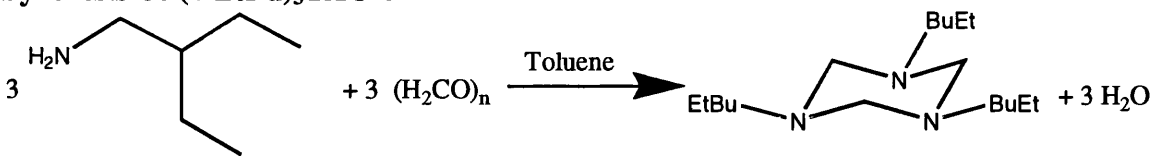

2-Ethyl-n-butylamine (2g) was dissolved in 30ml of toluene in a round-bottomed flask. Paraformaldehyde (1.103g) was added to the solution and stirred until all had gone into solution. This was followed by distillation of half the toluene with the water produced in the reaction. The remaining toluene was pumped off under vacuum, resulting in a colourless liquid of EtBu$_3$TAC (2.03g, 91 %). ^{1}H NMR (300MHz): δ(CDCl$_3$) 3.22 (6H, bs, N-CH$_2$-N), 2.24 (6H, d, $J_{H,H}$=5.3Hz, N-CH$_2$-C), 1.28 (15H, m, C-CH-[CH$_2$]$_2$), 0.81 (18H, t, $J_{H,H}$=7.2Hz, C-CH$_3$). ^{13}C{^{1}H} NMR (75.5MHz): δ(CDCl$_3$) 75.71 (s, N-CH$_2$-N), 56.70 (s, N-CH2-C), 39.13 (s, C-CH-[C]$_2$), 24.63 (s, C-CH$_2$-C), 11.21 (s, C-CH$_3$).

Synthesis Of (2-EtHex)$_3$TAC 5

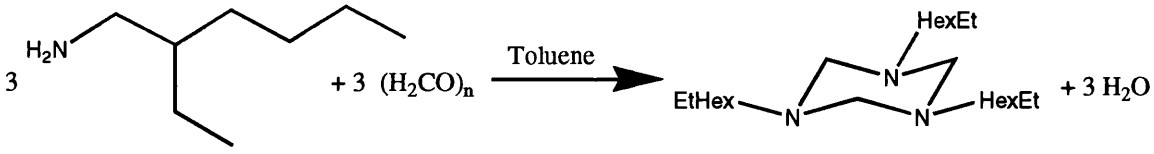

2-Ethyl-n-hexylamine (10g) was dissolved in 100ml of toluene in a round-bottomed flask. Paraformaldehyde (2.32g) was added to the solution and stirred until all had gone into solution. This was followed by distillation of half the toluene with the water produced in the reaction. The remaining toluene was pumped off under vacuum, resulting in a colourless liquid of EtHex$_3$TAC (5.094g, 83 %). ^{1}H NMR (300MHz): δ(CDCl$_3$) 3.22 (6H,

bs, N-CH_2-N), 2.17 (6H, d, $J_{H,H}$=5.3Hz, N-CH_2-C), 1.23 (27H, m, C-CH-[CH_2]$_2$$CH_2CH_2$), 0.80 (18H, t, $J_{H,H}$=7.2Hz, C-CH_3). $^{13}C\{^1H\}$ NMR (75.5MHz): δ($CDCl_3$) 75.67 (s, N-CH_2-N), 57.10 (s, N-CH2-C), 37.66 (s, C-CH-[C]$_2$), 31.79 (s, C-CH_2-C), 29.33 (s, C-CH_2-C), 24.96 (s, C-CH_2-C), 23.53 (s, C-CH_2-C), 14.49 (s, C-CH_3 [Et]), 11.15 (s, C-CH_3 [Bu]).

Synthesis Of Do_3TAC 1 [194]

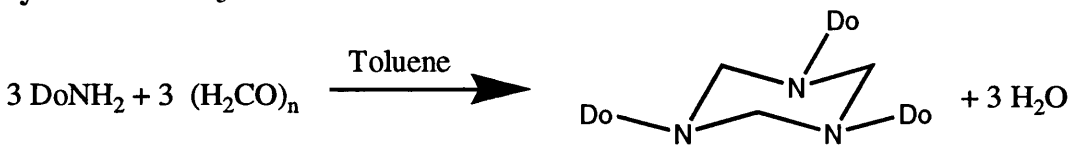

Dodecylamine (3g) was dissolved in 30ml of toluene in a round-bottomed flask. Paraformaldehyde (0.486g) was added to the solution and stirred until all had gone into solution. This was followed by distillation of half the toluene with the water produced in the reaction. The remaining toluene was pumped off under vacuum, resulting in a colourless liquid of Do_3TAC (2.49g, 78 %). ^1H NMR (300MHz): δ($CDCl_3$) 3.48 (6H, bs, N-CH_2-N), 2.57 (6H, t, $J_{H,H}$=5.3Hz, N-CH_2-C), 1.60 (6H, m, C-CH_2-C), 1.38 (56H, m, C-CH_2-C), 0.99 (9H, t, $J_{H,H}$=7.2Hz, C-CH_3). $^{13}C\{^1H\}$ NMR (75.5MHz): δ($CDCl_3$) 75.62 (s, N-CH_2-N), 53.46 (s, N-CH_2-C), 32.74, 30.57, 30.55, 30.53, 30.49, 30.24, 28.62, 28.33, 27.72, 23.51 (s, C-CH_2-C), 14.76 (s, C-CH_3).

Synthesis Of d_6-Do_3TAC 2

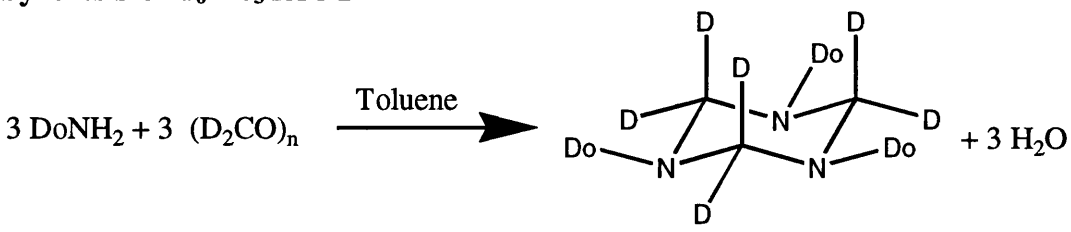

Dodecylamine (1g) was dissolved in 30ml of toluene in a round-bottomed flask. d^2-Paraformaldehyde (0.162g) was added to the solution and stirred until all had gone into

solution. This was followed by distillation of half the toluene with the water produced in the reaction. The remaining toluene was pumped off under vacuum, resulting in a colourless liquid of d^6-Do_3TAC (0.80g, 74 %). ^1H NMR (400MHz): δ($CDCl_3$) 2.38 (6H, t, $J_{H,H}$=7.7Hz, N-CH_2-C), 1.43 (6H, m, C-CH_2-C), 1.25 (56H, bs, C-CH_2-C), 0.87 (9H, t, $J_{H,H}$=6.9Hz, C-CH_3). ^2H NMR (61.4MHz): δ($CDCl_3$) 3.37 (6D, bs, N-CD_2-N). $^{13}C\{^1H\}$ NMR (100MHz): δ($CDCl_3$) 75.62 (quin, $J_{D,C}$=32Hz, N-CD_2-N), 53.46 (s, N-CH_2-C), 32.74, 30.57, 30.55, 30.53, 30.49, 30.24, 28.62, 28.33, 27.72, 23.51 (s, C-CH_2-C), 14.76 (s, C-CH_3).

Synthesis Of $Allyl_3TAC$ 3

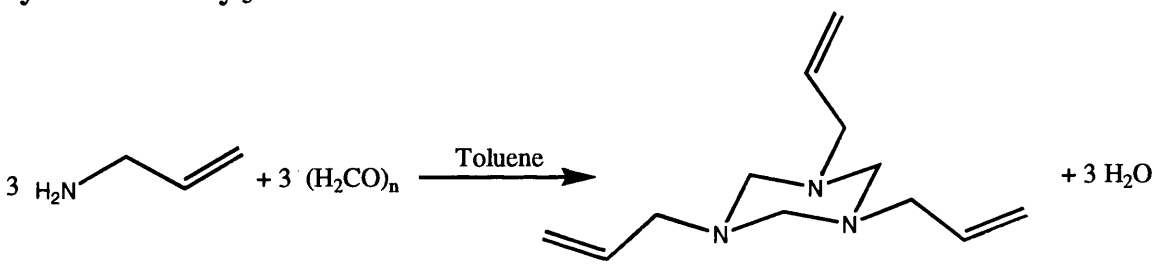

Allylamine (8.68g) was dissolved in 50ml of toluene in a round-bottomed flask. Paraformaldehyde (4g) was added to the solution and stirred until all had gone into solution. This was followed by distillation of half the toluene with the water produced in the reaction. The remaining toluene was pumped off under vacuum, resulting in a colourless liquid of $Allyl_3TAC$ (8.28g, 79 %). ^1H NMR (300MHz): δ($CDCl_3$) 5.82 (3H, m, C=CH-C), 5.17 (6H, m, CH_2=C), 3.34 (6H, bs, N-CH_2-N), 3.10 (6H, d, $J_{H,H}$=6.4Hz, N-CH_2-C). $^{13}C\{^1H\}$ NMR (75.5MHz): δ($CDCl_3$) 134.76 (s, C=CH-C), 116.93 (s, CH_2=C), 73.13 (s, N-CH_2-N), 55.33 (s, N-CH_2-C).

Synthesis Of $(Sen)_3TAC$ 7

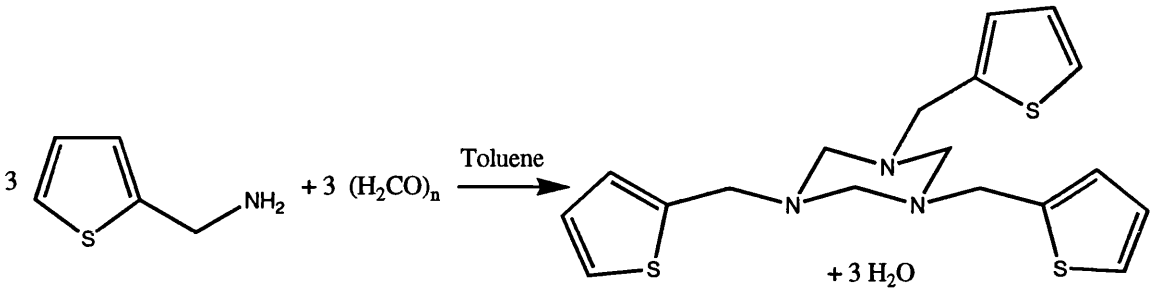

2-Thiophenemethylamine (5g) was dissolved in 50 ml of toluene in a round-bottomed flask. Paraformaldehyde (1.327g) was added to the solution and stirred until all had gone into solution. This was followed by distillation of half the toluene with the water produced in the reaction. The remaining toluene was pumped off under vacuum, resulting in a colourless liquid of $(Sen)_3TAC$ (5.42g, 98 %). ^1H NMR (300MHz): $\delta(CDCl_3)$ 6.90 (3H, d, $J_{H,H}$=4.0Hz, S-CH=C), 6.59 (6H, m, C=CH-CH=C), 3.66 (6H, s, N-CH_2-C), 3.27 (6H, bs, N-CH_2-N). $^{13}C\{^1H\}$ NMR (75.5MHz): $\delta(CDCl_3)$ 142.34 (s, S-C(-C)=C), 126.47 (s, C=CH-C), 125.64 (s, C-CH=C), 124.86 (s, C=CH-C), 72.81 (s, N-CH_2-N), 51.61 (s, N-CH_2,-C).

Synthesis Of (p-FBz)$_3$TAC 6 [195]

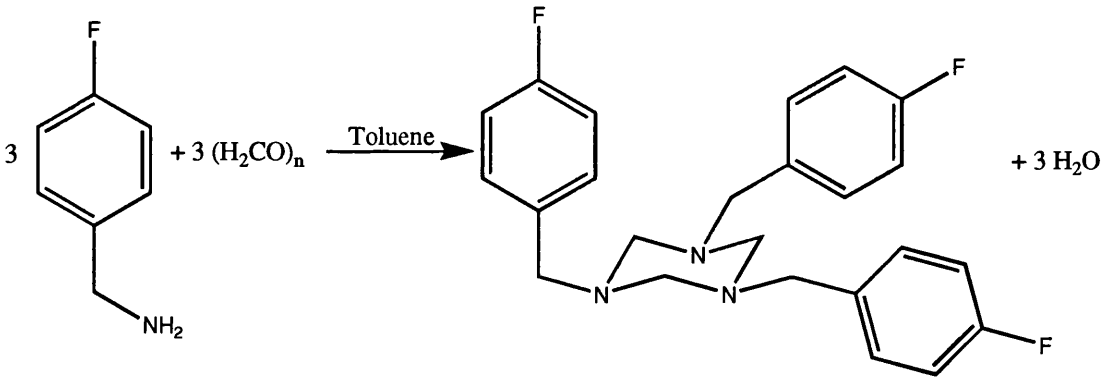

4-Fluorobenzylamine (5g) was dissolved in 50 ml of toluene in a round-bottomed flask. Paraformaldehyde (1.226g) was added to the solution and stirred until all had gone into solution. This was followed by distillation of half the toluene with the water produced in the reaction. The remaining toluene was pumped off under vacuum, resulting in a colourless liquid of (p-FBz)$_3$TAC (3.89g, 71 %). 7.26 (6H, m, m-FC_6H_4), 6.96 (6H, dd, $J_{H,H}$= 8.7Hz, $J_{H,F}$= 8.7Hz, o-FC_6H_4), 3.60 (6H, s, N-CH_2-PhF), 3.37 (6H, bs, N-CH_2-N). $^{13}C\{^1H\}$ NMR (75.5MHz): δ($CDCl_3$) 161.92 (d, $J_{C,F}$= 245Hz, $ipso$-FC_6H_4), 133.91 (d, $J_{C,F}$= 3.0Hz, p-FC_6H_4), 130.29 (d, $J_{C,F}$= 8.0Hz, m-FC_6H_4), 115.02 (d, $J_{C,F}$= 21.2Hz, o-FC_6H_4), 73.54 (s, N-CH_2-N), 56.13 (s, N-CH_2-PhF).

Synthesis Of [(EtO)$_3$SiPr]$_3$TAC 8

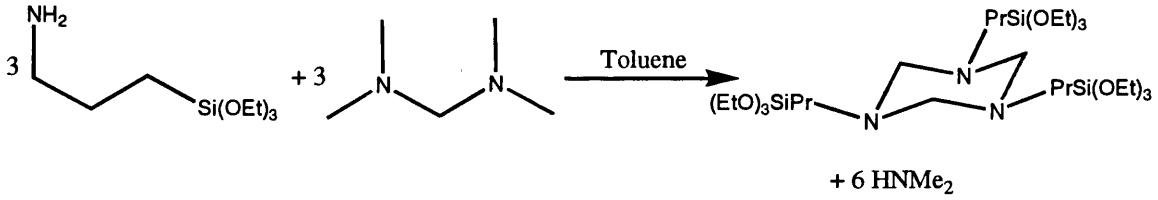

3-Aminopropyltriethoxysilane (1.623g) was dissolved in 50ml of toluene in a round-bottomed flask. N,N,N',N'-tetramethylmethylenediamine (0.749g) was added to the solution and refluxed at 110 °C for 3h. The toluene was pumped off under vacuum with any di-methylamine produced, resulting in a colourless liquid of [(EtO)$_3$SiPr]$_3$TAC (1.64g, 96 %). ^1H NMR (300MHz): δ($CDCl_3$) 3.89 (18H, q, $J_{H,H}$=6.2Hz, O-CH_2-C), 3.37 (6H, bs, N-CH_2-N), 2.48 (6H, t, $J_{H,H}$=5.2Hz, N-CH_2-C), 1.65 (6H, m, C-CH_2-C), 1.29 (27H, t, $J_{H,H}$=6.2Hz, C-CH_3), 0.70 (6H, t, $J_{H,H}$=5.7Hz, Si-CH_2-C). $^{13}C\{^1H\}$ NMR (75.5MHz): δ($CDCl_3$) 75.14 (s, N-CH_2-N), 58.64 (s, O-CH_2-C), 56.30 (s, N-CH_2-C), 21.88 (s, C-CH_2-C), 18.77 (s, C-CH_3), 8.47 (s, Si-CH_2-C).

Synthesis Of (*o*-MeOPh)$_3$TAC 9 [51]

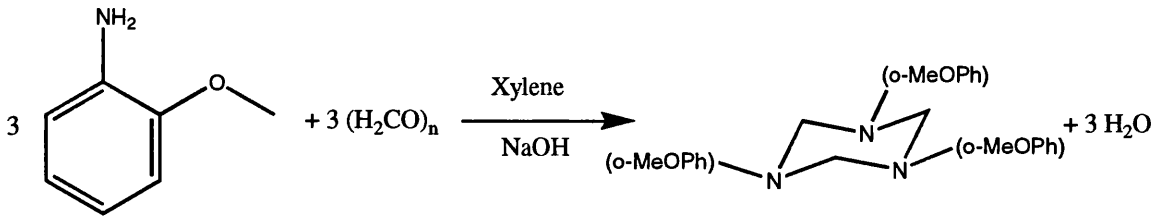

o-Anisidine (1g) was dissolved in 50ml of toluene in a round-bottomed flask. Paraformaldehyde (0.749g) was added to the solution and stirred for 8h. The toluene was pumped off under vacuum with any di-methylamine produced, resulting in a colourless liquid of (*o*-MeOPh)$_3$TAC (0.97g, 88 %). ^{1}H NMR (300MHz): δ($CDCl_3$) 7.4 (3H, m, Ar), 6.8 (3H, m, Ar), 6.7 (3H, m, Ar), 6.7 (3H, m, Ar), 4.8 (6H, bs, N-CH_2-N), 3.7 (9H, s, O-CH_3). $^{13}C\{^1H\}$ NMR (75.5MHz): δ($CDCl_3$) 147.50 (s, Ar-O), 136.97 (s, Ar-N), 123.33 (s, Ar), 121.27 (s, Ar), 111.00 (s, Ar), 110.23 (s, Ar), 55.84 (s, O-CH_3).

6.3: Mixed Triazacyclohexanes

The mixed triazacyclohexanes were prepared by dissolving a primary amine (1g) and primary aniline, in the ratios stated, in a round-bottomed flask with toluene. The given amount of paraformaldehyde was then added and stirred for 8 hours, or until completely consumed. The solution was then distilled to reduce the toluene volume by half and remove the water produced. During this distillation any remaining formaldehyde is reacted. The remaining toluene was pumped off under vacuum. The mixture of products was then dried under vacuum in a water bath at 40 °C. Where stated the products were separated by

crystallization from petroleum spirit at –80 °C followed by a second purifying crystallization at 5 °C. Relative amounts of the different products were determined by ^1H NMR and are given in the equation.

Synthesis Of Do_2PhTAC And Ph_2DoTAC

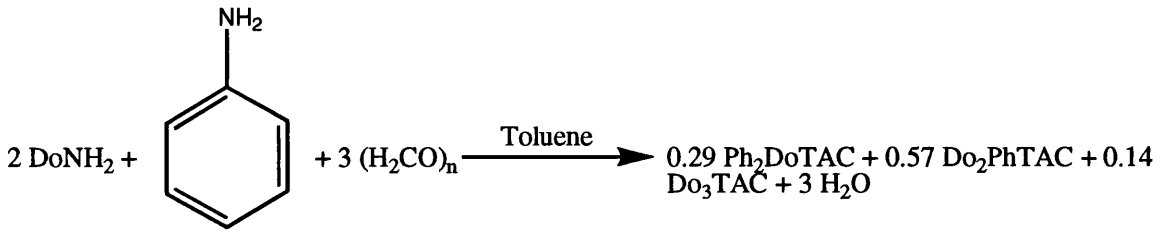

Do_2PhTAC ^1H NMR (300MHz): δ($CDCl_3$) 6.8-7.3 (5H, m, Ar), 4.15 (4H, s, N-CH_2-N), 3.64 (2H, s, N-CH_2-N), 1.60 (4H, m, C-CH_2-C), 1.38 (36H, m, C-CH_2-C), 1.04 (6H, t, C-CH_3). $^{13}C\{^1H\}$ NMR (75.5MHz): δ($CDCl_3$) 149.85 (s, ArN), 129.50 (s, Ar), 120.22 (s, Ar), 117.35 (s, Ar), 74.79 (s, N-CH_2-N), 71.50 (s, N-CH_2-N), 52.84 (s, N-CH_2-C), 32.34 (s, C-CH_2-C), 30.09 (s, C-CH_2-C), 29.99 (s, C-CH_2-C), 29.93 (s, C-CH_2-C), 29.78 (s, C-CH_2-C), 28.06 (s, C-CH_2-C), 27.98 (s, C-CH_2-C), 27.96 (s, C-CH_2-C), 27.88 (s, C-CH_2-C), 23.11 (s, C-CH_2-C), 14.54 (s, C-CH_3).

Ph_2DoTAC ^1H NMR (300MHz): δ($CDCl_3$) 6.8-7.3 (10H, m, Ar), 4.72 (2H, s, N-CH_2-N), 4.32 (4H, s, N-CH_2-N), 1.60 (2H, m, C-CH_2-C), 1.38 (18H, m, C-CH_2-C), 1.04 (3H, t, C-CH_3). $^{13}C\{^1H\}$ NMR (75.5MHz): δ($CDCl_3$) 150.45 (s, ArN), 129.62 (s, Ar), 120.90 (s, Ar), 117.72 (s, Ar), 71.58 (s, N-CH_2-N), 68.85 (s, N-CH_2-N), 52.47 (s, N-CH_2-C), 32.34 (s, C-CH_2-C), 30.09 (s, C-CH_2-C), 29.99 (s, C-CH_2-C), 29.93 (s, C-CH_2-C),

29.78 (s, C-CH_2-C), 28.06 (s, C-CH_2-C), 27.98 (s, C-CH_2-C), 27.96 (s, C-CH_2-C), 27.88 (s, C-CH_2-C), 23.11 (s, C-CH_2-C), 14.54 (s, C-CH_3).

Synthesis Of Do_2(*p*-BrPh)TAC And (*p*-BrPh)$_2$DoTAC

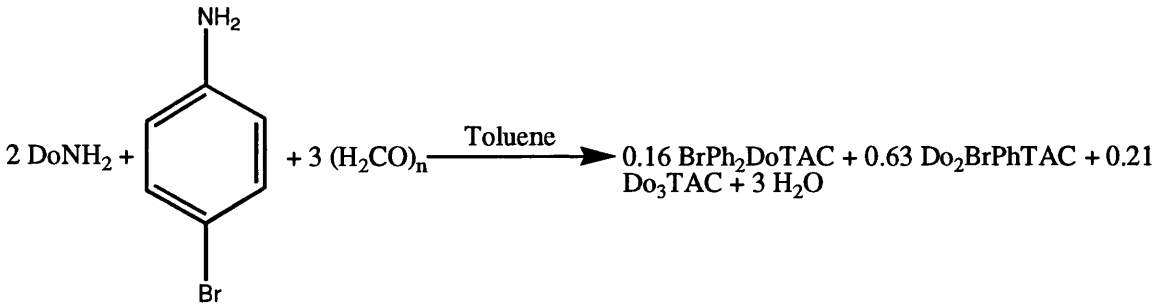

Do_2(*p*-BrPh)TAC ^{1}H NMR (300MHz): δ($CDCl_3$) 7.32 (2H, d, $J_{H,H}$=9Hz, Ar), 6.86 (2H, d, $J_{H,H}$=9Hz, Ar), 4.08 (4H, s, N-CH_2-N), 3.52 (2H, s, N-CH_2-N), 2.41 (4H, t, $J_{H,H}$=7.2Hz, N-CH_2), 1.45 (4H, m, C-CH_2-C), 1.26 (36H, m, C-CH_2-C), 0.89 (6H, t, $J_{H,H}$=6.9Hz, C-CH_3). ^{13}C{^{1}H} NMR (75.5MHz): δ($CDCl_3$) 149.68 (s, ArN), 132.29 (s, Ar), 119.00 (s, Ar), 112.34 (s, ArBr), 74.71 (s, N-CH_2-N), 71.34 (s, N-CH_2-N), 52.77 (s, N-CH_2-C), 32.32 (s, C-CH_2-C), 30.08 (s, C-CH_2-C), 29.98 (s, C-CH_2-C), 29.90 (s, C-CH_2-C), 29.76 (s, C-CH_2-C), 28.04 (s, C-CH_2-C), 27.94 (s, C-CH_2-C), 27.88 (s, C-CH_2-C), 27.83 (s, C-CH_2-C), 23.09 (s, C-CH_2-C), 14.53 (s, C-CH_3).

(*p*-BrPh)$_2$DoTAC ^{1}H NMR (300MHz): δ($CDCl_3$) 7.33 (4H, d, $J_{H,H}$=6.6Hz, Ar), 6.85 (4H, d, $J_{H,H}$=6.6Hz, Ar), 4.74 (2H, s, N-CH_2-N), 4.25 (4H, s, N-CH_2-N), 2.56 (2H, t, $J_{H,H}$=7.2Hz, N-CH_2), 1.45 (2H, m, C-CH_2-C), 1.26 (18H, m, C-CH_2-C), 0.89 (3H, t, $J_{H,H}$=6.9Hz, C-CH_3). ^{13}C{^{1}H} NMR (75.5MHz): δ($CDCl_3$) 148.76 (s, ArN), 132.46 (s, Ar), 119.49 (s, Ar), 113.41 (s, ArBr), 71.55 (s, N-CH_2-N), 68.69 (s, N-CH_2-N), 52.48 (s, N-CH_2-C), 32.32 (s, C-CH_2-C), 30.08 (s, C-CH_2-C), 29.98 (s, C-CH_2-C), 29.90 (s, C-CH_2-C),

29.76 (s, C-CH_2-C), 28.04 (s, C-CH_2-C), 27.94 (s, C-CH_2-C), 27.88 (s, C-CH_2-C), 27.83 (s, C-CH_2-C), 23.09 (s, C-CH_2-C), 14.53 (s, C-CH_3).

Synthesis Of Do_2(*p*-FPh)TAC And (*p*-FPh)$_2$DoTAC

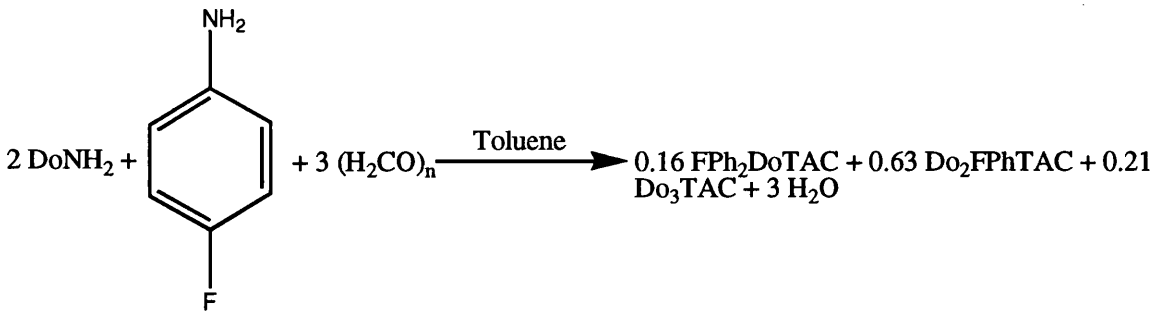

Do_2(*p*-FPh)TAC ^{1}H NMR (300MHz): δ($CDCl_3$) 7.18 (2H, d, $J_{H,H}$=9Hz, Ar), 6.63 (2H, d, $J_{H,H}$=9Hz, Ar), 4.04 (4H, s, N-CH_2-N), 3.51 (2H, s, N-CH_2-N), 2.43 (4H, t, $J_{H,H}$=1.8Hz, N-CH_2), 1.46 (4H, m, C-CH_2-C), 1.27 (36H, m, C-CH_2-C), 0.89 (6H, t, $J_{H,H}$=6.9Hz, C-CH_3). ^{13}C{^{1}H} NMR (75.5MHz): δ($CDCl_3$) 147.01 (s, ArN), 129.41 (s, Ar), 119.18 (s, Ar), 115.81 (d, $J_{C,F}$=9Hz, ArF), 74.78 (s, N-CH_2-N), 72.28 (s, N-CH_2-N), 52.88 (s, N-CH_2-C), 32.33 (s, C-CH_2-C), 30.08 (s, C-CH_2-C), 29.98 (s, C-CH_2-C), 29.91 (s, C-CH_2-C), 29.77 (s, C-CH_2-C), 28.05 (s, C-CH_2-C), 27.94 (s, C-CH_2-C), 27.92 (s, C-CH_2-C), 27.86 (s, C-CH_2-C), 23.09 (s, C-CH_2-C), 14.52 (s, C-CH_3). ^{19}F NMR (376MHz): δ($CDCl_3$) –122.9 (1F, bm, ArF).

(*p*-FPh)$_2$DoTAC ^{1}H NMR (300MHz): δ($CDCl_3$) 7.25 (4H, d, $J_{H,H}$=6.6Hz, Ar), 6.60 (4H, d, $J_{H,H}$=6.6Hz, Ar), 4.67 (2H, s, N-CH_2-N), 4.20 (4H, s, N-CH_2-N), 2.58 (2H, t, $J_{H,H}$=7.2Hz, N-CH_2), 1.46 (2H, m, C-CH_2-C), 1.27 (18H, m, C-CH_2-C), 0.89 (3H, t, $J_{H,H}$=6.9Hz, C-CH_3). ^{13}C{^{1}H} NMR (75.5MHz): δ($CDCl_3$) 146.98 (s, ArN), 128.6 (s, Ar), 119.28 (s, Ar), 116.11 (d, $J_{C,F}$=9Hz, ArF), 72.40 (s, N-CH_2-N), 70.67 (s, N-CH_2-N), 52.64

(s, N-CH_2-C), 32.33 (s, C-CH_2-C), 30.08 (s, C-CH_2-C), 29.98 (s, C-CH_2-C), 29.91 (s, C-CH_2-C), 29.77 (s, C-CH_2-C), 28.05 (s, C-CH_2-C), 27.94 (s, C-CH_2-C), 27.92 (s, C-CH_2-C), 27.86 (s, C-CH_2-C), 23.09 (s, C-CH_2-C), 14.52 (s, C-CH_3). ^{19}F NMR (376MHz): δ($CDCl_3$) –121.7 (2F, bm, ArF).

Synthesis Of Do_2(*p*-ClPh)TAC And (*p*-ClPh)$_2$DoTAC

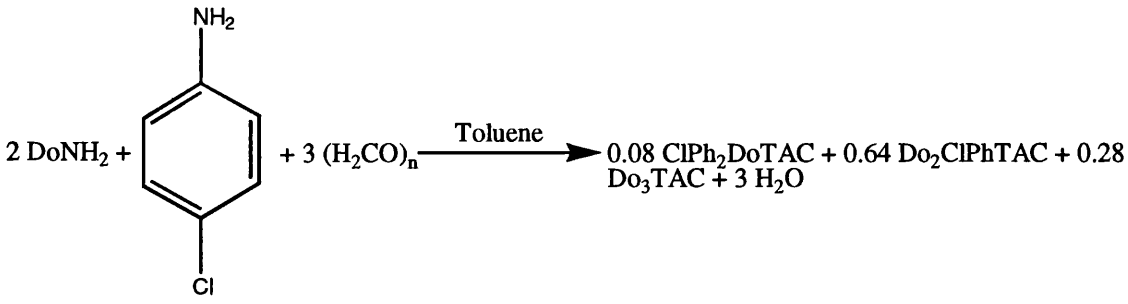

Do_2(*p*-ClPh)TAC ^1H NMR (300MHz): δ($CDCl_3$) 7.18 (2H, d, $J_{H,H}$=9Hz, Ar), 6.91 (2H, d, $J_{H,H}$=9Hz, Ar), 4.08 (4H, s, N-CH_2-N), 3.52 (2H, s, N-CH_2-N), 2.42 (4H, t, $J_{H,H}$=6.6Hz, N-CH_2), 1.45 (4H, m, C-CH_2-C), 1.26 (36H, m, C-CH_2-C), 0.89 (6H, t, $J_{H,H}$=6.3Hz, C-CH_3). $^{13}C\{^1H\}$ NMR (75.5MHz): δ($CDCl_3$) 149.24 (s, ArN), 129.37 (s, Ar), 125.04 (s, ArCl), 118.61 (s, Ar), 74.73 (s, N-CH_2-N), 71.48 (s, N-CH_2-N), 52.78 (s, N-CH_2-C), 32.33 (s, C-CH_2-C), 30.08 (s, C-CH_2-C), 29.98 (s, C-CH_2-C), 29.90 (s, C-CH_2-C), 29.77 (s, C-CH_2-C), 28.04 (s, C-CH_2-C), 27.94 (s, C-CH_2-C), 27.88 (s, C-CH_2-C), 27.83 (s, C-CH_2-C), 23.09 (s, C-CH_2-C), 14.52 (s, C-CH_3).

(*p*-ClPh)$_2$DoTAC ^1H NMR (300MHz): δ($CDCl_3$) 7.18 (4H, d, $J_{H,H}$=9Hz, Ar), 6.91 (4H, d, $J_{H,H}$=6.6Hz, Ar), 4.71 (2H, s, N-CH_2-N), 4.25 (4H, s, N-CH_2-N), 2.37 (2H, t, $J_{H,H}$=3.6Hz, N-CH_2), 1.45 (2H, m, C-CH_2-C), 1.26 (18H, m, C-CH_2-C), 0.89 (3H, t, $J_{H,H}$=6.3Hz, C-CH_3). $^{13}C\{^1H\}$ NMR (75.5MHz): δ($CDCl_3$) 149.24 (s, ArN), 129.52 (s, Ar), 125.67 (s, ArCl), 119.14 (s, Ar), 71.48 (s, N-CH_2-N), 66.10 (s, N-CH_2-N), 52.78 (s, N-CH_2-

C), 32.33 (s, C-CH_2-C), 30.08 (s, C-CH_2-C), 29.98 (s, C-CH_2-C), 29.90 (s, C-CH_2-C), 29.77 (s, C-CH_2-C), 28.04 (s, C-CH_2-C), 27.94 (s, C-CH_2-C), 27.88 (s, C-CH_2-C), 27.83 (s, C-CH_2-C), 23.09 (s, C-CH_2-C), 14.52 (s, C-CH_3).

Synthesis Of Do_2[*p*-(F_3C)Ph]TAC And [*p*-(F_3C)Ph]$_2$DoTAC

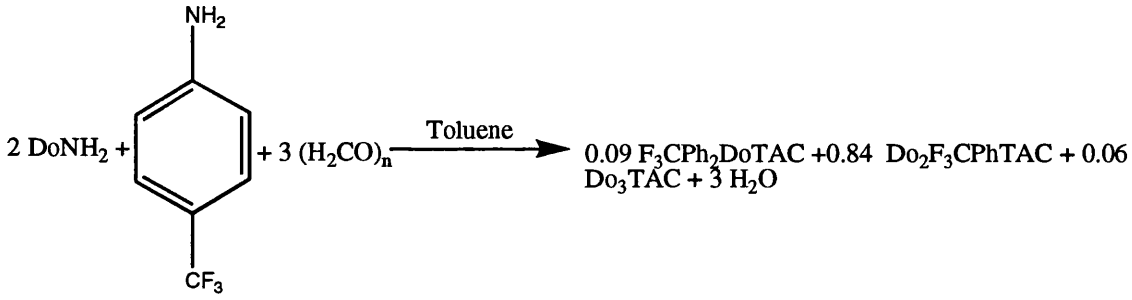

Do_2[*p*-(F_3C)Ph]TAC ^{1}H NMR (300MHz): δ($CDCl_3$) 7.47 (2H, d, $J_{H,H}$=6.6Hz, Ar), 6.69 (2H, d, $J_{H,H}$=6.6Hz, Ar), 4.20 (4H, s, N-CH_2-N), 3.56 (2H, s, N-CH_2-N), 2.43 (4H, t, $J_{H,H}$=5.4Hz, N-CH_2), 1.48 (4H, m, C-CH_2-C), 1.23 (36H, m, C-CH_2-C), 0.91 (6H, t, $J_{H,H}$=4.8Hz, C-CH_3). ^{13}C{^{1}H} NMR (75.5MHz): δ($CDCl_3$) 152.44 (s, ArN), 128.06 (s, Ar), 120.40 (q, $J_{C,F}$=30Hz, $ArCF_3$), 115.40 (s, Ar), 74.42 (s, N-CH_2-N), 70.08 (s, N-CH_2-N), 52.31 (s, N-CH_2-C), 29.78 (s, C-CH_2-C), 29.75 (s, C-CH_2-C), 29.66 (s, C-CH_2-C), 29.59 (s, C-CH_2-C), 29.47 (s, C-CH_2-C), 27.72 (s, C-CH_2-C), 27.66 (s, C-CH_2-C), 27.61 (s, C-CH_2-C), 27.53 (s, C-CH_2-C), 22.82 (s, C-CH_2-C), 14.26 (s, C-CH_3). ^{19}F NMR (376MHz): δ($CDCl_3$) –61.7 (1F, s, ArF).

[*p*-(F_3C)Ph]$_2$DoTAC ^{1}H NMR (300MHz): δ($CDCl_3$) 7.47 (4H, d, $J_{H,H}$=6.6Hz, Ar), 6.69 (4H, d, $J_{H,H}$=6.6Hz, Ar), 4.92 (2H, s, N-CH_2-N), 4.40 (4H, s, N-CH_2-N), 2.55 (2H, t, $J_{H,H}$=7.2Hz, N-CH_2), 1.46 (2H, m, C-CH_2-C), 1.23 (18H, m, C-CH_2-C), 0.89 (3H, t, $J_{H,H}$=4.8Hz, C-CH_3). ^{13}C{^{1}H} NMR (75.5MHz): δ($CDCl_3$) 152.44 (s, ArN), 128.87 (s, Ar), 120.40 (q, $J_{C,F}$=30Hz, $ArCF_3$), 116.03 (s, Ar), 70.37 (s, N-CH_2-N), 66.81 (s, N-CH_2-N),

51.96 (s, N-CH_2-C), 29.78 (s, C-CH_2-C), 29.75 (s, C-CH_2-C), 29.66 (s, C-CH_2-C), 29.59 (s, C-CH_2-C), 29.47 (s, C-CH_2-C), 27.72 (s, C-CH_2-C), 27.66 (s, C-CH_2-C), 27.61 (s, C-CH_2-C), 27.53 (s, C-CH_2-C), 22.82 (s, C-CH_2-C), 14.26 (s, C-CH_3). ^{19}F NMR (376MHz): δ($CDCl_3$) –62.0 (2F, s, ArF).

Synthesis Of $Do_2(F_5Ph)TAC$ And $(F_5Ph)_2DoTAC$

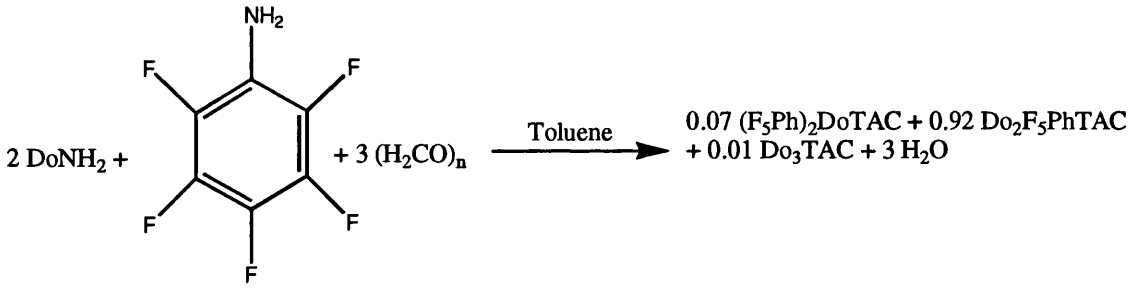

$Do_2(F_5Ph)TAC$ ^1H NMR (300MHz): δ(CDCl3) 4.08 (4H, s, N-CH_2-N), 3.62 (2H, s, N-CH_2-N), 2.63 (4H, t, $J_{H,H}$=7.5Hz, N-CH_2), 1.45 (4H, m, C-CH_2-C), 1.26 (36H, m, C-CH_2-C), 0.88 (6H, t, $J_{H,H}$=6.3Hz, C-CH_3). $^{13}C\{^1H\}$ NMR (75.5MHz): δ($CDCl_3$) 128.56 (s, ArN), 73.48 (s, N-CH_2-N), 72.25 (s, N-CH_2-N), 52.47 (s, N-CH_2-C), 32.31 (s, C-CH_2-C), 30.07 (s, C-CH_2-C), 30.04 (s, C-CH_2-C), 30.02 (s, C-CH_2-C), 29.96 (s, C-CH_2-C), 29.91 (s, C-CH_2-C), 29.75 (s, C-CH_2-C), 28.17 (s, C-CH_2-C), 27.78 (s, C-CH_2-C), 21.78 (s, C-CH_2-C), 14.46 (s, C-CH_3).

$(F_5Ph)_2DoTAC$ ^1H NMR (300MHz): δ($CDCl_3$) 4.69 (2H, s, N-CH_2-N), 4.40 (4H, s, N-CH_2-N), 2.40 (2H, t, $J_{H,H}$=7.2Hz, N-CH_2), 1.45 (2H, m, C-CH_2-C), 1.26 (18H, m, C-CH_2-C), 0.88 (3H, t, $J_{H,H}$=4.8Hz, C-CH_3). $^{13}C\{^1H\}$ NMR (75.5MHz): δ($CDCl_3$) 129.37 (s, ArN), 72.25 (s, N-CH_2-N), 68.90 (s, N-CH_2-N), 52.47 (s, N-CH_2-C), 32.31 (s, C-CH_2-C), 30.07 (s, C-CH_2-C), 30.04 (s, C-CH_2-C), 30.02 (s, C-CH_2-C), 29.96 (s, C-CH_2-C), 29.91 (s,

C-CH_2-C), 29.75 (s, C-CH_2-C), 28.17 (s, C-CH_2-C), 27.78 (s, C-CH_2-C), 21.78 (s, C-CH_2-C), 14.46 (s, C-CH_3).

Synthesis Of (2-EtBu)$_2$PhTAC And Ph$_2$(2-EtBu)TAC

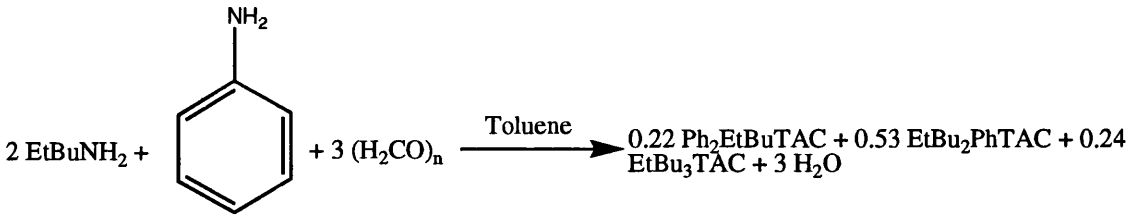

(2-EtBu)$_2$PhTAC ^{1}H NMR (300MHz): δ($CDCl_3$) 6.8-7.2 (5H, m, Ar), 4.03 (4H, s, N-CH_2-N), 3.42 (2H, s, N-CH_2-N), 2.23 (4H, d, $J_{H,H}$=5.4Hz, N-CH_2), 1.25 (10H, m, C-CH-[CH_2]$_2$-C), 0.75 (12H, t, $J_{H,H}$=7.2Hz, C-CH_3). $^{13}C\{^1H\}$ NMR (75.5MHz): δ($CDCl_3$) 150.75 (s, ArN), 129.83 (s, Ar), 120.05 (s, Ar), 117.31 (s, Ar), 75.78 (s, N-CH_2-N), 74.95 (s, N-CH_2-N), 56.17 (s, N-CH_2-C), 39.08 (s, C-CH-[C]$_2$), 24.39 (s, C-CH_2-C), 11.22 (s, C-CH_3).

Ph$_2$(2-EtBu)TAC ^{1}H NMR (300MHz): δ($CDCl_3$) 6.8-7.2 (10H, m, Ar), 4.70 (2H, s, N-CH_2-N), 4.22 (4H, s, N-CH_2-N), 2.40 (2H, d, $J_{H,H}$=6.1Hz, N-CH_2), 1.32 (5H, m, C-CH-[CH_2]$_2$-C), 0.69 (6H, t, $J_{H,H}$=7.2Hz, C-CH_3). $^{13}C\{^1H\}$ NMR (75.5MHz): δ($CDCl_3$) 149.98 (s, ArN), 129.45 (s, Ar), 120.85 (s, Ar), 117.74 (s, Ar), 72.13 (s, N-CH_2-N), 68.87 (s, N-CH_2-N), 55.92 (s, N-CH_2-C), 39.20 (s, C-CH-[C]$_2$), 24.29 (s, C-CH_2-C), 11.16 (s, C-CH_3).

Synthesis Of (2-EtBu)$_2$(*p*-BrPh)TAC And (*p*-BrPh)$_2$(2-EtBu)TAC 13

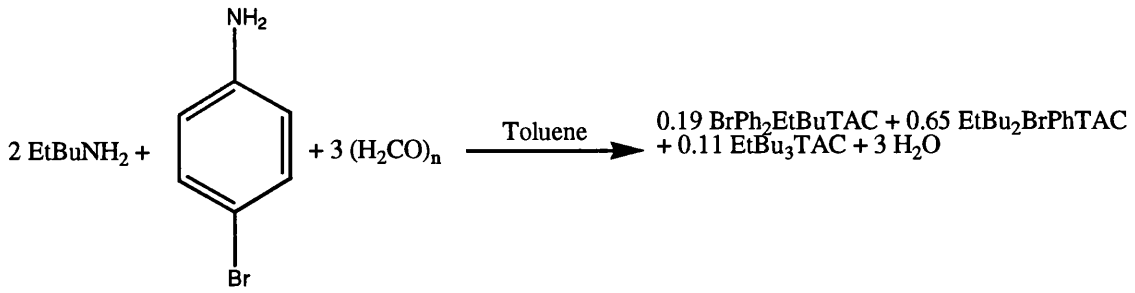

(2-EtBu)$_2$(*p*-BrPh)TAC ^{1}H NMR (300MHz): δ($CDCl_3$) 7.18 (2H, d, $J_{H,H}$=9.0Hz, Ar), 6.91 (2H, d, $J_{H,H}$=9.0Hz, Ar), 4.01 (4H, s, N-CH_2-N), 3.41 (2H, s, N-CH_2-N), 2.20 (4H, d, $J_{H,H}$=5.1Hz, N-CH_2), 1.23 (10H, m, C-CH-[CH_2]$_2$-C), 0.75 (12H, t, $J_{H,H}$=7.2Hz, C-CH_3). ^{13}C{^{1}H} NMR (75.5MHz): δ($CDCl_3$) 149.99 (s, ArN), 132.22 (s, Ar), 118.96 (s, Ar), 112.10 (s, ArBr), 74.81 (s, N-CH_2-N), 71.99 (s, N-CH_2-N), 56.13 (s, N-CH_2-C), 39.04 (s, C-CH-[C]$_2$), 24.36 (s, C-CH_2-C), 11.19 (s, CH_3).

(*p*-BrPh)$_2$(2-EtBu)TAC ^{1}H NMR (300MHz): δ($CDCl_3$) 7.19 (2H, d, $J_{H,H}$=9.0Hz, Ar), 6.91 (2H, d, $J_{H,H}$=9.0Hz, Ar), 4.64 (2H, s, N-CH_2-N), 4.15 (4H, s, N-CH_2-N), 2.32 (2H, d, $J_{H,H}$=5.7Hz, N-CH_2), 1.23 (5H, m, C-CH-[CH_2]$_2$-C), 0.72 (6H, t, $J_{H,H}$=3.6Hz, C-CH_3). ^{13}C{^{1}H} NMR (75.5MHz): δ($CDCl_3$) 148.88 (s, ArN), 132.43 (s, Ar), 119.50 (s, Ar), 113.33 (s, ArBr), 71.99 (s, N-CH_2-N), 68.64 (s, N-CH_2-N), 55.95 (s, N-CH_2-C), 39.04 (s, C-CH-[C]$_2$), 24.30 (s, C-CH_2-C), 11.19 (s, CH_3).

Synthesis Of (2-EtBu)$_2$(*p*-FPh)TAC And (*p*-FPh)$_2$(2-EtBu)TAC 11

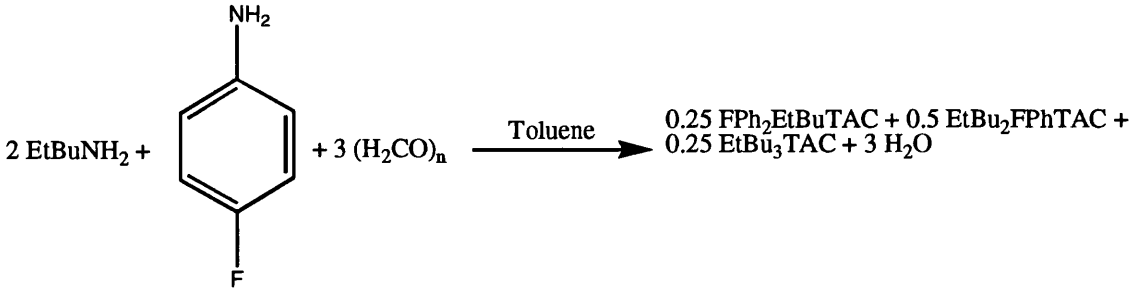

(2-EtBu)$_2$(p-FPh)TAC ^{1}H NMR (400MHz): δ($CDCl_3$) 7.21 (2H, dd, $J_{H,H}$=9.6Hz, $J_{H,F}$=18Hz, Ar), 6.94 (2H, d, $J_{H,H}$=9.6Hz, Ar), 4.07 (4H, s, N-CH_2-N), 3.51 (2H, s, N-CH_2-N), 2.32 (4H, d, $J_{H,H}$=3.9Hz, N-CH_2), 1.34 (10H, m, C-CH-[CH_2]$_2$-C), 0.86 (12H, t, $J_{H,H}$=5.4Hz, C-CH_3). ^{13}C{^{1}H} NMR (100MHz): δ($CDCl_3$) 147.10 (s, ArN), 128.90 (s, Ar), 119.58 (s, Ar), 115.74 (d, $J_{C,F}$=9Hz, ArF), 74.71 (s, N-CH_2-N), 72.83 (s, N-CH_2-N), 56.18 (s, N-CH_2-C), 39.04 (s, C-CH-[C]$_2$), 24.40 (s, C-CH_2-C), 11.26 (s, CH_3). ^{19}F NMR (376MHz): δ($CDCl_3$) –124.9 (1F, bm, ArF).

(*p*-FPh)$_2$(2-EtBu)TAC ^{1}H NMR (400MHz): δ($CDCl_3$) 7.21 (4H, dd, $J_{H,H}$=9.6Hz, $J_{H,F}$=18Hz, Ar), 6.94 (4H, d, $J_{H,H}$=9.6Hz, Ar), 4.68 (2H, s, N-CH_2-N), 4.20 (4H, s, N-CH_2-N), 2.45 (2H, d, $J_{H,H}$=3.9Hz, N-CH_2), 1.36 (5H, m, C-CH-[CH_2]$_2$-C), 0.83 (6H, t, $J_{H,H}$=5.4Hz, C-CH_3). ^{13}C{^{1}H} NMR (100MHz): δ($CDCl_3$) 146.07 (s, ArN), 128.90 (s, Ar), 119.65 (s, Ar), 115.91 (d, $J_{C,F}$=9Hz, ArF), 72.76 (s, N-CH_2-N), 70.55 (s, N-CH_2-N), 56.07 (s, N-CH_2-C), 39.11 (s, C-CH-[C]$_2$), 24.36 (s, C-CH_2-C), 11.22 (s, CH_3). ^{19}F NMR (376MHz): δ($CDCl_3$) –123.5 (1F, bm, ArF).

Synthesis Of (2-EtBu)$_2$(*p*-ClPh)TAC And (*p*-ClPh)$_2$(2-EtBu)TAC 12

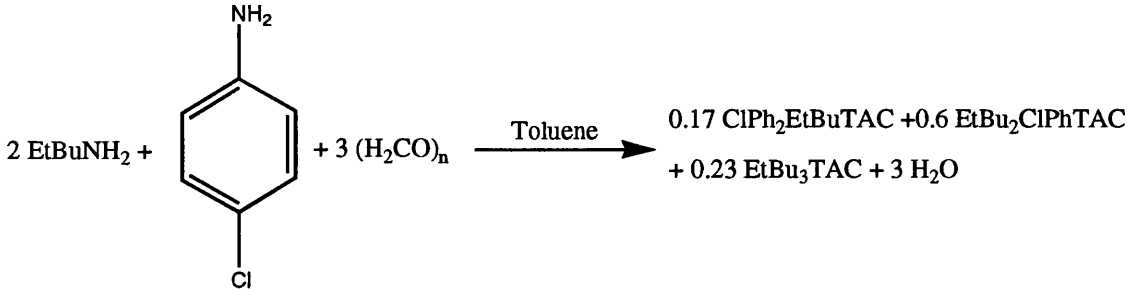

(2-EtBu)$_2$(*p*-ClPh)TAC ^{1}H NMR (300MHz): δ($CDCl_3$) 7.18 (2H, d, $J_{H,H}$=9.0Hz, Ar), 6.91 (2H, d, $J_{H,H}$=9.0Hz, Ar), 4.09 (4H, s, N-CH_2-N), 3.50 (2H, s, N-CH_2-N), 2.28 (4H, d, $J_{H,H}$=4.8Hz, N-CH_2), 1.33 (10H, m, C-CH-[CH_2]$_2$-C), 0.84 (12H, t, $J_{H,H}$=6.9Hz, C-CH_3). ^{13}C{^{1}H} NMR (75.5MHz): δ($CDCl_3$) 149.56 (s, ArN), 129.31 (s, Ar), 124.81 (s, ArCl), 115.07 (s, Ar), 74.81 (s, N-CH_2-N), 72.12 (s, N-CH_2-N), 56.14 (s, N-CH_2-C), 39.04 (s, C-CH-[C]$_2$), 24.37 (s, C-CH_2-C), 11.20 (s, CH_3).

(*p*-ClPh)$_2$(2-EtBu)TAC ^{1}H NMR (300MHz): δ($CDCl_3$) 7.19 (2H, d, $J_{H,H}$=9.0Hz, Ar), 6.91 (2H, d, $J_{H,H}$=9.0Hz, Ar), 4.72 (2H, s, N-CH_2-N), 4.23 (4H, s, N-CH_2-N), 2.48 (2H, d, $J_{H,H}$=5.3Hz, N-CH_2), 1.39 (5H, m, C-CH-[CH_2]$_2$-C), 0.89 (6H, t, $J_{H,H}$=6.9Hz, C-CH_3). ^{13}C{^{1}H} NMR (75.5MHz): δ($CDCl_3$) 148.46 (s, ArN), 129.49 (s, Ar), 125.96 (s, ArCl), 119.15 (s, Ar), 72.12 (s, N-CH_2-N), 69.03 (s, N-CH_2-N), 55.97 (s, N-CH_2-C), 39.04 (s, C-CH-[C]$_2$), 24.31 (s, C-CH_2-C), 11.15 (s, CH_3).

Synthesis Of (2-EtBu)$_2$[*p*-(F$_3$C)Ph]TAC And [*p*-(F$_3$C)Ph]$_2$(2-EtBu)TAC

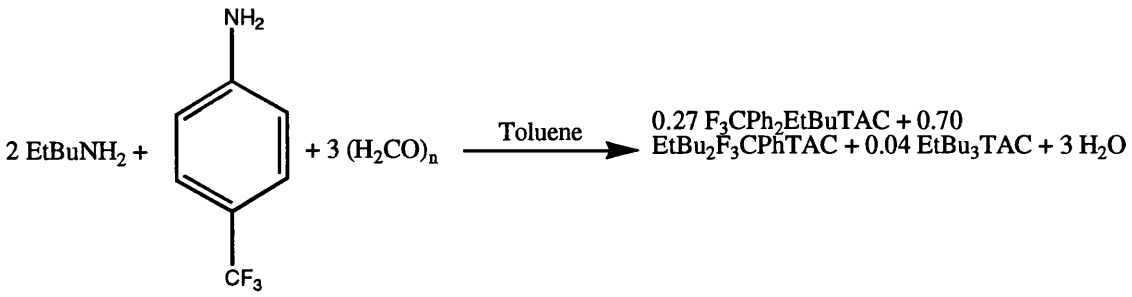

(2-EtBu)$_2$[(*p*-F$_3$C)Ph]TAC ^{1}H NMR (300MHz): δ(CDCl$_3$) 7.50 (2H, d, $J_{H,H}$=8.7Hz, Ar), 7.01 (2H, d, $J_{H,H}$=8.7Hz, Ar), 4.21 (4H, s, N-CH$_2$-N), 3.55 (2H, s, N-CH$_2$-N), 2.29 (4H, d, $J_{H,H}$=5.4Hz, N-CH$_2$), 1.34 (10H, m, C-CH-[CH$_2$]$_2$-C), 0.85 (12H, t, $J_{H,H}$=3.9Hz, C-CH$_3$). ^{13}C{^{1}H} NMR (75.5MHz): δ(CDCl$_3$) 153.44 (s, ArC), 126.78 (s, ArN), 120.91 (q, $J_{C,F}$=30Hz, C-CF$_3$), 115.89 (s, Ar), 115.89 (s, Ar), 75.08 (s, N-CH$_2$-N), 71.07 (s, N-CH$_2$-N), 55.99 (s, N-CH$_2$-C), 38.98 (s, C-CH-[C]$_2$), 24.30 (s, C-CH$_2$-C), 11.14 (s, CH$_3$). ^{19}F NMR (376MHz): δ(CDCl$_3$) –61.80 (1F, s, C-CF$_3$).

[(*p*-F$_3$C)Ph]$_2$(2-EtBu)TAC ^{1}H NMR (300MHz): δ(CDCl$_3$) 7.50 (2H, d, $J_{H,H}$=8.7Hz, Ar), 7.01 (2H, d, $J_{H,H}$=8.7Hz, Ar), 4.93 (2H, s, N-CH$_2$-N), 4.39 (4H, s, N-CH$_2$-N), 2.43 (2H, d, $J_{H,H}$=6.0Hz, N-CH$_2$), 1.34 (5H, m, C-CH-[CH$_2$]$_2$-C), 0.81 (6H, t, $J_{H,H}$=7.2Hz, C-CH$_3$). ^{13}C{^{1}H} NMR (75.5MHz): δ(CDCl$_3$) 152.23 (s, ArC), 126.97 (s, ArN), 121.83 (q, $J_{C,F}$=30Hz, C-CF$_3$), 116.56 (s, Ar), 116.56 (s, Ar), 71.20 (s, N-CH$_2$-N), 67.20 (s, N-CH$_2$-N), 55.79 (s, N-CH$_2$-C), 39.09 (s, C-CH-[C]$_2$), 24.30 (s, C-CH$_2$-C), 11.07 (s, CH$_3$). ^{19}F NMR (376MHz): δ(CDCl$_3$) –62.21 (1F, s, C-CF$_3$).

Synthesis Of $(2\text{-EtBu})_2(F_5Ph)TAC$ And $(F_5Ph)_2(2\text{-EtBu})TAC$

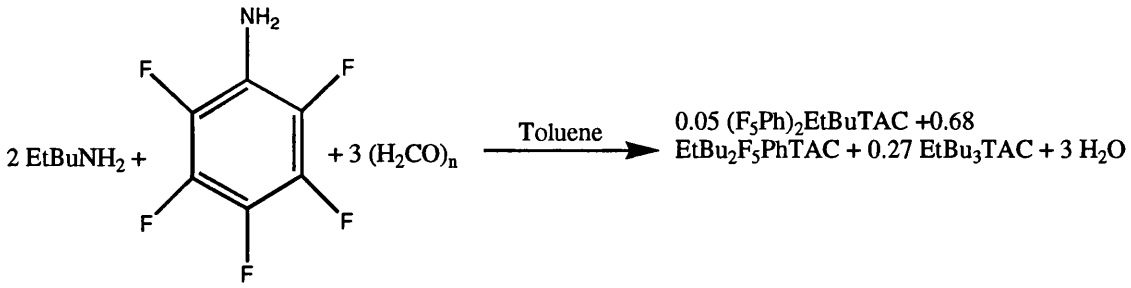

$(2\text{-EtBu})_2(F_5Ph)TAC$ ^1H NMR (300MHz): $\delta(CDCl_3)$ 4.07 (4H, s, N-CH_2-N), 3.58 (2H, s, N-CH_2-N), 2.48 (4H, d, $J_{H,H}$=5.4Hz, N-CH_2), 1.34 (10H, m, C-CH-[CH_2]$_2$-C), 0.86 (12H, t, $J_{H,H}$=5.4Hz, C-CH_3). $^{13}C\{^1H\}$ NMR (75.5MHz): $\delta(CDCl_3)$ 129.40 (s, ArN), 73.89 (s, N-CH_2-N), 72.81 (s, N-CH_2-N), 55.71 (s, N-CH_2-C), 39.17 (s, C-CH-[C]$_2$), 24.29 (s, C-CH_2-C), 11.13 (s, CH_3).

$(F_5Ph)_2(2\text{-EtBu})TAC$ ^1H NMR (300MHz): $\delta(CDCl_3)$ 4.68 (2H, s, N-CH_2-N), 4.38 (4H, s, N-CH_2-N), 2.28 (2H, d, $J_{H,H}$=5.1Hz, N-CH_2), 1.38 (5H, m, C-CH-[CH_2]$_2$-C), 0.84 (6H, t, $J_{H,H}$=5.4Hz, C-CH_3). $^{13}C\{^1H\}$ NMR (75.5MHz): $\delta(CDCl_3)$ 128.59 (s, ArN), 72.81 (s, N-CH_2-N), 71.20 (s, N-CH_2-N), 55.71 (s, N-CH_2-C), 39.17 (s, C-CH-[C]$_2$), 24.29 (s, C-CH_2-C), 11.13 (s, CH_3).

Synthesis Of $(4\text{-PhBu})_2(p\text{-FPh})TAC$ And $(p\text{-FPh})_2(4\text{-PhBu})TAC$

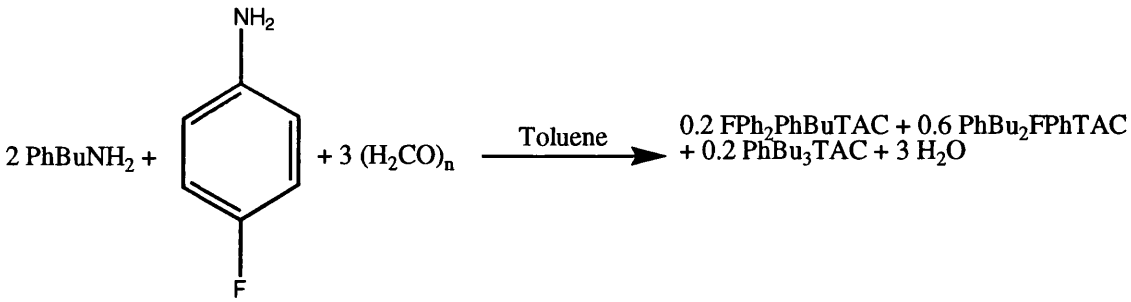

(4-PhBu)$_2$(*p*-FPh)TAC ^{1}H NMR (300MHz): δ(CDCl$_3$) 6.7-7.2 (14H, m, Ar), 3.88 (4H, s, N-CH$_2$-N), 3.35 (2H, s, N-CH$_2$-N), 2.48 (4H, t, $J_{H,H}$=7.2Hz, C-CH$_2$-Ph), 2.32 (4H, t, $J_{H,H}$=6.6Hz, C-CH$_2$-N), 1.48 (4H, m, C-CH$_2$-C), 1.36 (4H, m, C-CH$_2$-C). ^{13}C{^{1}H} NMR (75.5MHz): δ(CDCl$_3$) 119-147 (m, Ar), 74.73 (s, N-CH$_2$-N), 72.26 (s, N-CH$_2$-N), 52.62 (s, N-CH$_2$-C), 36.15 (s, C-CH$_2$-C), 29.64 (s, C-CH$_2$-C), 27.51 (s, C-CH$_2$-C). ^{19}F NMR (376MHz): δ(CDCl$_3$) –123.1 (1F, bm, ArF).

(*p*-FPh)$_2$(4-PhBu)TAC ^{1}H NMR (300MHz): δ(CDCl$_3$) 6.7-7.2 (13H, m, Ar), 4.51 (2H, s, N-CH$_2$-N), 4.04 (4H, s, N-CH$_2$-N), 2.45 (2H, t, $J_{H,H}$=3.9Hz, C-CH$_2$-Ph), 2.29 (2H, t, $J_{H,H}$=8.1Hz, C-CH$_2$-N), 1.54 (2H, m, C-CH$_2$-C), 1.36 (2H, t, C-CH$_2$-C). ^{13}C{^{1}H} NMR (75.5MHz): δ(CDCl$_3$) 119-147 (m, Ar), 72.38 (s, N-CH$_2$-N), 70.50 (s, N-CH$_2$-N), 52.60 (s, N-CH$_2$-C), 36.15 (s, C-CH$_2$-C), 29.51 (s, C-CH$_2$-C), 27.51 (s, C-CH$_2$-C). ^{19}F NMR (376MHz): δ(CDCl$_3$) –122.3 (1F, bm, ArF).

6.4: Triazacyclohexane Chromium Trichloride Complexes

Synthesis Of (2-EtBu)$_3$TACCrCl$_3$ 16

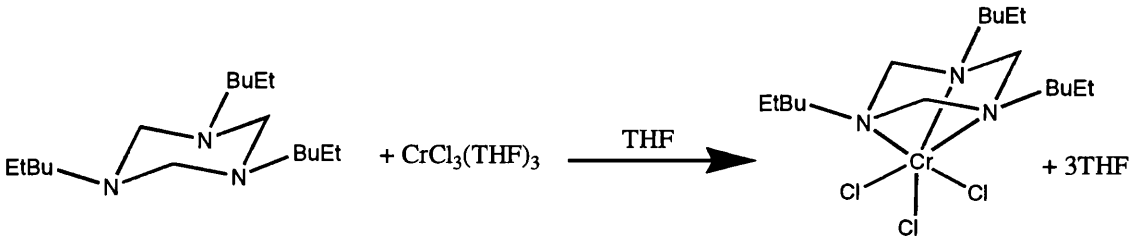

Chromium trichloride-tris-THF (1.103g) was added to (2-EtBu)$_3$TAC (1g) in a Schlenk tube under argon. THF (30ml) was added and the solution stirred for 12 hours. The purple precipitate (2-EtBu)$_3$TACCrCl$_3$ was filtered, then dried under vacuum in a 40 °C water bath (1.2g, 78 %). ^{1}H NMR (400MHz): δ(CDCl$_3$/DMSO) 1.67 (3H, bs, C-CH-[C]$_2$),

1.30 (12H, bs, C-CH_2-C), 0.91 (18H, bs, C-CH_3). $^{13}C\{^1H\}$ NMR (100MHz): δ($CDCl_3$/DMSO) 39.22 (bs, C-CH_2-C), 12.98 (bs, C-CH_3). Anal. Calc. for $C_{21}H_{45}Cl_3CrN_3$ (497.96): C, 50.7; H, 9.11; N, 8.44%. Found: C, 50.1; H, 9.03; N, 8.21%. m.p > 250 °C.

Synthesis Of (2-PhEt)$_3$TACCrCl$_3$ 15 [195]

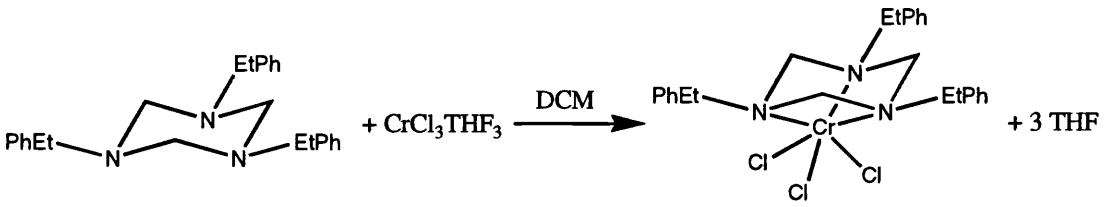

Chromium trichloride-tris-THF (1. g) was added to (2-PhEt)$_3$TAC (1.175g) in a Schlenk tube under argon. DCM (30ml) was added and the solution stirred for 12 hours. After this time the purple solution was layered with hexane, on standing for 24 hours purple crystals of (2-PhEt)$_3$TACCrCl$_3$ formed (0.613g, 41 %). Anal. Calc. for $C_{27}H_{33}Cl_3CrN_3$ (557.94): C, 58.1; H, 5.96; N, 7.53%. Found: C, 55.5; H, 5.75; N, 6.89%.

Synthesis Of (Sen)$_3$TACCrCl$_3$

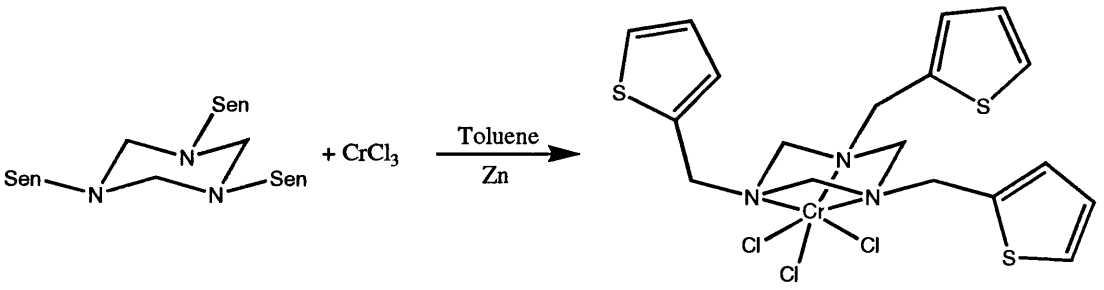

To a solution of (Sen)$_3$TAC (5.42g) in toluene (50ml) in a round-bottomed flask was added chromium trichloride (2.29g) and zinc powder (2 spatulas). The solution was stirred under gentle heat (50 °C) until a purple solution was formed. The purple solution was decanted into another round-bottomed flask to remove the zinc powder. The remaining

toluene was removed under vacuum to result in a purple solid of $(Sen)_3TACCrCl_3$ (5.55g, 72 %). Anal. Calc. for $C_{18}H_{21}Cl_3CrN_3$ (533.94): C, 40.5; H, 3.96; N, 7.87%. Found: C, 40.2; H, 3.85; N, 7.77%. T_{dec} 241 °C.

Synthesis Of d_6-Do_3TACCrCl$_3$ 20

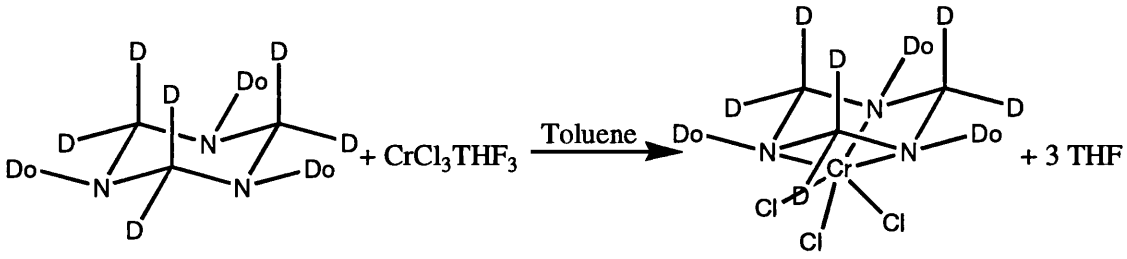

Chromium trichloride-tris-THF (0.45 g) was added to d_6-Do_3TAC (0.8g) in a Schlenk tube under argon. Toluene (30ml) was added and the solution stirred for 12 hours. The purple precipitate d^6-Do_3TACCrCl$_3$ was filtered, then dried under vacuum in a 40 °C water bath (0.87g, 86 %). $^{13}C\{^1H\}$ NMR (100MHz): δ($CDCl_3$) 53.8 (bs, C-CH_2-C), 30.9 (bs, C-CH_2-C), 29.9 (bs, C-CH_2-C), 29.1 (bs, C-CH_2-C), 28.8 (bs, C-CH_2-C), 28.4 (bs, C-CH_2-C), 21.7 (bs, C-CH_2-C), 13.2 (bs, C-CH_3), -43 (bs, C-CH_2-C). ^2H NMR (61.4MHz): δ($CDCl_3$) 41.8 (3D, bs, N-$CD_{a,b}$-N), -5.7 (3D, bs, N-$CD_{b,a}$-N). Anal. Calc. for $C_{39}H_{75}D_6Cl_3CrN_3$ (756.53): C, 61.90; H, 10.78; N, 5.55%. Found: C, 59.5; H, 10.6; N, 5.06%. T_{dec} 194 °C. χ^{dia} = -0.765, μ_{eff} (Toluene) = 3.773 μ_B.

Synthesis Of $Allyl_3TACCrCl_3$ 14

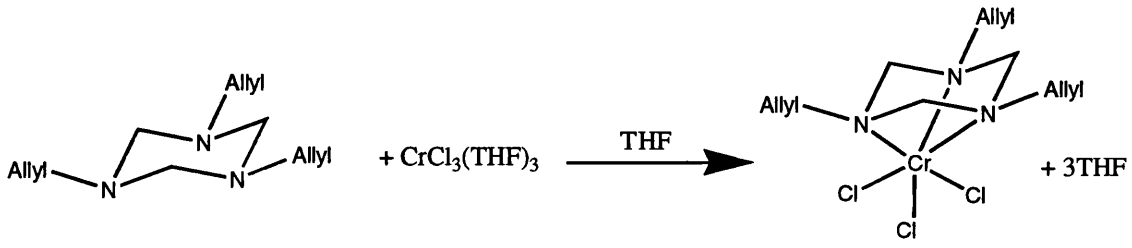

Chromium trichloride-tris-THF (0.2g) was added to $Allyl_3TAC$ (0.224g) in a Schlenk tube under argon. THF (30ml) was added and the solution stirred until all solids had dissolved. The resultant solution was left to stand for 24h. The purple crystals of $Allyl_3TACCrCl_3$ that formed were dried under vacuum in a 40 °C water bath (0.21g, 72 %). $^{13}C\{^1H\}$ NMR (100MHz): $\delta(CDCl_3\backslash MeNO_2)$ 137.90 (bs, C-CH=C), 94.50 (bs, $C=CH_2$). Anal. Calc. for $C_{12}H_{21}Cl_3CrN_3$ (365.68): C, 39.4; H, 5.79; N, 11.49%. Found: C, 39.67; H, 5.84; N, 11.03%. m.p > 250 °C.

Synthesis Of $(p\text{-FBz})_3TACCrCl_3$ [195]

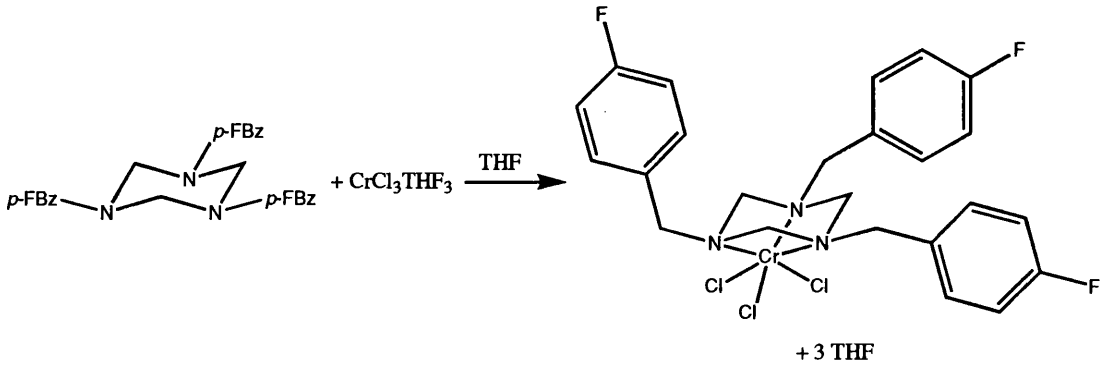

Chromium trichloride-tris-THF (0.2g) was added to $(p\text{-Bz})_3TAC$ (0.22g) in a Schlenk tube under argon. THF (20ml) was added and the solution stirred for 12 hours. The purple precipitate $(p\text{-FBz})_3TACCrCl_3$ was filtered, then dried under vacuum in a 40 °C

water bath (0.22g, 72 %). Anal. Calc. for $C_{24}H_{24}Cl_3CrF_3N_3$ (569.83): C, 50.59; H, 4.25; N, 7.37%. Found: C, 51.0; H, 4.77; N, 6.69%. m.p > 250 °C.

Synthesis Of $[(EtO)_3SiPr]_3TACCrCl_3$ 18

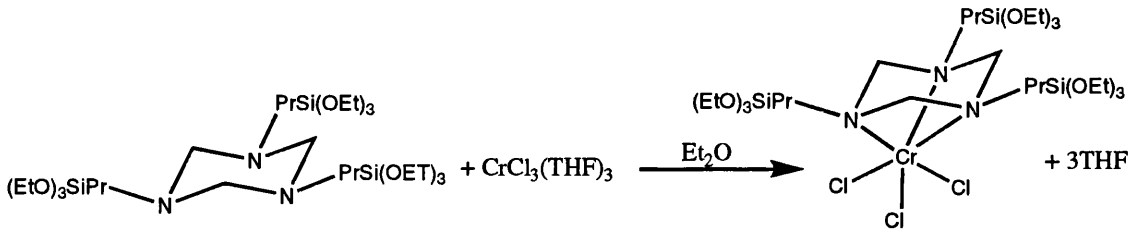

Chromium trichloride-tris-THF (0.876g) was added to $([EtO]_3SiPr)_3TAC$ (1.637g) in a Schlenk tube under argon. Diethyl ether (30ml) was added and the solution stirred for 12 hours. The solvent was pumped off under vacuum and the resultant purple solid of $([EtO]_3SiPr)_3TACCrCl_3$ was washed with hexane then dried under vacuum in a 40 °C water bath (1.63g, 81 %). ^1H NMR (400MHz): $\delta(C_6D_6)$ 3.83 (18H, bs, O-CH_2-C), 1.28 (27H, bs, C-CH_3). $^{13}C\{^1H\}$ NMR (100MHz): $\delta(C_6D_6)$ 62.18 (bs, O-CH_2-C), 21.60 (bs, C-CH_3). T_{dec} 178 °C.

Synthesis Of $(2\text{-EtHex})_3TACCrCl_3$ 17

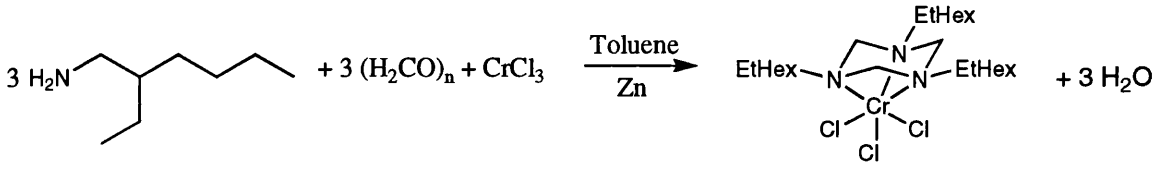

(+/-)-2-Ethylhexylamine (3g) was dissolved in 30ml of toluene in a round-bottomed flask. Paraformaldehyde (0.718g) was added to the solution and stirred until all had gone into solution. This was followed by distillation of half the toluene with the water produced in the reaction. Chromium (III) chloride (1.472g) was added to the solution with zinc

powder (2 spatulas). The solution was stirred under gentle heat (50 °C) until a purple solution was formed. The purple solution was decanted into another round-bottomed flask to remove the zinc powder. The remaining toluene was removed under vacuum to result in a purple solid of (2-EtHex)$_3$TACCrCl$_3$ (2.93g, 65 %). $^{13}C\{^1H\}$ NMR (100MHz): δ($CDCl_3$) 46.15 (bs, C-CH_2-C), 42.14 (bs, C-CH_2-C), 29.39 (bs, C-CH_2-C), 21.86 (bs, C-CH_2-C), 14.45 (bs, C-CH_3), 12.02 (bs, C-CH_3), -49.56 (bs, C-CH_1-[C]$_2$). Anal. Calc. for $C_{27}H_{57}Cl_3CrN_3$ (582.11): C, 55.7; H, 9.87; N, 7.22%. Found: C, 57.1; H, 9.80; N, 6.01%. (2-EtHex)$_3$TACCrCl$_3$·0.4toluene: C, 57.8; H 9.80; N, 6.79. T_{dec} 219 °C. χ^{dia} = -0.742, μ_{eff} (Toluene) = 3.751 μ_B.

Synthesis Of (4-PhBu)$_3$TACCrCl$_3$

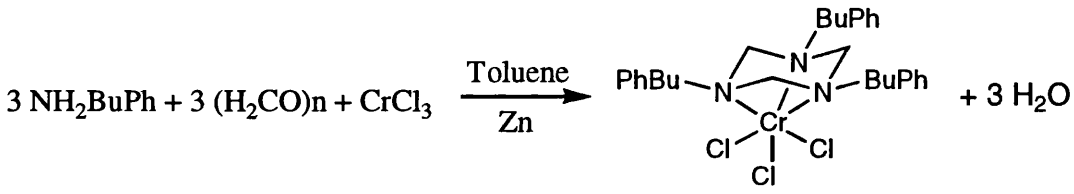

4-Phenyl-1-butylamine (3g) was dissolved in 30ml of toluene in a round-bottomed flask. Paraformaldehyde (0.604g) was added to the solution and stirred until all had gone into solution. This was followed by distillation of half the toluene with the water produced in the reaction. Chromium (III) chloride (1.3g) was added to the solution with zinc powder (2 spatulas). The solution was stirred under gentle heat (50 °C) until a purple solution was formed. The purple solution was decanted into another round-bottomed flask to remove the zinc powder. The remaining toluene was removed under vacuum to result in a purple solid of (4-PhBu)$_3$TACCrCl$_3$ (2.90g, 68 %). $^{13}C\{^1H\}$ NMR (100MHz): δ($CDCl_3$) 141.23 (bs, ArN), 128.00 (bs, Ar), 125.46 (bs, Ar), 54.52 (bs, C-CH_2-C), 29.02 (bs, C-CH_2-C). Anal.

Calc. for $C_{33}H_{45}Cl_3CrN_3$ (642.03): C, 61.7; H, 7.06; N, 6.54%. Found: C, 59.1; H, 6.80; N, 6.16%. T_{dec} 180 °C.

Synthesis Of (2-EtHex)$_3$TACCr(OTf)$_3$ 26

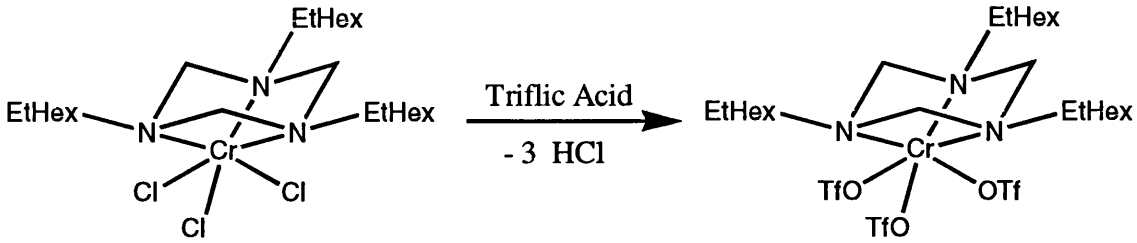

Into a round-bottomed flask with (2-EtHex)$_3$TACCrCl$_3$ (0.5g) was distilled an excess of triflic acid (10ml) under reduced pressure. Upon solvation of the chromium complex an immediate colour change was observed from a purple solid to a blue/green solution. After stirring at room temperature for 10 minutes the excess triflic acid was distilled off. The resulting chromium triflate complex was washed thrice with diethyl ether, to remove any unreacted triflic acid, to produce a blue/green solid of the (2-EtHex)$_3$TACCr(OTf)$_3$ complex that was dried under reduced pressure (0.63g, 80%). $^{13}C\{^1H\}$ NMR (100MHz): δ($CDCl_3$/$SOCl_2$) 28.09 (bs, C-CH_2-C), 22.40 (bs, C-CH_2-C), 14.52 (bs, C-CH_3), 10.03 (bs, C-CH_3). ^{19}F NMR (376MHz): δ($CDCl_3$/$SOCl_2$) –77.55 (9F, bs, S-CF_3). Anal. Calc. for $C_{30}H_{57}CrF_9N_3O_9S_3$ (922.97): C, 39.04; H, 6.22; N, 4.55%. Found: C, 37.1; H, 6.54; N, 4.34%. (2-EtHex)$_3$TACCr(OTf)$_3$·H_2O: C, 38.3; H, 6.32; N, 4.47.

Synthesis Of $Do_3TACCr(OTf)_3$ 27

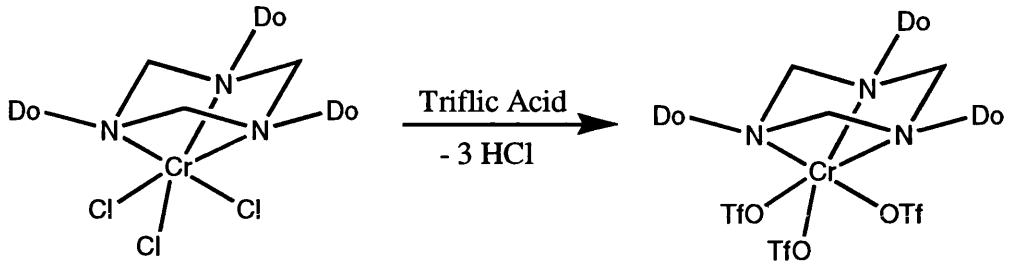

Into a round-bottomed flask with $Do_3TACCrCl_3$ (0.35g) was distilled an excess of triflic acid (10ml) under reduced pressure. Upon solvation of the chromium complex an immediate colour change was observed from a purple solid to a blue/green solution. After stirring at room temperature for 10 minutes the excess triflic acid was distilled off. The resulting chromium triflate complex was washed thrice with diethyl ether, to remove any unreacted triflic acid, to produce a sticky blue/green solid of the $Do_3TACCr(OTf)_3$ complex. On repeated washing and drying under reduced pressure the solid remained sticky (0.39g, 76%). $^{13}C\{^1H\}$ NMR (100MHz): $\delta(C_6D_6)$ 42.76 (bs, C-(10^{th})CH_2-C), 3.35 (bs, C-(4^{th})CH_2-C), 28.8 (bs, C-(5^{th}-9^{th})CH_2-C), 24.16 (bs, C-(11^{th})CH_2-C), 15.40 (bs, C-(12^{th})CH_3), -43 (bs, C-(2^{nd})CH_2-C). ^{19}F NMR (376MHz): $\delta(C_6D_6)$ –77.74 (9F, bs, S-CF_3). Anal. Calc. for $C_{42}H_{81}CrF_9N_3O_9S_3$ (1091.29): C, 46.23; H, 7.48; N, 3.85%. Found: C, 35.7; H, 6.43; N, 3.32%. $Do_3TACCr(OTf)_3.TfOH.H_2O$: C, 41.04; H, 6.65; N, 3.34%.

Synthesis Of $Do_2(Ph)TACCrCl_3$ 21

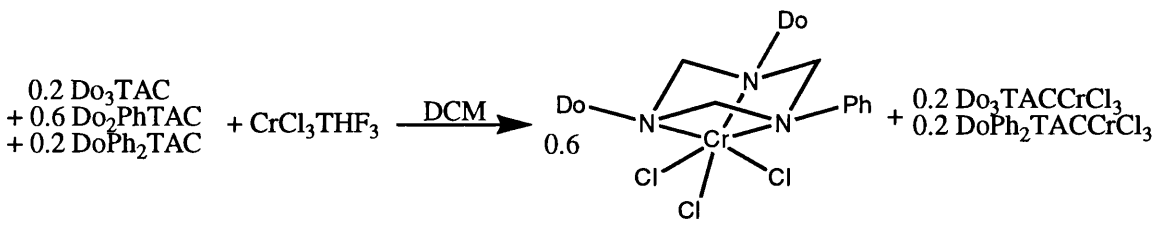

To a mixture of Do_3TAC, Do_2PhTAC, and $DoPh_2TAC$ (1.253g) in DCM (50ml), in a Schlenk tube under a nitrogen atmosphere, was added chromium trichloride-tris-THF (0.938g). The mixture was stirred for 12 hours followed by filtration to remove any unreacted chromium trichloride-tris-THF. The solution was passed through a 25 mm dia. column of silica gel approximately 300mm long. Two fractions were recovered from the column, the first of $Do_3TACCrCl_3$, and the second of $Do_2PhTACCrCl_3$. The $DoPh_2TACCrCl_3$ fraction moved very slowly through the column and decomposed before collection. The solvent from the second fraction was removed under reduced pressure to give a purple solid of the $Do_2PhTACCrCl_3$ complex (0.69g, 42%). Anal. Calc. for $C_{33}H_{61}CrCl_3N_3$ (658.21): C, 60.2; H, 9.34; N, 6.39%. Found: C, 60.1; H, 8.99; N, 6.12%.

Synthesis Of (2-EtHex)$_2$(*p*-FPh)TACCrCl$_3$ 23

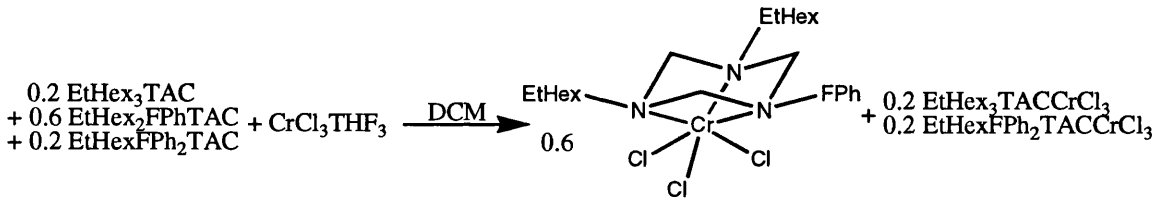

To a mixture of (2-EtHex)$_3$TAC, (2-EtHex)$_2$(FPh)TAC, and (2-EtHex)(FPh)$_2$TAC (2.6g) in DCM (50ml), in a Schlenk tube under a nitrogen atmosphere, was added chromium trichloride-tris-THF (2.39g). The mixture was stirred for 12 hours followed by filtration to remove any unreacted chromium trichloride-tris-THF. The solution was passed through a 25 mm dia. column of silica gel approximately 300mm long. Two fractions were recovered from the column, the first of (2-EtHex)$_3$TACCrCl$_3$, and the second of (2-EtHex)$_2$(FPh)TACCrCl$_3$. The (2-EtHex)(FPh)$_2$TACCrCl$_3$ fraction moved very slowly through the column and decomposed before collection. The solvent from the second

fraction was removed under reduced pressure to give a purple solid of the (2-EtHex)$_2$(FPh)TACCrCl$_3$ complex (1.48g, 41%). ^{19}F NMR (376MHz): δ(C_6D_6) –115.00 (1F, bs, ArF). Anal. Calc. for $C_{25}H_{44}CrCl_3FN_3$ (564.00): C, 53.2; H, 7.86; N, 7.45%. Found: C, 52.9; H, 7.68; N, 7.39%.

Synthesis Of Do$_2$(*p*-F$_3$CPh)TACCrCl$_3$ 22

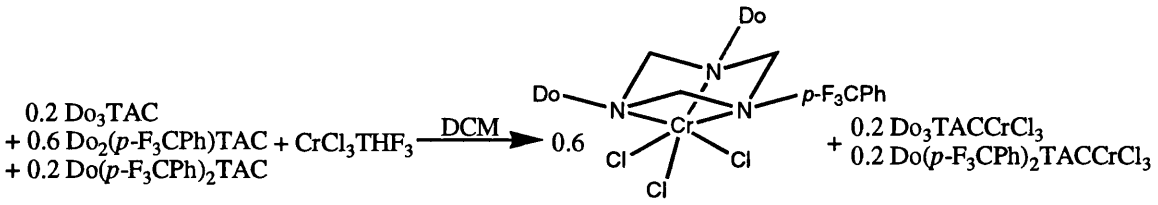

To a mixture of Do$_3$TAC, Do$_2$(*p*-F$_3$CPh)TAC, and Do(*p*-F$_3$CPh)$_2$TAC (1.533g) in DCM (50ml), in a Schlenk tube under a nitrogen atmosphere, was added chromium trichloride-tris-THF (1.012g). The mixture was stirred for 12 hours followed by filtration to remove any unreacted chromium trichloride-tris-THF. The solution was passed through a 25 mm dia. column of silica gel approximately 300mm long. Two fractions were recovered from the column, the first of Do$_3$TACCrCl$_3$, and the second of Do$_2$(*p*-F$_3$CPh)TACCrCl$_3$. The Do(*p*-F$_3$CPh)$_2$TACCrCl$_3$ fraction moved very slowly through the column and decomposed before collection. The solvent from the second fraction was removed under reduced pressure to give a purple solid of the Do$_2$(*p*-F$_3$CPh)TACCrCl$_3$ complex (0.69g, 35%). ^{19}F NMR (376MHz): δ(C_6D_6) –64.90 (3F, bs, Ph-CF$_3$). Anal. Calc. for $C_{34}H_{60}CrCl_3F_3N_3$ (726.22): C, 56.23; H, 8.32; N, 5.79%. Found: C, 56.9; H, 8.53; N, 5.65%. T_{dec} 131 °C.

Synthesis Of (2-EtBu)(p-FPh)$_2$TACCrCl$_3$

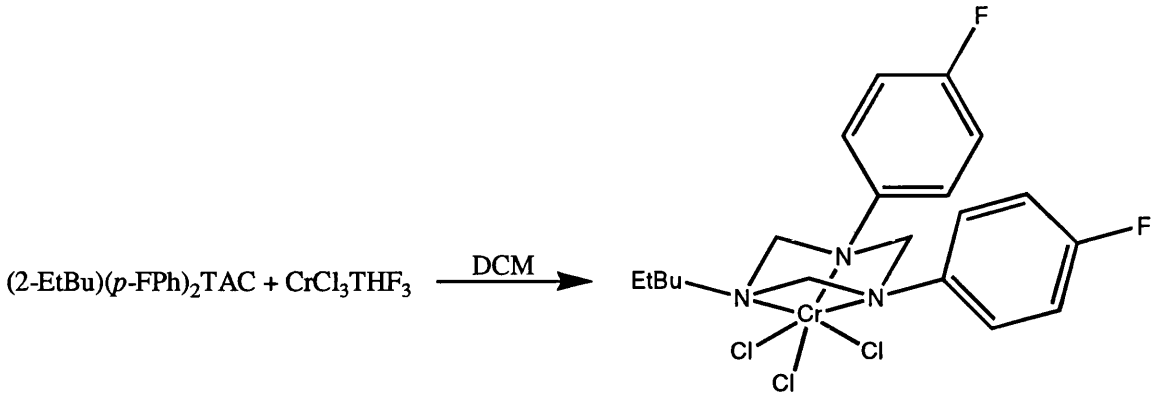

Chromium trichloride-tris-THF (0.146g) was added to (2-EtBu)(p-FPh)$_2$TAC (0.14g) in a Schlenk tube under argon. DCM (15ml) was added and the solution stirred for 12 hours. The purple precipitate (2-EtBu)(p-FPh)$_2$TACCrCl$_3$ was filtered, then dried under vacuum in a 40 °C water bath (0.16g, 77 %). ^{19}F NMR (376MHz): $\delta(C_6D_6)$ –129.20 (2F, bs, ArF). Anal. Calc. for $C_{21}H_{27}Cl_3CrF_2N_3$ (517.82): C, 48.7; H, 5.26; N, 8.11%. Found: C, 46.2; H, 6.87; N, 7.60%. (2-EtBu)(p-FPh)$_2$TACCrCl$_3$·2H$_2$O: C, 45.5; H, 5.64; N, 7.59%. T_{dec} 148 °C.

NMR Tube Synthesis Of [R$_3$TACCrCl$_3$(PhMe$_2$NH)]B(C$_6$F$_5$)$_4$

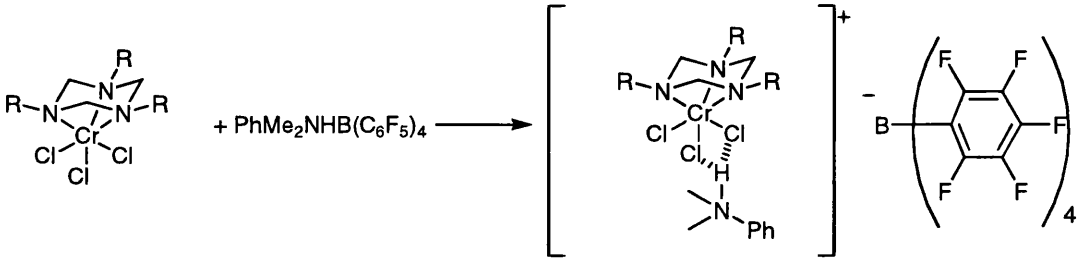

$R_3TACCrCl_3$ (0.035mmol) was dissolved in a given solvent (1ml). $PhMe_2NHB(C_6F_5)_4$ (0.035mmol) was added to the solution and shaken until a homogeneous solution was achieved. The resultant species in solution was $[R_3TACCrCl_3(PhMe_2NH)]B(C_6F_5)_4$.

$[(2\text{-}EtHex)_3TACCrCl_3(PhMe_2NH)]B(C_6F_5)_4$ **33**: $^{13}C\{^1H\}$ NMR (100MHz): $\delta(C_6D_6)$ 44.55 (bs, C-CH_2-C), 37.39 (bs, C-CH_2-C), 29.86 (bs, C-CH_2-C), 24.03 (bs, C-CH_2-C), 14.68 (bs, C-CH_3), 12.49 (bs, C-CH_3). ^{19}F NMR (400MHz): $\delta(C_6D_6)$ –131.65 (8F, bs, *o*-ArF), -161.60 (4F, bs, *p*-ArF), -164.83 (8F, bs, *m*-ArF). μ_{eff} (Toluene) = 3.689 μ_B.

$[Do_3TACCrCl_3(PhMe_2NH)]B(C_6F_5)_4$ **34**: ^{19}F NMR (400MHz): $\delta(C_6D_6)$ –131.07 (8F, bs, *o*-ArF), -161.74 (4F, bs, *p*-ArF), -164.90 (8F, bs, *m*-ArF). μ_{eff} (Benzene) = 3.729 μ_B.

$[(p\text{-}FBz)_3TACCrCl_3(PhMe_2NH)]B(C_6F_5)_4$ **35**: ^{19}F NMR (400MHz): $\delta(CDCl_3)$ – 107.70 (3F, bs, *p*-FBz), –130.14 (8F, bs, *o*-ArF), -160.01 (4F, bs, *p*-ArF), -163.76 (8F, bs, *m*-ArF).

$[Me_3TACCrCl_3(PhMe_2NH)]B(C_6F_5)_4$ **37**: ^{19}F NMR (400MHz): δ(Toluene) –131.83 (8F, bs, *o*-ArF), -164.68 (4F, bs, *p*-ArF), -168.60 (8F, bs, *m*-ArF).

[(2-EtHex)$_2$(FPh)TACCrCl$_3$(PhMe$_2$NH)]B(C$_6$F$_5$)$_4$ **38**: ^{19}F NMR (400MHz): δ(C$_6$D$_6$) –114.34 (1F, bs, *p*-FPh), –131.37 (8F, bs, *o*-ArF), -161.03 (4F, bs, *p*-ArF), -164.28 (8F, bs, *m*-ArF).

Synthesis Of [(2-EtBu)$_3$TACCrCl$_3$(PhMe$_2$NH)]B(C$_6$F$_5$)$_4$ 32

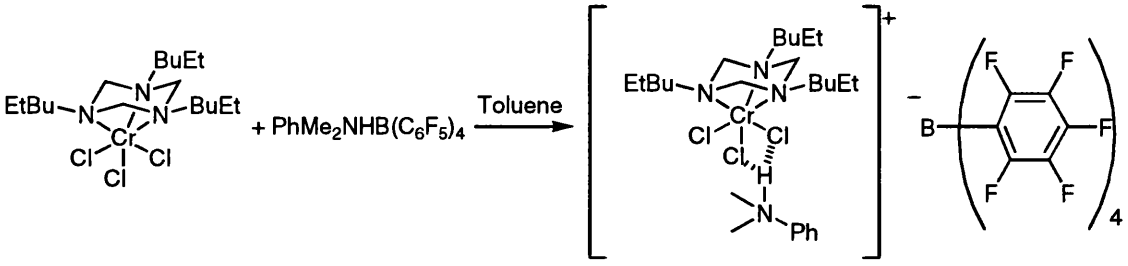

(2-EtBu)$_3$TACCrCl$_3$ (0.1g) was dissolved in toluene (20ml). PhMe$_2$NHB(C$_6$F$_5$)$_4$ (0.161g) was added to the solution and stirred until a homogeneous solution was achieved. This solution was layered with hexane. Purple crystals of [(2-EtBu)$_3$TACCrCl$_3$(PhMe$_2$NH)] B(C$_6$F$_5$)$_4$ were formed (0.23g, 89 %). ^{1}H NMR (400MHz): δ(C$_6$D$_6$) 1.312 (12H, bs, C-CH$_2$-C), 0.933 (18H, bs, C-CH$_3$). ^{13}C{^{1}H} NMR (100MHz): δ(C$_6$D$_6$) 36.67 (bs, C-CH$_2$-C), 12.00 (bs, C-CH$_3$). ^{19}F NMR (376MHz): δ(C$_6$D$_6$) –132.91 (8F, bs, *o*-ArF), -162.47 (4F, bs, *p*-ArF), -165.93 (8F, bs, *m*-ArF). Anal. Calc. for C$_{53}$H$_{57}$BCl$_3$CrF$_{20}$N$_4$ (1299.94): C, 49.0; H, 4.42; N, 4.31%. Found: C, 49.9; H, 4.34; N, 4.02%. m.p 106 °C.

Synthesis Of [(2-PhEt)$_3$TACCrCl$_3$(PhMe$_2$NH)]B(C$_6$F$_5$)$_4$ 31

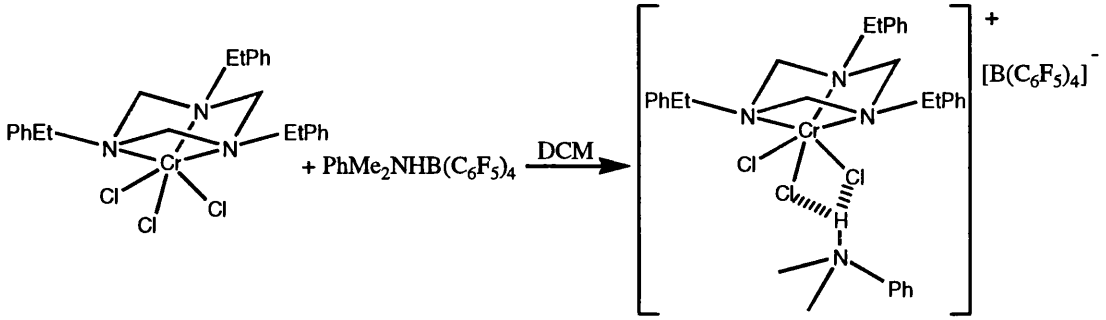

(2-PhEt)$_3$TACCrCl$_3$ (0.1g) was dissolved in DCM (20ml). PhMe$_2$NHB(C$_6$F$_5$)$_4$ (0.144g) was added to the solution and stirred until a homogeneous solution was achieved. This solution was layered with hexane. Purple crystals of [(2-PhEt)$_3$TACCrCl$_3$(PhMe$_2$NH)] B(C$_6$F$_5$)$_4$ were formed (0.20g, 82 %). ^{19}F NMR (376MHz): δ(C$_6$D$_6$) –130.48 (8F, bs, *o*-ArF), -159.95 (4F, bs, *p*-ArF), -163.30 (8F, bs, *m*-ArF). Anal. Calc. for C$_{59}$H$_{45}$BCl$_3$CrF$_{20}$N$_4$ (1359.16): C, 52.14; H, 3.34; N, 4.12%. Found: C, 52.6; H, 3.37; N, 4.21%.

Synthesis Of [^{t}Bu$_3$TACCrCl$_3$(PhMe$_2$NH)]B(C$_6$F$_5$)$_4$ 36

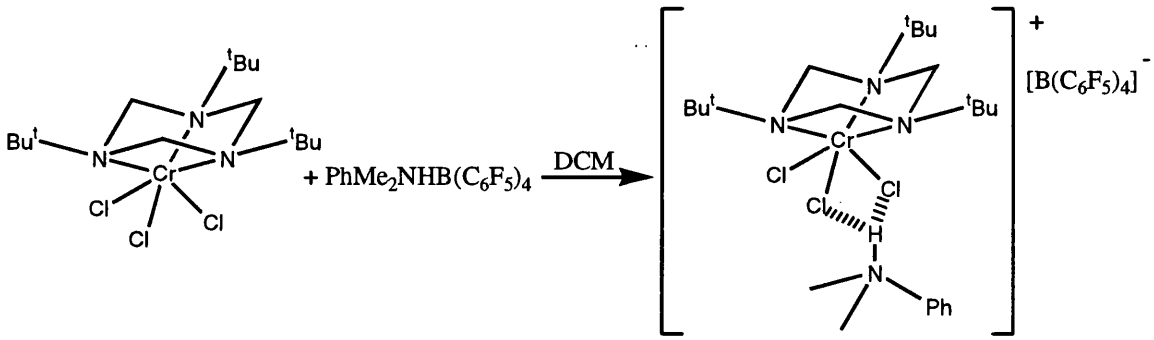

To a suspension of ^{t}Bu$_3$TACCrCl$_3$ (0.1g) in toluene (20ml) was added PhMe$_2$NHB(C$_6$F$_5$)$_4$ (0.194g) and stirred until a homogeneous solution was achieved. The solvent was removed under reduced pressure to give a purple powder of [^{t}Bu$_3$TACCrCl$_3$(PhMe$_2$NH)]B(C$_6$F$_5$)$_4$ (0.28g, 97 %). ^{19}F NMR (376MHz): δ(C$_6$D$_6$) –132.08

(8F, bs, *o*-ArF), -162.48 (4F, bs, *p*-ArF), -165.86 (8F, bs, *m*-ArF). Anal. Calc. for $C_{47}H_{45}BCl_3CrF_{20}N_4$ (1215.03): C, 46.5; H, 3.73; N, 4.61%. Found: C, 46.5; H, 3.83; N, 4.18%. m.p 115 °C.

6.5: Borates

Synthesis Of DMAHB$(C_6F_5)_4$ 28 [164,165]

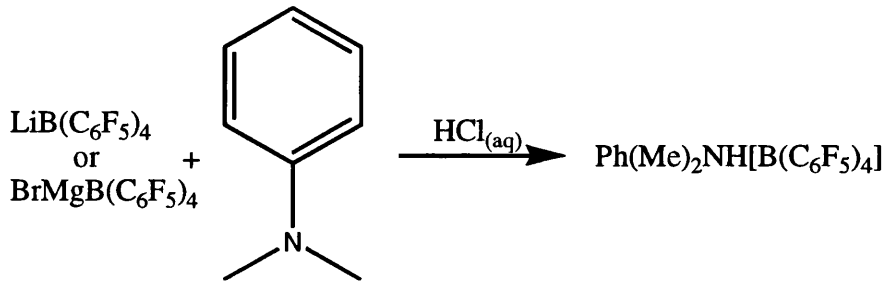

To an aqueous solution of either the lithium borate salt (12mmol) or $BrMgB(C_6F_5)_4$ (12mmol), prepared from literature procedures was added an aqueous solution of dimethylanilinium chloride (12mmol). On addition immidiate precipitation of a white solid occured. Filtration to give the crude product was followed by redissolving in toluene and removal of water by an azeotropic distillation. Any remaining solvents were removed under reduced pressure to give a white powder of $Ph(Me)_2NH[B(C_6F_5)_4]$ (11mmol, 92%). ^1H NMR (300MHz): $\delta(CD_2Cl_2)$ 7.57 (1H, t, $J_{H,H}$=4.5Hz, *p*-Ph), 7.56 (2H, d, $J_{H,H}$=9Hz, *o*-Ph), 7.33 (2H, m, *m*-Ph), 3.28 (6H, s, N-CH_3). ^{19}F NMR (376MHz): $\delta(CDCl_3)$ –133.19 (8F, bs, *o*-ArF), -163.42 (4F, t, $J_{F,F}$=21Hz, *p*-ArF), -167.42 (8F, t, $J_{F,F}$=16Hz, *m*-ArF). Anal. Calc. for $C_{32}H_{12}BF_{20}N$ (801.22): C, 47.97; H, 1.51; N, 1.75%. Found: C, 48.7; H, 1.76; N, 1.64%. T_{dec} 223 °C.

Synthesis Of DEAHB(C_6F_5)$_4$ 29

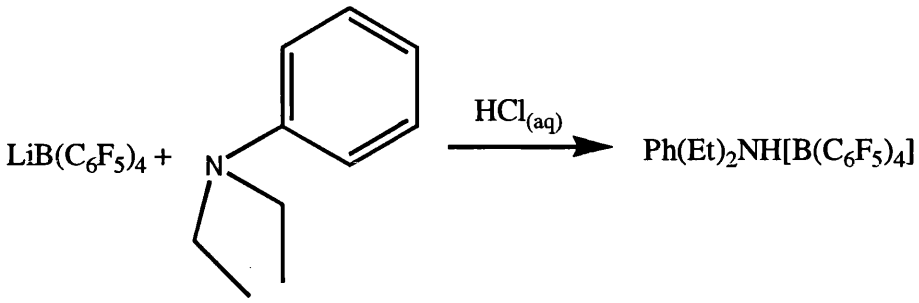

To an aqueous solution of the lithium borate salt (12mmol) was added an aqueous solution of diethylanilinium chloride (12mmol). On addition immediate precipitation of a white solid occured. Filtration to give the crude product was followed by redissolving in toluene and removal of water by an azeotropic distillation. Any remaining solvents were removed under reduced pressure to give a white powder of $Ph(Et)_2NH[B(C_6F_5)_4]$ (11mmol, 91%). ^1H NMR (300MHz): $\delta(CD_2Cl_2)$ 7.59 (1H, t, $J_{H,H}$=4.5Hz, *p*-Ph), 7.57 (2H, d, $J_{H,H}$=9Hz, *o*-Ph), 7.20 (2H, m, *m*-Ph), 3.58 (4H, q, $J_{H,H}$=7.5Hz, N-CH_2-C) 1.14 (6H, t, $J_{H,H}$=7.5Hz, C-CH_3). ^{19}F NMR (376MHz): $\delta(CDCl_3)$ –133.26 (8F, bs, *o*-ArF), -163.38 (4F, t, $J_{F,F}$=21Hz, *p*-ArF), -167.41 (8F, t, $J_{F,F}$=16Hz, *m*-ArF). Anal. Calc. for $C_{34}H_{16}BF_{20}N$ (829.28): C, 49.2; H, 1.9; N, 1.7%. Found: C, 48.8; H, 1.98; N, 1.70%. m.p 186 °C.

Synthesis Of [NBu_4]B(C_6F_5)$_4$ 30

$$LiB(C_6F_5)_4 + [n\text{-}Bu_4N]NO_3 \xrightarrow{H_2O} [n\text{-}Bu_4N][B(C_6F_5)_4]$$

To an aqueous solution of the lithium borate salt (3.583g) was added an aqueous solution of tetra-*n*-butylammonium nitrate (1.308g). On addition precipitation of a white solid occured. Filtration to give the crude product was followed by redissolving in toluene

and removal of water by an azeotropic distillation. Any remaining solvents were removed under reduced pressure to give a white powder of n-Bu_4N [$B(C_6F_5)_4$] (4.28g, 89%). ^1H NMR (400MHz): δ($CDCl_3$) 2.75 (8H, t, $J_{H,H}$=7.7Hz, N-CH_2-C), 1.27 (8H, m, C-CH_2-C), 1.08 (8H, m, C-CH_2-C), 0.71 (12H, t, $J_{H,H}$=4.7Hz, C-CH_3). ^{19}F NMR (376MHz): δ($CDCl_3$) –132.35 (8F, bm, o-ArF), -162.27 (4F, t, $J_{F,F}$=19.6Hz, p-ArF), -166.19 (8F, bm, m-ArF). Anal. Calc. for $C_{40}H_{36}BF_{20}N$ (921.50): C, 52.1; H, 3.9; N, 1.5%. Found: C, 52.2; H, 3.97; N, 1.54%. m.p 158 °C.

6.6: NMR Tube Reactions

Ethylene Trimerisation

To a Youngs NMR tube was added $R_3TACCrCl_3$ (0.013mmol) and either toluene or C_6D_6 (1ml). The complex was activated by MAO (0.13mmol) or by the co-activation of DMAB (0.013mmol) followed by either Al^iBu_3 or $AlEt_3$ (0.039mmol). Upon activation the solution instantaneously undergoes a colour change from purple to green. The solution was degassed and the NMR tube filled with ethylene (1 bar). By ^1H NMR spectroscopy the major product formed was 1-hexene. ^1H NMR (400MHz): δ(Toluene) 5.72 (1H, m, N-C=CH-C), 4.94 (2H, m, C=CH_2), 1.92 (2H, m, C-CH_2-C), 1.25 (4H, m, C-CH_2-CH_2-C), 0.81 (3H, t, $J_{H,H}$=4.2Hz, C-CH_3).

α-olefin Trimerisation

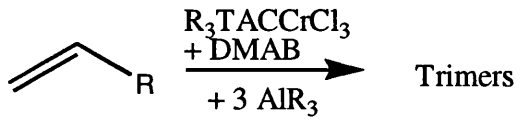

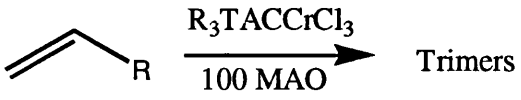

To a Youngs NMR tube was added $R_3TACCrCl_3$ (0.013mmol) and either toluene or C_6D_6 (1ml). The complex was activated by MAO (0.13mmol) or by the co-activation of DMAB (0.013mmol) followed by either Al^iBu_3 or $AlEt_3$ (0.039mmol). Upon activation the solution instantaneously undergoes a colour change from purple to green. To the solution was added either 1-hexene (2.3mmol) or allylbenzene (2.3mmol). By ^1H NMR spectroscopy the composition of the products were determined between trimers and isomerisation of the monomer. ^1H NMR (400MHz): δ(Toluene) 6.3-5.0 (olefinic protons), 2.1-0.7 (aliphatic protons).

All activations of $R_3TACCrCl_3$ complexes with the co-catalyst mixture of DMAB / AlR_3 led to decomposition within 14 days, on addition of olefin this process was accelerated to 2 hours. In solution the complex $R_3TACAlR_2[B(C_6F_5)_4]$ is produced (66 %), and yellow crystals also form of the complex $[(toluene)_2Cr][B(C_6F_5)_4]$ (33 %).

$R_3TACAlR_2[B(C_6F_5)_4]$: ^1H NMR (400MHz): δ(Toluene) 3.48 (3H, d, $J_{Ha,Hb}$=8.9Hz, N-CH_aH_b-N), 2.93 (3H, d, $J_{Hb,Ha}$=8.9Hz, N-CH_bH_a-N),

(toluene)$_2$Cr[B(C$_6$F$_5$)$_4$]: Anal. Calc. for $C_{38}H_{16}BCrF_{20}$ (915.3): C, 49.9; H, 1.76; N, 0%. Found: C, 49.0; H, 2.10; N, 0.12%.

NMR Tube Synthesis Of Do$_3$TACAl^{i}Bu$_2$[B(C$_6$F$_5$)$_4$

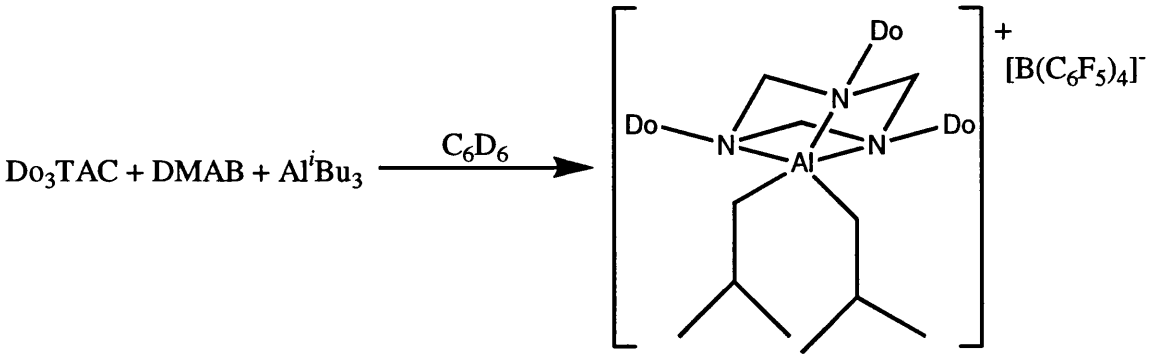

Do$_3$TAC (0.037mmol), DMAB (0.037mmol), and Al^{i}Bu$_3$ as a 1.0M solution in hexane (0.12mmol) were dissolved in benzene-d$_6$ (1ml) to form a colourless solution of Do$_3$TACAl^{i}Bu$_2$[B(C$_6$F$_5$)$_4$]. Isolation was attempted by crystallisation and distillation of excess Al^{i}Bu$_3$ but both methods failed. ^{1}H NMR (300MHz): δ(C$_6$D$_6$) 3.48 (3H, d, $J_{Ha,Hb}$=8.9Hz, N-CH$_a$H$_b$-N), 2.88 (3H, d, $J_{Hb,Ha}$=8.9Hz, N-CH$_b$H$_a$-N), 1.76 (2H, m, C-CH-C), 0.95 (12H, d, $J_{H,H}$=6.3Hz,C-CH$_3$), 0.07 (4H, d, $J_{H,H}$=8.0Hz, Al-CH$_2$-C).

NMR Tube Synthesis Of (2-EtBu)$_3$TACAl^{i}Bu$_2$[B(C$_6$F$_5$)$_4$]

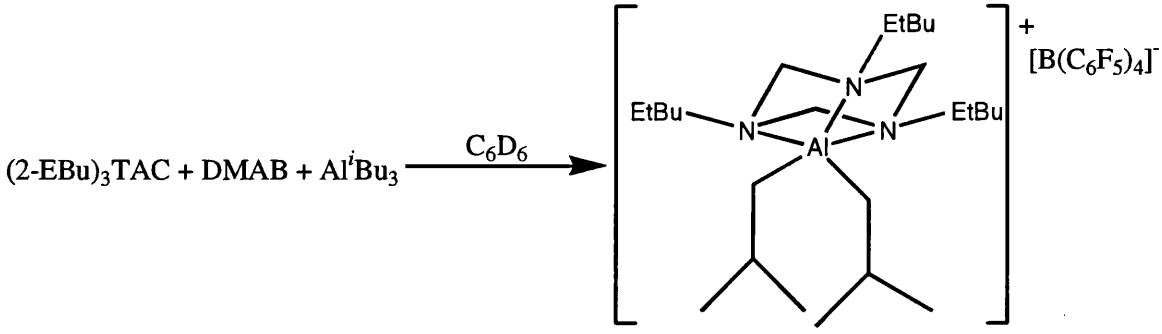

$(2\text{-EtBu})_3$TAC (0.094mmol), DMAB (0.094mmol), and Al^iBu_3 as a 1.0M solution in hexane (0.29mmol) were dissolved in benzene-d_6 (1ml) to form a colourless solution of $(2\text{-EtBu})_3TACAl^iBu_2[B(C_6F_5)_4]$. Isolation was attempted by crystallisation and distillation of excess Al^iBu_3 but both methods failed. ^{1}H NMR (300MHz): $\delta(C_6D_6)$ 3.73 (3H, d, $J_{Ha,Hb}$=8.9Hz, N-CH_aH_b-N), 3.08 (3H, d, $J_{Hb,Ha}$=8.9Hz, N-CH_bH_a-N), 1.70 (2H, m, C-CH-C), 0.92 (12H, d, $J_{H,H}$=6.4Hz,C-CH_3), 0.24 (4H, d, $J_{H,H}$=7.0Hz, Al-CH_2-C).

Conclusion

In this thesis there has been shown the synthesis of a variety of triazacyclohexane chromium complexes that have vast differences in solubility and catalytic reactivity towards polymerisation and selective trimerisation of α-olefins. Activation of these systems with DMAB followed by AlR_3 has been monitored by ^{19}F NMR to give valuable information on aggregation of species in solution and the close contact of the weakly coordinating anion to the activated complex. T_2 measurements show a significant interaction between the chromium cation and a *meta* fluorine atom of the anion to be a key feature of the activated complex. Manipulations of these measurements determine a structure in concurrence with DFT calculations. Effective magnetic moment measurements along with formation of a Cr(I) decomposition product both lead to strong evidence for a Cr(III) / Cr(I) couple being active in this system. Ring slippage of the triazacyclohexane ring and aluminium has been identified as key contributors to decomposition of the catalyst. Addressing these issues is vital to the lifetime of this catalyst system.

References

1. M. S. Reisch, Chem. Eng. News, 1997, 14
2. [a] K. Ziegler, Belgian Patent 1954, **533**,362, [b] K. Ziegler, E. Holzkamp, H. Martin, and H. Breil, Angew. Chem. 1955, **67**, 541. [c] G. Natta, J. Polym. Sci. 1955, **16**, 143
3. H. H. Brintzinger, D. Fischer, R. Mulhaupt, B. Rieger, and R. M. Waymouth, Angew. Chem. Int. Ed. Engl. 1995, **34**, 1143
4. [a] J. P. Hogan, R. L. Banks, Phillips Petroleum, US 2,825,721 1958; CA = 52:8621h [b] C. E. Marsden, Plast. Rubber Compos. Process. Appl., 1994, **21**, 193 [c] T. E. Nowlin, Prog. Polym. Sci., 1985, **11**, 29 [d] S. M. Augustine, and J. P. Blitz, J. of Catalysis, 1996, **161**, 641
5. M. R·tzsch, Polymerwerkstoffe 1998, 23
6. M. P. McDaniel, Adv. Catalysis 1985, **33**, 47
7. H. L. Krauss, and H. Stach, Inorg. Nucl. Chem. Lett. 1968, **4**, 393.
8. K. H. Theopold, Eur. J. Inorg. Chem., 1998, 15.
9. [a] D. S. Richeson, S. –W. Hsu, N. H. Fredd, G. Van Duyne, and K. H. Theopold, J. Am. Chem. Soc. 1986, **108**, 1491. [b] B. J. Thomas, S. –K. Noh, G. K. Schulte, S. C. Sendlinger, and K. H. Theopold, J. Am. Chem. Soc. 1991, **113**, 893. [c] B. J. Thomas, and K. H. Theopold, J. Am. Chem. Soc. 1988, **110**, 5902
10. M. L. H. Green, J. Organomet. Chem. 1995, **500**, 127
11. B. J. Thomas, J. F. Mitchell, J. A. Leary, and K. H. Theopold, J. Organomet. Chem. 1988, **348**, 333
12. R. A. Heintz, Ph. D. thesis, Cornell University, 1994
13. P. A. White, J. Calabrese, and K. H. Theopold, Organometallics, 1996, **15**, 5473
14. R. Emrich, O. Heinemann, P. W. Jolly, C. Krüger, and G. P. J. Verhovnik, Organometallics, 1997, **16**, 1511
15. M. Enders, P. Fernández, G. Ludwig, and H. Pritzkow, Organometallics, 2001, **20**, 5005
16. [a] G. J. P. Britovsek, V. C. Gibson, and D. F. Wass, Angew. Chem., 1999, **111**, 448. [b] G. J. P. Britovsek, V. C. Gibson, and D. F. Wass, Angew. Chem. Int. Ed. Engl., 1999, **38**, 428
17. V. C. Gibson, C. Newton, C. Redshaw, G. A. Solan. A. J. P. White, and D. J. Williams, J. Chem. Soc. Dalton Trans., 1999, 827
18. F. J. Wu, EP 0537609 (Albemarle Corporation), July 10, 1992
19. R. D. Köhn, M. Haufe, S. Mihan, and D. Lilge, Chem. Commun., 2000, 1927
20. R. D. Köhn, G. Kociok- Köhn, and M. Haufe, J. Organomet. Chem., 1995, **501**, 303
21. T.Yoshida, T. Yamamoto, and H. Murakita, US2002/0035029 (Tosoh Corporation), March 21, 2002
22. S. Ittel, L. K. Johnson, and M. Brookhart, Chem. Rev., 2000, **100**, 1169
23. K. Iwanaga, and M. Tamura, GB 2314518 (Sumitomo Chemical Company), June 27, 1997
24. F. T. Wu, US5811618 (Amoco Corporation), August 25, 1995
25. S. J. Dossett, A. Gillon, A. G. Orpen, J. S. Fleming, P. G. Pringle, D. F. Wass, and M. D. Jones, Chem. Commun., 2001, 699
26. N. A. Cooley, S. M. Green, D. F. Wass, K. Heslop, A. G. Orpen, and P. G. Pringle, Organometallics, 2001, **20**, 4769

27. A. Carter, S. A. Cohen, N. A. Cooley, A. Murphy, J. Scutt, and D. F. Wass, Chem. Commun., 2002, 858
28. D. F. Wass, WO 02/04199 (BP Chemicals Ltd), January 17, 2002
29. J. T. Dixon, J. J. C. Grove, P. Wasserchеid, D. S. McGuinness, F. M. Hess, H. Maumela, D. H. Morgan, and A. Bollman, WO 03053891 (Sasol Technology (Pty) Ltd), December 20, 2001
30. D. S. McGuinness, P. Wasserchеid,W. Keim, J. T. Dixon, J. J. C. Grove, C. Hu, and U. Englert, Chem. Commun., 2003, 334
31. A. Bollmann, K. Blann, J. T. Dixon, F. M. Hess, E. Killian, H. Maumela, D. S. McGuinness, D. H. Morgan, A. Neveling, S. Otto, M. Overett, A. M. Z. Slawin, P. Wasserscheid, and S. Kuhlmann, J. Am. Chem. Soc., 2004, **126**, 14712
32. M. J. Overett, K. Blann, A. Bollmann, J. T. Dixon, F. Hess, E. Killian, H. Maumela, D. H. Morgan, A. Neveling, and S. Otto, Chem. Commun., 2005, 622
33. D. S. McGuinness, P. Wasserchеid,W. Keim, D. H. Morgan, J. T. Dixon, A. Bollman, H. Maumela, F. M. Hess and U. Englert, J. Am. Chem. Soc., 2003, **125**, 5272
34. R. M Manyik, W. E. Walker, and T. P. Wilson, US 3300458 (Union Carbide Corporation), January 24, 1967
35. W. K. Reagan, J. W. Freeman, B. K. Conroy, T. M. Pettijohn, and E. A. Benham, US 5,451,645 (Phillips Petroleum Company), Septermber 19, 1995
36. R. Santi, A. M. Romano, M. Grande, A. Sommazzi, F. Masi and A. Proto, WO 01/68572 (Enichem S.P.A), September 20, 2001
37. S. Murtuza, S. B. Harkins, G. S. Long and A. Sen, J. Am. Chem. Soc., 2000, **122**, 1867
38. C. Andes, S. B. Harkins, S. Murtuza, K. Oyler and A. Sen, J. Am. Chem. Soc., 2001, **123**, 7423
39. C. Pellecchia, D. Pappalardo and G. Gruter, Macromolecules, 1999, **32**, 4491
40. P. J. W. Deckers, B. Hessen, and J. H. Teuben, Angew. Chem. Int. Ed., 2001, **40**, 13, 2516
41. K. Sugimura, T. S. Nitabara and T. Fujita, JP 10324710 (Mitsui Chemicals Incorporated), December 8, 1998
42. K. Ban, T. Hayashi and Y. Suzuki, JP 10101587 (Mitsui Chemicals Incorporated), April 21, 1998
43. R. D. Köhn, M. Haufe, G. Kociok- Köhn, S. Grimm, P. Wasserscheid, and W. Keim, Angew. Chem. Int. Ed., 2000, **39**, 23, 4337
44. J. R. Briggs, J. Chem. Soc., Chem. Commun., 1989, 674
45. C. Wellington, and T. Tollens, Chem. Ber., 1885, **18**, 3298
46. L. Henry, Bull. Acad. Sci. Belge., 1885, **26**, 200
47. E. Brocher, and J. L. Cambier, Compt. Rend., 1895, **120**, 449
48. P. Duden, and M. Scharff, Chem. Ber., 1895, **28**, 936
49. (a) J. Graymore, J. Chem. Soc., 1924, **125**, 2283; (b) 1931, 1490; (c) 1932, 1353; (d) 1935, 865; (e) 1938, 1311; (f) 1941, 39
50. C. W. Hoerr, E. Rapkin, A. E. Brake, K. N. Warner, and H. J. Harwood, J. Am. Chem. Soc., 1956, **78**, 4667
51. D. Adam, P. H. McCabe, G. A. Sim, and A. Bouchemma, Acta. Cryst., 1995, **C51**, 246
52. A. Bouchemma, P. H. McCabe, and G. A. Sim, J. Chem. Soc. Perkin Trans. II, 1989, 583

53. M. Squillacote, R. S. Sheridan, O. L. Chapman, and F. A. L. Anet, J. Am. Chem. Soc., 1975, **97**, 3244
54. T. A. Crabb, and A. R. Katritzky, Adv. Heterocycl. Chem., 1984, **36**, 3
55. K. B. Wiberg, J. D. Hammer, H. Castejon, W. F. Bailey, E. L. DeLeon, and R. M. Jarret, J. Org. Chem., 1999, **64**, 2085
56. R. A. Y. Jones, A. R. Katritzky, and M. Snarey, J. Chem. Soc., 1970, 135
57. C. H. Bushweller, M. Z. Lourandos, and J. A. Brunelle, J. Am. Chem. Soc., 1974, **96**, 1591
58. V. J. Baker, I. J. Ferguson, A. R. Katritzky, R. C. Patel, and S. J. Rahimi-Rastgoo, J. Chem. Soc. Perkin Trans. II, 1978, **11**, 377
59. E. Juaristi, and G. Cuevas, The Anomeric Effect; CRC Press: Boca Raton, FL, 1995
60. J. G. Jewett, J. J. Breeyear, J. H. Brown, and C. H. Bushweller, J. Am. Chem. Soc., 2000, **122**, 308
61. J. W. Larson, and T. B. McMahon, J. Am. Chem. Soc., 1984, **106**, 517
62. A. Bouchemma, P. H. McCabe, and G. A. Sim, Acta. Cryst., 1988, **C44**, 1469
63. G. A. Sim, J. Chem. Soc. Chem. Commun., 1987, 1118
64. A. Bouchemma, P. H. McCabe, and G. A. Sim, Acta. Cryst., 1990, **C46**, 671
65. A. G. Giumanini, G. Verardo, L. Randaccio, N. Bresciani-Pahor, and P. Traldi, J. Prakt. Chem., 1985, **327**, 739
66. N. L. Allinger, and M. T. Tribble, Tetrahedron Lett., 1971, **35**, 3259
67. A. Bouchemma, P. H. McCabe, and G. A. Sim, Acta. Cryst., 1990, **C46**, 410
68. B.Schichtel, Project report for M. Chem, 2001
69. M. B. Hursthouse, M. Moteevalli, P. O'Brien, and J. R. Walsh, Organometallics, 1991, **10**, 3196
70. J. L.Atwood, F. R. Bennett, C. Jones, G. A. Koutsantonis, C. L. Raston, and K. D. Robinson, J. Chem. Soc. Chem. Commun., 1992, 541
71. R. D. Köhn, Z. Pan, M. F. Mahon, and G. Kociock- Köhn, Chem. Commun., 2003, 1272
72. R. D. Köhn, G. Seifert, Z. Pan, M. F. Mahon, and G. Kociock- Köhn, Angew. Chem. Int. Ed., 2003, **42**, 793
73. D. C. Bradley, H. Dawes, D. M. Frigo, M. B. Hursthouse, and B. Husain, J. Organomet. Chem., 1987, **325**, 55
74. D. C. Bradley, D. M. Frigo, I. S. Harding, M. B. Hursthouse, and M. Motevalli, J. Chem. Soc. Chem. Commun., 1992, 577
75. D. C. Bradley, and I. S. Harding, J. Chem. Soc. Dalton. Trans., 1997, 4637
76. P. J. Wilson, A. J. Blake, P. Mountford, and M. Schröder, J. Organomet. Chem., 2000, **600**, 71
77. J. Sandström, Dynamic NMR Specroscopy, Academic Press, London, 1992
78. N. L. Armanasco, M. V. Baker, M. R. North, B. R. Skelton, and A. H. White, J. Chem. Soc. Dalton Trans., 1997, 1363
79. G. R. Willey, T. J. Woodman, U. Somasundaram, D. R. Aris, and W. Errington, J. Chem. Soc. Dalton Trans., 1998, 2573
80. N. L. Armanasco, M. V. Baker, M. R. North, B. W. Skelton, and A. H. White, J. Chem. Soc. Dalton Trans., 1997, 1363
81. A. Lüttringhaus, and W. Kullick, Tetrahedron Lett., 1959, 13
82. H. Schumann, Z. Naturforsch, Teil B, 1995, **50**, 1038
83. N. L. Armanasco, M. V. Baker, M. R. North, B. W. Skelton, and A. H. White, J. Chem. Soc. Dalton Trans., 1998, 1145

84. M. V. Baker, and M. R. North, J. Organomet. Chem., 1998, **565**, 225
85. N. D. Fenton, and M. Gerloch, J. Chem. Soc. Dalton Trans.,1988, 2201
86. F.A. Cotton, E. V. Dikarev, and S. Herrero, Inorg. Chem., 1998, **37**, 5862
87. R. G. Abbott, F. A. Cotton, and L. R. Falvello, Inorg. Chem., 1990, **29**, 514
88. R. D. Köhn, and G. Kociok-Köhn, Angew. Chem. Int. Ed. Engl., 1994, **33**, 1877
89. M. V. Baker, D. H. Brown, B. W. Skelton, and A. H. White, J. Chem. Soc. Dalton Trans., 2000, 763
90. S. –J. Wu, G. P. Stahly, F. R. Fronczek, and S. F. Watkins, Acta Crystallogr. C, 1995, **51**, 18
91. B. R. McGarvey, J. Phys. Chem., 1957, **61**, 1232
92. M. Rubinstein, A. Baram, and Z. Luz, Mol. Phys., 1971, **20**, 67
93. G. N. La Mar, and F. A. Walker, J. Am. Chem. Soc., 1973, **95**, 6950
94. [a] I. Bertini, and C. Luchinat, In Coordination Chemistry Reviews- NMR of Paramagnetic Substances; Lever, A. B. P., Ed.; Elsevier; New York, 1996, Vol. 150. [b] R. D. Köhn, Habilitationsschrift, University of Berlin, 1996
95. D. F. Evans, J. Chem. Soc., 1959, 2003
96. R. D. Köhn, Private communication
97. W. Beck, and K. H. Sünkel, Chem. Rev. 1988, **88**, 1405
98. N. M. N. Gowda, S. B. Naikar, and G. K. N. Reddy, Adv. Inorg. Chem. Radiochem., 1984, **28**, 255.
99. G. A. Lawrence, Chem. Rev., 1993, **93**, 17.
100. W. H. Hersh, Inorg. Chem, 1990, **29**, 713.
101. R. V. Honeychuck and W. H. Hersh, Inorg. Chem, 1989, **28**, 2869.
102. K. Shelly, T. Bartczak, W. R. Scheidt, and C. A. Reed, Inorg. Chem, 1985 , **24**, 4325.
103. H. W. Turner, European Patent Appl., 277,004 (assigned to Exxon)
104. G. Fachinetti, T. Funaioli, and P. F. Zanazzi, Chem. Commun., 1988, 1100
105. L. C. Ananias de Carvalho, M. Dartiguanave, Y. Dartiguanave, and A. L. Beauchamp, J. Am. Chem. Soc. 1984, **106**, 6848
106. M. Pasquali, C. Floriani, and A. Gaetani-Manfredotti, Inorg. Chem., 1980, **19**, 1191
107. G. G. Hlatky, H. W. Turner, and R. R. Eckman, J. Am. Chem. Soc., 1989, **111**, 2728
108. A. D. Horton, and J. H. G. Frijna, Angew. Chem. Int. Ed. Engl., 1991, **30**, 1152
109. E. E. Bancroft, H. N. Blount, and E. G. Jansen, J. Am. Chem. Soc., 1979, **101**, 3692
110. A. G. Massey, and A. J. Park, J. Organomet. Chem., 1964, **2**, 245
111. J. H. Golden, P. F. Mutolo, E. B. Lobrovski, and F. J. DiSalvo, Inorg. Chem., 1994, **33**, 5374
112. X. Yang, C. L. Stern, and T. J. Marks, Organometallics, 1991, **10**, 840
113. R. D. Shannon, Acta. Crystallogr., 1976, A**32**, 751
114. www.sdsc.edu/CCMS/Packages/Cambridge/started/gs-appendix-5.html
115. Z. Lin, J. F. LeMarechall, M. Sabat, and T. J. Marks, J. Am. Chem. Soc., 1987, **109**, 4127
116. M. R. Kesti, and M. R. Waymouth, J. Am. Chem. Soc., 1992, **114**, 3565
117. X. Yang, C. L. Stern, and T. J. Marks, J. Am. Chem. Soc., 1991, **113**, 3623
118. S. B. Jones, and J. L. Petersen, Inorg. Chem., 1981, **20**, 2889
119. X. Song, M. Thornton-Pett, and M. Bochmann, Organometallics, 1998, **17**, 1004
120. X. Yang, C. L. Stern, and T. J. Marks, J. Am. Chem. Soc., 1994, **116**, 10015

121. X. Yang, C. L. Stern, and T. J. Marks, J. Am. Chem. Soc., 1996, **118**, 12451
122. L. Li and T. J. Marks, Organometallics, 1998, **17**, 3996
123. M. V. Metz, D. J. Schwartz, C. L. Beswick, C. L. Stern, and T. J. Marks, Abstracts of papers, 217th National Meeting Of The American Chemical Society, Anaheim, CA March, 1999, INOR 015
124. X. Yang, C. L. Stern, and T. J. Marks, J. Am. Chem. Soc., 1997, **119**, 2582
125. S. M. Miller, O. P. Anderson, and S. H. Strauss, J. Mol. Catal., 1998, **128**, 289
126. X. Yang, C. L. Stern, and T. J. Marks, J. Am. Chem. Soc., 1998, **120**, 6287
127. C. Reed, Acc. Chem. Res., 1998, **31**, 133
128. J. Plesek, T. Jelinek, S. Hermanek, and B. Stibr, Collect. Czech. Chem. Commun., 1986, **51**, 819
129. C. –W. Tsang, Q. Yang, E. Tung-Po Sze, T. C. W. Mak, T. D. W. Chan, and Z. Xie, Inorg. Chem., 2000, **39**, 5851
130. B. T. King, Z. Janousek, B. Grüner, M. Tramell, B. C. Noll, and J. Michl, J. Am. Chem. Soc., 1996, **118**, 3313
131. D. Stasko, and C. A. Reed, J. Am. Chem. Soc., 2002, **124**, 1148
132. J. Boar, Ziegler – Natta Catalysts and Polymerizations, Academic Press: New York 1979
133. J. C. W. Chien, Ed. Coordination Polymerization, Academic Press: New York 1975
134. G. Natta, I. Pasquon, and A. Zambelli, J. Am. Chem. Soc., 1962, **84**, 1488
135. D. S. Breslow, and N. R. Newburg, J. Am. Chem. Soc., 1957, **79**, 5072
136. W. P. Long, and D. S. Breslow, J. Am. Chem. Soc., 1960, **82**, 1953
137. J. C. W. Chien, J. Am. Chem. Soc., 1959, **81**, 86
138. J. Skupinska, J. Chem. Rev., 1991, **91**, 613
139. A. K. Zefirova, and A. E. Shilov, Dokt. Akad. Nauk. SSSR, 1961, **136**, 599
140. F. S. Dyachkovskii, A. K. Shilova, and A. E. Shilov, J. Polym. Sci., Part C, 1967, **16**, 2333
141. J. J. Etsch, A. M. Plotrowski, S. K. Brownstein, E. J. Gabe, and E. L. Lee, J. Am. Chem. Soc., 1985, **107**, 7219
142. R. Mynott, G. Fink, and W. Fenzl, Angew. Makromol. Chem., 1987, **154**, 1
143. J. J. Etsch, S. I. Pombrik, and G. X. Zheng, Organometallics, 1993, **12**, 3856
144. M. Y. He, G. Xiong, P. J. Toscano, R. L. Burwell, and T. J. Marks, J. Am. Chem. Soc., 1985, **107**, 641
145. M. Bochmann, A. J. Jagger, I. M. Wilson, M. B. Hursthouse, and M. Motevalli, Polyhedron, 1989, **8**, 1838
146. W. P. Long, and D. S. Breslow, J. Am. Chem. Soc., 1960, **82**, 1953
147. A. D. Horton, and J. de With, Organometallics, 1997, **16**, 5424
148. M. Brookhart, B. Grant, and A. F. Volpe, Organometallics, 1992, **11**, 3920
149. X. Bei, D. C. Swenson, and R. F. Jordan, Organometallics, 1997, **16**, 3282
150. Y. Yokota, T. Inoue, S. Naganuma, H. Shozaki, N. Tomotsu, M. Kuramoto, and N. Ishithara, Ed Metalorganic Catalysts for Synthesis and Polymerization: Recent Results by Ziegler-Natta and Metallocene Investigations: Springer-Verlag: Berlin, 1999, 435
151. M. Bochmann, and S. J. Lancaster, J. Organomet. Chem., 1992, 434, C1-C5
152. J. A. Ewen, and M. J. Elder, J. Makromol. Chem. Macromol. Symp., 1993, **66**, 179
153. A. Andresen, H. G. Cordes, H. Herwig, W. Kaminsky, A. Merk, R. Mottweβer, J. Petit, H. Sinn, and H. Vollmer, J. Angew. Chem. Int. Ed. Engl., 1976, **15**, 630

154. H. Sinn, and W. Kaminsky, Adv. Organomet. Chem., 1980, **18**, 99
155. H. Sinn, W. Kaminsky, and H. Hoker, Eds. Aluminoxanes, Macromolecular Symposia 97; Huthig and Wepf.: Heidelberg, Germany, 1995
156. S. Srinivasa Reddy, and S. Sivaram, Prog. Polym. Sci., 1995, **20**, 309
157. H. Sinn, Macromol. Symp., 1995, **97**, 27
158. D. W. Imhoff, L. S. Simeral, S. S. Sangokoya, and J. H. Peet, Organometallics, 1998, **17**, 1941
159. T. Sugano, K. Matsubara, T. Fujita, and T. Takahashi, J. Mol. Catal., 1993, **82**, 93
160. W. Kaminsky, and R. Steiger, Polyhedron, 1988, **7**, 2375
161. A. R. Siedle, W. M. Lamanna, R. A. Newmark, and J. N. Schroepher, J. Mol. Catal., 1998, **128**, 257
162. I. Tritto, S. X. Li, M. C. Sacchi, P. Locatteli, and G. Zannoni, Macromolecules, 1995, **28**, 5358
163. I. Tritto, R. Donnetti, M. C. Sacchi, P. Locatteli, and G. Zannoni, Macromolecules, 1997, **30**, 1247
164. A. G. Massey, and A. J. Park, J. Organomet. Chem., 1964, **2**, 245
165. D.W. Owens, and J. F. Balhoff, US 6241917 (Albemarle Corporation), June 5, 2001
166. I. Katsumi, H. Mitsui, and N. Yamamoto, EP 0838466 (Nippon Catalytic Chem. Ind.), April 29, 1998
167. J. C. W. Chien, W. M. Tsai, and M. D. Rausch, J. Am. Chem. Soc., 1991, **113**, 8570
168. C.J. Pouchert, and J. Behnke, The Aldrich Library of ^{13}C and ^{1}H FT-NMR Spectra
169. R. D. Köhn, D. Smith, M. F. Mahon, M. Prinz, S. Mihan, and G. Kociock-Köhn, J. Organomet. Chem., 2003, **683**, 200
170. B. Binotti, A. Macchioni, C. Zuccaccia, and D. Zuccaccia, Comments on Inorganic Chemistry, 2002, **23**, 417
171. H. Matthias, R. D. Köhn, R. Weimann, G. Seifert, and D. Zeigan, J. Organomet. Chem., 1996, **520**, 121
172. H.Brunner, A. Winter, and B. Nuber, J. Organomet. Chem., 1998, **558**, 213
173. F. Molnar, BASF, DFT Calculations
174. S. K. Noh, R. A. Heintz, C. Janiak, S.C. Sendlinger, and K. H. Theopold, Angew. Chem. Int. Ed. Engl., 1990, **29**, 775
175. S. K. Noh, S. C. Sendlinger, C. Janiak, and K. H. Theopold, J. Am. Chem. Soc., 1989, **111**, 9127
176. G. V. Z. Schulz, Phys. Chem., Abt. B **30**, 1935, 379
177. E. J. Arlman, and P. Cossee, J. Catal., 1964, **3**, 99
178. J. X. McDermott, J. F. White, and G. M. Whitesides, J. Am. Chem. Soc., 1973, **95**, 4451
179. R. M. Manyik, W. E. Walker, and T. P. Wilson, J. Catal., 1977, **47**, 197
180. J. X. McDermott, J. F. White, and G. M. Whitesides, J. Am. Chem. Soc., 1976, **98**, 6521
181. L. A. MacAdams, G. P. Buffone, C. D. Incarvito, J. A. Golen, A. L. Rheingold, and K. H. Theopold, Chem. Commun., 2003, 1164
182. T. Agapie, S. J. Schofer, J. A. Labinger, and J. E. Bercaw, J. Am. Chem. Soc., 2004, **126**, 1304
183. N. Meijboom, C. J. Schaverien, and A. G. Orpen, Organometallics, 1990, **9**, 774

184. D. H. Morgan, S. L. Schwikkard, J. T. Dixon, J. J. Nair, and R. Hunter, Adv. Synth. Catal., 2003, **345**, 939
185. F. A. Cotton, G. Wilkinson, C. A. Murillo, and M. Bochmann, Advanced Inorganic Chemistry, Wiley, New York, 1999, 1355
186. Y. Fang, Y. Liu, Y. Ke, C. Guo, N. Zhu, X. Mi, Z. Ma, and Y. Hu, Appl. Catal. A, 2002, **235**, 33
187. W. J. van Rensburg, C. Grove, J. P. Steynberg, K. B. Stark, J. J. Huyser, and P. J. Steyenberg, Organometallics, 2004, **23**, 1207
188. C. Andes, S. B. Harkins, S. Murtuza, K. Oyler, and A. Sen, J. Am. Chem. Soc., 2001, **123**, 7423
189. P. J. W. Deckers, B. Hessen, and J. H. Teuben, Organometallics, 2002, **21**, 5122
190. Z. Yu, and K. N. Houk, Angew. Chem. Int. Ed. Engl., 2003, **42**, 808
191. A. N. J. Blok, P. H. M. Budzelaar, and A. W. Gal, Organometallics, 2003, **22**, 2564
192. T. J. M. de Bruin, L. Magna, P. Raybaud, and H. Toulhoat, Organometallics, 2003, **22**, 3404
193. S. Tobisch, and T. Ziegler, Organometallics, 2003, **22**, 5392
194. M. Haufe, PhD thesis, Berlin, 1998, D 83
195. R. D. Köhn, Habilitationsschrift, University of Berlin, 1996

Appendix

Crystal data and structure refinement for $(Allyl)_3TACCrCl_3$

Identification code	david1 alias k01rdk17
Empirical formula	C12 H21 Cl3 Cr N3
Formula weight	365.67
Temperature	150(2) K
Wavelength	0.71073 A
Crystal system	hexagonal
Space group	P 6_3 (no.173)
Unit cell dimensions	a = 11.9100(3) A alpha = 90 deg. b = 11.9100(3) A beta = 90 deg. c = 6.9350(2) A gamma = 120 deg.
Volume	851.92(4) A^3
Z, Calculated density	2, 1.425 Mg/m^3
Absorption coefficient	1.132 mm^-1
F(000)	378
Crystal size	0.20 x 0.10 x 0.10 mm
Colour, shape	dark purple hexagonal column
Theta range for data collection	3.95 to 27.50 deg.
Limiting indices	-15<=h<=15, -13<=k<=15, -8<=l<=8
Reflections collected / unique	12016 / 1300 [R(int) = 0.0469]
Completeness to theta = 27.50	99.6 %
Max. and min. transmission	0.8952 and 0.8052
Refinement method	Full-matrix least-squares on F^2
Data / restraints / parameters	1300 / 1 / 59
Goodness-of-fit on F^2	1.133
Final R indices [I>2sigma(I)]	R1 = 0.0337, wR2 = 0.0897
R indices (all data)	R1 = 0.0361, wR2 = 0.0912
Absolute structure parameter	0.43(4)
Largest diff. peak and hole	1.321 and -0.356 e.A^-3

Crystal data and structure refinement for $(2\text{-PhEt})_3TACCrCl_3[Me_2NHPh][B(PhF_5)_4]$

Identification code	david2 alias k01rdk19
Empirical formula	C59 H45 B Cl3 Cr F20 N4
Formula weight	1359.15
Temperature	150(2) K
Wavelength	0.71073 A
Crystal system	triclinic
Space group	P $\bar{1}$
Unit cell dimensions	a = 13.4030(2) A alpha = 63.8900(6) deg. b = 15.0830(2) A beta = 82.3890(6) deg. c = 16.2570(2) A gamma = 80.4760(6) deg.
Volume	2903.81(7) A^3
Z, Calculated density	2, 1.554 Mg/m^3
Absorption coefficient	0.443 mm^-1
F(000)	1374
Crystal size	0.38 x 0.25 x 0.10 mm
Colour, shape	yellow plate
Theta range for data collection	3.56 to 27.52 deg.
Limiting indices	-17<=h<=17, -19<=k<=19, -20<=l<=21
Reflections collected / unique	41201 / 13271 [R(int) = 0.0410]
Completeness to theta = 27.52	99.2 %
Max. and min. transmission	0.9570 and 0.8496
Refinement method	Full-matrix least-squares on F^2
Data / restraints / parameters	13271 / 0 / 793
Goodness-of-fit on F^2	1.022
Final R indices [I>2sigma(I)]	R1 = 0.0358, wR2 = 0.0857
R indices (all data)	R1 = 0.0508, wR2 = 0.0943
Largest diff. peak and hole	0.271 and -0.487 e.A^-3

Crystal data and structure refinement for
$[(2\text{-EtBu})_3TACCrCl_3][B(PhF_5)_4][Me_2NHPh]*(C_7H_8)_{0.5}$

Identification code	david3
Empirical formula	C56.50 H60.50 B Cl3 Cr F20 N4
Formula weight	1344.75
Temperature	150(2) K
Wavelength	0.71073 A
Crystal system	monoclinic
Space group	P $2_1/n$
Unit cell dimensions	a = 12.31900(10) A alpha = 90 deg. b = 30.5470(3) A beta = 107.87 deg. c = 16.5740(2) A gamma = 90 deg.
Volume	5936.14(10) A^3
Z, Calculated density	4, 1.505 Mg/m^3
Absorption coefficient	0.432 mm^-1
F(000)	2750
Crystal size	0.50 x 0.40 x 0.15 mm
Colour, shape	purple brownish plate
Theta range for data collection	2.96 to 27.10 deg.
Limiting indices	-15<=h<=15, -39<=k<=38, -21<=l<=21
Reflections collected / unique	41284 / 12904 [R(int) = 0.0632]
Completeness to theta = 27.10	98.5 %
Max. and min. transmission	0.9380 and 0.8128
Refinement method	Full-matrix least-squares on F^2
Data / restraints / parameters	12904 / 0 / 775
Goodness-of-fit on F^2	1.015
Final R indices [I>2sigma(I)]	R1 = 0.0441, wR2 = 0.0984
R indices (all data)	R1 = 0.0771, wR2 = 0.1113
Largest diff. peak and hole	0.456 and -0.677 e.A^-3

Crystal data and structure refinement for $(2\text{-PhEt})_3TACCrCl_3$

Identification code	david4 alias h02rdk4
Empirical formula	C27 H33 Cl3 Cr N3
Formula weight	557.91
Temperature	150(2) K
Wavelength	0.71073 A
Crystal system	monoclinic
Space group	P $2_1/c$
Unit cell dimensions	a = 11.6360(2) A alpha = 90 deg. b = 17.1910(3) A beta = 109.7840(10) deg. c = 14.0810(3) A gamma = 90 deg.
Volume	2650.43(9) A^3
Z, Calculated density	4, 1.398 Mg/m^3
Absorption coefficient	0.755 mm^-1
F(000)	1164
Crystal size	0.50 x 0.15 x 0.08 mm
Colour, shape	purple plate
Theta range for data collection	3.87 to 27.51 deg.
Limiting indices	-15<=h<=14, -22<=k<=22, -18<=l<=18
Reflections collected / unique	45752 / 6064 [R(int) = 0.0737]
Completeness to theta = 27.51	99.4 %
Max. and min. transmission	0.9421 and 0.7039
Refinement method	Full-matrix least-squares on F^2
Data / restraints / parameters	6064 / 0 / 321
Goodness-of-fit on F^2	1.019
Final R indices [I>2sigma(I)]	R1 = 0.0396, wR2 = 0.0865
R indices (all data)	R1 = 0.0811, wR2 = 0.1006
Extinction coefficient	0.0054(7)
Largest diff. peak and hole	0.378 and -0.504 e.A^-3

Crystal data and structure refinement for $(FPh)_2$(2-EtBu)TAC

Identification code	david5
Empirical formula	C21 H27 F2 N3
Formula weight	359.46
Temperature	150(2) K
Wavelength	0.71073 A
Crystal system	triclinic
Space group	P $\bar{1}$
Unit cell dimensions	a = 6.6760(2) A alpha = 96.6740(10) deg. b = 11.1310(4) A beta = 104.4010(10) deg. c = 13.5710(5) A gamma = 100.619(2) deg.
Volume	946.04(6) A^3
Z, Calculated density	2, 1.262 Mg/m^3
Absorption coefficient	0.089 mm^-1
F(000)	384
Crystal size	0.25 x 0.20 x 0.13 mm
Colour, shape	clourless plate
Theta range for data collection	3.15 to 27.43 deg.
Limiting indices	-8<=h<=8, -14<=k<=14, -17<=l<=15
Reflections collected / unique	12218 / 4308 [R(int) = 0.0554]
Completeness to theta = 27.43	99.3 %
Max. and min. transmission	0.9885 and 0.9781
Refinement method	Full-matrix least-squares on F^2
Data / restraints / parameters	4308 / 0 / 235
Goodness-of-fit on F^2	1.025
Final R indices [I>2sigma(I)]	R1 = 0.0481, wR2 = 0.1072
R indices (all data)	R1 = 0.0790, wR2 = 0.1236
Largest diff. peak and hole	0.184 and -0.229 e.A^-3

Crystal data and structure refinement for (2-EtBu)$(BrPh)_2$TAC

Identification code	david6
Empirical formula	C21 H27 Br2 N3
Formula weight	481.28
Temperature	150(2) K
Wavelength	0.71073 A
Crystal system	Orthorhombic
Space group	P b c a
Unit cell dimensions	a = 9.85600(10) A alpha = 90 deg. b = 19.2690(2) A beta = 90 deg. c = 22.2230(3) A gamma = 90 deg.
Volume	4220.49(8) A^3
Z, Calculated density	8, 1.515 Mg/m^3
Absorption coefficient	3.851 mm^-1
F(000)	1952
Crystal size	0.35 x 0.25 x 0.05 mm
colour, shape	colourless plate
Theta range for data collection	3.60 to 27.47 deg.
Limiting indices	-12<=h<=12, -25<=k<=25, -28<=l<=28
Reflections collected / unique	67363 / 4819 [R(int) = 0.1159]
Completeness to theta = 27.47	99.7 %
Max. and min. transmission	0.8308 and 0.3459
Refinement method	Full-matrix least-squares on F^2
Data / restraints / parameters	4819 / 0 / 236
Goodness-of-fit on F^2	1.015
Final R indices [I>2sigma(I)]	R1 = 0.0404, wR2 = 0.0870
R indices (all data)	R1 = 0.0769, wR2 = 0.0991
Extinction coefficient	0.0018(2)
Largest diff. peak and hole	0.638 and -0.581 e.A^-3

Crystal data and structure refinement for $[Tol_2Cr][BPhF_5]_4*(Tol)_{0.5}$

Identification code	david7
Empirical formula	C41.50 H19.50 B Cr F20
Formula weight	960.88
Temperature	150(2) K
Wavelength	0.71073 A
Crystal system	monoclinic
Space group	P $2_1/c$
Unit cell dimensions	a = 10.4850(2) A alpha = 90 deg. b = 21.8690(4) A beta = 103.9710(10) deg. c = 16.8810(4) A gamma = 90 deg.
Volume	3756.25(13) A^3
Z, Calculated density	4, 1.699 Mg/m^3
Absorption coefficient	0.437 mm^-1
F(000)	1910
Crystal size	0.30 x 0.25 x 0.13 mm
Colour, shape	yellow wedge
Theta range for data collection	3.36 to 27.47 deg.
Limiting indices	-13<=h<=13, -25<=k<=28, -21<=l<=19
Reflections collected / unique	27245 / 8310 [R(int) = 0.0743]
Completeness to theta = 27.47	96.4 %
Max. and min. transmission	0.9453 and 0.8800
Refinement method	Full-matrix least-squares on F^2
Data / restraints / parameters	8310 / 0 / 660
Goodness-of-fit on F^2	1.011
Final R indices [I>2sigma(I)]	R1 = 0.0516, wR2 = 0.1138
R indices (all data)	R1 = 0.1031, wR2 = 0.1364
Largest diff. peak and hole	0.299 and -0.475 e.A^-3

Crystal data and structure refinement for $(ClPh)_2$(2-EtBu)TAC

Identification code	david8
Empirical formula	C21 H27 Cl2 N3
Formula weight	392.36
Temperature	150(2) K
Wavelength	0.71073 A
Crystal system	Orthorhombic
Space group	P b c a
Unit cell dimensions	a = 9.69500(10) A alpha = 90 deg. b = 18.9700(2) A beta = 90 deg. c = 22.2490(3) A gamma = 90 deg.
Volume	4091.91(8) A^3
Z, Calculated density	8, 1.274 Mg/m^3
Absorption coefficient	0.327 mm^-1
F(000)	1664
Crystal size	0.50 x 0.30 x 0.05 mm
Colour, shape	colourless plate
Theta range for data collection	3.49 to 27.48 deg.
Limiting indices	-12<=h<=12, -24<=k<=23, -28<=l<=28
Reflections collected / unique	60485 / 4681 [R(int) = 0.0844]
Completeness to theta = 27.48	99.6 %
Max. and min. transmission	0.9838 and 0.8535
Refinement method	Full-matrix least-squares on F^2
Data / restraints / parameters	4681 / 0 / 235
Goodness-of-fit on F^2	1.021
Final R indices [I>2sigma(I)]	R1 = 0.0423, wR2 = 0.0963
R indices (all data)	R1 = 0.0750, wR2 = 0.1105
Largest diff. peak and hole	0.244 and -0.252 e.A^-3

Crystal data and structure refinement for $[(0\text{-MeOPh})NH]_2CH_2$

Identification code	david9 (h04rdk1)
Empirical formula	C15 H18 N2 O2
Formula weight	258.31
Temperature	150(2) K
Wavelength	0.71073 A
Crystal system	orthorhombic
Space group	P n a 2_1
Unit cell dimensions	a = 8.2190(8) A alpha = 90 deg. b = 23.6120(2) A beta = 90 deg. c = 6.9850(2) A gamma = 90 deg.
Volume	1355.56(14) A^3
Z, Calculated density	4, 1.266 Mg/m^3
Absorption coefficient	0.085 mm^-1
F(000)	552
Crystal size	0.50 x 0.50 x 0.08 mm
Theta range for data collection	3.58 to 28.67 deg.
Limiting indices	-7<=h<=11, -30<=k<=31, -9<=l<=9
Reflections collected / unique	5868 / 2900 [R(int) = 0.0390]
Completeness to theta = 28.67	98.3 %
Max. and min. transmission	0.9932 and 0.9588
Refinement method	Full-matrix least-squares on F^2
Data / restraints / parameters	2900 / 1 / 182
Goodness-of-fit on F^2	1.054
Final R indices [I>2sigma(I)]	R1 = 0.0365, wR2 = 0.0823
R indices (all data)	R1 = 0.0490, wR2 = 0.0870
Absolute structure parameter	0.1(10)
Largest diff. peak and hole	0.139 and -0.148 e.A^-3